SPECIAL
Sun Spot Report

COMMUNICATIONS QUARTERLY

THE JOURNAL OF COMMUNICATIONS TECHNOLOGY

Summer 1991 $9.95

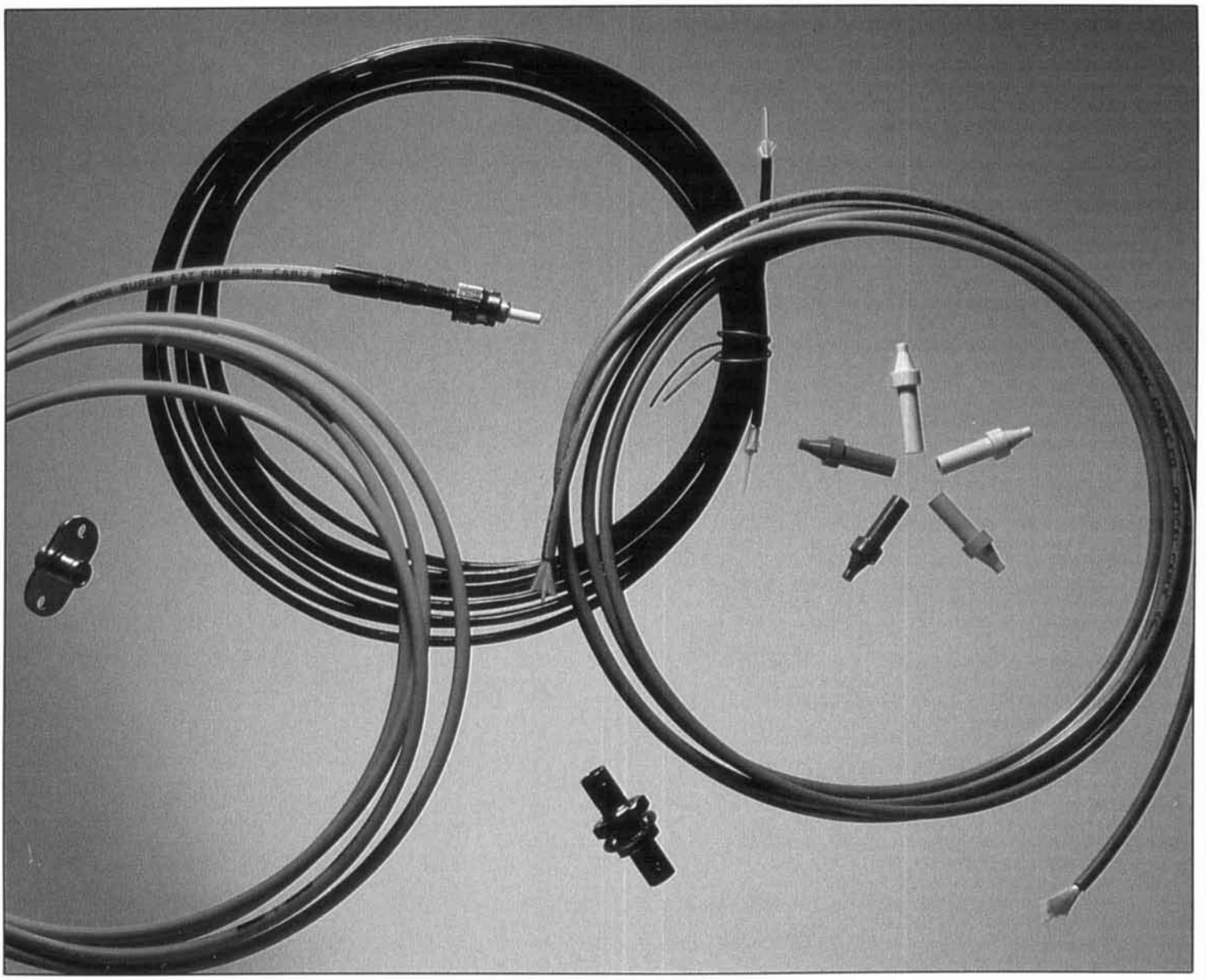

- Fiber Optics
- Outlining June's Strong Solar Flare Activity
- Recording Solar Flares Indirectly
- Antenna Angle of Radiation Considerations
- A Rapid Design Tool for Microstrip Filters
- Upgrading the FT-ONE Transceiver
- TX IMD Performance and Measurement Techniques
- A High-Level SSB Modulator for S Band
- Modifying The Heath SB220 Linear Amplifier

ISSN 1053-9433

F M T R A N S C E I V E R

IC-24AT
Dual Band
Transceiver

IC-W2A
Dual Band
Transceiver

ACTUAL SIZE

Icom continues to dominate the industry with exceptional product design and innovation. The IC-24AT firmly established Icom as the leader in dual band technology. Now the IC-W2A gives you the advantage of choosing the dual bander best suited for your needs.

The new IC-W2A dual band handheld sets the pace with its sleek design and superior characteristics. Designed for the user who demands the finest features available, the IC-W2A boasts simultaneous dual band receive. Listen to one band while talking on the other! Three tuning systems, high speed scanning with priority watch and 60 memory channels add to the luxurious IC-W2A.

Both the IC-W2A and IC-24AT give you full operation on the two-meter and 440MHz amateur bands with outstanding wideband receive capability.

Each unit features up to five watts of power, programmable scanning, priority watch, a battery saver, DTMF pad for memory channel autopatching, 24 hour clock with timing system, multi-function LCD readouts...the list is infinite. See the IC-W2A and the IC-24AT today at your authorized Icom dealer.

SETTING THE PACE IN DUAL BAND DESIGN

For full details and specifications on the IC-W2A and IC-24AT, call the Icom Brochure hotline at 1-800-999-9877.

CORPORATE HEADQUARTERS
ICOM America, Inc., 2380-116th Ave. N.E., Bellevue, WA 98004
Customer Service Hotline
(206) 454-7619
CUSTOMER SERVICE CENTERS
18102 Sky Park South, Suite 52-B, Irvine, CA 92714
1777 Phoenix Parkway, Suite 201, Atlanta, GA 30349
3071 - #5 Road, Unit 9, Richmond, B.C. V6X 2T4 Canada

All stated specifications are subject to change without notice or obligation. All ICOM radios significantly exceed FCC regulations limiting spurious emissions.
W2A691

ICOM

ICOM

First in Communications

CORPORATE HEADQUARTERS: ICOM America, Inc.
2380-116th Ave. N.E., Bellevue, WA 98004
CUSTOMER SERVICE HOTLINE (206) 454-7619
CUSTOMER SERVICE CENTERS:
18102 Sky Park South, Ste. 52-B, Irvine, CA 92714
1777 Phoenix Parkway, Suite 201, Atlanta, GA 30349
3071 - #5 Road, Unit 9, Richmond, B.C. V6X 2T4 Canada
2380-116th Ave. N.E., Bellevue, WA 98004

All stated specifications are subject to change without notice or obligation. All ICOM radios significantly exceed FCC regulations limiting spurious emissions. 3220791

KENWOOD

TM-731A/631A

144/450 and 144/220 MHz FM Dual Banders

- Extended receiver range (136.000 – 173.995 MHz) on 2 m; 70 cm coverage is 438.000 – 449.995 MHz; 1-1/4 m coverage is 215 – 229.995 MHz. (Specifications guaranteed on Amateur bands only. Two meter transmit range is 144 – 148 MHz. Modifiable for MARS/CAP. Permits required.)
- Separate frequency display for "main" and "sub-band."
- Versatile scanning functions. Dual scan, and carrier and time operated scan stop.
- 30 memory channels. Stores everything you need to make operating easier. Two channels for "odd splits."
- 50 Watts on 2 m, 35 watts on 70 cm, 25 watts on 1-1/4 m. Approx. 5 watts low power.
- Automatic offset selection.
- Dual antenna ports.
- Automatic Band Change (A.B.C.) Automatically changes between main and sub-band when a signal is present.
- Dual watch function allows VHF and UHF receive simultaneously.
- CTCSS encode/decode selectable from front panel or UP/DWN keys on microphone. (Encode built-in, optional TSU-6 needed for decode.)
- Balance control and separate squelch controls for each band.
- Full duplex operation.
- Dimmer switch.
- 16 key DTMF/control mic. included.
- Frequency (dial) lock.

Optional Accessories:
• **PG-4H** Extra interface cable for IF-20 (for three to four radios) • **PG-4J** Extension cable kit for IF-20 DC and audio • **PS-430** Power supply • **TSU-6** CTCSS decode unit • **SWT-1** 2 m antenna tuner • **SWT-2** 70 cm antenna tuner • **SP-41** Compact mobile speaker • **SP-50B** Deluxe mobile speaker • **PG-2N** DC cable • **PG-3B** DC line noise filter • **MC-60A, MC-80, MC-85** Base station mics. • **MA-700** Dual band 2 m/70 cm mobile antenna (mount not supplied) • **MB-11** Mobile bracket • **MC-43S** UP/DWN hand mic. • **MC-48B** 16-key DTMF hand mic.

KENWOOD U.S.A. CORPORATION
COMMUNICATIONS & TEST EQUIPMENT GROUP
P.O. BOX 22745, 2201 E. Dominguez Street
Long Beach, CA 90801-5745
KENWOOD ELECTRONICS CANADA INC.
P.O. BOX 1075, 959 Gana Court
Mississauga, Ontario, Canada L4T 4C2

KENWOOD

...pacesetter in Amateur Radio

"Dynamic Duals"

Complete service manuals are available for all Kenwood transceivers and most accessories. Specifications, features and prices are subject to change without notice or obligation.

COMMUNICATIONS QUARTERLY

THE JOURNAL OF COMMUNICATIONS TECHNOLOGY

CONTENTS

Volume 1, Number 3 Summer 1991

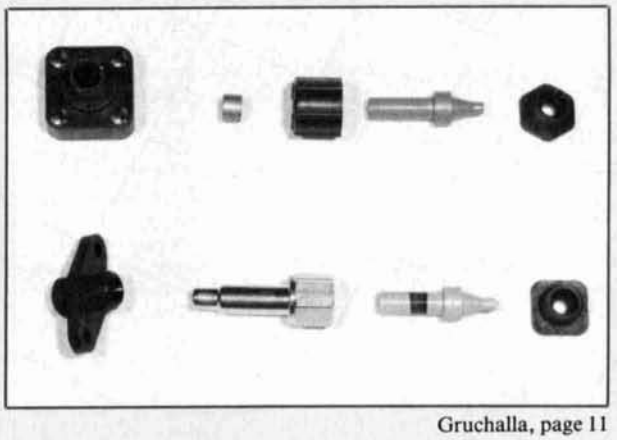

Gruchalla, page 11

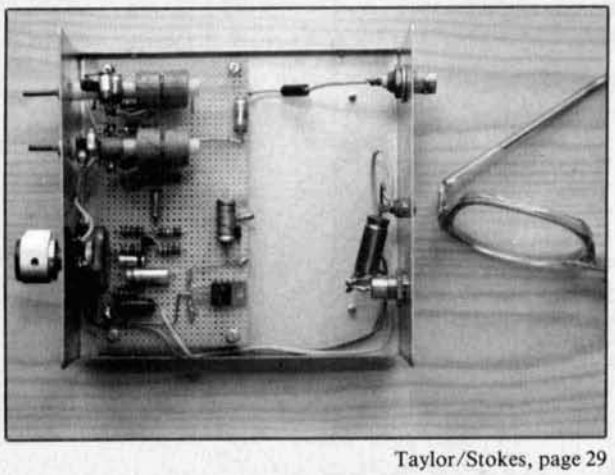

Taylor/Stokes, page 29

11 Fiber Optics
Michael E. Gruchalla

26 Outlining June's Strong Solar Flare Activity
Peter O. Taylor

29 Recording Solar Flares Indirectly
Peter O. Taylor and Arthur J. Stokes, N8BN

37 Antenna Angle of Radiation Considerations
Carl Luetzelschwab, K9LA

43 A Rapid Design Tool for Microstrip Filters
Jeff Crawford, KØZR

48 Upgrading the FT-ONE Transceiver
Cornell Drentea, WB3JZO

61 TX IMD Performance and Measurement Techniques
Marv Gonsior, W6FR

66 The Wonderful Transformer Power Splitter
David M. Barton, AF6S

71 A High-Level SSB Modulator for S Band
Norm Foot, WA9HUV

76 An Audio Imaging System for Enhanced CW Reception
Bryan Bergeron, NU1N

84 Super Yagi Beam
John Tyskiewicz, W1HXU

88 Making High-Q Air-Core Coils
Yardley Beers, WØJF

91 Modifying The Heath SB220 Linear Amplifier
George W. Carson, K4GDG

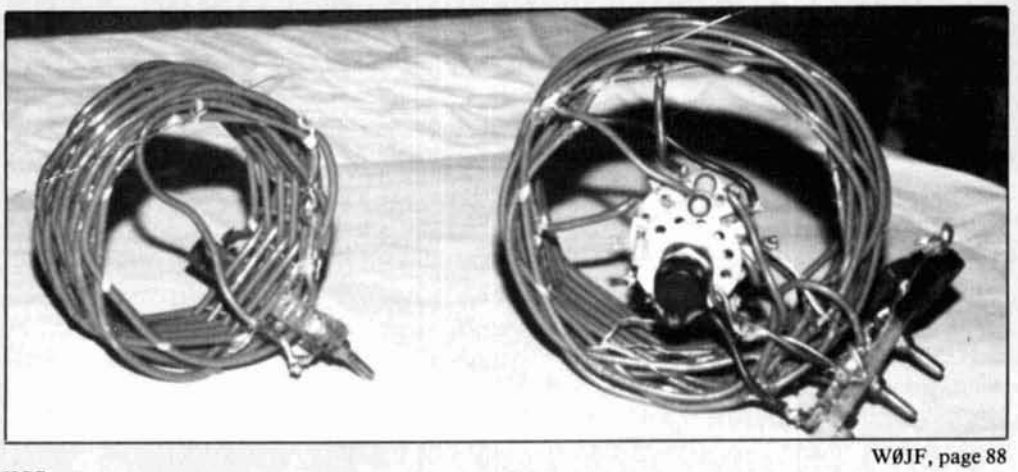

WØJF, page 88

Cover photo: Nick Thomas, KA1YGS

EDITORIAL

A Most Unique Solar Event

During the month of June 1991 there were a total of five solar flares so powerful that they surpassed the capabilities of state-of-the-art equipment used to measure such events. Indeed, this month was one of the most active in the current solar cycle (Cycle 22).

For most people, what was happening on the sun and in the ionosphere at this time was of little concern. Radio and TV reception was a little poorer than usual, and there were spotty power blackouts in some places. However, for radio amateurs these flares created a propagational nightmare.

June's solar storm began as NOAA/USAF Sunspot Region 6659 rotated to the Sun's edge with a massive X-class flare. This saturated the sensors of the Geostationary Operational Environment Satellite (GOES) and sent the displays of earth-bound equipment off the scale. Within eight minutes of the first flare, the Earth's ionosphere was jolted by a tremendous blast of radio signals, the total spectrum of light, and X-rays. Radio propagation began to deteriorate, if not disappear altogether, as the ionosphere became increasingly disturbed. Twenty-four to 36 hours later, heavier atomic particles arrived and bombarded the earth with even more energy, causing further disruption to radio communications. Propagation from 3 to 30 MHz became sporadic, at best. Many bands were subject to total blackouts. Polar paths were gone, and equatorial propagation was compromised.

Solar Cycle 22 has passed its peak. There are differences of opinion in the scientific community as to when this peak occurred—1989 or 1990. But no matter what the date, the sun storm of this past June tends to support recent studies which indicate that there is usually an increase in activity following the peak of a solar cycle.

Hams have always been acutely aware of the effects of solar events on their ability to work the bands. Those who monitor our power facilities and broadcast stations are also aware of just how damaging the sun's activities can be. Early in 1990, a major solar flare shorted out the relays at a power station in Quebec, causing an interruption of service that could have been far worse than it was. If the disturbance created by the flare had not impacted this area on a cold winter night when demand for electricity was relatively low, the power outages could have been much greater and more widespread. The limited effect of the June 1991 solar storm was the result of a number of factors, not the least of which included information learned from the flares of 1990 and a large dose of luck.

In an effort to help all of us understand the ramifications of Cycle 22's most unique solar outburst, Peter Taylor, chairman of the solar division of AAVSO in Athens, Georgia, documents the incidents of June 1991. Those of you who are interested participating in on-going solar research activities will also want to read the article by Taylor and his co-author Arthur Stokes on page 29. They tell you how to interface a simple three-transistor receiver to an inexpensive computer in order to compile, tabulate, and output data on solar events. Even though we're on the downside of this current cycle, there will be plenty more flares before it reaches solar minimum, and plenty of chances for you to play a part in this fascinating investigation of the sun.

Craig Clark, NX1G
Associate Publisher

EDITORIAL STAFF
Editor
Terry Northup, KA1STC
Consulting Technical Editor
Robert Wilson, WA1TKH
Senior Technical Editor
Alfred Wilson, W6NIF
Technical Editor
Peter Bertini, K1ZJH
Editorial Assistant
Elizabeth McCormack

EDITORIAL REVIEW BOARD
Forrest Gehrke, K2BT
Michael Gruchalla, P.E.
Hunter Harris, W1SI
Bob Lewis, W2EBS
Walter Maxwell, W2DU
William Orr, W6SAI

BUSINESS STAFF
Publisher
Richard Ross, K2MGA
Associate Publisher
J. Craig Clark, Jr., NX1G
Advertising Manager
Arnie Sposato
Sales Assistant
Tracy Parbst
Controller
Frank Fuzia
Circulation Manager
Catherine Ross
Data Processing
Melissa Kehrwieder
Carol Minervini
Customer Service
Denise Pyne

PRODUCTION STAFF
Art Director
Elizabeth Ryan
Asst. Art Director
Barbara Terzo
Artist
Susan Reale
Production Manager
Dorothy Kehrwieder
Production
Tracy Parbst
Phototypographers
Pat Le Blanc
Florence V. Martin
Typesetter
Kate Ross

A publication of
CQ Communications, Inc.
76 North Broadway
Hicksville, NY 11801-USA

Editorial Offices: Main Street, Greenville, NH 03048. Telephone: (603) 878-1441. FAX: (603) 878-1951.
Business Offices: 76 North Broadway, Hicksville, NY 11801. Telephone: (516) 681-2922. FAX: (516) 681-2926.
Communications Quarterly is published four times a year (quarterly) by *CQ Communications, Inc.* Subscription prices: Domestic—one year $29.95; Foreign—$39.95. Contents copyrighted CQ Communications, Inc. 1991. Communications Quarterly does not assume responsibility for unsolicited manuscripts. Allow six weeks for change of address.
Second-class postage paid at Hicksville, NY and additional mailing offices.
Postmaster: Please send change of address to Communications Quarterly, CQ Communications, Inc., 76 North Broadway, Hicksville, NY 11801. ISSN 1053-9344

KantronicsD4-10

19,200 off the shelf

No tweaking, no kludges, no kidding . . .The new Kantronics D4-10 transceiver provides robust 19,200 baud operation off the shelf, today. Manufactured to respond to your requests for a faster more powerful transceiver, the D4-10 represents state of the art design equalling that found in our DataEngine and beyond that found anywhere else in the industry.

The Kantronics D4-10 features user selectable narrow and wide bandwidth operation (60 KHZ). This provides conventional and high speed data modes at 1200, 9600, and up to 19,200 baud and beyond with our DataEngine and DE19200 plug-in module.

Add features like a DVR2-2 plug compatible analog port for experimentation, TTL port which supports internal DFSK modulation and threshold demodulation, fast TR switching and you have a 70 cm transceiver that is as fun to use as it is technologically advanced.

The Kantronics D4-10 transceiver, the state of the art available off the shelf from Kantronics.

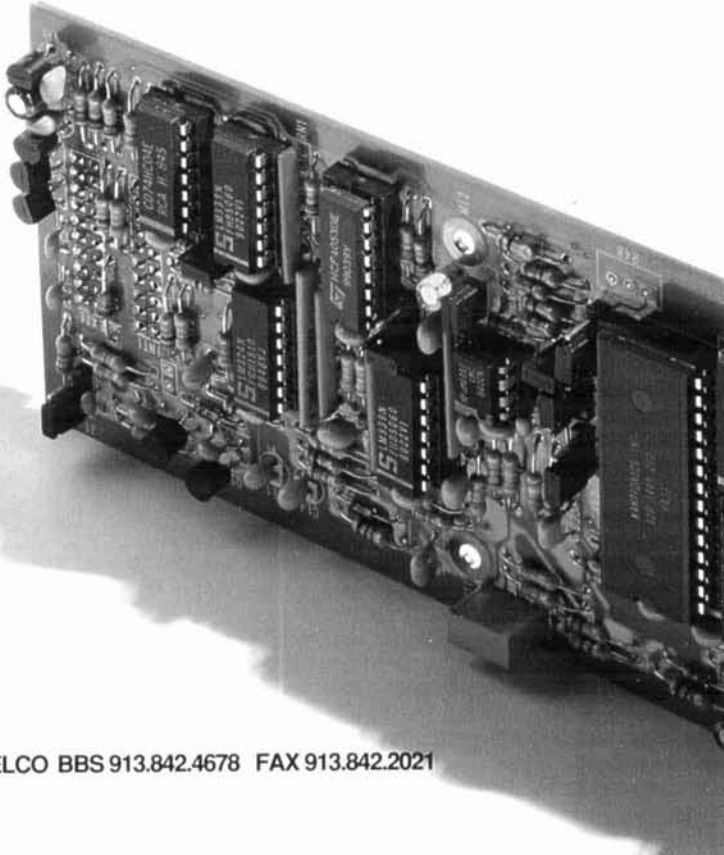

Kantronics 1202 E. 23rd St., Lawrence, KS 66046 913.842.7745 TELCO BBS 913.842.4678 FAX 913.842.2021

LETTERS

Confidence in the future

Hearty congratulations to you and all your staff members for a job well done! The premier issue is a testament to the dedication and hard work you have all endured. I for one am confident that this marks the beginning of a new and exciting phase of Amateur Radio. Keep up the good work!

Norman J. Foot, WA9HUV,
Elmhurst, Illinois

Constructive criticism

Good first issue. Here are some comments.

Keep the binding with the square edges, like *QST*. Stacks much better than the other style!

We don't need wide-open margins or slick, fancy paper. At the hefty price, we expect content, not artistic quality and doodling space.

Good technical content in issue number one, and a good spread of topics. Please don't aim toward the PhD/MSEE level (not saying that number one did). Remember, there are lots of us with BS, associates degrees, and high school diplomas with technical interests. Don't neglect tutorials on basics. K4IPV's column in *Ham Radio* was most helpful.

After you run low on high-powered topics, I might even send in my inductance tester, which uses a slightly different approach.

Michael A. Czuhajewski, WA8MCQ,
Severn, Maryland

Correction

In the article, "Upgrade Your 1296-MHz Converter," by Norm Foot, WA9HUV, found on page 93 of the Winter 1991 issue of *Communications Quarterly*, a 25-pF chip capacitor was omitted. The capacitor should be soldered between the junction of L1 and R7 and ground, as shown in the corrected version of **Figure 5**.

Omission of this capacitor will not prevent the oscillator from working, but its addition will reduce phase and flicker noise close in on each side of the carrier, thus improving PLO performance considerably. **Ed.**

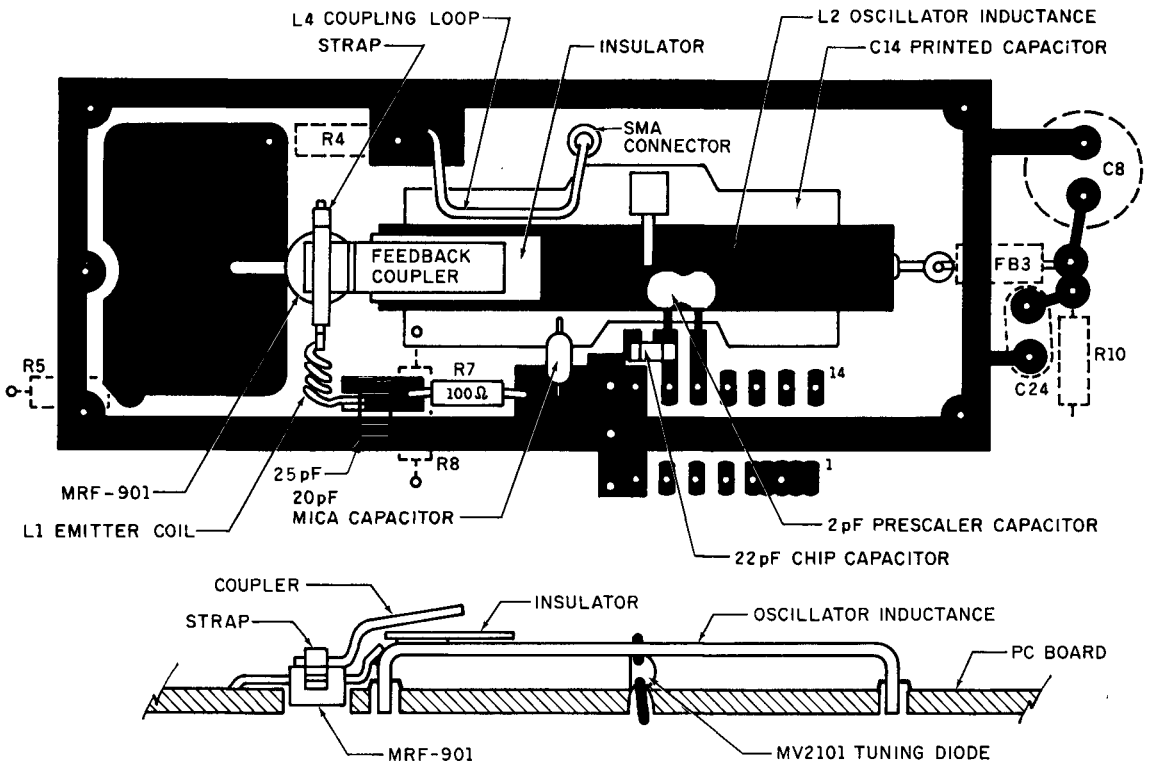

FLYWEIGHT BODY with HEAVYWEIGHT FEATURES

Alinco's New DJ-F1/F4T Realized Super Compact Body and Plenty of Features including:

*40 Memory Channels store Frequency, Shift direction, Split operation Setting, Tone encoder/Tone decoder setting (with optional Tone squelch unit), DSQ setting, Tone frequency and Offset frequency independently.

*Digital Signal Display and Memory Function
The DJ-F1T/F4T has special memory channels for transmitting, receiving, and store "Two Digit" DTMF Tones, for communication messages. This feature allows for the DJ-F1T/F4T to receive a "Two Digit" message and display it at any later time, at the convenience of the operator.

*Wide Band Receiving range
F1T:140-170MHz(AM Mode 118-136MHz after modification)
F4T:430-460MHz

*Battery Pack Lock
*Pager and Code Squelch
*Triple Stage Selective Power Output
*5W Output Power with Optional Battery Pack EBP-18N
*8 Scan Modes
*Programmable VFO Range Function
*Battery Save Function
*Six Channel Steps - 5, 10, 12.5, 15, 20, and 25KHz
*Priority Function (Dual Watch)
*Automatic Power Off (Programmable Timed)
*Automatic Dialer Function
*Illuminated DTMF Keypad
*Many Optional Accessories such as:
EMS-8:Remote Control Speaker/Mic.
EME-11:Earphone/Mic. with PTT/VOX
EME-10:Headset with PTT/VOX
EJ-2U:Tone squelch Unit
EDC-33:Quick Charger (Compatible with standard battery pack)

and many more. . . . .

DJ-S1T/S4T is Simple Type and Low-Priced But Offers Features such as:

*5W Output Power with Optional Battery Pack EBP-18N
*Triple Stage Slective Power Output
*Dry Cell Battery Case Lock
*Programmable VFO Range Function
*Frequency Lock, PTT Lock Function
*One Touch Squelch De-Activation Function
*8 Scan Modes
*Wide Band Receiving Range

Available Features with Optional DTMF Unit (DJ-10U) and DTMF Keypad (ESK-1) Include:

*Pager and Code Squelch
*Digital Signal Display and Memory Function
*Automatic dialer Function
*Many Optional Accessories Available

•Specifications

Frequency Range:
DJ-F1T/S1T
TX:144-148MHz
RX:140-170MHz (AM Mode 118-136MHz after Modification)
DJ-F4T/S4T
TX:440-450MHz
RX:430-460MHz

Output Power:
* with Battery Pack EBP-16N (Standard for F1T/F4T)
Hi:2W(F1T/S1T) 1.5W(F4T/S4T)
Mid:1W Low:0.1W
* with Optional Battery Pack EBP-18N
Hi:5W Mid:1W Low:0.1W
* at 9V
Hi:2.5W(F1T/S1T) 2W(F4T/S4T)
Mid:1W Low:0.1W

Weight:
DJ-F1T/F4T Approx.:13.2 oz.: with Standard Battery Pack
DJ-S1T/S4T Approx.:13 oz.: with Dry Battery case

Dimensions:
4.3(H) × 2.1(W) × 1.5(D) inch (Without Projections)

Specifications and features are guaranteed for amateur bands only and subject to change without notice.

ALINCO ELECTRONICS INC.
438 AMAPOLA AVE. LOT 130
TORRANCE, CALIFORNIA 90501
Phone: 213-618-8616
FAX : 213-618-8758

STAY TUNED with ALINCO

MAXIMUM RANGE MAXIMIZED SENSITIVITY

We've Carefully balanced the amount of gain used in our input amplifiers - too much or too little results in poor performance. **OPTOELECTRONICS' HANDI-COUNTERS™** with maximized sensitivity give you the maximum range for antenna pick-up.

Made in the USA

MODEL 3000
Multi-function Counter
10Hz-3GHz, 10 Digit LCD with frequency, period, ratio, interval & signal level bargraph....**$375.**

Maximum Security Device.
Increase your frequency finding™ by 10 times the distance *or more.*
Tunable Preselector APS-104 $995.

Counter Sold separately

MODEL 8030
With all the features of the 3000 plus enhanced input signal conditioning and enhanced TCXO time base **$579.**

OPTOELECTRONICS

$99.

Model 2300 - 1MHz-2.4GHz Available with NiCads and AC Charger Adapter. Complete Package only....$128.

$199.

Model 2210A
10Hz-2.4GHz Full range counter.Price includes Nicads & AC charger/adapter.

The Original Pocket-Sized LED Handi-Counter™

All of ***OPTOELECTRONICS'*** LED Handi-Counters™ will:

- Count frequencies above 2.4GHz.
- Have display saving Power Switch (avoids premature LED burn-out, leading cause of *counter failure.*)

Accept no substitutes - Look for the *OPTOELECTRONICS* name on the label!

Only *OPTOELECTRONICS* offers you *MAXIMIZED SENSITIVITY.*

Factory Direct Order Line **1-800-327-5912**

FL(305)771-2050 • FAX(305)771-2052

5821 NE 14th Ave. • Ft. Lauderdale, FL33334 • 5% Ship/Handling (Max. $10) U.S. & Canada. 15% outside continental U.S.A.
Visa and Master Card accepted.

Wide Dynamic Range and Low Distortion – The Key to Superior HF Data Communications

- Dynamic Range > 75 dB
- 400 to 4000 Hz
- BW Matched to Baud Rate
- BER < 1 X 10^{-5} for S / N = 0 dB
- 10 to 1200 Baud
- Linear Phase Filters

ST-8000 HF Modem

Real HF radio teleprinter signals exhibit heavy fading and distortion, requirements that cannot be measured by standard constant amplitude BER and distortion test procedures. In designing the ST-8000, HAL has gone the extra step beyond traditional test and design. Our noise floor is at -65 dBm, not at -30 dBm as on other units, an extra 35 dB gain margin to handle fading. Filters in the ST-8000 are all of linear-phase design to give minimum pulse distortion, not sharp-skirted filters with high phase distortion. All signal processing is done at the input tone frequency; heterodyning is NOT used. This avoids distortion due to frequency conversion or introduced by abnormally high or low filter Q's. Bandwidths of the input, Mark/Space channels, and post-detection filters are all computed and set for the baud rate you select, from 10 to 1200 baud. Other standard features of the ST-8000 include:

- 8 Programmable Memories
- Set frequencies in 1 Hz steps
- Adjustable Print Squelch
- Phase-continuous TX Tones
- Split or Transceive TX/RX
- CRT Tuning Indicator
- RS-232C, MIL-188C, or TTL Data
- 8, 600, or 10K Audio Input
- Signal Regeneration
- Variable Threshold Diversity
- RS-232 Remote Control I/O
- 100-130/200-250 VAC, 44-440 Hz
- AM or FM Signal Processing
- 32 steps of M/S filter BW
- Mark or Space-Only Detection
- Digital Multipath Correction
- FDX or HDX with Echo
- Spectra-Tune and X-Y Display
- Transmitter PTT Relay
- 8 or 600 Ohm Audio Output
- Code and Speed Conversion
- Signal Amplitude Squelch
- Receive Clock Recovery
- 3.5" High Rack Mounting

Write or call for complete ST-8000 specifications.

HAL Communications Corp.
Government Products Division
Post Office Box 365
Urbana, Illinois 61801
(217) 367-7373

VERSATILITY PLUS +

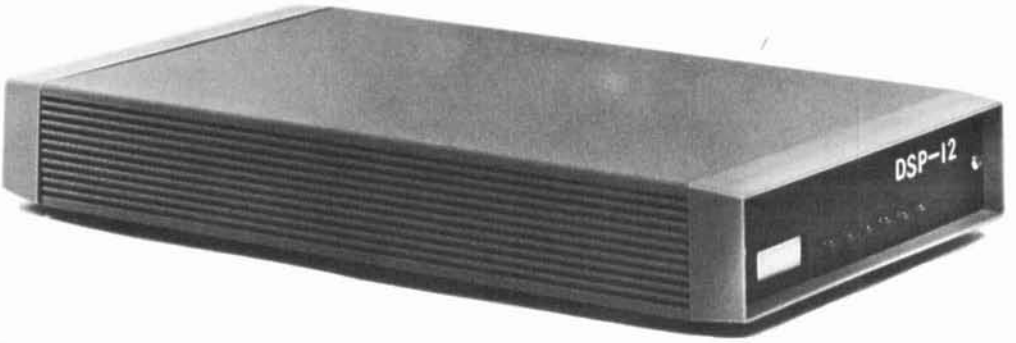

L.L. Grace introduces our latest product, the **DSP-12 Multi-Mode Communications Controller.** The **DSP-12** is a user programmable, digital signal processing (DSP) based communications controller.

FEATURES

- Multi-tasking operating system built in
- PC-compatible (V40) architecture allows development of custom applications using normal PC development tools and languages
- Motorola DSP56001 DSP processor
- Serial interface speeds from 110 to 19200 bps
- Optional 8-channel A-to-D & DAC for voice and telemetry applications
- 12-bit conversion architecture
- V40 source code and schematics available
- RAM expandable to one megabyte. Useable for mailbox feature, voice mail and development
- EPROM expandable to 384k bytes
- Low power requirements: 10-15vdc, 750ma
- 3 analog radio connectors. RX & TX can be split in any combination. Programmable tuning outputs are available on each connector
- Many modems available in the basic unit, including Packet, RTTY, ASCII, and PSK modems for high speed packet and satellite work
- Both V40 and DSP programs can be down-line-loaded from your PC or a bulletin board. You can participate in new development!
- Built in packet mailbox
- V40 and DSP debuggers built in
- Open programming architecture
- Free software upgrades
- Low cost unit
- Room for future growth

APPLICATIONS

- HF Packet
- HF RTTY & ASCII, including inverted mark/space and custom-split applications
- VHF Packet
- 400bps PSK (satellite telemetry)
- 1200bps PSK (satellite & terrestrial packet)
- V26.B 2400bps packet
- 9600bps direct FSK (UO-14)
- Morse Code

CUSTOM APPLICATIONS

- Voice compression
- Telemetry acquisition
- Message Store-and-Forward
- Voice Mail

COMING ATTRACTIONS

(Remember, software upgrades are free!)

- WEFAX and SSTV demodulators
- NAVTEX
- AMTOR and SITOR
- Multi-tone Modems
- ARINC ACARS

Commercial inquiries are welcomed. We offer rapid prototyping of custom commercial, civil, and government applications including intelligent radio, wireline, and telephone modems.

DSP-12 Multi-mode Communications Controller	$ 595.00
One Megabyte RAM Expansion Option	149.00
Date/Time Clock Backup Option	29.00
8-Channel A-To-D Telemetry/Experimentation Option	49.00
Wall-Mount Power Supply for DSP-12 (110 vac)	19.00

We accept MasterCard & VISA and can ship C.O.D. within the USA. All orders must be paid in US Dollars. Shipping & Handling: $5 ($20 International).

L. L. Grace Communications Products, Inc.
41 Acadia Drive, Voorhees, NJ 08043, USA
Telephone: (609) 751-1018
FAX: (609) 751-9705
Compuserve: 72677,1107

1/91

L. L. Grace also manufactures the Kansas City Tracker family of satellite antenna aiming systems. Call or write for more information.

Michael E. Gruchalla
4816 Palo Duro Avenue, NE
Albuquerque, New Mexico 87110

FIBER OPTICS

A brief introduction

The technology of fiber optics is developing at a very rapid rate. On a reasonably regular basis, you may hear of a new fiber optics application, some new installation, or a new fiber-optic technological breakthrough. Fiber optics is being used in a great many fields, but the most well-publicized uses are those related to telecommunication where the optical fiber offers tremendous advantages over any other transmission medium. However, this is only a single general application. Fiber optics is also used in many nontelecommunication applications in the medical, industrial, and commercial fields. Some of these applications include: surgery, accurate positioning, gyroscopes, lenses, nonlens imaging, and sensors of various types. In spite of its rapid development, there is little general information available for those outside the fiber-optic industry who wish to understand this technology more fully.

This article touches on some of the very basics of fiber optics. I've included only enough detail to give you a little better understanding of the technology, without going into the theory. For those who wish to pursue the particulars of fiber optics, I have listed some references that may be of additional interest and lead you deeper into the more theoretical concepts of fiber-optic technology. **Reference 1** is a very good introductory resource.

The fiber-optic system

There's a great variety of fiber-optic systems in use. Design details for each system depend on its application. Some are very specialized. However, in all fiber-optic systems there are certain elements which are always present in one form or another. These are:

- Optical fiber: The optical transmission path, or silica fiber, for which the fiber-optic technology was named.
- Optical connectors: A device which allows the interconnection of emitters, detectors, and fibers just as electrical connectors do in electronic systems.
- Optical emitter: A device which generates the optical signal, or light, to be processed by the fiber-optic system.
- Optical detector: A device which detects the optical signal at the output of the optical fiber.

Figure 1 shows a very basic fiber-optic system block diagram which incorporates these elements.

It may be argued that one or more of these elements is missing in many applications, but they are all generally present in one form or another. For example, in some sensing applications, a property of the fiber which causes it to emit light when exposed to certain stimuli is used as the light source rather than a more conventional emitter. In such a case, that portion of fiber being used as the light source would be the effective emitter (an intrinsic fiber-optic sensor) shown in **Figure 1**. The optical fiber is often welded together rather then joined with optical connectors. A fiber weld would still

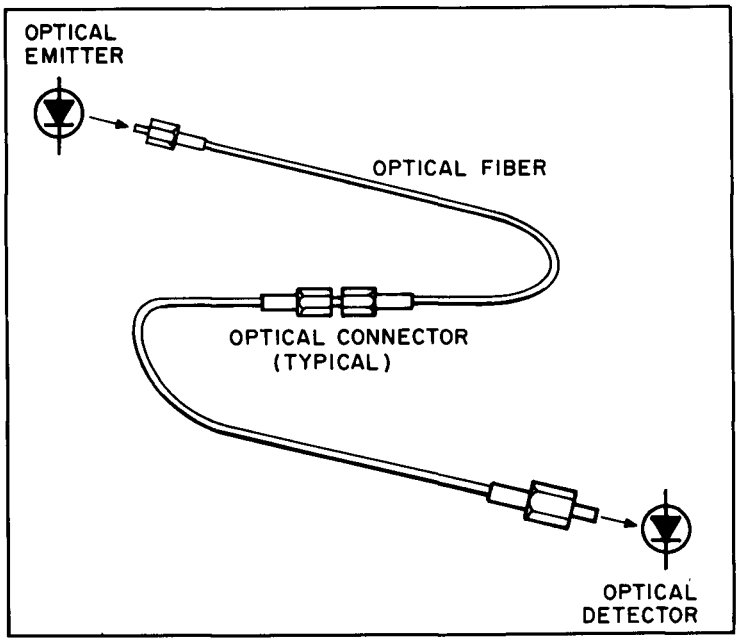

Figure 1. Basic fiber-optic system block diagram.

be considered a type of connector in **Figure 1**. In a very general sense, then, **Figure 1** represents the very minimum configuration of a fiber-optic system. Actual systems will include many other elements for input conditioning, power conditioning, modulation, RF detection, amplification, and other tasks associated with data communication. These are application specific and aren't of general concern in this review.

Fiber-optic light transmission

The key element of a fiber-optic system is the actual optical fiber. The fibers used in fiber-optic applications are a very pure silica material and are quite different from the optical fiber bundles that you may have seen used in flexible flash lights and optical-fiber lamps. In addition to the high degree of purity, the geometry of the fiber is very accurately controlled. It is this high-purity silica and tight geometric control that give modern communication fibers their high-performance.

The basic optical fiber is composed of two parts—the core and the cladding. The core is the part of the fiber that actually carries the light. The cladding keeps the light inside the core. Transmission through the fiber is by means of *total internal reflection*. This is the underlying principle of all optical fibers.

All optical materials have a property called the index of refraction. This property is related to the dielectric constant of the material. Just as the dielectric constant affects the propagation speed of electromagnetic fields in a material, the refractive index affects the propagation speed of optical signals. When light travels from a medium of one index to a medium of a different index, it is refracted, or bent. This phenomenon is described by Snell's Law, and is one of the basic principles of refractive optics—lenses. Snell's Law is found in **Equation 1**.

$$n_a \sin(\alpha_a) = n_b \sin(\alpha_b) \qquad (1)$$

where:

n_a is the index of refraction of medium a.

α_a is the incident angle in medium a. (measured from the interface normal)

You can see the effect of refraction by partially submerging an object, like a pencil, in a glass of water, as shown in **Photo A**. The pencil appears to be bent at the interface between the air (refractive index of 1) and the higher-index water (refractive index of approximately 1.3).

For this discussion, consider a light beam (a collection of photons) traveling from a medium of higher index to one of lower index (see **Figure 2**). If the beam is directed at the interface between the two materials at a 90-degree angle ($\alpha_a = 0$), most of the light goes from one medium to the other (though some is reflected back into the high-index medium), and the exiting beam in the low-index material leaves the interface at a 90-degree angle to the interface, in line with the incident beam. If the angle of the incident beam (the one in the higher index material) is increased to form a more acute angle with the plane of the interface, the exiting beam in the lower-index material leaves the interface at a different angle than the incident beam, and is no longer in line

Photo A. A demonstration of refraction.

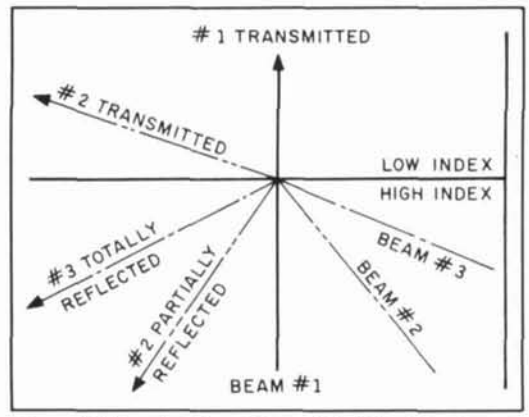

Figure 2. The refraction effects of light traveling from a material of high index to a material of low index.

Photo B. Aquarium demonstration. Effect of refraction at a near 90-degree angle of incidence.

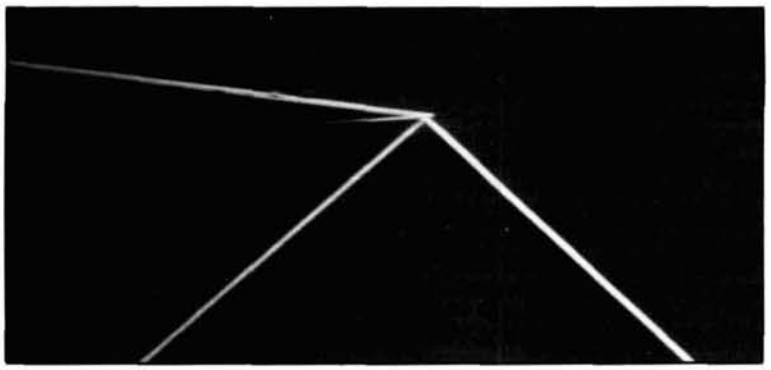

Photo C. Aquarium demonstration. Effect of refraction near the critical angle.

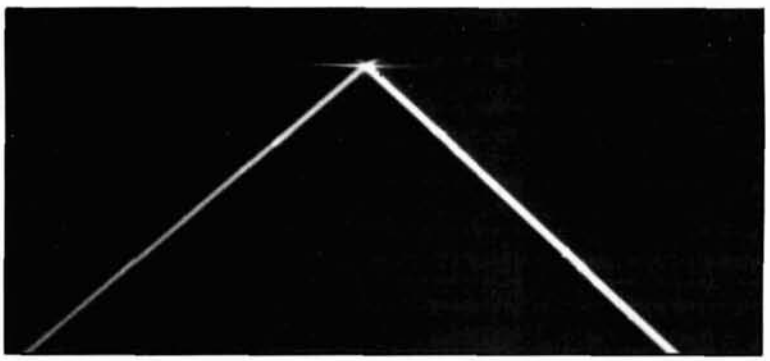

Photo D. Aquarium demonstration. Effect of refraction at the critical angle.

with it. This property is refraction and is described by Snell's Law. Now, when light travels from a medium of higher index to one of lower index, a peculiar thing happens. As the angle of incidence of the incident beam with the interface is increased from the reference normal, the exit beam is refracted at a greater and greater angle until, at a particular incident angle, the beam no longer exits at all, but is totally reflected from the interface back into the higher-index medium. This is total internal reflection, and the incident angle at which it *just* occurs is the critical angle.

I set up a simple demonstration to show this effect of refraction more clearly. In **Photos B,C**, and **D**, a helium-neon laser directed through an aquarium filled with water produces various angles of incidence with the water-air interface at the point where the beam exits the water into the air. I added a very small amount of detergent to the water to provide some scattering, so the beam could be seen and photographed. I also filled the air space above the water with a small amount of smoke for the same reason. Because the water has a higher refractive index than air, the beam at the exit point from the water is traveling from a medium of higher index to one of lower index. As the beam is moved from a 90-degree angle of incidence, the exit beam is bent down more and more until, at a particular angle, it no longer exits at all. In the photos, you can very easily see the incident, transmitted, and reflected beams. As the angle of incidence is increased with respect to normal incidence, the amount of light reflected increases. The angle at which the beam just fails to exit is the critical angle. Using Snell's Law and the indices of water (1.33) and air (1.0), that critical angle is found to be about 49 degrees from the interface normal.

Now let's apply this to optical fibers. Typical optical fibers are fabricated with a low-index cladding around a higher-index core. A typical fiber cross-section is shown in **Figure 3**. As the preceding demonstration indicates, light traveling in the core will be totally reflected at the core-clad interface for angles greater than the critical angle. The light will then be totally trapped in the core as it's totally reflected each time it hits the core-clad interface. This, again, is total internal reflection. Light incident at the interface at an angle less than the critical angle will be only partially reflected, and its propagation through the fiber will be highly attenuated (see **Figure 4**). The fiber, then, effectively has an acceptance angle in which it will accept light with low-loss propagation. This acceptance angle is described by the numerical aperture (NA), which is the sine of one-half of the total acceptance angle.* The angles of incidence accepted by the fiber are related to its propagating

*The acceptance angle of the fiber is related to, but not equal to, the internal critical angle of the fiber – the refractive effects of the air-core interface must be considered at the light entry point into the core).

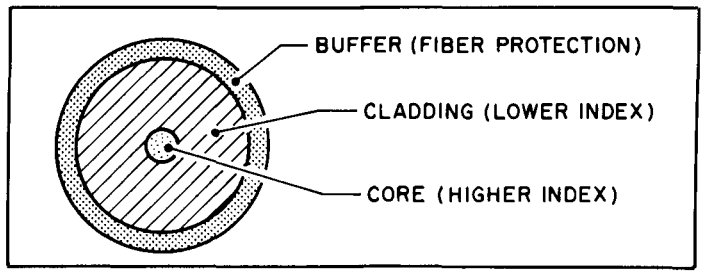

Figure 3. Basic optical-fiber cross section.

modes. These modes in optical fibers are essentially similar to those in electromagnetic wave guides. Light is an electromagnetic wave, and fiber-optic transmission is a true guided-wave phenomenon. Many fibers have acceptance angles which allow propagation of many modes. These are multimode fibers. **Figure 4** shows the effect of several modes propagating in a multimode fiber. Generally in these fibers, all the modes are excited and used. This is in contrast to an electrical waveguide, where the goal is usually to launch and maintain a single specific mode.

Electrical guides tend to have physical dimensions closely related to the wavelength to be propagated. Multimode fibers, however, are usually many wavelengths in diameter. For example, one of the common multimode fiber core diameters is on the order of 50 microns and one of the common optical wavelengths is nominally 830 nanometers in air—about 550 nanometers in the fiber core. The fiber core is almost 100 wavelengths in diameter. Among other things, this multimode propagation limits the maximum data frequency that a given length of fiber can carry. To see this, look again at **Figure 4.** A photon that travels down the center of the fiber without any reflections, travels the shortest path through the fiber and arrives at output faster than all the photons launched. A photon launched at the maximum acceptance angle experiences the maximum number of reflections and the longest path length, and requires the most time to travel through the fiber. If a pulse of light with a very fast rise time is launched, and all modes are excited, the rise time of the pulse at the output will be lengthened by the difference in transit times of the photons in the different modes. A similar effect occurs in television reception. Often, the transmitted signal is reflected off of a mountain or tall building. Two (or more) similar signals then arrive at the receiving antenna, but at slightly different times. The first to arrive is the direct transmission. The reflection, since it must travel from the transmitting antenna to the point of reflection and then to the receiving antenna, arrives later than the direct path. This causes multiple images, or ghosts, to appear on the television screen. For television, you need only one of the signals (usually the direct path) to obtain all the information needed to reconstruct the picture and, therefore, use various techniques to reject the unwanted signals. With multimode optical fibers, however, you need all the information from the various different optical paths. The upper limit of frequency performance is then established by the differences in the delay among the different path lengths. The longer the fiber, the greater the time difference between the arrival of the various photons at the fiber output, and the more the rise time is degraded. This phenomenon is called Modal Dispersion and results in a constant bandwidth-length product (MHz-km) for a specific fiber. The longer the fiber, the lower the available bandwidth. The unit of "MHz/km" often seen used to specify optical fiber bandwidth is incorrect. That designation would imply that the longer the fiber, the higher the bandwidth. The proper product unit of "MHz-km" is of a similar form as the gain-bandwidth product specification of an operational amplifier and the dielectric resistance specification for capacitors given in megohm-microfarads. A typical bandwidth-length product for the type of fiber discussed so far, the step-index fiber, is on the order of 5 MHz-km to perhaps 20 MHz-km. In order to increase the speed of a given fiber, several things may be done. For instance, the fiber may be designed with a narrower acceptance angle (more about this later). However, with optical fiber, the velocity properties of the core material may be optimized. In the step-index fiber, the various launched rays travel different distances through the fiber, and since the refractive index through which those rays travel is uniform, the propagation times of the various rays through the fiber

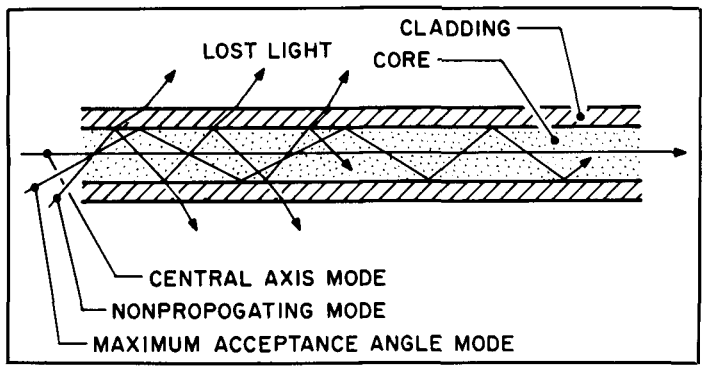

Figure 4. Step-index, multimode propagation.

are different. To speed up the fiber, a core material is needed which causes photons that travel down the fiber center to move at a slower speed than those that travel at the maximum acceptance angle. This can be done by making the index of the core higher in the center than at the outer edges. This type of fiber is a graded-index fiber. This modifying of the fiber index profile is a common practice in fiber design for optimizing fibers for specific applications. Several common index profiles are shown in **Figure 5A** through **D**. The index profile of a step-index fiber is shown in **5A** and that of graded fiber in **5B**. A ray launched down the center of the graded-index fiber will travel at a comparatively slow velocity. A ray launched at the maximum acceptance angle will travel at that same velocity near the core center, but will travel faster near the outer edges of the core because of the lower index in that region. Also, since the index isn't uniform, the ray will be bent as it travels from one side of the core to the other. Rays launched at the maximum acceptance angle still travel a longer physical distance than a central ray. However, since their velocities are variable, with the slowest velocity being equal to that of the central ray, the actual propagation time through the fiber of the high launch-angle rays may be made nearly equal to that of the central ray. **Figure 6** shows a sketch of how photons are diffracted in the core of a graded-index fiber. By carefully controlling the grading profile, accurate matching of mode velocities can be accomplished. The bandwidth-length product of graded-index fibers can be as high as 1 GHz-km, with typical values on the order of 500 MHz-km.

The partially graded-index fiber is a variation of the step and graded-index fibers. A sketch of its profile is shown in **Figure 5C**. This material is a compromise between the more expensive graded-index materials and the larger fibers. The core index of the partially graded fiber is only slightly graded to give some improvement in modal dispersion and provide a wider bandwidth-length product than a simple step-index fiber of the same core diameter. Partial grading is a less costly process than total grading, yet it does supply a reasonable improvement in performance. One of the popular fibers is a 100-micron core material with a typical bandwidth-length product of about 20 MHz-km and a loss of about 7 dB/km.

As mentioned, another method of increasing the fiber bandwidth is to reduce the acceptance angle of the fiber. This decreases the difference in propagation delay of the propagating modes. The limiting case is a fiber which will accept only light that is very nearly exactly on axis. This type of fiber is called a single-mode fiber because it will propagate only a single optical mode at a given optical wavelength. The index profile of a single-mode fiber is shown in **Figure 5D**. The core diameter of a typical single-mode fiber for use at 1.3 microns is about 8 microns. To give you a point of comparison, a human hair is about 50 microns in diameter. Since only a single photon path is available for transmission, it would appear that this fiber should be of infinite bandwidth. However, another form of dispersion, material dispersion (also called chromatic dispersion), limits the bandwidth to finite values. Material dispersion causes different optical wavelengths to travel at different velocities. Typical optical sources don't generate spectrally pure single-frequency light. Instead, their output has an optical bandwidth. That means the output is of various "colors" about the color of the center wavelength. This corresponds to the spectral purity specification of an electronic oscillator. An oscillator output isn't a single frequency, but a collection of frequencies near the center frequency. The narrower this collection of frequencies, the better the spectral purity. Now, since the optical output of a typical fiber-optic emitter isn't a single frequency, and since the fiber material dispersion causes different "color" components to travel at different velocities, the different wavelengths of a fast rise-time optical pulse

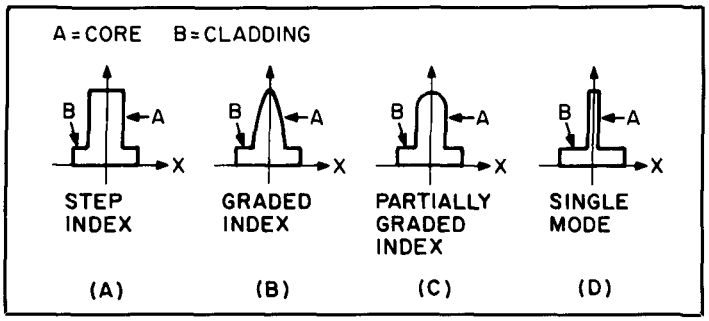

Figure 5. Common optical-fiber index profiles.

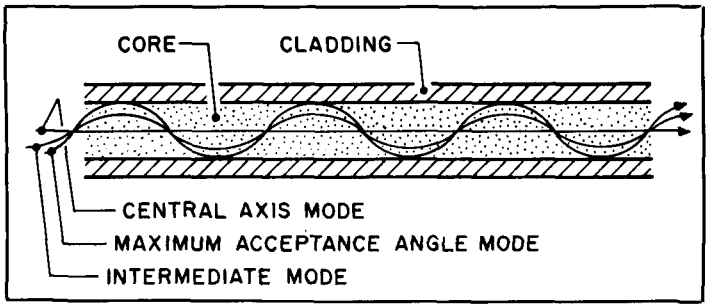

Figure 6. Graded-index, multimode propagation.

input to a single-mode optical fiber will arrive at the fiber output at different times—much like the various modes in the multimode fiber. The limiting bandwidths due to material dispersion are an order of magnitude or two higher than those caused by modal dispersion in multimode fibers. In general, material dispersion isn't too much of a problem in multimode materials, but it is a serious limitation in a single-mode fiber. However, it's possible to optimize the core material and modify the material dispersion. The material dispersion is wavelength dependent and, to some extent, can be controlled. At wavelengths of about 1.3 microns, the material dispersion may be made essentially zero (for particular sources) making the fiber bandwidth theoretically infinite. Various practical considerations limit the bandwidth, but values of several GHz-km aren't uncommon. A theoretical limit in excess of 1 terahertz-km has been suggested[2].

The final thing to consider about the actual fiber is its attenuation. You've seen that the bandwidth is both geometry and material dependent. Attenuation is basically a function of the fiber purity. (Mechanical considerations also affect attenuation, but generally an attempt is made to minimize these in cable design and installation.) One of the most critical impurities is the OH radical. This is sometimes called the water content. Other impurities also degrade the performance, and various impurities are added (doping) to enhance it. Very well-controlled processing techniques have lead to fibers with attenuations of less than 0.5 dB/km (yes, "dB/km" is the correct unit here) at a wavelength of about 1.55 microns. The trick now in the fiber-optic industry is to optimize the materials to make the zero material-dispersion wavelength and the minimum-attenuation wavelength the same. Ways to do so are still being researched.

This might be a good point to compare the performance of a typical communication fiber with high-quality coaxial and waveguide systems. It's difficult to do a direct comparison of optical fiber and coax or waveguide because the electrical components are specified somewhat differently. However, you can make some reasonable approximations from the specifications which will provide a good comparison. One kilometer is a very convenient reference length. Also, since cable loss per unit length is frequency dependent, I'll use a frequency of 100 MHz as the reference frequency at which the performance is compared. A good optical fiber (but not the best) will exhibit a loss of about 1 dB/km and a bandwidth-length product of about 500 MHz-km. One common cable with which almost everyone is familiar is RG-58C/U. The curves for this cable show its loss at 100 MHz is about 5 dB /100 feet. At a length of about 60 feet, a 100-MHz signal will be attenuated 3 dB. This may be considered the 3-dB *cutoff length* at 100 MHz. RG-58C/U then exhibits a loss at 100 MHz of 164 dB/km and a bandwidth-length product of 1.83 MHz-km. This is considerably poorer than the typical fiber selected for comparison. Most of us have used RG-58C/U, and although it doesn't have the best of properties, it's certainly acceptable for many applications. Optical fiber is so much better, the difference is actually difficult to comprehend. RG-214 is another familiar cable. It has a loss at 100 MHz of 65 dB/km and a bandwidth-length product of 4.6 MHz-km—still rather poor compared to fiber. Finally, a 5-inch air-dielectric, helical construction material, like an Andrew HJ9-50, is a very high-performance coaxial cable. This material exhibits a loss at 100 MHz of 26 dB/km and a bandwidth-length product of 11.5 MHz-km. Even this high-quality cable exhibits much poorer performance than an average optical fiber.

An RG-112/U waveguide exhibits a loss of approximately 14 dB/km and a bandwidth-length product of 652 MHz-km at 3 GHz. (I chose the 3-GHz frequency here because 100-MHz guide is somewhat hard to find, and 3 GHz is near the minimum loss frequency specified for RG-112/U.) WC281 was one of the best guides I could find. It has a loss of 9.3 dB/km and a 3.6 GHz-km bandwidth-length product at a frequency of 11 GHz. These examples show that even very good coaxial cable can't even come close to the performance of an average optical communication fiber. Waveguide can provide comparable bandwidth performance, but can't provide the same low loss as the average fiber chosen for comparison. If compared to the best available fibers (single-mode, perhaps 0.1 dB/km and >5 GHz-km), even waveguide falls short. The advantages of optical fiber as a transmission medium are obvious.

A final comparison that should be made for completeness is that of optical fiber to over-the-air transmission. In over-the-air transmission, the signal strength at a receiving antenna in the far field is proportional to the reciprocal of the range squared (atmospheric effects and other variable loss effects are not considered here). This is not really a loss, as such (the receiver simply collects less and less power with increasing range), but to a receiver, it effectively

appears to be a loss. Therefore, if you were to successively double the range, the signal strength would be reduced by 6 dB each time the range was doubled. So, theoretically, the loss is 6 dB per each range doubling for any range. The transmission in an optical fiber is a constant fraction per unit length. Its loss per unit length (measured in dB/km) is then constant for any length. Let's assume you have a 6 km length of fiber with a loss of 1 dB/km. The total loss would be 6 dB. If you double its length (range) once, the loss will increase by 6 dB to a total of 12 dB. This is the same increase in loss that would be seen when doubling the range of an over-the-air transmission. If you double the length of the fiber again, the loss will increase by 12 dB, to a total of 24 dB (12 km to 24 km length). That increase in loss is 6 dB higher than would occur for a second doubling in an over-the-air system. Therefore, for a given set of operating conditions, there will always be a range for which the over-the-air transmission yields lower theoretical loss than a specific optical fiber. For this reason, as well as obvious practical considerations (how do you attach an optical fiber from earth to an interplanetary spacecraft), fiber optics won't displace all over-the-air communication. Fiber optic technology can be expected to find a niche where its specific properties provide significant operational or cost improvement.

Optical fiber construction

I've discussed three basic types of optical fiber: step-index, graded-index, and single-mode. Now let's take a quick look at their actual construction. In the discussion which follows, refer to **Figures 5A** through **D** for construction drawings of the specific fibers discussed.

The earliest and simplest fiber used was the step-index fiber. In the modern telecommunication fibers, the core is almost always a high-purity silica (some plastic core materials are seen in very specialized applications). Cladding is either plastic or silica. The plastic-clad fibers are called plastic-clad silica, or PCS. A variation of the plastic cladding is a hard cladding. This is still a plastic cladding, but it is very thin compared with the typical PCS cladding and formulated differently. These fibers are called hard-clad silica, or HCS. The PCS and HCS materials are available in a variety of core diameters. The most popular core diameters are 100 and 200 micron, but diameters as large as one millimeter and as small as 50 microns are available. Remember, a typical human hair is about 50 microns in diameter. The cladding of the PCS material is generally several hundred microns thick, while that of the HCS fibers is about 15 microns in thick.

The silica-clad materials are more popular than the plastic-clad fibers. These are also called glass-on-glass fibers because both the core and cladding are silica. The compositions of the core and cladding, however, are different because the core must be of higher index than the cladding. Popular core diameters in these fibers with step-index construction are 100 and 200 microns. A typical diameter of a 200-micron glass-on-glass fiber is about 250 microns.

The 200-micron core materials, both plastic clad and glass-on-glass, are quite popular for relatively short data communication paths, like those between computers within the same building. The typical bandwidth-length product of these fibers is on the order of 5 to 20 MHz-km and loss is on the order of 5 to 10 dB/km.

The graded-index fiber is currently the most widely used material, although single mode is gaining in popularity. Its construction is almost always a glass-on-glass configuration. The cladding consists of a low-index silica and the core a higher-index silica material with a radially graded index profile. The core index is highest at the core center, decreasing to a lower value (but still higher than the cladding) at the cladding interface. Fibers with core diameters near 50 microns and overall diameters of 125 microns are perhaps the most popular of all optical fibers. Fibers with bandwidth-length products higher than 500 MHz-km and loss below 1 dB/km are routinely available in this construction. Some partially graded index materials are becoming popular, but are still in a type of probationary state. One of the available materials is a 100-micron core with a 140-micron clad diameter. These materials exhibit bandwidth-length products of 20 MHz-km and greater, and loss on the order of 7 dB/km, or less.

At this point it's useful to touch on another very important point regarding the basic optical fiber—cost. In a very basic sense, the optical fiber is simply glass manufactured from some of the most abundant and least costly natural resources. High-quality optical fiber is considerably more complicated but, at this time, most of the cost of the basic fiber lies in the processing and not in the materials. The cost of fiber is, for the most part, a function of the length purchased (fiber vendors talk in fiber orders of tens or hundreds of thousands of kilometer lengths and longer), but the cost of even a modest length of one

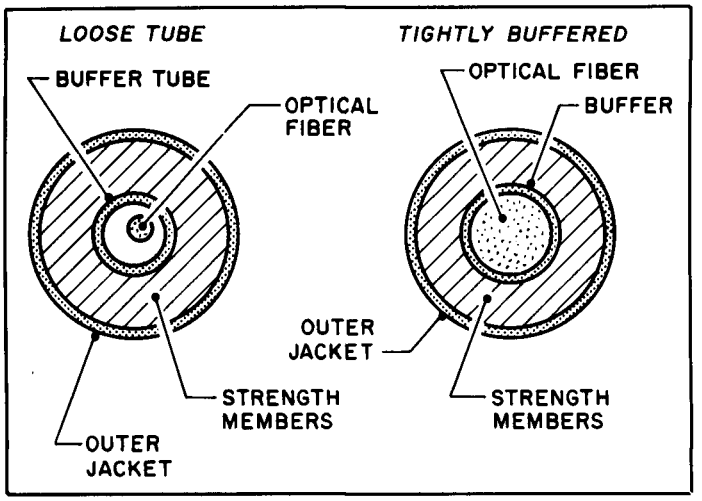

Figure 7. Basic fiber-optic cable geometries.

of the high-performance fibers is just $1 per meter or less. The cabled cost is somewhat higher, but is still typically below $2 per meter for single-fiber cables. A comparable electrical cable or waveguide could cost as much as $200 per meter, or about $60 per foot! The optical fiber medium, then, has a very significant cost advantage. That, in itself, is sufficient incentive to promote the use of fiber optics.

Fiber-optic cable construction

In most applications, the optical fiber is too delicate to be used as a simple bare fiber. The optical fiber is usually protected by some type of cable structure. There are a very wide variety of optical-fiber cables ranging from single-fiber cables, to cables with a large number of individual optical fibers. However, the basic cable geometries may be grouped into two general classes—loose tube and tightly buffered. The basic construction of these two cable geometries is shown in **Figure 7**.

In the loose-tube configuration, the optical fiber is placed in a flexible plastic tube with an inside diameter that is much larger than the fiber. Various strength members (to provide tensile strength) and buffers are placed around the tube, and a final outer jacket is included to provide the desired cable properties for the intended application of the specific cable. Multifiber cables are manufactured by including multiple loose tubes, or in some cases loose channels, in some type of a central cable core assembly (this cable core is not related to the optical-fiber core) with appropriate strength members, buffers, and jacketing. The loose-tube construction has the advantage in installations where the cable must be pulled through conduits and other areas during installation, because the loose mounting of the fiber results in almost no stress on the fiber during the pulling process. All of the pulling load is carried by the cable strength members. This cable configuration, however, can prove to be a poor choice in field applications where the cable is handled continuously and exposed to various abuses. Loose-tube cable commonly fails when it is bent sharply (well beyond its recommended bend radius). This often occurs when the cable is being moved and is pulled tightly around the edge of some object. In such a case, the internal tube carrying the fiber will kink, breaking the fiber. It's important to note that the fiber damage isn't due to the actual bending of the fiber, but rather failure of the loose tube. Of course, this is a gross abuse of the cable; however, it is a realistic concern in field environments. The cable could be made more rugged by increasing its mechanical resistance to bending. That, however, would be undesirable because of increased cost and greater handling difficulties.

The tightly buffered cable geometry provides a generally smaller and more flexible cable than the loose-tube structure. In this construction, a buffer material is applied directly to the optical fiber. Various strength members are incorporated to provide tensile strength, and an outer jacket is included to provide the desired external properties. In general, this cable geometry doesn't provide the same tensile protection for the fiber as does the loose-tube construction, but it does provide much better tolerance to abusive bending.

The tightly buffered cable's smaller diameter and better flexibility make it a preferred choice for field applications. However, in applications where high-load pulling operations are required for the cable installation, the loose-tube structure is the preferred cable type.

Fiber-optic connectors

A very important element in an optical system is the optical connector used to interconnect optical fibers. The optical connector serves the same purpose in fiber-optic systems as electrical connectors do in electrical systems. They allow convenient connection and disconnection of system elements. There are almost as many types of optical connectors as there are fibers to be connected. However, the list may be narrowed down to a few general types.

The most common type of connector is the straight "pin-and-sleeve" design. In this

type of connector, the fibers to be mated are each bonded into a precision pin using epoxy or another suitable adhesive. The end of the fiber is then polished to provide the needed optical finish and physical length. Accurate mating is accomplished by inserting the pins into the opposite ends of a precision sleeve. The accuracy of the pin-and-sleeve connection provides the necessary optical alignment. A typical pin-and-sleeve connector manufactured by Amphenol is shown in **Photo E**. **Photo F** shows a variation of this design in a connector by AMP Special Industries. The AMP connector is an all-plastic part, with the exception of a metal crimp ring (some versions have a metal nut and crimp sleeve). Alignment accuracy is provided by a combination of the pin-and-sleeve design, a precision taper, and plastic deformation. These are just two examples of very common connectors of this style. There are a variety of others which could be classed as pin and sleeve. The optical loss of a connector of this design can be below 1 dB, but in practice it ranges from about 1.5 to 3 dB. Loss of that magnitude is generally unacceptable in telecommunication systems, but is generally tolerable in short-haul data acquisition and communication applications. The major advantages of these connectors is their low cost, ease of termination (attachment to the fiber), and ruggedness.

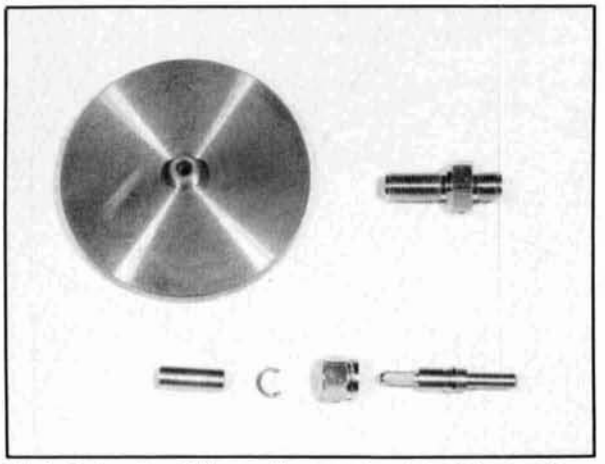

Photo E. Amphenol fiber-optic connector. A typical example of a pin-and-sleeve connector design.

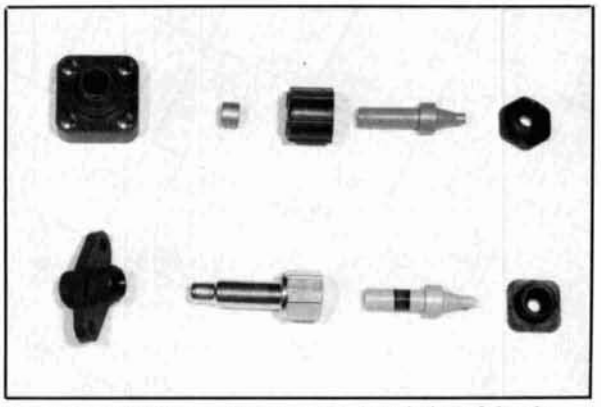

Photo F. AMP fiber-optic connector. A variation of the pin-and-sleeve design.

Another variation which could be considered a type of pin-and-sleeve design is the connector family which incorporates a conical tapered pin that mates into a conical sleeve. An example of this connector type, manufactured by AT&T, is shown in **Photo G**. This configuration has a great advantage over the straight pin. In a straight pin connector, a certain amount of clearance must be allowed between the pin and the sleeve. A value of 10 to 20 microns is about the minimum that will allow a field-worthy connector. This "looseness" then determines the limits of alignment that can be expected from this type of connector—10 to 20 microns. This is quite adequate for the larger core fibers of 100 and 200 microns, and actually provides acceptable short-haul performance for 50-micron fibers. However, in the case of single-mode fibers with core diameters of about 8 microns and smaller, the straight-pin design can't provide the necessary mechanical alignment. If the clearance were reduced to perhaps even one micron, the alignment accuracy would still be marginal, and the connector would become very costly to manufacture due to the extreme precision needed (1 micron is about 0.00004 inch, or about 40 millionths of an inch). Also, the extremely close fit would lead to binding of the pin and sleeve if there was even the slightest contamination or a difference in temperature. This makes the design a very poor choice for field applications.

To a large extent, the alignment problem is solved by the tapered pin-and-sleeve configuration. With modern manufacturing techniques, these tapers can be constructed to the high level of accuracy needed, at reasonable cost. Such a connector design can provide the alignment accuracy needed for even single-mode fibers. Losses on the order of 0.5 dB can be achieved with 1.3-micron wavelength single-mode fiber (a core diameter of about 8 microns). Also, if the connector is mated while contaminated with dirt, the taper will not mate properly, but it will not generally bind. Connector performance may be restored, provided the optical surfaces aren't damaged by the contaminant, simply by taking the connector apart, cleaning, and reconnecting it.

In the basic pin-and-sleeve configurations, the polished fiber ends are simply butted together to form a connection. Since

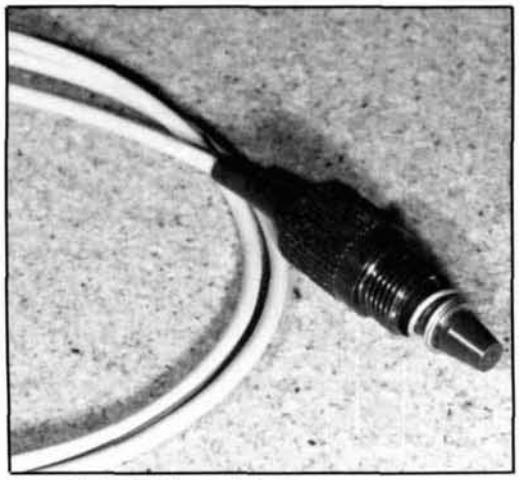

Photo G. AT&T bi-connical connector.

the fiber is quite small, any contamination on the fiber face will cause a significant loss in performance. This problem of contamination can be eliminated by proper cleaning procedures, but that isn't always practical. The effect of contamination can be minimized by expanding the beam at the mating plane, so any contaminant blocks a much smaller amount of the total optical power. A sketch of a beam expanding connector is shown in **Figure 8**. Mechanical alignment is still generally provided by a pin-and-sleeve configuration. The loss performance of this type connector is similar to that of other pin-and-sleeve components (1 to 3 dB), but its tolerance of contaminants is quite good, making it a good candidate for use in harsh field and industrial environments.

The loss with most connectors is too high for long-haul telecommunication applications. Also, those applications generally have no need for connecting and disconnecting elements on a regular basis. For these reasons, the fibers in telecommunication systems are routinely welded together. This can provide connection losses well below 0.5 dB. However, fiber welding tends to be more of an art than a science, and the welding equipment can be quite expensive. Fiber welding is most useful in applications where disconnection of the fiber isn't required once installed and where highly trained personnel are available to provide installation and maintenance.

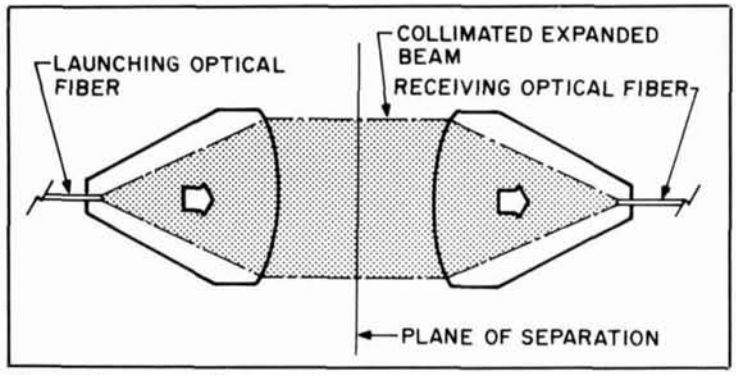

Figure 8. Beam-expanding connector.

These are examples of just a few of the numerous types of connectors used in fiber-optic systems. As the applications and uses of fiber optics increase, the available connector variations will also increase. This is particularly true in the rapidly expanding area of single-mode fiber systems, where the alignment accuracy is most critical. In many applications, it's very likely that the loss due to the optical connectors will be the major contributing factor to the total optical loss in the fiber-optic system. Selection of the optimum connector for each specific application is a very important part of the design of a fiber-optic system. The requirements of loss must be weighed against such considerations as convenience, ruggedness, and cost, if a well-engineered system with the best possible performance is to result.

Optical emitters

There are two emitter types that are the most common signal sources in the majority of fiber-optic systems—light emitting diodes (LED) and laser diodes (LD). Each of these sources has definite advantages and disadvantages. For a specific application, a tradeoff must generally be made between desired performance and device properties to arrive at the optimum part for the application.

LED sources have the advantage over LDs. They are comparatively inexpensive, rugged, and easy to use. The LED sources used in fiber optics are essentially the same technologically as the visible LEDs used as optical indicators. One significant difference is that most fiber-optic LEDs operate at near-infrared wavelengths, like 830 nanometers, rather than the visible wavelengths of the indicator devices. The longer wavelength is chosen because the fiber typically shows lower loss, and the LEDs show better efficiency in the infrared. Another difference is the actual size of the emitting area of the LED. Indicator LEDs must have a source size large enough to see easily in the intended applications. Optical fibers have core diameters on the order of several hundred microns or less, and cannot take advantage of large-area sources. Therefore, LEDs for fiber-optic applications are generally much smaller than visible LEDs. The small area leads to another advantage—

speed. One of the speed limitations of an LED is the time constant of the equivalent series resistance and the device capacitance. As the junction area is made smaller, the device capacitance is reduced, in turn, reducing this time constant and allowing higher operating speeds.

The LED is a very rugged device. It will tolerate a reasonable amount of physical and electrical abuse, with minimal degradation in performance. It can also operate over a comparatively wide temperature range without the need for complicated thermal control or compensation. The LED also exhibits a modest frequency performance. Units with optical bandwidths of 100 MHz are common. The optical power launched into a fiber using LED sources ranges from a few tens of microwatts to several hundred microwatts, depending on the LED and the fiber. Although this isn't a large amount of power, it's certainly acceptable for many applications. The LED is most useful in "short-haul" applications of perhaps one or two kilometers or less, where the bandwidths are below 100 MHz. A typical application would be a fiber-optic communication link between several computers in a building. The LED source is also quite useful in harsh industrial environments where it must often operate with a high degree of thermal or mechanical abuse. Finally, the LED source is relatively inexpensive when compared with a laser source. Typical fiber-optic LEDs range in price from a few dollars to several hundred. (Custom devices can be much more expensive.)

The laser diode offers several significant advantages over the LED, but not without sacrifice. The two most important are speed and launched power. Laser diodes with flat frequency response through X-band (about 10 GHz) are available[3] This is significantly higher than that available with any other simple optical source presently in distribution. Laser diodes can also launch several milliwatts of optical power into even the small-core, single-mode optical fibers. The higher speed has the obvious advantage of higher data rates. The higher launched power allows longer transmission path lengths in a given system (fewer repeaters) and better signal-to-noise ratio. Another advantage of the laser is that it's much more "coherent" than the LED. That means that its optical output has a very narrow spectral width (or, in other words, it is very nearly a single color). The fiber discussion showed that the spectral content of the source has a direct effect on the usable bandwidth of the fiber (material dispersion). The narrow spectral width of the laser results in the very wide bandwidth of the optical fiber.

Although the laser is an attractive source for fiber-optic transmission in many respects, it does have several serious limitations. Of particular concern is optical safety. The coherence of the laser diode and its output power make it a formidable optical hazard. Its safety is further compromised by typical operating wavelengths in the near-infrared region. In the vicinity of 830 nanometers the laser output is essentially invisible; but it is fully transmitted in the eye, making the hazard more serious than higher-power sources of visible wavelength. Any system using a laser source must be carefully engineered to provide adequate optical safety and assure the protection of casual users who may not be familiar with the seriousness of the hazard.

Another disadvantage of the laser diode is that it is much more delicate than the LED. It can be destroyed by currents of as little as 10 percent above its normal operating current. Also, even very narrow reverse-bias spikes (even as narrow as a few nanoseconds, or less) can degrade, or totally destroy, a laser diode. Since laser diodes are used in very high-speed applications, damaging spikes can easily occur as a result of improper transmission-line design and termination, or even from the excitation of parasitic elements in the circuit. Very careful circuit design and construction is necessary to ensure that the laser isn't destroyed by these phenomena.

The laser diode is also very temperature sensitive. In most applications, some form of temperature compensation is necessary. A limited amount of compensation can be achieved by controlling the quiescent bias current as a function of temperature, but that is limited to a reasonably narrow temperature range. In high-performance applications, the laser diode chip is mounted on a small solid-state refrigerator, called a *Peltier Device* (also called a thermoelectric device, or thermoelectric cooler—TEC) which provides cooling by means of the *Peltier Effect*. A control system then maintains the laser chip at a constant temperature.

Another difficulty encountered with the use of laser sources, generally in analog applications, is modal noise. Because the laser is a coherent source, a spatial interference pattern in the power distribution within the optical fiber results. An exaggerated view of the modal distribution pattern at an optical connector is shown in **Figure 9**. When the fiber is disturbed as the laser is driven through its dynamic range, that modal distribution is altered. This, in turn,

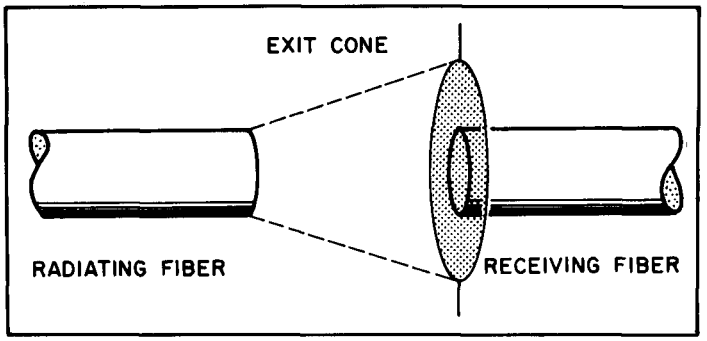

Figure 9. Modal power distribution at a connector interface.

results in variations in the amount of optical power received by the detector. Since the large majority of optical transmission systems use amplitude modulation of the optical signal as the means of information transmission, the variations in collected power caused by modal variations result in "noise" in the received signal. The modal noise problem may be eliminated by using an incoherent source (an LED), but the advantages of the laser are then lost. It may also be eliminated by the use of single-mode fiber, if the extremely small fiber diameter can be handled successfully.

A final disadvantage of the laser diode, perhaps the most significant in many applications, is expense. A simple laser diode for fiber-optic use will range from several hundred to $1,000. A top-of-the-line part could easily be as much as $10,000. The laser diode is most useful in "long-haul" telecommunication applications where its environment can be well defined, and its high cost is offset by the improved performance it offers.

Fiber-optic detectors

There are basically two types of optical detectors used in fiber-optic detection: PIN photodiodes and avalanche photodiodes. The PIN photodiode is a high-speed photovoltaic part (the output is a current proportional to the optical input). The "responsivity," or output current for input light, is roughly 0.5 A/W near the wavelength of peak response. The limiting speed of the device is a function of the junction and mounting capacitance, the device resistance, and the load impedance. It can be as high as several gigahertz for the small-area parts typically used for fiber-optic applications. The PIN-type photodiodes are available for operation at wavelengths from the visible (shorter than 600 nanometers) to beyond the 1.55-micron fiber minimum-loss wavelength. The longer wavelength parts (beyond about 850 nanometers) become somewhat complex and correspondingly expensive. The prices for PIN components range from less than $1 to several hundred dollars depending on operating wavelength, speed, and package style.

The avalanche photodiode is, in effect, the solid-state counterpart of the photomultiplier tube. It consists of a photovoltaic-type photoreceptor structure of roughly similar performance as the PIN photodiode, followed by an amplifying structure. These two elements are integrated into a single solid-state structure. The avalanche photodiode, as does the PIN photodiode, operates in the photovoltaic mode. However, the gain of the avalanche structure results in a responsivity of much greater than 0.5 A/W. The gain is a function of the applied bias and can be as high as several hundred, yielding responsivities of 100 A/W and higher. Gain-bandwidth products as high as 200 GHz have also been reported. In fiber-optic systems, gains of 10 to 100 are more common with typical limiting gain-bandwidth products of several GHz, or below. The cost of the avalanche photodiode is considerably higher than that of a typical PIN device due to its more complex structure. Typical prices range from roughly $100 to perhaps $1000; again, price is a function of wavelength, speed, and packaging.

Data transmission over optical fiber

In many ways, fiber-optic communication is very similar to the more familiar electromagnetic communication. In fact, light is still an electromagnetic phenomenon. It just occurs at a very high frequency. The equivalent frequency of typical light used for fiber-optic transmission (a wavelength of 1.5 microns in air) is about 2×10E14 Hz, or 200,000 GHz. Wavelengths from about 820 nanometers (0.82 microns) to about 1.6 microns are commonly used in fiber-optic systems. There are various others for specialized applications. The visible wavelengths fall in the approximate range of 400 to about 750 nanometers. Did you know that you could *see* 600,000 GHz (500 nanometers, a blue-green color)? Wavelengths slightly longer than the visible (frequencies slightly lower than visible) are called *near infrared.*

The simplest of fiber-optic systems modulate the intensity of a suitable light source for transmission of data. In such cases, the light source is a CW carrier and it is amplitude modulated (AM) with the information

to be communicated. This is exactly the same as conventional AM of an RF carrier. In certain applications, particularly in sensing systems, the phase of a carrier light is modulated as in conventional phase modulation (PM). The common RF-modulation technique of frequency modulation (FM) of the actual optical carrier hasn't found widespread use due, in part, to difficulties in implementation with the fiber-optic materials available. Amplitude modulation is the most widely used modulation technique in fiber-optic systems.

The very high effective carrier frequency of typical fiber-optic systems allow the use of a lot of individual RF carriers or subcarriers on the actual optical signal. For example, a 1-GHz analog fiber-optic data link can carry all the information found over-the-air from VLF (below 10 kHz) through L-band (1 to 2 GHz) on a single wavelength of a single fiber. Each of the individual signals appearing in that range would effectively be a subcarrier. Of equal importance is the capability of the optical fiber to carry this information over long distances at very low loss. Fiber-optic technology, like most others, has coined terms unique to its applications. The use of effective subcarriers is called frequency division multiplexing, or FDM. Experimental systems are available which provide operation into X-band, and it appears that this will be extended much farther in the near future. This will allow a tremendous capability for FDM.

Another form of signal multiplexing used is time division multiplexing, or TDM. This is most often employed for digital signals. An example of TDM would be a typical computer data bus, where the various computer elements use the bus at different times with different data. Each collection of signals that is TDMed requires a particular bandwidth determined by the data. The very wide bandwidth capability of fiber-optic systems allow a large number of TDM signals to be FDMed. For example, many telephone conversations (perhaps several thousand) may be digitized (put into digital form), combined using TDM, and then modulated onto a single RF carrier. A number of such modulated RF carriers (How many discrete carriers are available from VLF to X-band?) may then be combined onto a single fiber using FDM. This allows a very high data density in the usable band space of a given wavelength of operation of a single fiber.

Of course, FDM and TDM can also be used very effectively in over-the-air communication. Fiber optics offers one additional form of signal multiplexing—wavelength division multiplexing, or WDM. A typical communication-type optical fiber can carry several different optical wavelengths (or colors) simultaneously. WDM makes use of several suitable optical wavelengths in the available optical band space of the fiber, and is therefore analogous to the use of various RF carriers in the radio-frequency band space of conventional radio transmission. The characteristics of operation at each wavelength differ but, in general, each different wavelength can carry the full analog bandwidth of the system—roughly VLF to X-band. If a particular fiber can carry ten different wavelengths in a particular application, that single fiber can then carry ten times the information of the same air-wave bandwidth.

Now this can be confusing, so I'll put all the multiplexing together in a single thought. First, you can use several different optical wavelengths on a single fiber by using wavelength division multiplexing. Then, you can modulate each wavelength with individual RF carriers through about X-band using frequency division multiplexing. Finally, you can combine many individual signals by time division multiplexing on each RF carrier. While this should put multiplexing on optical fiber in perspective, the issue can be further complicated by the fact that any form of signal multiplexing available for use in conventional RF-transmission can generally be used in a fiber-optic system. Consequently, quite a bit of information can be packed onto a single optical fiber.

As yet, the present state of development of fiber-optic materials doesn't allow the total exploitation of the potential capabilities of the medium. However, each of the individual capabilities have been demonstrated and many are in regular use. In theory, these can all be combined in a single system, and it's only a matter of time until the various capabilities are integrated.

This very high information-carrying capacity, coupled with very low transmission loss, are the principle properties which have made fiber optics a very attractive data-transmission medium. Its low cost when compared with that of high-quality cable, also gives optical fiber a definite advantage. Finally, although optical fiber is somewhat more difficult to terminate than electrical cable (this is not totally true because some of the more exotic electrical cables are quite difficult to terminate), other installation procedures are much simpler than those for typical high-quality cable or waveguide, reducing both the time and cost of installation.

Fiber-optic sensors

One of the most rapidly advancing applications of fiber optics is the development of sensors of numerous types for sensing various physical phenomena and general process parameters. Two of the more definitive works on the subject of fiber-optic sensors are **References 4** and **5**. The first work[4] includes 133 references, providing anyone interested in this subject a very good starting point for their research.

There are two general classes of fiber-optic sensors: intrinsic and extrinsic. The intrinsic class of sensors uses some basic property of the fiber as the actual sensing phenomenon. An example of this would be the measurement of a magnetic field by the change in the polarization of an optical signal in a fiber segment caused by exposure to the field. Here, a basic property of the fiber, the Verdet Constant, is used to sense the quantity of interest—a magnetic field. The extrinsic class of sensors are those that use the optical fiber only as a signal path. The actual sensing is accomplished by other materials. An example of this would be a temperature sensor which uses an optical fiber coated at the sensing point (the fiber end for example) with a fluor that exhibits a color change with temperature. The color of the fluor is monitored by means of the optical fiber, but the actual thermal properties of the fiber aren't involved in the actual sensing task. Some sensors are somewhat difficult to classify since it could be argued that they could be placed in either, or both classes. An example would be a fiber-optic strain sensor using the change in length of the fiber as the sensing mechanism. It could be argued that the physical properties of the fiber result in the output signal when the fiber is "stretched," implying an intrinsic sensor. It could be argued equally that the same sensor could be fabricated with active materials other than the optical fiber—free space for example—with similar results, implying an extrinsic sensor where the fiber is only a signal carrier. However, since this classification of fiber-optic sensors is generally of tutorial interest only, with no particular value in application, it's of little consequence which class one chooses to include those sensors exhibiting properties of both.

This technology of fiber-optic sensors is much too broad to be treated usefully in this brief review. Those interested in more information are directed to the literature where the latest in developments are reported. However, it would be useful to examine briefly a single fiber-optic sensor. A fiber-optic strain gauge is a suitable example. There are a number of approaches suitable to measure strain fiber optically. One of the most sensitive, and most complicated, is the use of optical fibers in a Mach-Zhender interferometer.[4,5,6] The principle of this sensor is the optical interference of two identical optical signals of different phase. As the active path is subjected to some stress, the resulting strain produces a change in path length in the active path, causing a shift of the phase of its optical signal. This results in a change in the optical interference at the detector, and a corresponding output signal from the detector. The minimum signal that can be detected is limited by factors such as the various noises of the system and the optical power launched into the sensor. It has been suggested that a theoretical limit of the phase sensitivity in this type of sensor is on the order of 1 microradian.[4] If the optical wavelength (in the fiber) of the optical source is 1 micron (one wavelength is 2 π radians), the limit of displacement measurement would be about 1.6E−13 meter, or 0.0016 angstrom.[7] That is, indeed, a very small displacement. However, phase variations in optical systems may be related to time differences, and time is the likely physical parameter which you can measure with the highest accuracy and highest resolution. A force of about 2.5 micronewtons, a stress of 0.032 Newtons per square meter, would be required in a 1-cm diameter steel rod (E = 21E+10 Newtons per square meter) 1 meter in length to produce that strain—a microstrain of 1.5E−7 for the 1-meter length. A more practical resolution is on the order of 0.01 wavelength—a displacement of about 1.0E−8 meters, or 100 angstroms, or a microstrain of 0.01. Although considerably poorer than the theoretical limit, it still represents a relatively small displacement. This is roughly the ultimate sensitivity that might be expected of a laboratory-quality conventional strain system.[6]

The practical limit of the fiber-optic strain system is then near the ultimate limit of more conventional strain systems, and the ultimate limit of the fiber-optic system is perhaps as much as five orders of magnitude better than more conventional approaches. It must be remembered, however, that even though much higher ultimate sensitivity might be available from a fiber-optic system, such sensitivity may be of no practical value in the physical world—at least at this time. The gauge system chosen for a specific task must be selected using sound engineering, considering all the merits of the measurement technologies available and the rigors of the application.

Conclusions

A minimal fiber-optic system consists of an optical fiber, optical connectors, optical emitter, and an optical detector. The basic principle of fiber-optic transmission is total internal reflection, which is described by Snell's Law of refraction. Total internal reflection is used in an optical fiber by constructing a fiber with a high-index central core surrounded by a lower index cladding. Both step-index and graded-index geometries are manufactured. The limiting case of the step-index design is the single-mode fiber, where the core diameter is very near the optical wavelength of the propagating optical power. Step-index fibers are generally the least costly and easiest to apply, but are generally of lower bandwidth. Graded-index materials provide much higher bandwidths, but are generally available only in smaller core diameters. Single-mode fiber provides the maximum possible bandwidth and minimum loss, but at the expense of a very small core diameter which is difficult to use effectively. Typical optical fibers offer a large improvement in bandwidth and loss over conventional cable and waveguide systems. Bandwidths in excess of 1 GHz-km and losses below 0.5 dB/km are available.

Optical fibers are typically cabled to provide mechanical protection for the fiber. Both loose-tube and tightly buffered configurations are used. The loose-tube structure is the better choice in pulling applications, while the tightly buffered configuration is better for abusive field applications.

Optical connectors are required to interconnect optical fibers and other optical elements. In some applications, the optical fibers may be welded together to provide a very low-loss, but permanent, optical connection. Because the optical connectors will likely be the major contributor to optical loss in a fiber-optic system, the selection and installation of the optical connectors represent very important aspects of fiber-optic system design and use.

The two most common optical sources used in fiber-optic systems are the light emitting diode and the laser diode. The LED has the advantages of ruggedness, simple use, and low cost, at the expense of limited speed and power. The laser diode provides much higher speed and power, but at the expense of being more difficult to use, more delicate, and much more expensive. Also, the higher available power and coherence makes the laser source a potential optical hazard. An additional problem encountered with laser sources in analog applications is modal noise.

The two basic optical detectors used in fiber-optic systems are the PIN photodiode and the avalanche photodiode. The PIN detector offers the advantage of high speed and simple application at relatively low cost. The avalanche detector offers high internal gain, at the expense of increased circuit complexity and higher cost.

Data may be communicated over an optical fiber in essentially any manner available in over-the-air transmission. Typical methods include WDM, FDM, and TDM. The very high ultimate-fiber bandwidth, extremely low loss, and relatively low cost when compared with cable and waveguide systems, makes fiber-optic transmission a very attractive medium for communication of large amounts of information.

In addition to data communication, optical-fiber technology is used in fiber-optic sensors. In intrinsic sensors, some basic property of the fiber is used as the sensing mechanism. In extrinsic sensors, the optical fiber is used as a low-loss controlled means of signal transmission. In many applications, fiber-optic sensing can provide several orders of magnitude improvement in the resolution and accuracy over more traditional approaches.

This has been only a brief introduction into the very interesting and rapidly expanding technology of fiber optics. The treatment of the subject has by necessity been quite brief, touching on only a few basic principles and highlights. However, I hope that this article has at least helped stimulate your curiosity, provided you with a little basic background of this rapidly developing field, and encouraged you to watch the media for references of fiber-optic technology. When you see a reference to fiber-optic technology, like a news release stating that a researcher has successfully transmitted some signal over a record length of fiber, this should provide you enough basic background to understand just what that means. ■

REFERENCES

1. J.M. Rowell, "Photonic Materials," *Scientific American*, Vol. 255, No. 4, October 1986, pages 146-157.
2. Fred Guterl and Glenn Zorpette, "Fiber Optics: Poised To Displace Satellites," *IEEE Spectrum*, Vol. 22, No. 8, August 1985, pages 30-37.
3. N. Lau, Bar-Chaim, and I. Ury, "Wideband Laser Diodes Spark New Designs," *Microwaves and RF*, Vol. 23, No. 11, November 1984, pages 109-117.
4. Thomas Giallorenzi, Joseph A. Bucaro, Anthony Dandridge, G.H. Sigel, James H. Cole, Scott Rashleigh, and Richard G. Priest, "Optical Fiber Sensor Technology," *IEEE Journal Of Quantum Electronics*, Vol. QE-18, No. 4, April 1982, pages 626-665.
5. Thomas Giallorenzi, Joseph A. Bucaro, Anthony Dandridge, and James H. Cole, "Optical-Fiber Sensors Challenge The Competition," *IEEE Spectrum*, Vol. 23, No. 9, September 1986, pages 44-49.
6. Mario Martinelli, "The Dynamical Behavior Of A Single-Mode Optical Fiber Strain Gage," *IEEE Journal Of Quantum Electronics*, Vol. QE-18, No. 4, April 1982, pages 666-669.
7. James H. Cole, Private Communication, November, 1986.

SPECIAL REPORT

Peter O. Taylor, Chairman
AAVSO Solar Division
P.O. Box 5685
Athens, Georgia 30604-5685

OUTLINING JUNE'S STRONG SOLAR FLARE ACTIVITY

An overview of a series of remarkable solar events

On June 1st a powerful solar flare erupted from just behind the Sun's east limb, signaling the beginning of a remarkable period of solar activity that lasted for more than two weeks. By the 7th, the large sunspot group which spawned this event, NOAA/USAF Region 6659, had produced three flares which saturated the X-ray sensors aboard the Geostationary Operational Environmental Satellites (GOES). In doing so, it became the first spot cluster of solar cycle 22 to generate three or more flares of this magnitude, and eventually the only group on record to yield five such events.

The particulars

The first of these flares was accompanied by a strong shock in the solar atmosphere and a dramatic spray of material visible out to 0.5 solar radii. The event's X-ray intensity (X12+) was the most potent to be detected since a flare with an estimated strength of X15 occurred during October 1989. The Space Environment Services Center X-ray classification[1] ranks flares according to their peak flux in the 1 to 8 Å range, in units of Watts/square meter. The letters B, C, M, or X stand for powers of 10 beginning at 10^{-7} Wm^{-2}. Each class is subdivided into steps represented by a number appended to the appropriate letter, which acts as a multiplier. Thus, M6.5 symbolizes a flare with peak flux of 6.5×10^{-5} Watts/square meter. The X-class is extended by several measurable steps (X10 to X12), but flares with higher intensities overwhelm the GOES sensors and their maxima must be estimated. Major flares are events of magnitude M5.0 or greater; those that occurred in Region 6659 are listed in **Table 1**.

As you can see by referring to **Table 1** and the plot of GOES data in **Figure 1**, Region 6659 continued to produce major flares during the second and third weeks of June, yielding a fifth and final X12+ flare on the 15th (**Photo A**). Many of these were Tenflares; flares with associated 10-centimeter radio bursts that exceed 100 percent of the pre-event flux level. Region 6659 was extremely dynamic during its entire disk passage, and generated M5 and M4 flares even while passing behind the Sun's western limb on the 17th.

With an area of approximately 2200 millionths solar hemisphere (about thirteen times the surface area of the Earth), Region 6659 was the largest group on the visible hemisphere during June, and one of the more sizable to emerge this cycle. In all, this complex sunspot group produced twenty-nine M, and six X-level flares of sufficient intensity to yield the highest X-ray Region Index recorded since satellite monitoring began in 1964. For comparison, the largest group of this cycle (Region 5395 at ≈3500 millionths solar hemisphere) spawned forty-eight M, and eleven X-level flares during its transit in March 1989, but only one saturated the GOES sensors. One explanation for the numerous super-flares in Region 6659 suggests that energy was stored until a high triggering threshold was finally surpassed. The process would then repeat and another highly energetic flare would occur.

As would be expected, the geomagnetic

Day	Max (UT)	Peak X-ray	Peak Radio Flux 245 MHz	2695 MHz
1	1520	X12+	20000	5400
2	0746	M5.2	--------	37
4	0352	X12+	37000	11000
6	0108	X12+	65000	55000
9	0143	X10.0	3100	8600
10	1358	M6.4	8200	500
11	0209	X12+	6200	10000
	2132	M5.3	1200	260
13	1804	M5.4	---------	--------
14	0142	M7.3	---------	45
15	0821	X12+	6400	14000
17	0355	M5.2	330	1300

Peak Radio Flux is given in units of 10^{-22} Wm^{-2} Hz^{-1}

Table 1. Major solar flares in Region 6659.

field experienced minor to severe storm conditions throughout much of this interval, and aurorae were both frequent and spectacular at mid-latitudes and above. A satellite-level proton event and sudden commencement-type shock were recorded on the 4th, and severe storm levels were encountered by the 5th. During the days which followed, the daily magnetic index (e.g., **Figure 2**) became the second highest to be recorded this cycle (behind March 1989). GOES spacecraft underwent magnetopause crossings on the 4th and 5th as a strong surge in solar wind compressed the sunward portion of the magnetosphere.

Magnetic observatories at mid and high-latitudes continued to record major or severe storm conditions into the third week of June. The proton event which began on the 4th was repeatedly strengthened by the major flares in Region 6659 until it eventually reached a peak flux of 3000 particle flux units (p.f.u.) on the 11th, as a ground level event (GLE) was recorded by the Deep River Neutron Monitor. A Forbush decrease (indicating a sudden decrease in galactic cosmic rays caused by a magnetically enhanced solar wind) with a maximum decrease of ≈ 18 percent occurred on the 13th.

The long-duration proton event and associated polar cap absorption (PCA) finally ended on the 14th. Nonetheless, by the 15th a new proton event at satellite altitude and PCA were in progress. This event was bolstered by the group's final X12+ flare to a maximum of 1400 p.f.u. on the 15th, at approximately the same time that a second GLE was detected. Both GLEs were confirmed by increases in the (HEPAD) proton sensor on the GOES-6 satellite, and reports from South Africa indicate that a disruption of frequencies between 500 kHz and 30 MHz also occurred. Boulder noted an additional storm commencement on the 17th, but by the 19th both PCA and proton events ended and the magnetic field had calmed to quiet or unsettled conditions.

Surprisingly limited effects

The relatively benign effect of this activity on the terrestrial environment came as somewhat of a surprise, especially for events after the first two monster flares which erupted near the Sun's eastern limb. According to NOAA's Joe H. Allen,* HF and VHF

*Solar-Terrestrial Physics Division Chief, NOAA National Geophysical Data Center, Boulder, Colorado.

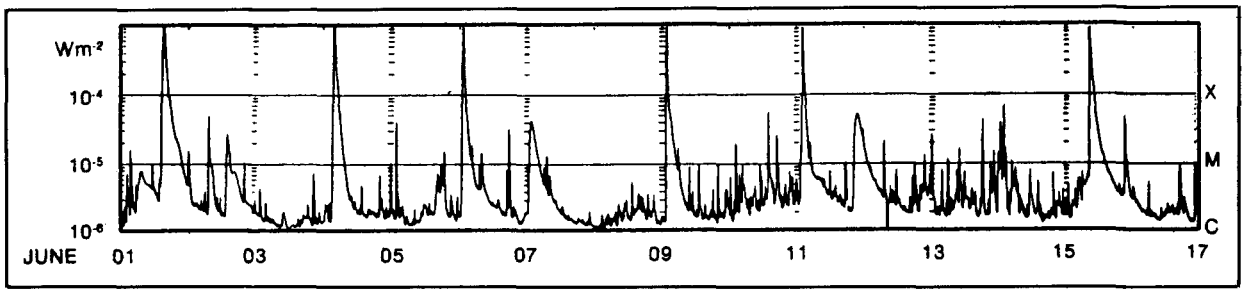

Figure 1. X-ray flux between 1 and 8 A, as measured by detectors aboard the GOES-7 spacecraft. Note that several events exceed the sensors' capacity (X12).

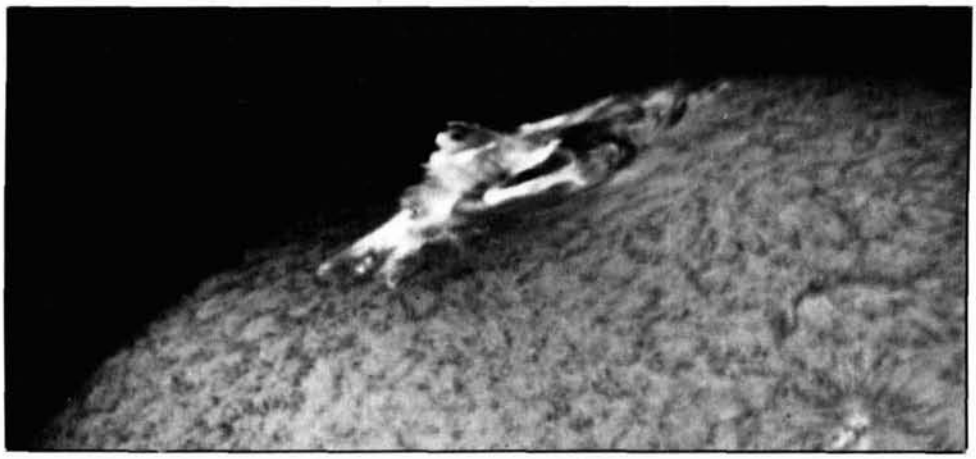

Photo A. The final solar flare in Region 6659 to saturate the GOES sensors occurred on June 15th. Dr. Jean Dragesco (la Riviere, France) secured this fine hydrogen-alpha photograph less than one hour after the event reached maximum.

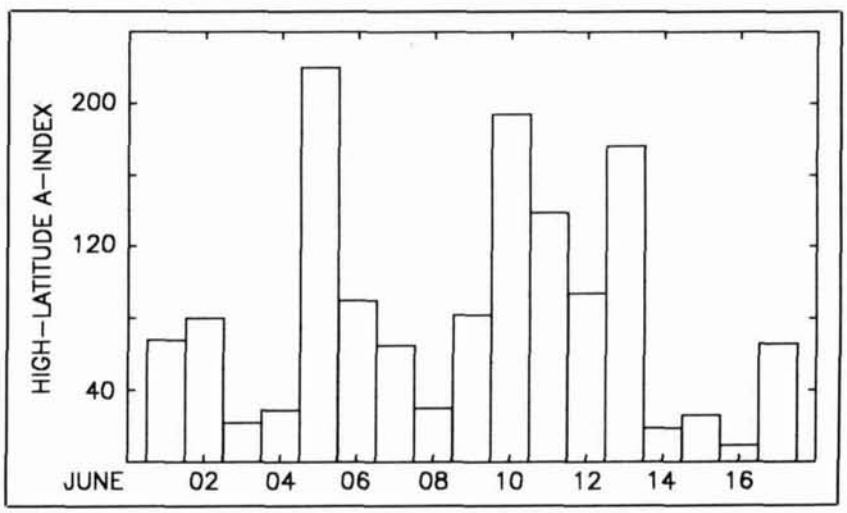

Figure 2. The daily high-latitude geomagnetic A-index recorded at Anchorage, Alaska between the 1st and 17th of June. Values between 50 and 100 indicate major magnetic storms, those equal to or greater than 100 signify severe conditions.

telecommunications were the most seriously affected facilities. Effects at the ground, other than those already mentioned, appear to have been confined to fairly insignificant problems at older power systems in the East and Northeast.

Presumably only comparatively minor anomalies occurred with civilian and DoD spacecraft, although GOES-6 did suffer a single event upset (the latest of over thirty such events), and satellite communications were occasionally disrupted. However, Mr. Allen suggests that these consequences appear to have been much softer than anticipated considering the intensity of the flares which took place, and the fact that several originated far to the west of the first events—in a location where they were more likely to influence the Earth. Moreover, the GOES satellites' power panels did not record any degradation during the particle events, as they have in all others since 1989. A similar scenario unfolded with the INTELSAT satellites; the proton increases were sudden and dramatic, but of lower amplitude than might have been expected. One factor that could partially account for this behavior is the orbital position of the Earth during June, as the planet is most vulnerable to solar emissions during the spring and fall.

Acknowledgment

Portions of the information presented here were taken from the *Preliminary Report and Forecast of Solar Geophysical Data*, Nos. 822-25, and from reports that originated at the NOAA Space Environment Laboratory. ■

REFERENCE

1. *NOAA Technical Memorandum* ERL SEL-48, NOAA Space Environment Laboratory, Boulder, Colorado, June 1977.

Peter O. Taylor and
Arthur J. Stokes, *N8BN*
AAVSO Solar Division
P.O. Box 5685
Athens, Georgia 30604-5685

RECORDING SOLAR FLARES INDIRECTLY

Your data input is welcomed for the continuing success of this project

The combination of solar phenomena and the terrestrial effects that arise when powerful events occur on the sun is a topic that can be both ambiguous and arcane. On the one hand (as Amateur Radio buffs realize all too well), the consequences of very strong solar activity frequently reach into many areas of daily life and occasionally result in millions of dollars in damage. At the same time, however, those of us who are not directly affected may be unaware that lesser influences are felt almost every day.

Background

In elementary school, we learned that incidents on the sun affect the earth's environment in a manner somehow connected with those enigmatic curiosities called sunspots; emerging concentrations of magnetic flux that originate deep within the sun. Of course, since the mid-nineteenth century* it

*English astronomers Richard Carrington and Richard Hodgson independently observed the first solar flare in 1859. The inferred relationship between this event and the geomagnetic storm which followed did much to establish a relationship between the two phenomena.

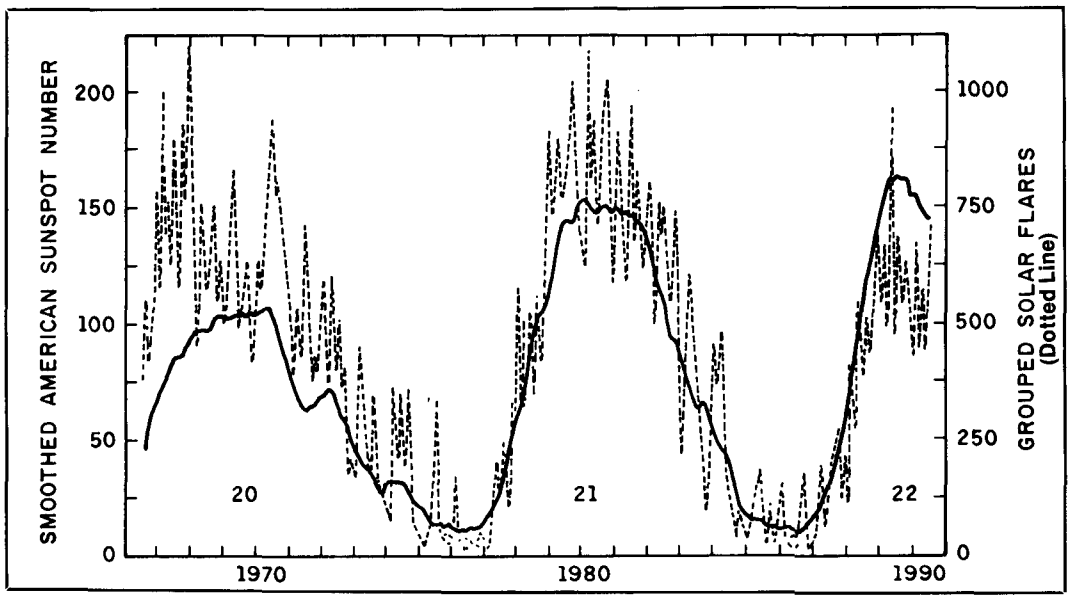

Figure 1. The monthly total of grouped solar flares[5] closely parallels the smoothed monthly sunspot number. (When flares are grouped, events recorded by more than one observatory, either optically or through other means, are counted as one.) Flare totals for the previous six months are particularly likely to increase as reports continue to be received.

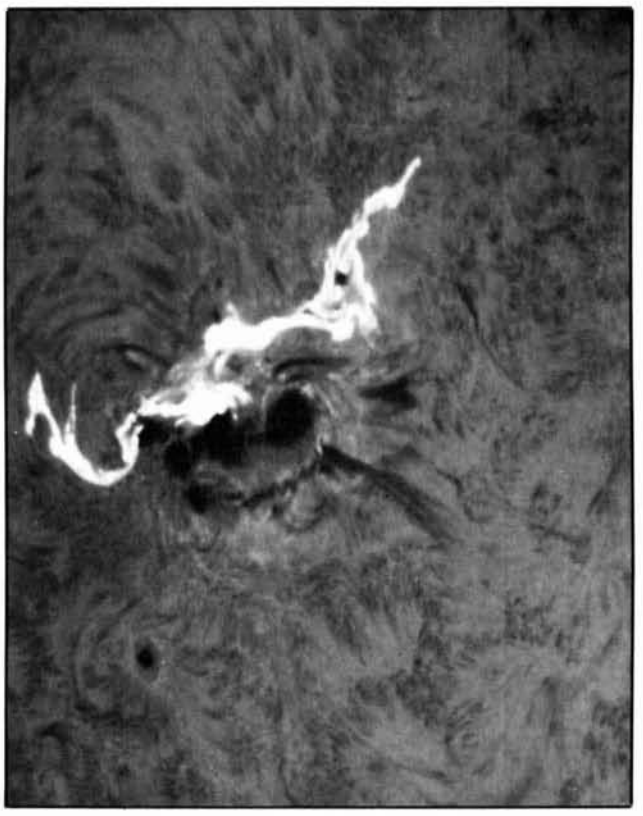

Photo A. An intense solar flare is recorded in the red light of atomic hydrogen during March 1989, one of the most active months of solar cycle 22.

has been acknowledged that the specific source of these effects is often rooted in the enormous energy eruptions that generally take place in groups of spots—solar flares. The strong correlation between these two solar activities is shown in **Figure 1.**

This aspect continues to be a significant part of what is believed today. However, recent research by Hewish, Tappin, Gapper,[1] and others has shown that this is not necessarily the entire story. It's now generally accepted that "coronal holes" (low-density areas of the sun's atmosphere), and the continuous flow of matter and magnetic fields from the sun known as the "solar wind," play prominent roles in influencing the geomagnetic field. At the very least these phenomena help propel bursts of solar radiation into the interplanetary environment, giving rise to both 27-day recurrent and random magnetic disturbances.

Occasionally, within hours of the occurrence of a major flare **(Photo A)**, the effect upon the earth is so severe that it culminates in the temporary loss of an affected communications facility. A typical example is the "polar cap absorption" when HF and VHF radio waves are rapidly absorbed in the polar ionosphere and transpolar-radio paths can be disrupted for days. Spacecraft, power-generating systems, and even long pipelines can also be damaged by intense solar activity. Explanations for several of the mechanisms that cause these conditions can be found in *Observing the Sun,*[2] *Astrophysics of the Sun,*[3] and in similar texts that reflect a consensus of current opinion.

Fortunately, not all flare-related effects result in drastic alterations of the terrestrial environment; some are commonplace throughout much of each solar cycle. One of the more familiar ramifications of this activity is an outgrowth of the interaction between shortwave radiation catapulted into space in flare eruptions and constituents of the ionosphere. When flare emission from this portion of the electromagnetic spectrum—mainly x-rays and ultraviolet radiation—enters the earth's atmosphere, the ability of the ionosphere to propagate radio waves at some frequencies can be enhanced rather than degraded.

Radio signals, like those within the VLF and lower-LF range between 5 and 100 kHz, use the ground wave for transmission. They are commonly propagated in the space between the earth's surface and the D-region, the lowest portion of the ionosphere. This layer is only active above the sunlit hemisphere because it requires constant ir-

radiation to maintain its ionospheric integrity. When the shortwave emission from flares reaches this area of the atmosphere a temporary, but significant, increase in the D-region's ionization level occurs. Signals broadcast at these frequencies are improved accordingly.

The x-ray and ultraviolet radiation that accompanies many solar flares travels to the earth at nearly the speed of light. Therefore its arrival, and the flare associated with it, can be detected at virtually the same moment as the flare's optical appearance. Monitors aboard the Geostationary Operational Environmental Satellites (GOES) normally collect these data, but the same conditions can also be observed by recording a convenient VLF station. When the station's signal is intensified in the manner described, the corresponding atmospheric anomaly is referred to as a sudden ionospheric disturbance (SID).

Furthermore, since VLF radio signals are less attenuated in water than their counterparts, their use constitutes a principal means of communication with submarines. This feature has resulted in a worldwide array of VLF stations that broadcast almost continuously, creating a unique network that can be monitored from anywhere in the world and exploited in the discovery of flare-induced SIDs. When VLF station signals are employed in this way, the detection technique is called a "sudden enhancement of signal."

Purpose of acquired data

Information obtained by this procedure is useful in radio propagation and flare research, and for studies of the solar-terrestrial relationship. Consequently, in 1956 the AAVSO Solar Division began a structured program to record these events as a part of the American contribution to the International Geophysical Year.[4]

Today, the data we obtain from this intriguing work are regularly supplied to the National Oceanic and Atmospheric Administration (NOAA), who fund the program through an annual grant to the association. Our results, along with those from observatories throughout the world, appear in each issue of *Solar-Geophysical Data*,[5] and in other media that delve into the solar-terrestrial relationship.

Required equipment

The simple arrangement of a SID monitoring station is shown in **Figure 2** and **Photo B**. Until recently, the accepted method of recording these interesting events was to funnel data from the receiver to a small strip-chart recording device, such as Rustrak's Model 288.* A majority of our collaborators have continued to follow this approach, but in the future many are likely to opt for our latest technique. Our newest procedure allows us to collect data as before, but now the information is sent directly to a small computer.

When we decided to upgrade our existing system, one objective was to use an older, used computer—the type that can be purchased at Amateur Radio hamfests for a fraction of its original price. With this in mind, we were able to obtain a Tandy Model III computer for less than $100. We have also used an IBM XT for this project, but the low-cost Model III is the workhorse of our present system.

The output of our VLF receiver is a DC analog signal of about 1 volt that must be digitized for input to the computer's bus. We accomplished this with an analog-to-digital converter. Many A-to-D converters are available in the commercial market; however, we found that the eight-channel, 12-bit device made by Alpha Products** (the Alpha FA-154) is ideal for our purposes, and is very reasonably priced. The FA-154 has

* Rustrak Instrument Division, Gulton Industries, Manchester, New Hampshire 03103.
** Alpha Products, 242-M West Avenue, Darien, Connecticut 06820.

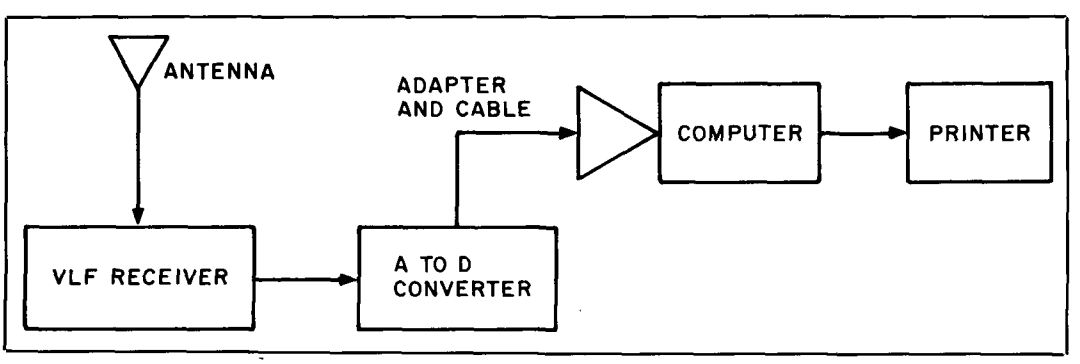

Figure 2. The arrangement of components for a SID monitoring station that uses a small computer to record data.

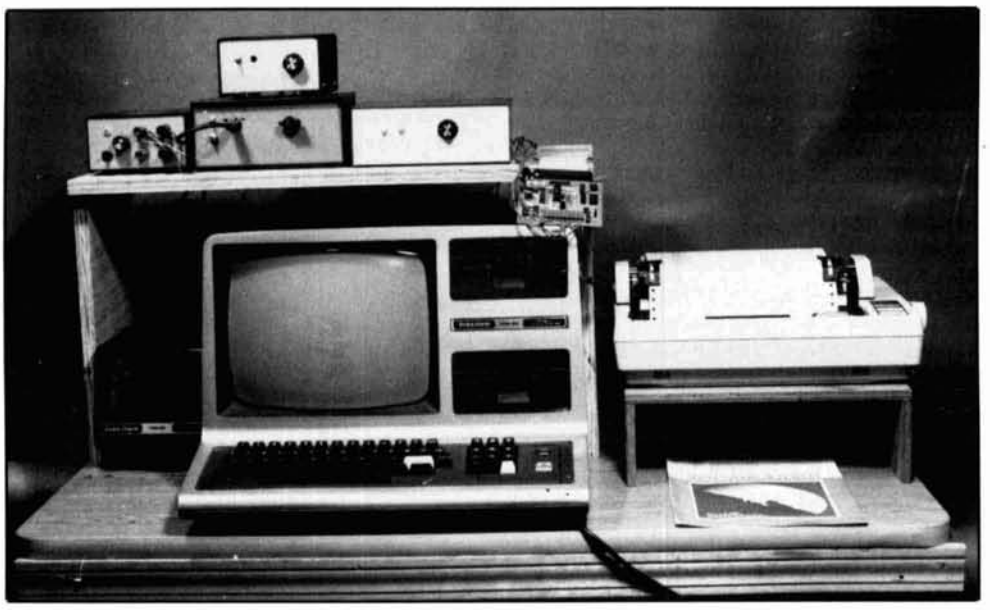

Photo B. The authors' monitoring station.

seven input ports that can be programmed for many functions.

An adapter and cable are required to connect the converter to the computer. These items are also available from Alpha Products in several different styles, which accommodate various computer models. If an IBM-PC or similar computer is used, power for the converter is obtained from the computer bus. (The IBM A-to-D system has a card that plugs into one of the slots in the computer board.) With the Model III however, it's necessary to use a separate 12-volt power supply.

The converter is attached to the receiver by a simple twisted pair of wires that can be up to 20 or 30 feet long. A 4.7-K resister should be connected across the receiver output terminals shunting the 100-μF capacitor (see **Figure 3**).

VLF receiver

Our latest generation of receiver (**Photo C**) is a three-transistor, capacitor-coupled high-gain amplifier, with a tuned LC circuit on the first stage. Two slug-tuned inductors couple the antenna signal to the base of the first transistor. Inductive coupling is used between the two coils. The third transistor output is connected to a rectifier-integrator network with a long time constant to smooth the signal. A reasonable separation should be made between the input and output portions of the circuit to avoid oscillation.

We have built many of these little receivers, and they have proven to be quite stable in operation. A tuning range of about 20 to 32 kHz can be obtained with the components shown in **Figure 3**. This band of frequencies has been found to be ideal for recording SIDs.

Antennas

The antenna is an important part of our monitoring system; consequently, we have experimented with a variety of sizes and types. We have tested loop antennas that ranged between 16 and 36 inches on a side, with different numbers of turns on the loop. Not surprisingly, the larger the size of the loop and the more turns of wire, the stronger the signal sent to the receiver. There are some practical limits on size however. We have settled on a 16 to 24-inch loop with about 125 turns of no. 26 enameled copper wire as a convenient compromise, (**Photo D**.

To be effective, a loop antenna should be sharply tuned with the proper capacitance across the loop terminals. A metal minibox with a half-dozen slide switches joined to several capacitors with values distributed between 50 pF and 0.001 μF provides a satisfactory tuning device. A variable tuning capacitor could also be added to fine tune the loop. The circuit is attached to the receiver by a short length of coaxial cable. Of course, no ground to earth is required in the case of the loop antenna.

We have also learned that vertical antennas, made of aluminum tubing 1 to 1-1/2 inches in diameter, are very effective. One of the more successful units consists of a 24-foot length of 1-1/4 inch diameter aluminum tubing mounted vertically on PVC insulators, with its lower end approximately 2 feet above ground. This antenna is

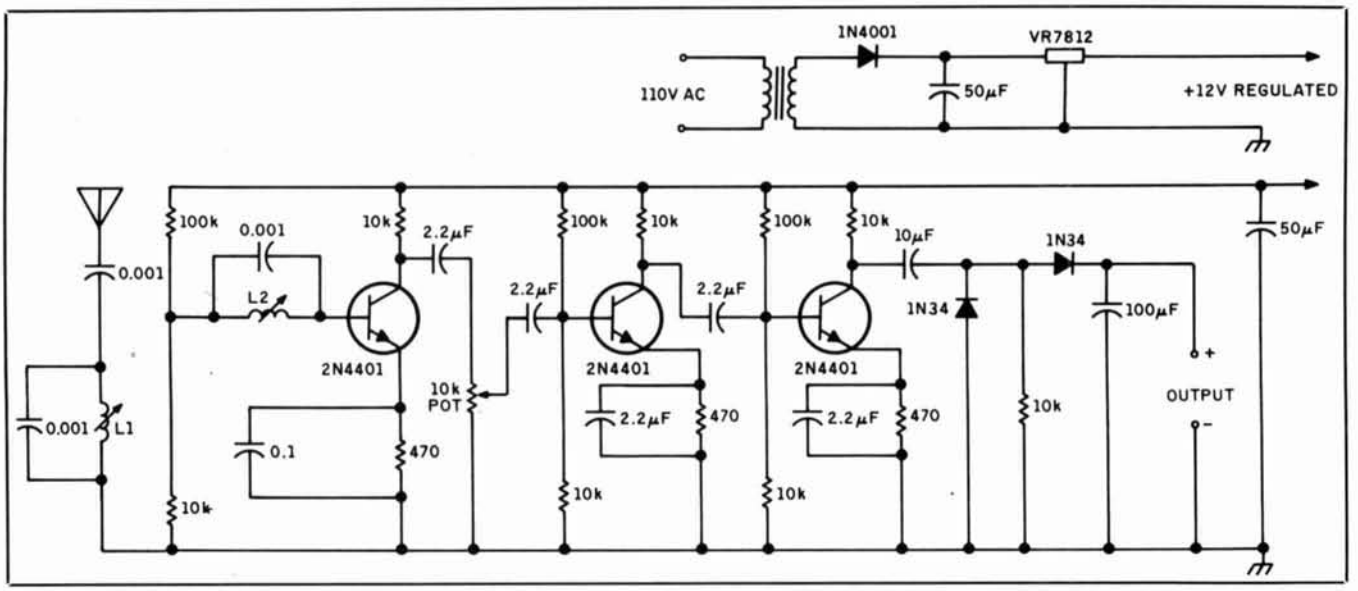

Figure 3. VLF receiver schematic. With the exception of the slug-tuned inductors (L1 and L2) all of the parts are readily obtainable. These inductors, Miller 6319, are no longer listed in the company's catalogues but are available from the authors.

about 20 feet from the receiver, connected by a 30-foot length of RG-58/U coax. In this case, the system must be grounded. Our practice is to wind the braided outer shield of the coax together and attach it to a ground rod at the antenna's base.

Tuning

Tuning the system is mainly a matter of finding the correct blend of inductor settings and sensitivity. If a loop antenna is used, its capacitance should be optimized for the selected frequency by experimenting with different capacitor combinations (values are additive). Since it is highly directional, the loop should be slowly rotated about its vertical axis until the strongest signal is obtained. It's helpful to use either a voltmeter or a 100-μA microammeter attached to the receiver output when the system is set up. The effects of tuning the inductors and loop can be seen, making it simpler to maximize an incoming signal.

Software

Because the FA-154 has multiple input ports, we designed our present system so it uses three separate receivers, and developed software that allows their output to be stacked and plotted simultaneously (see **Figure 4**). With this technique, we can directly compare three different frequencies and/or antenna combinations, as well as the abilities of different receivers. Information concerning

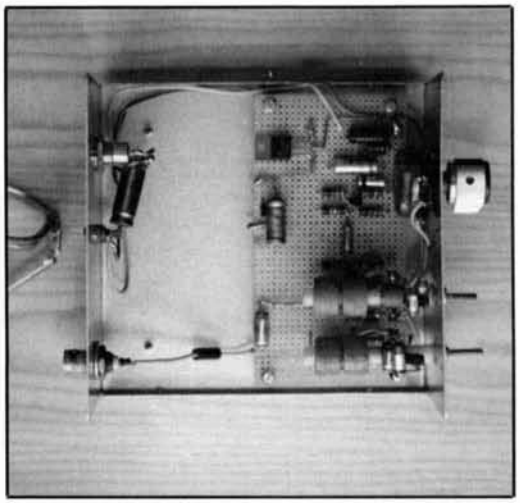

Photo C. The recommended parts arrangement for the simple VLF receiver described in the text is shown with the receiver's cover removed.

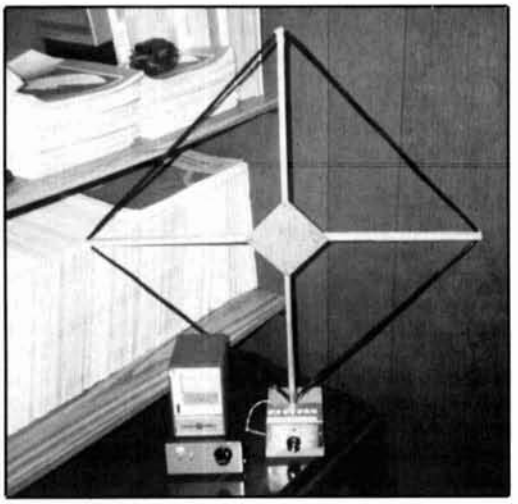

Photo D. One design of loop antenna that can be used in the detection of SIDs. Note the location of the tuning circuit, which is mounted on the unit's base.

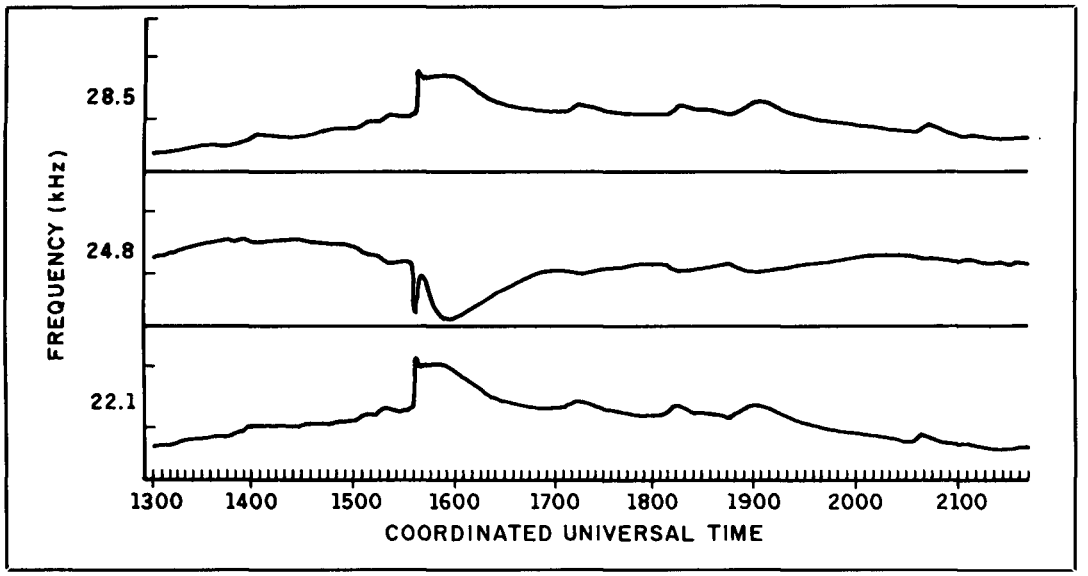

Figure 4. A group of SIDs recorded at frequencies of 22.1, 24.8, and 28.5 kHz. (The X and Y coordinate labels have been simplified for illustrative purposes.) The diversity among identical events at different frequencies results from variations in signal path, sensitivity, and local strength. Irregularities in amplitude and shape are thought to be caused by disparate event intensities and by the source-flare's X-ray and ultraviolet emission.

several of the many VLF stations which can be monitored is included in **Table 1.**

A number of versions of BASIC software have been written for this system. One approach stores the acquired data on disk and allows it to be plotted by the printer at a later date. Alternatively, the data can be plotted in real time. We have found the latter method to be better, as any SIDs are displayed immediately. This technique has enabled us to observe a disturbance's source flare while it is in progress, with the aid of a telescope equipped with a hydrogen-alpha filter.

The plotting program uses the dot-image capability of a standard nine-pin printer. In essence, the computer reads the three input ports in rapid succession, along with the time of the readings. After a specified time limit, typically 30 seconds, the ports are read again. Eight such data sets are taken and then converted to a firing sequence for the printer pins, which results in one line of hard copy. A line feed is then sent to the printer to prepare it for the next set of data. Since only eight pins are used when the printer is in the graphics mode, each pass of the print head produces 24 plotted points.

We have prepared additional software that plots one, two, or three inputs, depending on our requirements. In the process of developing this software, we learned that some modifications to the program code may be necessary if the type of computer is altered. The program shown in **Listing 1** is the three-input version for the Model III computer. This software has worked well with the various models of Epson and Panasonic printers that we have tried, but other models may require some minor program changes.

Moreover, if an IBM PC-type computer is

Frequency (kHz)	Call	Output	Location
21.4	NSS	400 kW	Annapolis, Maryland
22.3	NWC	1 MW	NW Cape, Australia
23.4	NPM	600 kW	Oahu, Hawaii
24.0	NAA	1 MW	Cutler, Maine
24.8	NLK	125 kW	Jim Creek, Washington
26.1	NPG	1MW	San Francisco, California
28.5	NAU	100 kW	Aquada, Puerto Rico
30.6	NPL	500 kW	San Diego, California

Table 1. These VLF radio stations are typical of those that can be monitored in the detection of sudden ionospheric disturbances (SIDs). A number of these stations broadcast on additional frequencies within the 21 to 32-kHz band.

used, the address port for the A-to-D converter will be different. In this case, the installation instructions supplied with the converter should be followed. With small modifications, the existing software should run well on both Model III and IBM-compatible computers. The rapid clock rate of the PC will be evident by its much faster speed of execution when compared with the Model III.

Fundamental data analysis

One of the more distinctive features of these recordings occurs around sunrise, as the D-Region forms. Appropriately enough, this characteristic is commonly called the "sunrise effect." Its general appearance is shown in **Figure 5**. Although many explanations for this pattern have been put forward,[4] a precise accounting for the entire

```
  5 CLEAR 3000:DIM A(1200)
  7 POKE 16912,PEEK(16912):OUT 250,27:OUT 250,65:OUT 250,8
 10 PRINT "A PROGRAM TO PLOT DATA FROM AN ALPHA FA-154 A TO D CONVERTER"
 20 PRINT "           FOR THE RADIO SHACK MODEL III COMPUTER":PRINT:PRINT
 30 PRINT:INPUT "PUT PRINTER ON LINE AND PRESS ENTER";Q
 40 REM PRINT Y-AXIS AND VOLTAGE SCALE
 50 LPRINT "                VOLTS              VOLTS              VOLTS"
 60 LPRINT "         0      .2      .4   0     .2      .4   0     .2      .4"
 70 LPRINT "
      +------+-------+----+------+-------+----+------+-------+----+"
 75 REM INTERVAL IN 80 DETERMINED BY EXPERIMENT - DEPENDENT ON CLOCK SPEED
 80 INPUT "ENTER NUMBER FOR TIME INTERVAL BETWEEN SAMPLES (3450=30 SEC)";AA
 90 PRINT
100 OUT 236,16
110 INPUT "CONNECT 0 INPUT TO GROUND AND PRESS ENTER";Q
120 OUT P,0:D=INP(P):H=INP(P):L=INP(P)
130 OF=(H*256+L)*5/4095
140 CLS:PRINT "DUMMY=";D,"HIGH=";H,"LOW=";L,"OFFSET=";OF
150 INPUT "PRESS ENTER TO CONTINUE";Q
160 CLS
170 REM RECORD VOLTS AND TIME FROM A TO D PORTS #3, #4, #5
180 FOR E=1 TO 8
190 T=0:J=0:R=0
200 FOR A=1 TO 2
210 OUT 236,16:OUT P,5:D=INP(P):H=INP(P+1):L=INP(P)
220 V=(L+(H*256))*5/4095:T=T+V
230 OUT P,4:D=INP(P):H=INP(P+1):L=INP(P)
240 I=(L+(H*256))*5/4095:J=J+I
250 OUT P,3:D=INP(P):H=INP(P+1):L=INP(P)
260 W=(L+(H*256))*5/4095:R=R+W
270 NEXT A
280 B=T/2:U=J/2:C=R/2
290 F=INT(B*10000+.5)/10000
300 Q=INT(U*10000+.5)/10000
310 K=INT(C*10000+.5)/10000
320 W(E)=F:O(E)=Q:Z(E)=K
330 H$(E)=RIGHT$(TIME$,8)
340 PRINT E;TAB(7)H$(E);TAB(18)W(E);TAB(30)O(E);TAB(42)Z(E)
350 FOR M=1 TO AA:NEXT M
360 NEXT E
370 REM CONVERT VOLTAGE TO DOTS AND ADD OFFSET
380 REM VOLTAGE SCALE IS 6 INCHES LONG * 120 DOTS PER INCH
390 REM TAKE EIGHT VOLTAGE VALUES FOR CONVERSION
400 E=1
410 FOR X=1 TO 8
420 V(X)=INT(6+W(E)*480):VA(X)=INT(246+O(E)*480)
430 VB(X)=INT(486+Z(E)*480)
440 E=E+1
450 NEXT X
460 REM INITIALIZE ALL PINS TO ZERO
470 FOR X=1 TO 960:A(X)=0:NEXT X
480 REM SET PRINTER FOR DOT MODE AND PRINT 8 COLUMNS
490 C=128:FOR X=1 TO 8:D=V(X):A(D)=A(D)+C:C=C/2:NEXT X
500 C=128:FOR X=1 TO 8:D=VA(X):A(D)=A(D)+C:C=C/2:NEXT X
510 C=128:FOR X=1 TO 8:D=VB(X):A(D)=A(D)+C:C=C/2:NEXT X
520 E=4
530 LPRINT"  ";LEFT$(H$(E),5);" -";
540 REM SET PRINTER FOR DOT IMAGE MODE
550 LPRINT CHR$(27)+"*"+CHR$(2)+CHR$(192)+CHR$(3);
560 REM PRINT OUT DATA POINTS
570 FOR Y=1 TO 960
580 A(5)=255:A(245)=255:A(485)=255
590 Z=A(Y):LPRINT CHR$(Z);:NEXT Y
600 REM REPEAT FOR NEXT SET OF READINGS
610 GOTO 180
620 LPRINT CHR$(27)+"P";
```

Listing 1. This BASIC program will store and plot information from three VLF receivers when a Tandy Model III or similar computer is used to record ionospheric anomalies.

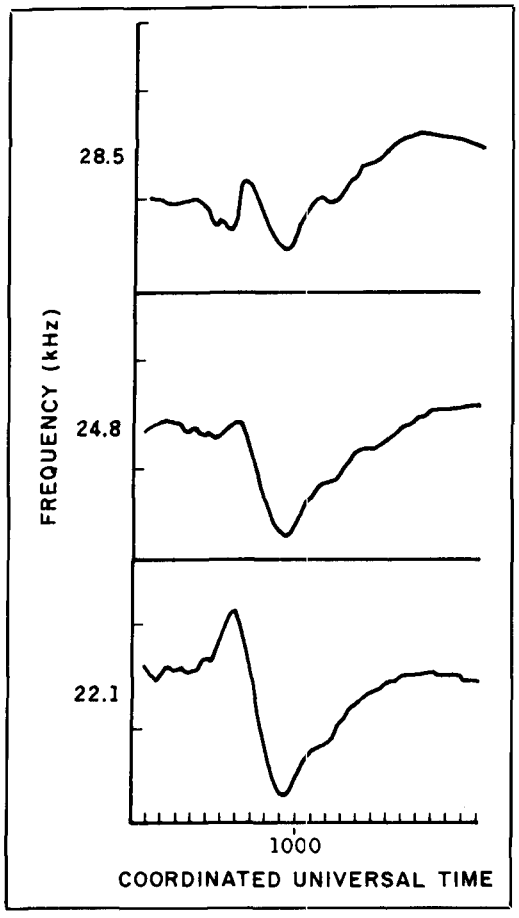

Figure 5. The "sunrise effect" occurs as the ionospheric D-Region forms over the sunlit hemisphere at an altitude near 70 km. When the recording system is properly tuned, a similar pattern appears each morning around daybreak.

phenomenon remains elusive. The sunrise effect is a considerable aid to the tuning process however, because its presence indicates that an adequate station has been located.

A detailed description of the analytical technique employed in the reduction of these data can be obtained from **Reference 2** or from the authors. Briefly though, the procedure is carried out in the following way.

The "classic" SID is depicted by the examples shown in **Figure 4**. Note that the amplitude of individual events varies considerably and some may appear to be inverted. The analyst's task is to determine the precise times that each of three event-phases occur, and then to use this information to find the SID's duration, or "importance." Last of all, the reality, or "definiteness" of the event is estimated subjectively. These latter parameters are given ratings in accordance with simple numerical scales.

The required time measurements (the event's beginning, maximum, and end) are all recorded with reference to the Coordinated Universal Time scale. A SID's maximum is not (necessarily) the time of its peak intensity. Rather, it is considered to be the instant when the ascending branch of the event ceases its initial sharp rise. The more difficult of the three measurements is the end time, which theoretically is the point at which the descending branch of the SID returns to the diurnal trend line. Unfortunately, this moment can seldom be pinpointed with great accuracy.

Happily for many contributors, we don't require each monitoring station to reduce its data. However, we do encourage them to do so because the process forms such an interesting part of this work. Those who lack the time or inclination to conduct their own analyses may simply send their raw recordings to us for event determination.

We strongly solicit participation in this rewarding and scientifically productive pursuit. All interested parties are urged to contact us for additional information. ■

REFERENCES
1. A. Hewish, S.J. Tappen, and G.R. Gapper, *Nature*, 314, 1985.
2. P.O. Taylor, *Observing the Sun*, Cambridge University Press, Cambridge, England, 1991.
3. H. Zirin, *Astrophysics of the Sun*, Cambridge University Press, Cambridge, England, 1988.
4. C.M. Chernan, *The Handbook of Solar Flare Monitoring and Propagation Forecasting*, TAB Books, Summit, Pennsylvania, 1978.
5. *Solar-Geophysical Data* , National Geophysical Data Center, NOAA/NESDIS, E/GC2, 325 Broadway, Boulder, Colorado 80303.

Parts List - VLF Receiver

Quantity	Description
Capacitors	
3	*0.001 μF*
1	*0.1 μF*
5	*2.2 μF*
1	*10 μF*
2	*50 μF*
1	*100 μF*
Diodes	
2	*1N34*
1	*1N4001*
Resistors	
7	*10 k, 1/2 watt*
3	*100 k, 1/2 watt*
3	*470 ohm, 1/2 watt*
Miscellaneous	
1	*10-k potentiometer*
1	*7812 12-volt regulator*
1	*12-volt transformer*
3	*1N4401 transistors*
2	*Miller 6319 inductors**
1	*perfboard*
1	*metal cabinet*
1	*BNC connector*
Assortment of screws and hardware	

*Available from the authors.

Carl Luetzelschwab, *K9LA*
1227 Pion Road
Ft. Wayne, Indiana 46845

ANTENNA ANGLE OF RADIATION CONSIDERATIONS

Performance comparison of Quads and Yagis mounted at low heights

Over the years, the Quad antenna has gained a reputation for outperforming a comparable Yagi when both are mounted low (generally, at heights of approximately 0.5 wavelength and below). This superiority has been attributed to the Quad's lower angle of radiation! This reputation persists in spite of the efforts and conclusions made by Overbeck[2] In this article, I'll show why the Quad has a lower angle of radiation than a comparable Yagi at the same height. I'll expand this information into a general statement with respect to *all* antennas. The results of this effort lay the groundwork for a new on-the-air comparison of a Quad and Yagi focusing on low height performance.

Previous work

In addition to the previously cited works by Bergren and Overbeck, many other articles have been written about Quads and Yagis. Of all these articles, only Parrott[3] Fitz[4] and Overbeck have compared a Quad and Yagi on a real-time basis. Overbeck's comparisons were at low-to-high heights, while Parrott's and Fitz's were only at high heights.

Why antennas at the same height can have different angles of radiation

It's best to begin by reviewing the way vertical patterns of horizontal antennas are formed over ground. I've done this in detail for a half-wave dipole and a one-wavelength square loop at 0.5 wavelength (the center of the loop is at 0.5 wavelength, where the boom of a multi-element Quad would be).

Remember that the vertical pattern of an antenna over ground is the product (the sum when expressed in dB) of the free-space vertical pattern and the ground-reflection factor.* The ground-reflection factor for horizontal antennas over perfectly conducting earth is $2 \times \sin(h \times \sin a)$, where h is the height above ground in degrees (1 wavelength = 360°) and a is the angle above the horizon (horizon = 0°)[5] For a given height, h, this function maximizes at a numerical value of 2 at a certain angle (or angles), a. Since $20 \times \log 2 = 6$ dB, putting an antenna over ground can result in up to 6 dB additional gain.

Figure 1 depicts the free-space vertical pattern, the ground-reflection factor, and the resulting total vertical pattern for both the dipole and square loop at the 0.5-wavelength height. The patterns were generated using K6STI's MN version 1.66 software.

Note the difference in the angles of radiation over ground. Although the difference is small, it is noticeable. To understand why

*This is strictly true only if the antenna in question doesn't change when put over ground. In reality, antennas change when put over ground. At reasonable heights, this change is minor. For example, a relatively thin resonant dipole in free space (0 dBd), when placed at 0.61 wavelengths over perfectly conducting ground, results in 7.01 dBd at 24° elevation angle. The extra 0.99 dB above the theoretical 6.02-dB ground-reflection factor is due to the decrease in the dipole's radiation resistance at this height. This effect is well documented by the damped sinusoidal "radiation resistance versus height above ground" curve found in many references. This effect (referred to in this article as the Rr factor) will be included in subsequent calculations, so the math is correct.

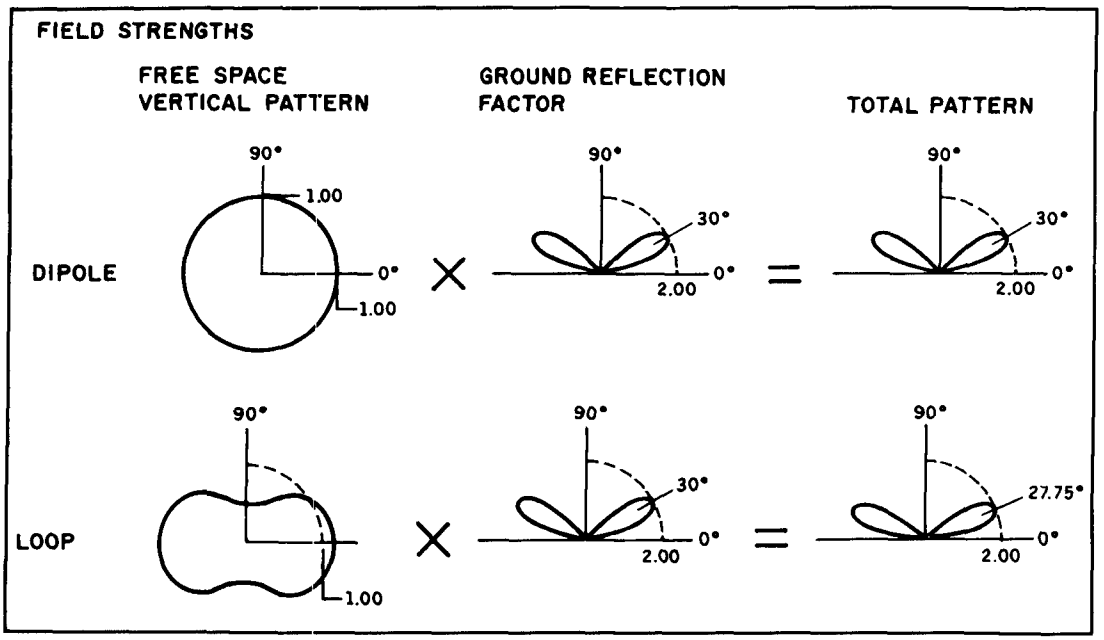

Figure 1. The free-space vertical pattern, the ground reflection factor, and resulting total vertical pattern for both the dipole and square loop at the 0.5-wavelength height.

the square loop's angle is lower, refer to **Table 1**. This table gives the values of the free-space vertical pattern, the ground-reflection factor, the Rr factor, and the total vertical pattern (the product) for both the dipole and square loop (in numerical values, not dB, with the dipole's free-space pattern as the reference) in the vicinity of 30°.

For the dipole, because its free space vertical pattern is constant, the total pattern in the vertical plane is simply that of the ground-reflection factor plus the slight modification due to the Rr factor.

For the square loop, consider the value of the ground-reflection factor at 30°, and the value of the free-space pattern at this angle. The product is 2.097.

Now consider a slightly higher angle (32°). The free-space pattern and the ground-reflection factor are both decreasing. Thus, the product (2.066) is also decreasing, and is less than that at 30°, indicating that 32° is moving away from the product peak.

Finally, consider a slightly lower angle (28°). The ground-reflection factor is decreasing again, but the free-space pattern is *increasing*. The product is now 2.106, which is more than that at 30°, indicating that 30° is *not* the peak of the product (total pattern). It should now be clear why the square loop has a lower angle of radiation than a dipole at this height. On the low side of the ground-reflection factor peak, the free-space vertical pattern of the square loop is increasing faster than the ground-

Dipole				
Angle (degrees)	**Free-space pattern**	**Ground-reflection factor**	**Rr factor**	**Product**
28	1.00	1.99	1.028	2.046
30	1.00	2.00	1.028	2.056
32	1.00	1.99	1.028	2.046
Loop				
Angle (degrees)	**Free-space pattern**	**Ground-reflection factor**	**Rr factor**	**Product**
28	1.05	1.99	1.008	2.106
30	1.04	2.00	1.008	2.097
32	1.03	1.99	1.008	2.066

Table 1. Values of the free-space vertical pattern, the ground-reflection factor, and the total vertical pattern for the dipole and square loop at 0.5 wavelengths height.

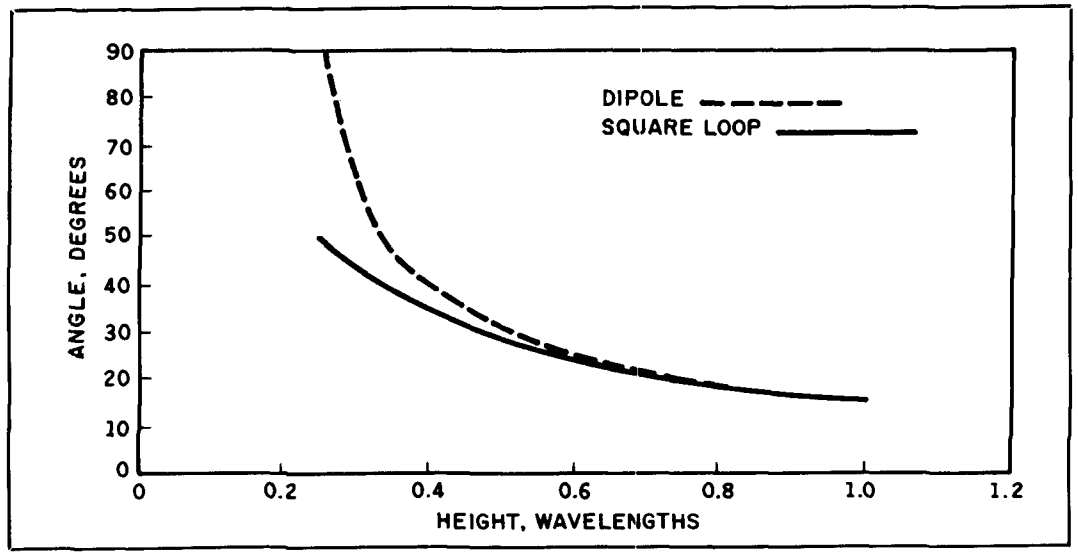

Figure 2. Elevation and angle of major lobe versus height in wavelengths,λ, at 14.175 MHz.

reflection factor is decreasing. As a result, the product of the two functions maximizes at a lower angle (27.75°).*

Thus, antennas with different free-space vertical patterns can perform differently at the same height over ground. It's interesting to perform these calculations on the dipole and the square loop for various heights above ground. You can do this using MN or, for those more mathematically inclined, by setting the derivative of the product of the ground-reflection factor and the free-space vertical pattern to zero and solving for the angle of radiation. (N4FDK performed this stimulating exercise on LOTUS Symphony using a second order polynomial curve fit to the free-space vertical pattern). The results of these two methods are identical, and are presented in **Figure 2.****

Figure 2 clearly shows that the vertical pattern of an antenna over ground is not only dependent on the height, but is also tied into the free-space vertical pattern. The specific parameter of the free-space vertical pattern which can be used as an indicator of this effect is the free-space half-power vertical beamwidth, or θh.

Summary statement

It should be obvious that the effect of θh is not confined to dipoles and square loops. It applies equally to all antennas. In general:

> The angle of radiation of an antenna is dependent not only on its height above ground, but also on its free space half-power vertical beamwidth (θh). The effect of θh on the radiation angle is most pronounced at low height, and diminishes as height increases.

To reiterate, two antennas at the same boom height can have different angles of radiation, when both are mounted low. The antenna with the smaller θh (narrower free-space half-power vertical beamwidth) will generally have a lower angle of radiation.†† Above 3/4 wavelength or so, the angles will essentially be identical.

Multi-element arrays in free space

Now that I've defined the effect of θh on radiation angle, I'd like to focus on the long-standing Quad versus Yagi controversy: Does a Quad at low height have a lower angle of radiation than a comparable Yagi, and if so, will the Quad outperform the Yagi? I looked at this question by designing

---

* In general, when beginning at an elevation angle above the peak of the lobe, the more narrow the vertical beamwidth θh, the more rapidly the free-space field increases as the elevation decreases, thus, the lower the resultant elevation angle of the radiation that includes the ground-reflection factor. Ed.

This concept isn't new. In fact, **Figure 2 is very similar to **Figure 5A** of "Loop versus Dipole – Analysis and Discussion" by Belcher, WA4JVE, and Casper, K4HKX, in the August 1976 issue of *QST*. Unfortunately, their calculation of loop gain is in error (see April 1977 Technical Correspondence in *QST* for corrections). This concept is also presented indirectly in Tables 5.2 and 5.3 of "The Effects of Ground" chapter in *Yagi Antenna Design* by Lawson, W2PV. It was also discussed by Regier, OD5CG, on page 60 of the July 1981 issue of *Ham Radio*, Kraus, W8JK, on page 21 of the January 1938 issue of *QST* (the earliest literature found on this subject), Landskov, W7KAR, on page 32 of the March 1977 issue of *QST*, and Orr, W6SAI, on page 53 of the May 1983 issue of *Ham Radio* (note that it is erroneously implied that a Yagi and dipole have the same angle of radiation at a height of three-eighths wavelength).

† Interestingly enough, two antennas with the same θh can have slightly different angles of radiation at the same height. This is a second order effect due to the shape of the pattern between the 3-dB points.

Antenna	θe	θh	Gain dBi	F/B dB	2:1 VSWR BW at 20m	Boom length
Commercial	65°	108°	7.64	31	>350 kHz	20′
Three-element NBS	55°	74°	9.64	9	175 kHz	28′

Table 2. Free-space performance of broadband and narrowband designs at the central design frequency (f_c = 14.175 MHz).

Antenna	θh	Gain dBi	F/B dB	Max VSWR over 20-m band	Boom length
Two-element Yagi	137°	6.16	11	2.00	7′5″
Two-element Quad	96°	7.02	17	2.00	7′5″
W8JK	91°	5.90	0	–	8′8″
Three-element Yagi	111°	7.51	42	1.60	19′2″

Table 3. Comparison of broadband designs for free-space performance at the central design frequency of 14.175 MHz.

several representative Yagis and Quads, and making on-the-air comparisons.

However, before I proceed, I'd like to address one major issue which seems to have been overlooked in the Yagi versus Quad comparisons found in the literature. This is the fact that an n-element Yagi (or an n-element Quad) can be tuned (element lengths and spacings) in a variety of ways. Different tuning gives different free-space E-plane (θe) and H-plane (θh) patterns. This means you may see different performances over ground, even at the same height. For example, consider a well-known manufacturer's three-element Yagi and another three-element Yagi that's tuned for maximum gain as described by W1LJ in the August 1982 issue of *QST*.[6] The free-space performance of each antenna at the central design frequency (f_c = 14.175 MHz) is shown in **Table 2.**

The commercial Yagi is a "broadband" design. This means it maintains gain within ±0.3 dB, F/B > 20 dB, and VSWR < 1.6:1 over the entire 20-meter band. The three-element NBS "max-gain" design sacrifices F/B and VSWR bandwidth for an extra 2 dB gain. Note the difference in θh. The three-element NBS design will give a lower angle of radiation than the commercial Yagi when both are at low heights. Thus, even two three-element Yagis could perform differently. Since tuning is a factor, what tuning condition should be used?

It is of primary importance that the antennas be tuned to the same goal. It isn't valid to compare a broadband design to a max-gain design. The following multi-element arrays are designed to broadband specifications, with the following performance criteria over the entire 20-meter band:

VSWR: less than 2:1
Gain: within ±0.6 dB referenced to gain at f_c
F/B: peaked at the center of the band

Using these constraints, which brought me as close to an "apple versus apple" condition as possible, I began the designs. For practical reasons, I restricted my designs to a two and three-element Yagi and a two-element Quad. The two-element designs employ a driven element and a reflector, with the Quad in a square configuration fed at the bottom center. I also included a single-section W8JK array. Also called a flattop array, it is two half-wave dipoles spaced 0.125 wavelengths apart and fed out-of-phase.[7] The designs were done manually with the aforementioned MN software.* The free-space performance of these designs at the central design frequency of 14.175 MHz is shown in **Table 3.** All designs used the equivalent of at least 20 segments per wavelength.

It's interesting to compare the free-space performances of these antennas. For these limited results, the two-element Quad exhibits about a 1-dB advantage over a two-element Yagi.** What's more, the two-element Quad is within 0.5 dB of the three-element Yagi. Also note the differences in θh: the

*K6STI's YO software could be used for the Yagi designs.

This agrees with calculations by the late Dr. Lawson, W2PV, in his book *Yagi Antenna Design*, and is about 1 dB less than the measurements of scale models at 400 MHz by Lindsay, W0HTH, in the May 1968 issue of *QST*. For a discussion of this see **Reference 2.

Antenna	Free space θh	Boom at 30 feet Angle	Gain dBi	Boom at 64 feet Angle	Gain dBi
Two-element Yagi	137°	30.00°	10.18	15.00°	11.36
Two-element quad	96°	27.50°	10.42	14.50°	12.04
W8JK	91°	27.75°	9.11	14.75°	10.96
Three-element Yagi	111°	28.50°	11.24	14.75°	12.69

Table 4. Evaluation of performance for multi-element arrays over ground.

two-element Quad should have a lower angle of radiation than either Yagi. The single-section W8JK should be fairly identical angle-wise to the two-element quad.

Multi-element arrays over ground

With the designs completed, I put these antennas over ground to evaluate their performance in the real world. I called upon MN once again, using average ground conditions (dielectric constant = 13, conductivity = 5). I evaluated two heights—30 feet (0.432 wavelength) and 64 feet (0.962 wavelength). Remember that the height for the Quad is to the center of the loops. The results are shown in **Table 4**. The angle is that of the lowest maximum and the gain in dBi at this angle.

There are three items worth noting about the data in **Table 4**. First, at low height, the antennas with the narrowest θh have lower angles of radiation. At the upper height, all the antennas are within 0.5°. This is in agreement with the summary statement presented earlier. For the two-element Yagi and two-element quad at 30 feet, the angle difference is 2.5°, and **Figure 3** depicts the vertical patterns. It shows that the main lobes are very broad, making it easy to conclude that the 2.5° difference is insignificant. On the other hand, a 2.5° lower angle in a multi-hop propagation model to a long-path DX station (W9 to JA, for example) calculates to two fewer hops, which should show a very noticeable improvement. According to Lew McCoy, W1ICP: "I have long argued that for the same boom height, a Quad has a lower angle of radiation than a Yagi. In the comparison mode, the meat of the radiation angle for the Quad was 2 to 4 degrees lower than a Yagi. Some Amateurs may argue that 2 or 4 degrees isn't worth debating about. However, my answer to that is to actually calculate the ionosphere hops for long DX. I am sure you'll be surprised."[8]

Second, although the data isn't presented, putting an antenna over real earth (for example, dielectric constant = 13, conductivity = 5) lowers the angle of radiation even further than if it was over perfectly

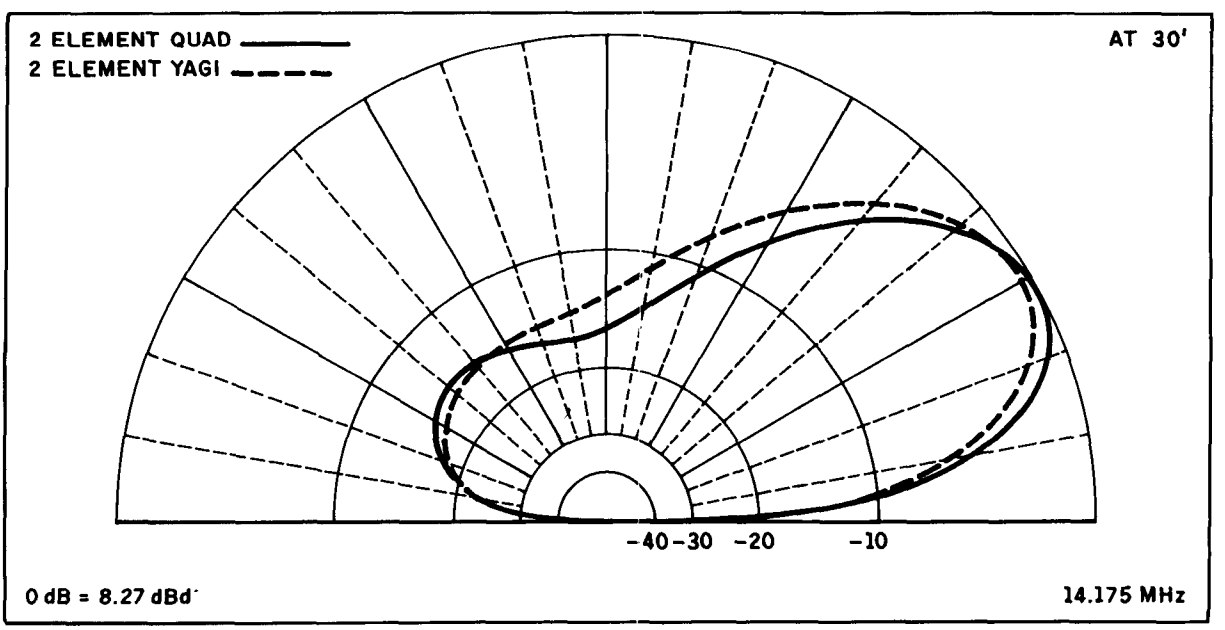

Figure 3. Vertical patterns for the two-element Yagi and two-element Quad at 30 feet.

conducting ground. This is because the ground-reflected wave suffers partial loss upon reflection from the earth. In essence, one small step toward free space has been taken. (The limit of totally absorbent earth is a 0° angle of radiation, with no "gain" enhancement by the ground-reflection factor because there's nothing reflected).

Third, note that the single-section W8JK is very comparable angle-wise to the two-element Quad.* I included the W8JK to illustrate that the Quad isn't the only antenna which offers a low-angle advantage over a comparable Yagi.** It's interesting to note that this advantage is achieved in the W8JK antenna without a vertical dimension, thus eliminating any possible confusion about the boom height.

Conclusion

I've shown that antennas with narrower free-space half-power vertical beamwidths have lower angles of radiation at low heights, whether they are Quads, Yagis, quagis, driven arrays, or any other variety. Specifically, a two-element Quad (and the single-section W8JK array) has a lower angle of radiation at low height than two and three-element Yagis, which, in turn, have lower angles of radiation than a dipole.

There shouldn't be any controversy regarding my conclusion. It simply shows how two mathematical functions interact when multiplied together. Rather, the controversy should focus on the question, "Does the Quad's lower-angle advantage truly matter in the real world?" Although there's much literature showing that a high antenna is better than a low antenna due to a large difference in the angle of radiation,† there doesn't appear to be any literature beyond Overbeck's proving this for angle of radiation differences in the 2.5° range.

To find out if the 2.5° difference matters, I performed on-the-air comparisons of two-element Yagis and two-element Quads at low height. I'll discuss the results in a future article. ■

*The W8JK, although having a narrower θh than the Quad, has a higher angle of radiation (see the fourth footnote).

**If both the quad and the W8JK result in significant narrowing of θh, why not combine these two antennas? I took a brief look at a dual-driven Quad (two loops spaced 0.125 wavelengths apart and fed 180° out-of-phase). Its θh was about 73°, resulting in an angle of radiation of about 25° at 30 feet. This appears to be the concept behind "The Evolution of the Four-Element Double-Driven Quad Antenna" by Martinez, W6PU, in the December 1983 issue of *CQ*.

†Several good references are: Overbeck, *QST*, March 1970; Utlaut, *Journal of Research of the NBS*, March/April 1961; and Epstein, Frank, Barry, and Villard, *Radio Science*, July 1966.

REFERENCES

1. Bergren, W0A1W, *QST*, May 1963, page 11.
2. Wayne Overbeck, N6NB, "Quads vs. Yagis," *Ham Radio*, May 1979, page 12.
3. Col. John H. Parrott, Jr., W4FRU, "Quad vs. Triband Yagi," *QST*, February 1971, page 11.
4. Fitz, W4RBZ, *QST*, October 1966, page 20.
5. Kraus, *Antennas*, Section 11-7a, Second Edition, page 464.
6. Dennis J. Lusis, W1LJ, "Go for the Gain, NBS Style," *QST*, August 1982, page 34.
7. John Kraus, "The W8JK Antenna: Recap and Update," *QST*, June 1982, page 11. This article gives a history of the W8JK antenna.
8. Lew McCoy, W1ICP, "The MN and YO Software Programs for Antenna Analysis," *CQ*, August 1989, page 34.

PRODUCT INFORMATION

RSSI Feature Added to FM IF ICs

Two low-power FM IFs have been added to Motorola's line of RF communication ICs. The MC3371 and MC3372 are basic single conversion narrowband FM IF receivers which include a received signal strength indicator (RSSI). The MC3371 is designed for use with parallel LC quadrature detector components, while the MC3372 can be used with either a 445-kHz ceramic discriminator or parallel LC components.

The MC3371 and MC3372 both feature a multipurpose local oscillator, a double-balanced mixer, a high gain limiting RF amplifier, quadrature detector, an active filter, squelch, and an RSSI output. Both devices operate with inputs beyond 100 MHz and are available in 16-pin DIP and SOIC surface mount packages.

Samples of the MC3371 and MC3372 are available. Contact Motorola Inc.—Media Relations, P.O. Box 52073, Mail Drop 56-102, Phoenix, Arizona 85072 for additional information. To obtain technical data on the low power narrowband FM IF contact: Motorola Literature Distribution, P.O. Box 20912, Phoenix, Arizona 85036. Ask for data sheet MC3371/D.

Rectifier Selector Guide Available

Motorola Inc. is offering a revised *Rectifier Selector Guide and Cross Reference*. The book includes information on application specific rectifiers, Schottky, fast and ultrafast rectifiers. To obtain a copy call Motorola Literature Distribution at 1-800-441-2447, or write: Motorola Inc., Literature Distribution Center, P.O. Box 20924, Phoenix, Arizona 85063. Ask for publication SG160/D.

Jeff Crawford, *K0ZR*
9441 Julie Beth Street
Cypress, California 90630

A RAPID DESIGN TOOL FOR MICROSTRIP FILTERS

Macintosh™ program aids in filter design and analysis

If you need a bandpass filter, and you're not sure how to proceed, you'll find this program helpful. I've found that very good results are possible up to at least 15 GHz.

The relationships used in this program are nothing new or exotic; they've been well documented in engineering journals[1-5] The ChebFilter program runs on the Macintosh™. The user interface is Macintosh friendly and I've endeavored to make it as foolproof as possible. Read on, and you can follow a design from start to finish!

Program organization

ChebFilter is organized into three sections: theoretical loss and group delay calculations, synthesis of the microstrip filter, and analysis for resonator Q. A brief outline of **Section 1** begins with the Chebychev relationship in **Equation 1.**

$$|H(j\omega)|^2 = \frac{1}{1 + \epsilon^2 C_n^2(\omega)}$$

where:

$$C_n(\omega) = \cos(n \cos^{-1}(\omega)) \quad \omega \le 1.0$$
$$= \cosh(n \cosh^{-1}(\omega)) \quad \omega > 1.0 \quad \textbf{(1)}$$

n = filter order
ϵ = passband ripple
dB ripple = $10\text{Log}_{10}(\epsilon)$
ω = normalized radian frequency
H(jω) = lowpass loss function

You can calculate a first estimate of the filter's characteristics using this equation; but, it's possible to do better. It's known that the realistic losses associated with a filter are directly influenced by the "Q"uality factor of the associated resonators making up the filter.[6] An approximation of the midband loss, L_o, is thus given by **Equation 2.**

F Ripple:	95 MHz, 105 MHz
Order:	6
Ripple, dB:	0.01
Unloaded Q	**Midband Loss, dB**
50	6.57
75	4.38
100	3.29
150	2.20
500	0.67

Table 1. Midband losses versus "average" unloaded resonator Q.

$$L_o(dB) = \frac{4.343(1-\alpha^2)}{W\,Q_u} \sum_{i=1}^{N} g_i \qquad \textbf{(2)}$$

where:
W = fractional bandwidth
Q_u = unloaded element Q, for L's and C's
Σg_i = the sum of the respective element values

$$1-\alpha^2 = \frac{4g_o \times g_{n+1}}{(g_o + g_{n+1})^2}$$

The g_i's are the element values of the i^{th} resonator (see the appendix for details). Q_u is best described as an average unloaded Q. Intuition should tell you that the Q of each resonator is probably different, because it's dependent upon the actual resistance and reactance present. **Equation 2** is further

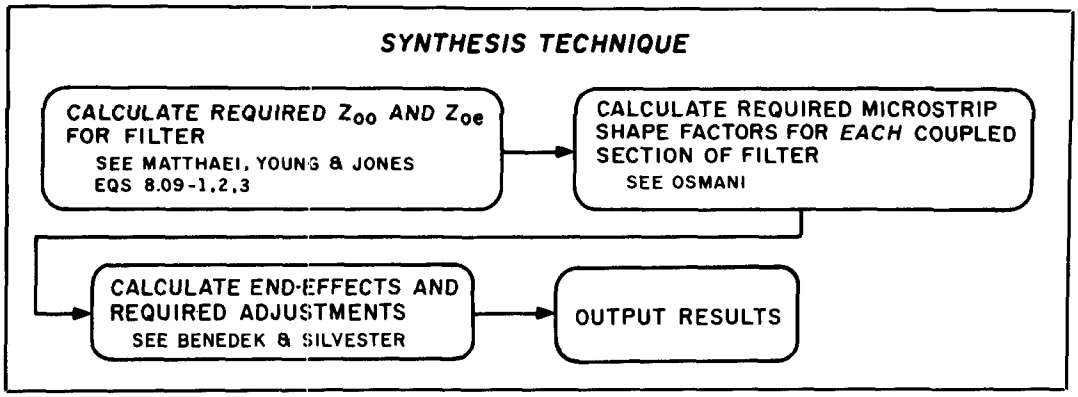

Figure 1. Synthesis flowchart.

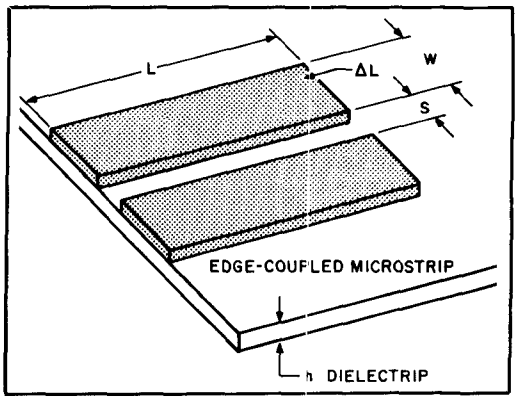

Figure 2. Dimensions and variables on microstrip.

modified by a ratio to obtain an approximation at other frequencies *within* the passband of the filter (see **Equation 3**).

$$\text{Addl Loss at } \omega' = \text{midband loss} \times \frac{\text{Group Delay}(\omega')}{\text{Group Delay}(\omega_o)} \quad (3)$$

where:
ω_o = band-center radian frequency
ω' = radian frequency of interest
midband loss = $\text{AntiLog}_{10}(L_o/10)$

The specifics behind the group delay calculation are also outlined in the appendix. For an example of the loss calculation, see the results obtained for parameters specified in **Table 1**.

Filter synthesis

The actual synthesis of the microstrip filter relies most heavily on relationships developed by Osmani.[7] Osmani reduced the synthesis problem from a two-variable, nonlinear analysis[8] to a one-variable solution. In his technique, the $(w/h)_{se}$, $(w/h)_{so}$, $(s/h)_{se}$, and $(s/h)_{so}$—even and odd-mode shape factors—are first calculated for noncoupled microstrip. He then uses these values to arrive at the final width-to-height and spacing-to-height information necessary to obtain the desired Z_{oo} and Z_{oe}—odd and even-mode impedances. The Z_{oo} and Z_{oe} are important because they directly affect the coupling between microstrip members composing the filter structure. ChebFilter solves **Equation 4**, a nonlinear equation, using a second-order Newton-Raphson technique. (This same procedure is appropriate for the synthesis of Lange couplers in microstrip.)

$$(w/h)_{so} = 2\cosh^{-1}\left[\frac{(x+1)f-2}{x^{-1}}\right] + (r)\cosh^{-1}\left[\frac{\cosh^{-1}[0.5*f*(x+1) + 0.5*(x-1)]}{\cosh^{-1}(x)}\right]$$

where

$$r = \begin{cases} f\cosh[\pi/2*(w/h)_{se}] & \epsilon r > 6 \\ \dfrac{8}{\pi(\epsilon_r + 2)} & \epsilon r \le 6 \end{cases} \quad (4)$$

The flowchart in **Figure 1** outlines the procedure from filter specification to final determination of the actual shape factors required.

An additional point must be made with respect to "end-effects." The result of the open-endedness associated with each microstrip resonator is an excess charge density which causes a disruption of the normal electric field intensities. To compensate for this effect, a small length (ΔL) is subtracted from the final length of each filter resonator (see **Figure 2**). Because ChebFilter relies upon curve-fit data[9] to perform its calculations, this information isn't available if you use a dielectric constant outside the range of approximation (not included in 2.0 to 2.4, 5.75 to 6.25, or 9.5 to 10.5). You'll be able to design the filter, but will be deprived of this additional information.

Idealized Filter Results

Magnitude v.s. Frequency

Freq	Mag	Freq	Mag	Freq	Mag	Freq	Mag
2000.00	-62.06	2240.00	-32.36	2480.00	-1.90	2720.00	-3.82
2020.00	-60.14	2260.00	-28.79	2500.00	-1.86	2740.00	-5.49
2040.00	-58.15	2280.00	-24.89	2520.00	-1.83	2760.00	-8.98
2060.00	-56.08	2300.00	-20.61	2540.00	-1.81	2780.00	-13.24
2080.00	-53.94	2320.00	-15.89	2560.00	-1.82	2800.00	-17.38
2100.00	-51.70	2340.00	-10.83	2580.00	-1.84	2820.00	-21.19
2120.00	-49.36	2360.00	-6.24	2600.00	-1.87	2840.00	-24.65
2140.00	-46.91	2380.00	-3.84	2620.00	-1.93	2860.00	-27.80
2160.00	-44.34	2400.00	0.00	2640.00	-2.01	2880.00	-30.71
2180.00	-41.62	2420.00	-2.29	2660.00	-2.13	2900.00	-33.39
2200.00	-38.73	2440.00	-2.10	2680.00	-2.32	2920.00	-35.89
2220.00	-35.66	2460.00	-1.98	2700.00	-2.71	2940.00	-38.22
						2960.00	-40.42
						2980.00	-42.48

Figure 3. Magnitude versus frequency.

Unloaded Q approximation

The final part of the program lets you obtain an approximate value for the expected unloaded Q for microstrip resonators exhibiting the specified characteristics entered into the program. I won't go into the equations used here as they are rather lengthy and found in numerous references.[10,11,12] The length, L, for each coupled section of the filter is also calculated for the designer's convenience.

A design example

Assume that you need a bandpass filter with a passband of 2400 to 2700 MHz and a theoretical loss which meets or exceeds 35 dB at 2000 and 2900 MHz. The material available for filter construction is Duroid with a dielectric constant of 5.9 and a dielectric thickness of 25 mils.

Begin by using the analysis section to best gauge the number of filter sections required and, if necessary, to obtain an estimate of the inband losses. **Figure 3** shows that a fifth-order Chebychev filter will meet each of the specified loss requirements: −62.06 dB at 2000 MHz and −33.39 dB at 2900 MHz. The required losses above the passband are always more difficult to achieve than those below the passband. Also, this type of filter has a multiple response at $2 \times f_0$,* which may influence your decision to use this type of filter. The same information is shown graphically in **Figure 4**. The autoscaling graphics are included within the ChebFilter program. Although not illustrated here, both tabulated and graphics output is available for the filter's group delay.

If you're unsure what magnitude of Q is

*f_0 is the geometric center of the passband; i.e., $f_o = \sqrt{f_1 \times f_2}$, where f_1 and f_2 are the filters' corner frequencies.

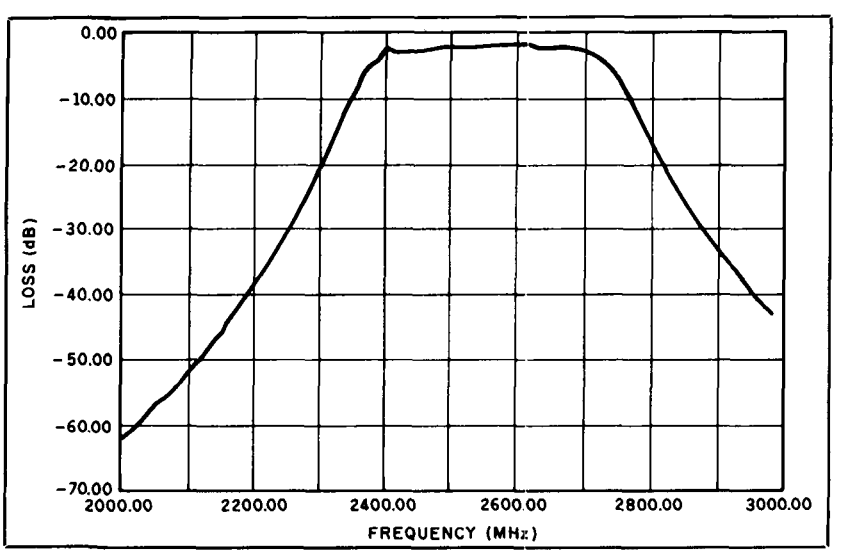

Figure 4. Calculation of unloaded resonator Q.

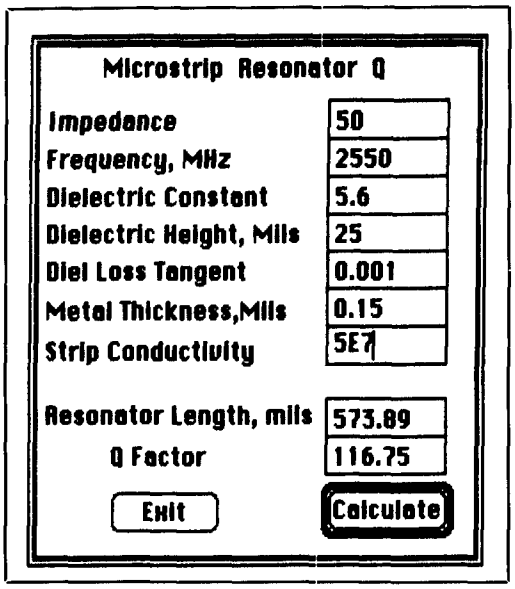

Figure 5. Calculation of unloaded resonator Q.

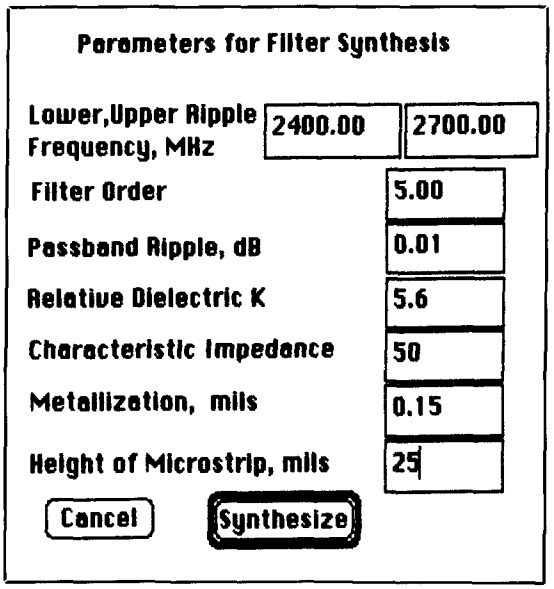

Figure 6. Required data inputs for the synthesis.

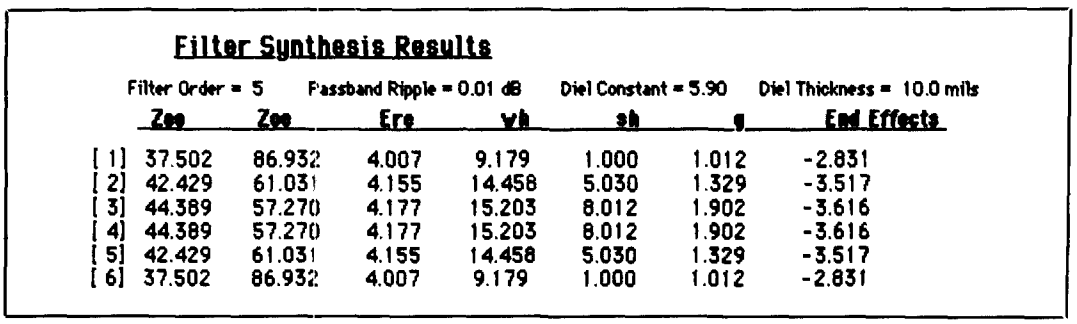

Figure 7. Sample synthesis output.

reasonable when analyzing a filter candidate, you should find the third option (discussed earlier), which calculates theoretical unloaded resonator Q, helpful. **Figure 5** shows a sample calculation illustrating what data is needed for input.

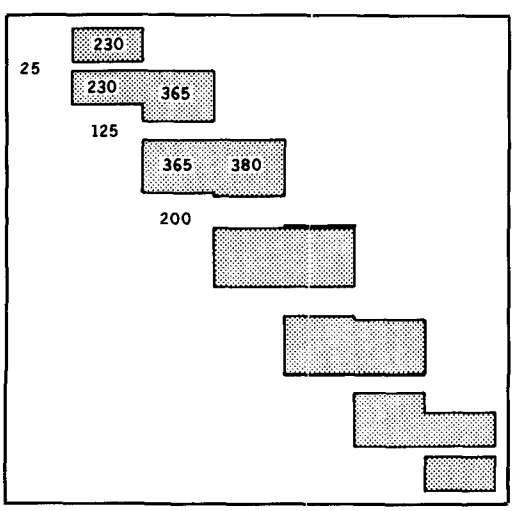

Figure 8. The finished filter to proportion (dimensions in mils; L = 574 mils).

Once you've defined the filter's primary characteristics, you're ready to execute the synthesis. **Figure 6** shows the required information inserted into the synthesis dialog. Clicking the mouse in "Synthesize" starts the procedure. In about 15 to 20 seconds (on a Macintosh SE), the output window shown in **Figure 7** appears. Any of the graphs or data windows may be written out to disk as a MacPaint file using one of the options from the "File" menu. **Figure 8** shows the finished filter, with dimensions for each filter section labeled. Because the filter is odd-order, it's symmetrical, and only the first half is dimensioned. Each coupled section is one-quarter wavelength long at the geometrical center of the passband, f_o.

Concluding Remarks

A large number of the required data inputs incorporate error trapping, so program operation should be very straightforward. The "g" factor shown in **Figure 7** is a convergence factor. A value of $g \geq 15$ indicates that the algorithm is having difficulty

reaching convergence. In such cases, widening the passband requirements or reducing the filter order may let you complete a successful synthesis. If the synthesis isn't converging, an alert notifies you of the problem. In most cases, I've found that if the exact dimensions given by Chebfilter are entered into Touchstone or SuperCompact, a return loss of 23 to 25 dB (VSWR $\leq$ 1.15) is generally found through the passband.

The program is available from the author for $10, if you provide your own disk, or $15, if the author must provide the disk and mailer. An additional description of the group delay calculation is included. ■

REFERENCES

1. G. Matthaei, E.M. Young, T. Jones, *Microwave Filters, Impedance-Matching Networks, and Coupling Structures*, Aertech House, 1980.
2. S.B. Cohn, "Parallel Coupled Transmission Line Resonator Filters," *IRE MTT*, April 1958, pages 253-231.
3. N. Volpicella, "Design Comb-Line and Parallel Coupled Filters," *Microwaves*, April 1979, pages 123-129.
4. S. Bharj, "Cal-Aided Lange Coupler Synthesis," *Microwave Journal*, January 1983.
5. "Accurate Wide Range Design Equations for the Frequency Dependent Characteristic of Parallel Coupled Microstrip Lines," *IEEE MTT-32* No. 1, January 1984, pages 83-90.
6. Harold L. Schumacher, "Dissipation Loss of Chebyshev Bandpass Filters," *The Microwave Journal*, August 1967, pages 41-43.
7. R.M. Osmani, "Synthesis of Lange Couplers," *IEEE MTT-29*, February 1981, pages 168-170.
8. T.C. Edwards, *Foundations for Microstrip Circuit Design*, John Wiley & Sons, 1981.
9. P. Silvester, P. Benedek, "Equivalent Capacitance of Microstrip Open Circuits," *IEEE MTT-20* No. 8, August 1972, pages 511-516.
10. Alan Tam, "Principles of Microstrip Design," *RF Design*, June 1988, pages 29-34.
11. G. Gonzalez, *Microwave Transistor Amplifiers, Analysis and Design*, Prentice-Hall, 1984.
12. I.J. Bahl, D.K. Trivedi, "A Design Guide to Microstrip Line," *Microwaves*, May 1977.

Appendix

Calculation of the g_i values:

$$\epsilon = \left[antilog_{10}\left[\frac{L_{AR}}{10}\right]\right] - 1$$

L_{AR} = attenuation at the passband edge
ϵ = passband ripple

$$\beta = Ln\left[coth\left[\frac{L_{AR}}{17.37}\right]\right]$$

$$a_k = sin((2k-1)\pi/(2n)) \quad k = 1,2,...n$$
$$b_k = \gamma^2 + sin^2(k\pi/n) \quad k = 1,2,...n$$
$$g_1 = 2a_1/\gamma$$

$$\gamma = sinh\,[\beta/(2n)] \qquad \text{where n = filter order}$$

$$g_k = \frac{4a_{k-1}a_k}{b_{k-1}\,g_{k-1}} \qquad k = 2,3,...n$$

$$g_{n+1} = 1 \qquad for\ n\ odd$$
$$g_{n+1}\ coth^2(\beta/4) \qquad n\ even$$

Calculation of the Z_{oo} and Z_{oe} for the filter:

For j=1 to n−1

$$\frac{J_{01}}{Y_o} = \sqrt{\frac{\pi\omega}{2g_0g_1}}$$

$$\frac{J_{j,j+1}}{Y_o} = \frac{\pi\omega}{2\omega'_1}\frac{1}{\sqrt{g_jg_{j+1}}} \quad for\ j = 1\ to\ n = 1$$

$$\frac{J_{n,n+1}}{Y_o} = \sqrt{\frac{\pi\omega}{2g_ng_{n+1}}}$$

$$\frac{\omega}{\omega'_1} = \frac{2}{\omega}\left[\frac{\omega-\omega_o}{\omega_o}\right]$$

$$\omega = \frac{\omega_2-\omega_1}{\omega_o}$$

$$\omega_o = \frac{\omega_2+\omega_1}{2}$$

$$Z_{oe_{j,j+1}} = \frac{1}{Y_o}\left[1 + \frac{J_{j,j+1}}{Y_o} + \left[\frac{J_{j,j+1}}{Y_o}\right]^2\right] \qquad j=0\ to\ n$$

$$Z_{oo_{j,j+1}} = \frac{1}{Y_o}\left[1 - \frac{J_{j,j+1}}{Y_o} + \left[\frac{J_{j,j+1}}{Y_o}\right]^2\right] \qquad j=0\ to\ n$$

where:
ω_o is the geometric center frequency
ω_1,ω_2 are the ripple frequencies

Calculation of group delay:

The calculation of group delay proceeds with the following equation. In this equation, each of the k poles is substituted to find its contribution to the total group delay.

$$Group\ Delay_{kth\ Pole} = \frac{-cos^2\left[\frac{\omega \pm \omega_k}{\sigma_k}\right]}{\sigma_k}$$

where:

ω is the frequency of interest
ω_k is the imaginary part of the kth pole
σ_k is the real part of the kth pole

Total group delay at $\omega = \Sigma$ delay$_k$
and the real and imaginary parts of the poles are given by:

$$\omega_k = cos\,[\pi(2k+1)/(2n)]cosh\left[\frac{1}{n}sinh^{-1}\left[\frac{1}{\epsilon}\right]\right]$$

$$\sigma_k = sin\,[\pi(2k+1)/(2n)]sinh\left[\frac{1}{n}sinh^{-1}\left[\frac{1}{\epsilon}\right]\right]$$

Cornell Drentea, *WB3JZO*

UPGRADING THE FT-ONE TRANSCEIVER

Improved synthesizer stability and a built-in 10-Hz digital display add new dimensions to an excellent radio.

With the cost of new radio equipment ever increasing, the need for modern used equipment has also grown. Remembering the old ham adage that good equipment can always be improved, I recently acquired a used Yaesu FT-ONE transceiver, upgraded it to long-term stability of ±2.5 Hz (room temperature) at any frequency within its range, and added a precise 10-Hz digital display to go along with this stability. The display has been incorporated into the radio's readout in such a way that it looks and feels like part of the original design. The upgrade is simple, and doesn't require changes in the electrical design of the radio. It takes advantage of existing features not fully used before.

The improvements described in this article are within the reach of any technically inclined Amateur and can be implemented totally or partially, as desired. However, I recommend you have a good understanding of how the FT-ONE's synthesizer and control circuits work before proceeding with the modifications. It would be helpful to read the FT-ONE service manual (available from Yaesu). I've tried to describe the modifications in sufficient detail here, but because of limited time, neither Yaesu nor I will be able

to provide additional information. Any mechanical or electrical modifications to your FT-ONE are made *at your own risk.*

Introduction

The FT-ONE is the forerunner of today's top-of-the-line radios. At an original price tag of over $2800, it was billed as the "super radio" which featured "unsurpassed performance" and was a "bold adventure in engineering." First produced in 1981, the radio was advertised as a breakthrough in spurious free dynamic range (SFDR), and still holds its outstanding reputation—even by today's standards. Its receiver exhibits superior performance, and is free of the phase-noise* and group/phase delay** distortion so common in some of the newer radios. The push-pull RF amplifier in the front end of its receiver uses high-power transistors with an intercept point exceeding +40 dBm, while doubling as a power amplifier predriver in transmit. The receiver uses a true high-level mixer approach equipped with Schottky diodes, a departure from the active balanced FET mixers used in other designs. Unlike some other radios, the first IF frequency of the FT-ONE is high enough (73 MHz) to keep the receiver remarkably free of images. (For good image rejection, the first IF of a radio should be at least 35 percent higher than the highest frequency of interest!)

The FT-ONE has outstanding IF filters and continuous bandwidth passband tuning which rival any Amateur or professional radio on the market today. The system can provide up to twenty-two poles of filtering in receive. Its unique front-end attenuator allows a wide AGC range. The FT-ONE's full-featured transmitter and receiver can provide coverage of any WARC or MARS bands now, or in the future. It features an automatically switched low-pass filter system designed for true rejection of harmonic content of better than 50 dB on any frequency within the transceiver's range. This is a feature not found on most other general coverage transceivers[2]. The packaging and reliability of the FT-ONE are unconditional, with G-10 boards used throughout in a plug-in approach. The rig uses quality Hewlett Packard displays and recognizable logic families.

Room for improvement

Although an outstanding design from a radio point of view, the shortcomings of the FT-ONE have been widely publicized in the literature.* Long-term stability has been one of the main complaints. First, the rig has been known to drift over long periods of time—a problem attributed to its synthesizer design. Many fixes have been offered, including painting the walls of the synthesizer enclosure black! Second, the rig doesn't have a 10-Hz digital readout, even though it tunes in 10-Hz increments—a feature considered mandatory today in RTTY or packet work.**

My recently acquired FT-ONE (lot 6) was no exception to these problems. I found it to be off in frequency by about 600 Hz. There is a good way to find out how far off frequency your FT-ONE may be without using expensive counters. Program in any active WWV frequency and listen in the SSB mode for the 500 or 600-Hz tones broadcast by this station as you switch between the upper and lower sidebands. If your radio is right on frequency, you'll hear the WWV tones (500 or 600 Hz) equally when switching between the two modes, and when the digital dial shows the exact expected frequency (5 MHz, 10 MHz, etc., for example). If you have a calibration/drift problem, there will be a difference between the two tones when the display shows zero beat. Tuning the main dial to hear the tones equally in frequency between the two modes will indicate the amount of drift as read directly from the digital readout. (When zeroing in with the FT-ONE, you must make sure that your dial is closest to the nearest 100 Hz on the display because the digital display doesn't show 10 Hz increments.) If a separate AM receiver is available, listen to the WWV tones concurrently with both receivers to match the received SSB tones with the AM detected tones. This will let you hear beat frequencies between the two receivers and modes of only a few Hz. By performing this test at periodic intervals from a cold start, you can plot out the rig's stability in time.†

*Phase noise is a short-term stability problem caused either by noisy reference oscillators, or by digital transients generated in the synthesizer's dividing chains. When used with noise-sensitive phase comparators and low-Q, wide-range VCOs, phase noise can reflect back into the IFs of radio receivers and transmitters affecting the received noise floor and the transmitted signal.

**Group/phase delay distortion impacts radio-data communications like RTTY or packet radio. It is caused primarily by inexpensively designed IF crystal filters, and shows up as IF and audio distortion which in turn interferes with the AGC systems of radio receivers, causing lost data.

*See all *International Radio Newsletters* published since 1982.

**The radio is equipped with a mechanical readout which can approximate 10 Hz resolution when calibrated properly.

†This procedure can also be applied to other synthesized radios.

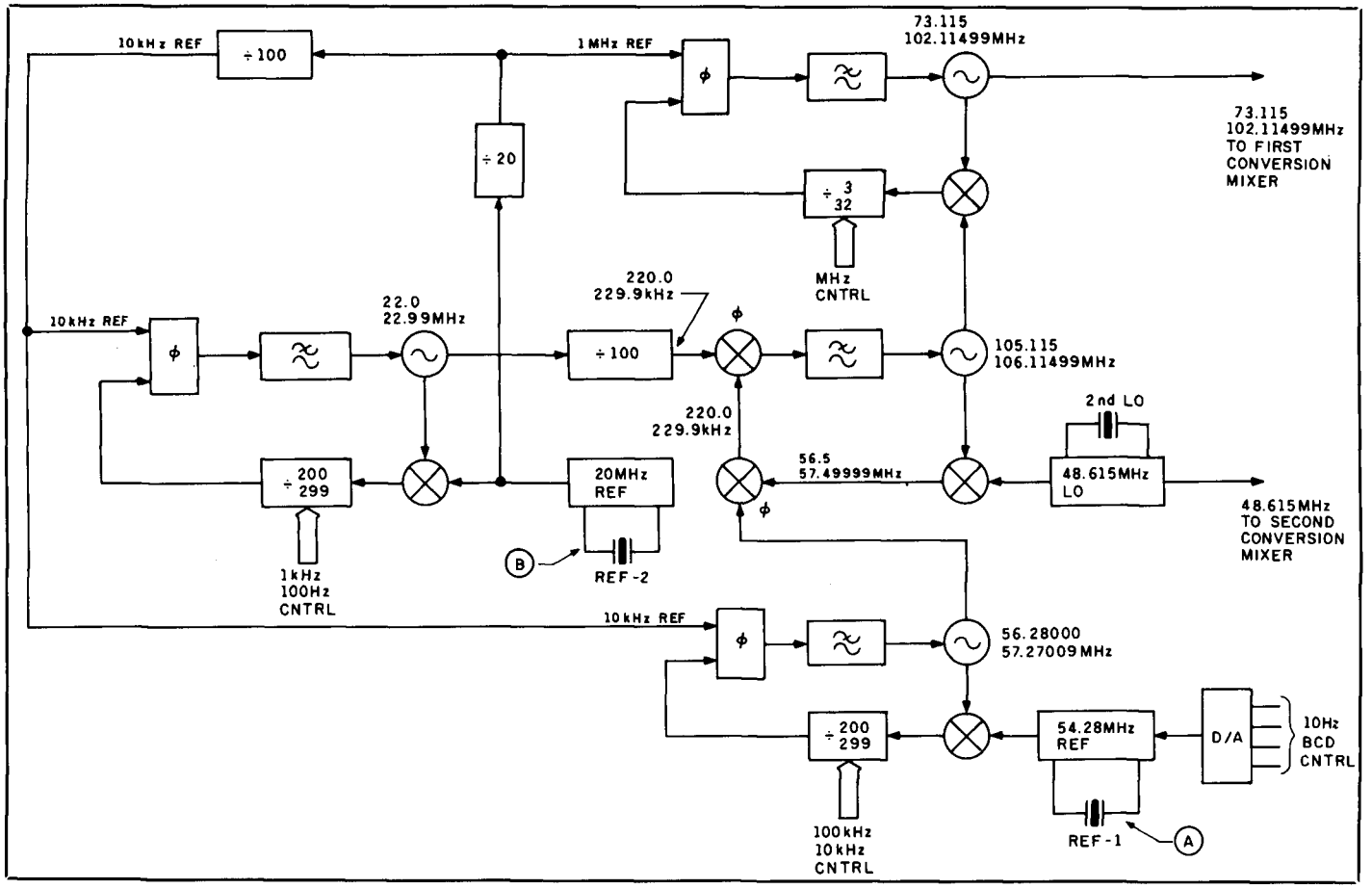

Figure 1. Block diagram of the FT-ONE's synthesizer shows that the radio's stability depends mainly on two reference oscillators running at 54.28 MHz (A) and 20 MHz (B).

Troubleshooting the drift

A quick look at the radio's block diagram revealed that the FT-ONE's engineers designed its synthesizer based on at least two important reference oscillators operating at 54.28 and 20 MHz. This means that the entire stability of the radio is based on more than one frequency source, and these sources can drift independently of each other and create problems (see **Figure 1**).

Elegant synthesizer design calls for mathematical derivation of all frequency sources (including the BFO) from a single reference oscillator[3] which isn't the case in the FT-ONE or many other modern Amateur transceivers. This is called full-frequency synthesis and requires a much more involved design process. In such a design, the job is to find the proper relationship between a main reference crystal oscillator, preferably running at nonfractional frequencies of 10 MHz or below, and derive all other frequencies from it. Although stable, VHF TCXOs (temperature-compensated crystal oscillators) have been produced recently with some success, conservative designers are still using the lower frequencies when it comes to reference oscillators (see Mil-Spec 1030 by Signal One which uses a 10-MHz reference for all oscillators in the radio). The reason for the relatively low reference frequencies is very simple. Temperature drift and crystal aging are much more manageable at lower frequencies than at higher ones. The FT-ONE's reference oscillators are shown in **Figure 2**.

The main reference oscillator in the FT-ONE runs at 54.28 MHz, an unusually high frequency for a reference oscillator (and a fractional number). The second reference runs at 20 MHz, a more manageable frequency. **Figure 2** shows that there are two parallel-series capacitors (one a trimmer) intended for calibrating the frequency of the crystals in the series-resonant tuned crystal oscillators. If these elements change their values over room temperature, the reference frequencies and, consequently, the rig's entire stability suffers. These capacitors must be compatible with the very high sta-

bility of the crystals in order to keep the radio's stability high. A quick look at my FT-ONE's 54.28-MHz crystal showed that it was totally out of specification due to aging, and couldn't be brought to the right frequency via its trimmer capacitor. Replacing this crystal with a new one from Yaesu corrected the immediate problem. However, a wandering drift of about ±100 Hz still remained in response to room temperature changes. This drift was within the manufacturer's specifications of 300 Hz, but still wasn't up to today's standards of 10 Hz or better. **Figure 3** shows the plot of the unmodified rig's frequency stability at room temperature.

A close look at the PLL unit's "guts" (PB-2257) indicated that the series trimmers and ceramic capacitors in the reference oscillators, which work in conjunction with the crystals in both reference oscillators, weren't compatible with this high-stability requirement (see test which follows). Also, the ratio of capacitance between the trimmers and the fixed capacitors was large, with the trimmers carrying most of the stability.

The solution

I decided that much more stable trimmers were needed in the circuits to improve long-term drift. In addition, I felt a better ratio between the capacitors would be desirable, especially in the 54.28-MHz reference oscillator. I needed a ratio that would base its stability on the fixed element, rather than the trimmer.

First, I performed a test by removing the 20-pF TC02 trimmer and C 218 (6 pF) from the 54.28-MHz oscillator. The capacitors were tested on the bench for capacitance changes over drastic temperature variations with the help of a digital capacimeter capable of reading to 0.1 pF. A change of 0.2 pF per degree C was found. I concluded that, over room temperatures, and at 54 MHz, this translated into at least ±100 Hz drift. The same was true (but to a lesser extent)

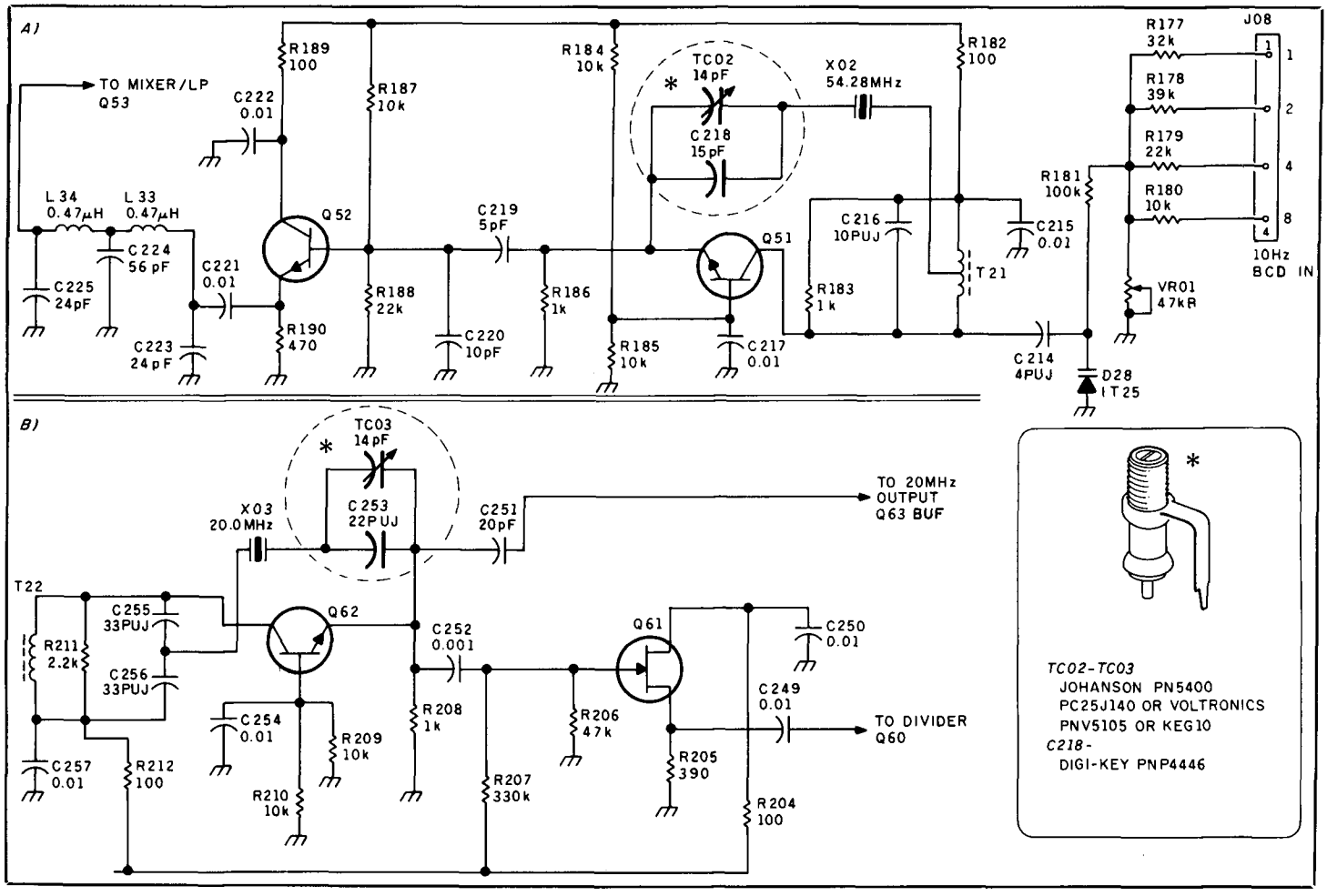

Figure 2. Schematic diagram of the FT-ONE's reference oscillators (A) 54,28 MHz, (B) 20.0 MHz, and a quick look at the synthesizer implementation reveals stability problems caused by the trimmers and fixed series-parallel capacitors in the circuits.

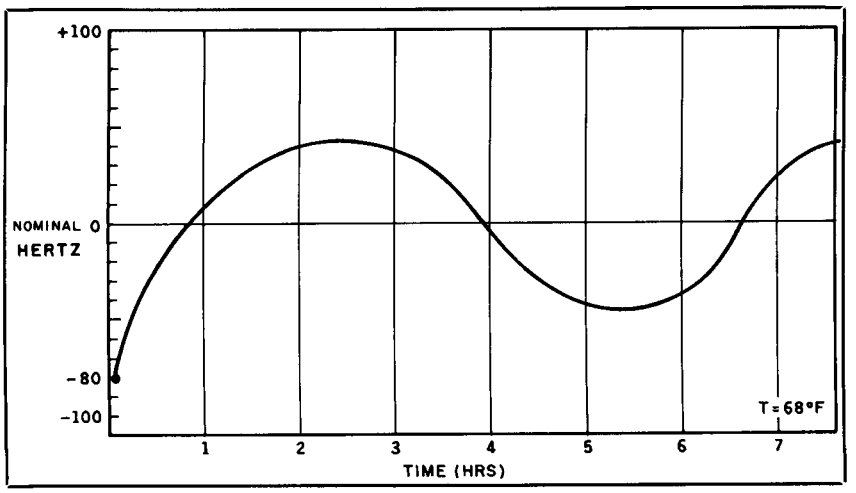

Figure 3. Frequency drift plot of the author's lot 6, unmodified FT-ONE at room temperature (68 degrees F) over time.

with the capacitors in the 20-MHz reference oscillator.

I substituted a 15-pF NPO capacitor for the fixed value, and replaced the original plastic-encased trimmer with an unconditionally stable 14-pF multi-turn air-piston trimmer from Johanson (part no. 5400 PC25J140). PC mountable precision trimmers can also be obtained from Voltronics or Trim-Tronics. Try the Voltronics V5105 or

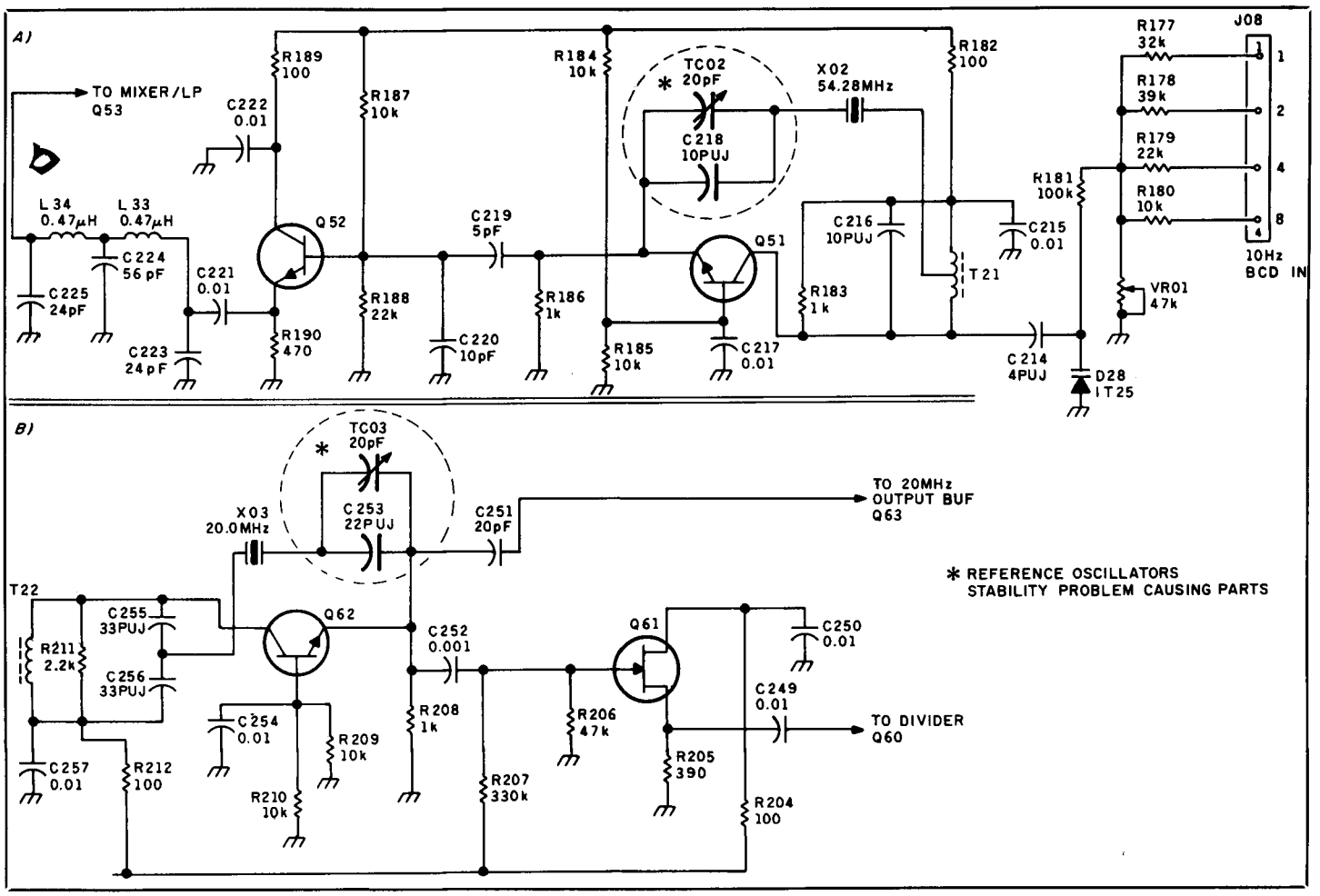

Figure 4. Modified reference oscillators in the FT-ONE feature new ratio between trimmers and fixed capacitors (54.28 MHz). The parts used are very high-quality precision piston trimmers, and NPO capacitors.

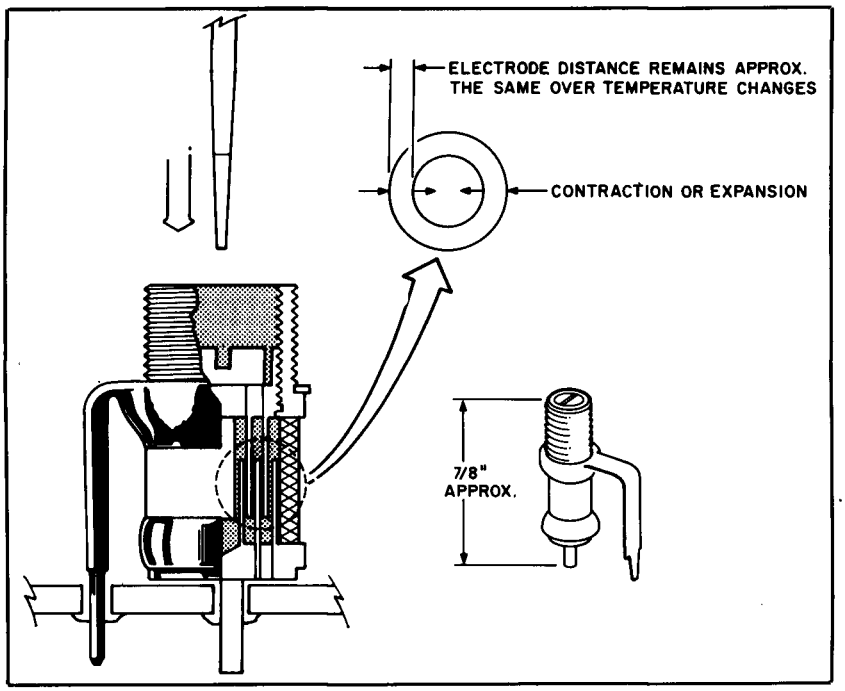

Figure 5. Construction of air-dielectric precision trimmers makes capacitance changes over temperature minimal. First, the air dielectric keeps capacitance shifting to a small value. Second, the concentric construction of electrodes keeps mechanical shift over temperature constant because the distance between the electrodes remains almost constant over a wide temperature range.

KEG 10 (a smaller model which costs about $6 per unit in quantities). If these sources are too expensive, or not accessible to you, reasonably priced precision trimmers can sometimes be found at hamfests. The same type of part was used in the 20-MHz oscillator, but I only changed the trimmer. The schematic diagram of the new circuit is shown in **Figure 4.**

The reasons for these changes were very clear. First, in a typical trimmer, capacitance changes are caused by shifting of the metal parts against the solid dielectric as temperature is raised or lowered. This capacitance shift can be extensive in sandwich-type trimmers.

In an air-piston trimmer, this shift is minimized by the use of an air dielectric. The concentric ring construction of the pistons also allows them to expand equally and in the same direction, keeping the electrode-to-electrode distance constant over temperature changes, as shown in **Figure 5.**

A near-zero capacitance change results—a very desirable feature for this application. In a multi-turn piston trimmer, this capacitance change is typically on the order of 50 PPM/degree C worst case over −55 C to +125 C. Consequently, for a temperature change of 1 degree, such a capacitance would change by only 0.001 pF for a trimmer capacitor adjusted to 9 pF. This would be considerably better by several orders of magnitude than the original plastic-encased trimmer adjusted for the same capacitance.

The same idea applies to the fixed capacitor. I used an NPO known for maintaining its capacitance over a certain temperature range. The 15-pF Digi-Key part no. P4446 I chose guarantees a maximum capacitance change of ±5 percent from −55 to +85 degrees C. This translates to 0.01 pF per degree C at 15 pF. With such wide temperature ranges and rigorous tolerances, these over designed parts will drift little at room temperature changes.

I performed the bench temperature test again using the new parts. The capacimeter didn't register any change as the two parts were heated and cooled over extreme temperature ranges using a hair dryer and freeze spray. The new parts were soldered onto the synthesizer board, and the radio was calibrated using the WWV test mentioned previously. Over the next several days, I performed an extended frequency stability test. No frequency drift larger than ±2.5 Hz was observed after warmup (measured with laboratory instrumentation). This performance is shown in **Figure 6.**

If you intend to perform this modification, it's important that you ground yourself against static electricity before removing the synthesizer assembly from the radio. This

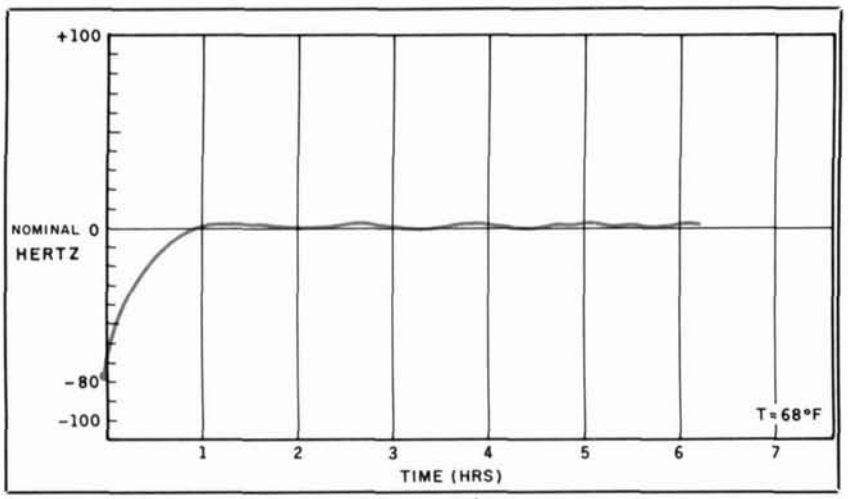

Figure 6. Plot of the frequency stability for the modified FT-ONE. Actual drift doesn't exceed ±2.5 Hz after warm up.

also applies when unsoldering and resoldering parts on the board itself. You can use solder wick to remove the original capacitors, but be careful not to destroy the copper foil in the layout. The capacitors in the 54.28-MHz oscillator TC02 and C218) are located in the middle top portion of the synthesizer board as viewed from the component side. The 20-MHz TC03 is located on the top left side of the board as viewed from the component side. The FT-ONE technical manual will prove invaluable for locating these parts. **Photo A** shows the implementation of these modifications in the FT-ONE synthesizer.

The 15-pF NPO capacitor replaced the old C 218. The precision piston trimmers install vertically at TC02 and TC03. They may be secured to the board with a touch of epoxy. Holes can be drilled into the synthesizer cover to allow for adjustment without removing the cover. In my FT-ONE, I've provided a hole for adjusting the 54.28-MHz reference through the side of the case—a feature usually found on other transceivers. If you intend to do the same, this hole should line up precisely with the one in the synthesizer cover. The ability to adjust the 54.28-MHz reference in the synthesizer without removing the covers proved to be a very useful feature because the rig exhibits different thermal characteristics when buttoned up. There's no need to do the same for the 20-MHz trimmer.

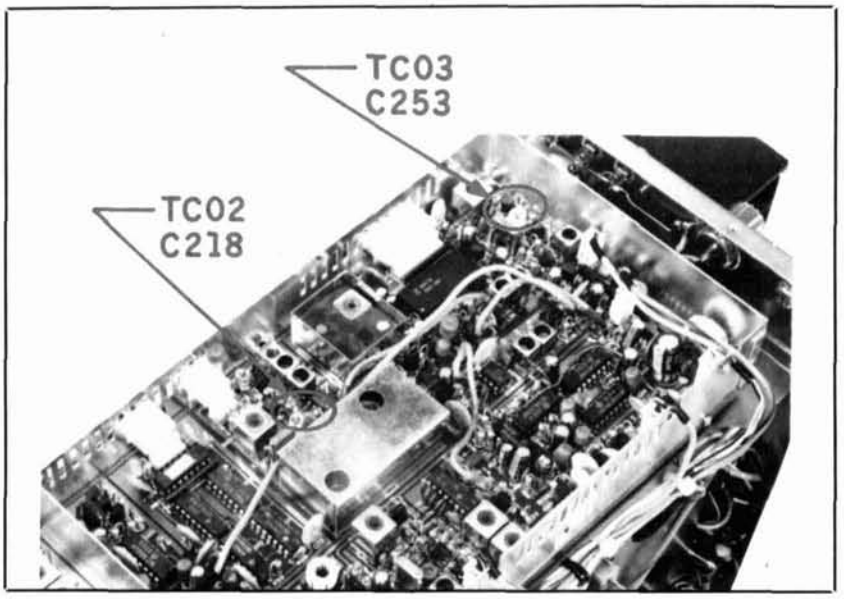

Photo A. Implementation of the high-stability modifications in the FT-ONE's synthesizer. Arrows show the location of parts that have been changed.

Calibrating the FT-ONE

To calibrate the radio, turn it on and observe the digital display. With all things working, you should have a steady readout. If the readout is blinking, it means that one or both of the oscillators aren't functioning. This can be caused by several things. First, the calibration of the trimmers could be out of range. This can be particularly true for the 54.28-MHz trimmer. If this is the case, turn the rig off and readjust the trimmer in one direction with the help of an insulated screwdriver. Remove the screwdriver and turn on the rig again. Repeat the adjustment in both directions for both oscillators until the display doesn't blink anymore. Don't forget to turn the rig off after each adjustment, or the display won't reset. If the oscillator doesn't start working, it probably means that your 54.28-MHz crystal has aged and needs replacing.

If things are in the ballpark, the radio should come back with a stable display every time the power is turned on and off. Once you've reached this point, leave the radio on for at least two hours before making the final adjustments. Make sure that the room temperature environment resembles that of your actual operating environment. In my case, this was about 68 to 70 degrees F.

The next step is to adjust the 20-MHz reference oscillator. With the radio opened, and looking at the front panel, set the "FINE" button to off (out). Connect the RF probe of a voltmeter and a precise frequency counter to pin 27 on the MJ8 connector, which is accessible through the bottom of the transceiver. Using an insulated screwdriver, adjust TC03 in the 20-MHz reference oscillator for an exact 20-MHz reading. If needed, adjust TC6022 for a reading of 160 to 240 mV RMS on the meter. If you don't have these tools, the 20-MHz oscillator can also be adjusted by tuning the radio to the 20-MHz WWV station and zero beating it against the internal 20-MHz oscillator which can be heard in the radio. Carefully adjust TC03 for the same tones to be heard in the speaker. To avoid confusion, do this by matching the beat tones when WWV doesn't transmit 500 and 600 Hz tones (at 45 minutes after the hour). Once you've completed this adjustment, reinstall the covers and wait for another half hour before proceeding. Then, adjust TC02 in the 54.28-MHz reference oscillator through the rig's side panel. This should also be done with the insulated screwdriver using the WWV procedure explained earlier. The multi-turn trimmer should be tuned exactly to the required frequency when the WWV tones are the same in upper and lower sideband and the digital display shows zero. When the adjustment is complete, the frequency won't move if room temperature remains within ±5 degrees F. The rig will stabilize consistently to the adjusted frequency from a cold start within an hour. Depending on the room temperature, it will start up about 80 Hz low in frequency and quickly arrive near the nominal frequency, with the last 10 to 20 Hz taking most of the time (see **Figure 6**). After the warm-up period, it will always be on frequency, regardless of where in the HF range the radio is tuned.

Some high-tech possibilities

I'm happy with the new stability of my FT-ONE. These simple modifications show that the rig's stability problem is very manageable and is caused mainly by one reference oscillator (not several as rumored). A TCXO circuit could be implemented by the more ambitious Amateur to compensate for the warm-up drift. Such a circuit could use a varistor to read the board's temperature rise and change the DC voltage to a varactor diode in the 54.28-MHz oscillator. The voltage curve produced by the varistor would ideally reverse mirror the frequency drift curve from **Figure 6**. Other possibilities include providing a programmable timer digital count-up circuit instead of the varistor, which would drive a digital-to-analog (D/A) converter. This, in turn, would drive the varactor circuit. The timer would have a variable rate reflecting the oscillator's drift curve from **Figure 6**. Although such design additions would be interesting from an amateur scientist point of view, they are commonly used by today's electronic industry. I've been satisfied with the stability provided by the simple modifications suggested in this article.

Displaying to 10 Hz

With the radio's improved stability, and because of the 10-Hz tuning steps, I thought it would be nice, and even necessary, to have a 10-Hz display.

A quick analysis of the synthesizer design indicated that the radio's 10-Hz resolution is achieved by using a BCD counter to add voltages in a simple D/A converter made of resistors (see **Figure 7**).

In this design, the binary count rolls over after reaching number 9. The resulting volt-

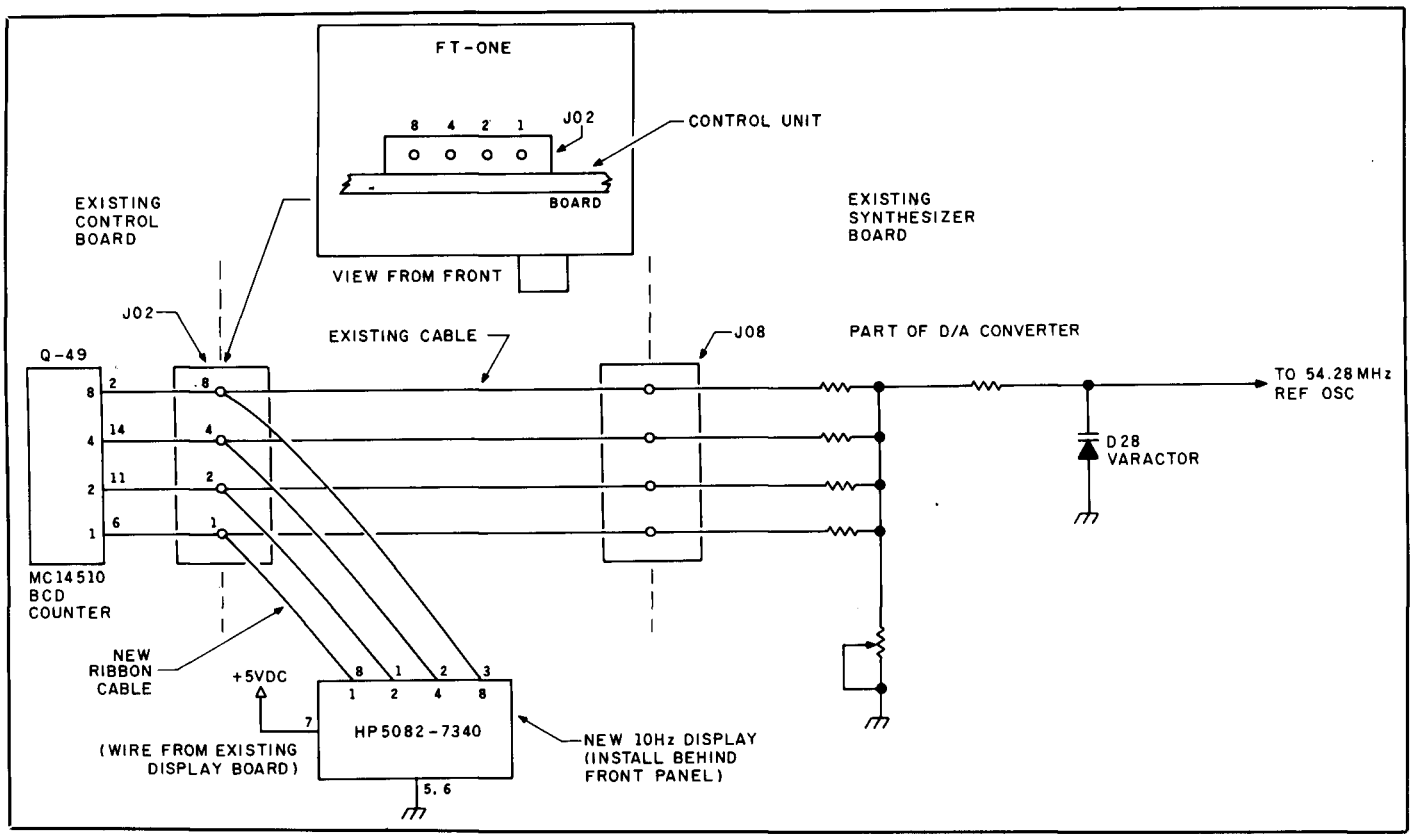

Figure 7. The FT-ONE's 10-Hz mechanism uses a BCD counter and a D/A converter to stir the 54.28-MHz reference oscillator over 100 Hz through the D28 varactor. The 10-Hz digit addition simply decodes and displays this parallel BCD information, which is readily available on the control-unit board at JO2. It requires only four wires and a display equipped with a built-in BCD decoder which can be mounted behind the front panel on the right side of 100-Hz display, just as if it were designed in.

age is applied to a small varactor (D28) in the 54.28-MHz reference oscillator. As the count goes from 0 to 9, the voltage causes the varactor to pull the 54.28-MHz crystal oscillator over a 100-Hz range, and a 10-Hz resolution results. However, this simple design is no substitute for complex synthesizers which use extra loops and direct digital synthesis (DDS) to achieve 10-Hz resolutions[3]

Implementing the 10-Hz display

The schematic diagram of the 10-Hz addition is shown in **Figure 7**. I used an HP 5082-7340 in my transceiver, but you could use other similar devices. The 7340 is a numeric hexadecimal indicator from Hewlett Packard. It has a built-in BCD decoder and a driver in one small package, and interfaces directly with the existing FT-ONE circuits. I chose this display to eliminate the use of additional parts and boards which would result in a cumbersome implementation. It's an elegant approach to achieving design simplicity. A transparent square window has been provided in the plastic front panel. Etching this window is by far the toughest job in the entire project and will test your patience, skill, and dexterity. First, lets look at the feasibility of implementing this feature. The FT-ONE's display pc board has ample space between the last digit and the "clarifier" display to allow a small board containing the 10-Hz display to be installed. Although not necessary, the more ambitious Amateur could even lay out a new display board which could contain the 10-Hz display (see **Photo B**.

Power to the 10-Hz display can be provided from the display board itself. **Photo C** shows my implementation of the 10-Hz addition in the display board of the FT-ONE. As I mentioned previously, a four-conductor ribbon cable carries the BCD information to the 10-Hz display directly from the control-unit board (connector JO2) located in the immediate proximity.

The HP 5082-7300 is among the other displays which could be used for this addition. An array of ten LEDs has also been

Photo B. The 10-Hz display has been implemented behind the front panel of the FT-ONE.

breadboarded to allow for a bar graph approach. This approach can be used independently, or in addition to the seven-segment display. The array has the feel of a mechanical dial and could be installed in small holes located in the square metal face just below the main digits. Miniature amber LED's can be used as indicators. A circuit diagram using CMOS logic compatible with the FT-ONE's original design (and mechanical layout) is shown in **Figure 8**. The bar graph approach can be used by itself, or in conjunction with the digital display. If you don't want to, or can't, implement these additions inside the FT-ONE, you can incorporate the changes into a small utility box and place it on top of the radio.

Now, let's look at what it takes to include the 10-Hz display behind the front panel of the FT-ONE. Again, this is the boldest of all approaches. First, remove the top of the radio. With the top off, unplug the control unit board (first board closest to the front). Detach all connectors carefully before completely extracting the board from the radio. Removing the board will give you space to work behind the front panel. Your goal is to get at, remove, modify, and reinstall the plas tic window so the new display shows through a transparent window located between the 100-Hz display and the clarifier display. This isn't a job for the beginner, so if you don't want to implement the display in the radio, you can always build an external box and wire it in.

Using a short Phillips screwdriver, unscrew and remove the display board through the back of the radio. The plastic

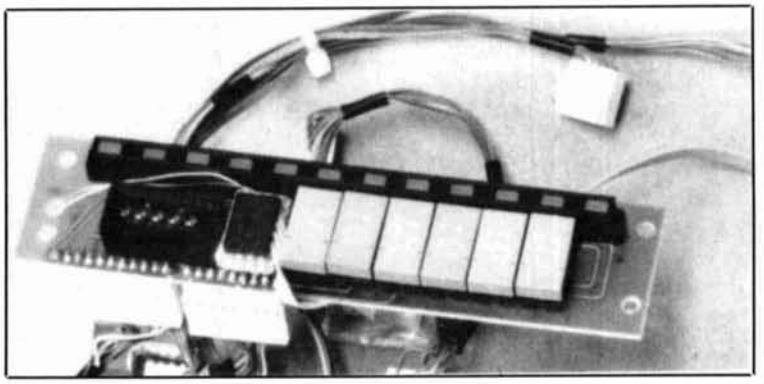

Photo C. Actual implementation of the 10-Hz display in the display board of the FT-ONE.

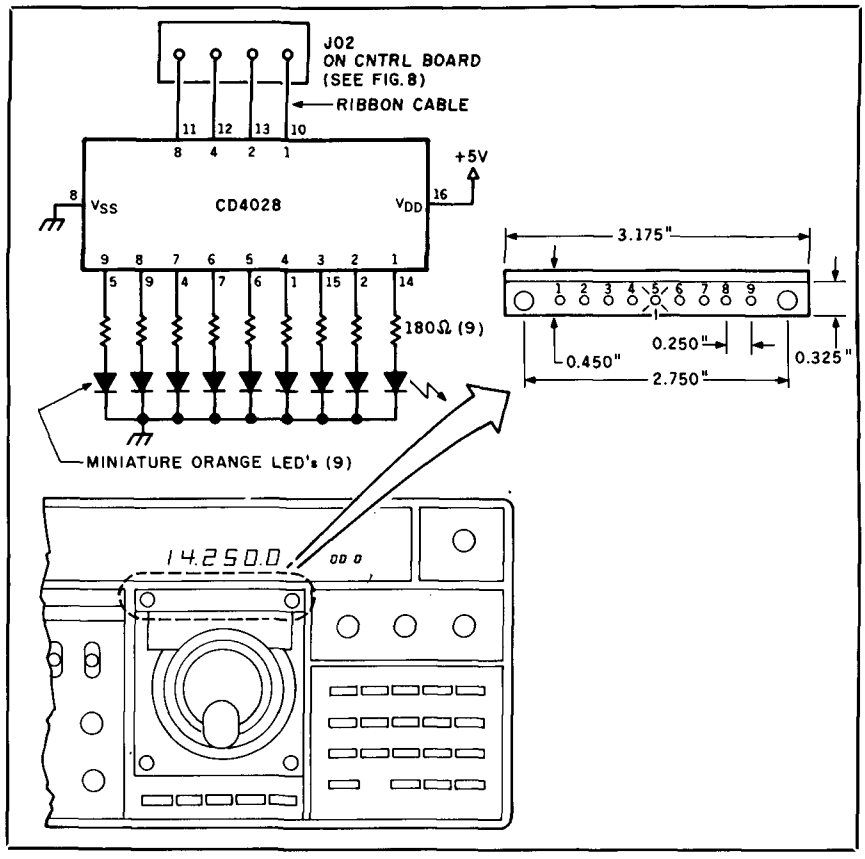

Figure 8. Schematic diagram (and mechanical layout) of a BCD-to-decimal decoder which can provide a bar graph approach to the 10-Hz readout. The LED's can be installed in the square front plate below the main digits. The bar graph approach can be used by itself, in addition to the extra digit approach, together with it, or in a separate box located outside the transceiver.

window will now be exposed through the back. Carefully unscrew the assembly containing the two meters, and rest it toward the back of the radio where it's out of the way. The entire transparent front-panel window is now exposed from the back. Carefully remove the two screws holding this piece, and slide out the window assembly through the left side of the radio. You may have to temporarily remove the meter switch located in the top left corner of the radio to make space for the window to be removed. This can be done from the front panel. Make sure not to scratch the plastic piece in the process. With the window out of the radio, you are ready to proceed. First, lay the window flat on a smooth surface with the painted surface up. Use masking tape to mask out a square window equivalent to the size of your display, exactly half way between the main display window and the clarifier window. Make sure that the new window bottom lines up exactly with the bottom of the main display window. Use good quality masking tape, because you'll be using chemicals to etch out the 10-Hz window. Purchase some lacquer thinner from a paint or hardware store. Lacquer thinner is a very powerful solvent which, among other things, will remove the silk-screen paint from the back of the plastic without affecting it. (Lacquer thinner can also be used to remove flux from pc boards.) If you're hesitant to remove the paint yourself, you may wish to take your window to someone who does silk screening and have them remove it.

To get the hang of things, dip a Q-tip into the thinner and gently rub out a corner area of paint which is not exposed through the front panel. This will give you a feel for the time it will take to remove the paint and how transparent the window will be. Now start rubbing the area inside the masked square. Exchange dirty Q-tips for clean ones as often as possible, and continue the process until you have a transparent square window. If you haven't succeeded in obtaining a perfect square, don't panic. You can later mask the cutout in reverse, along with the

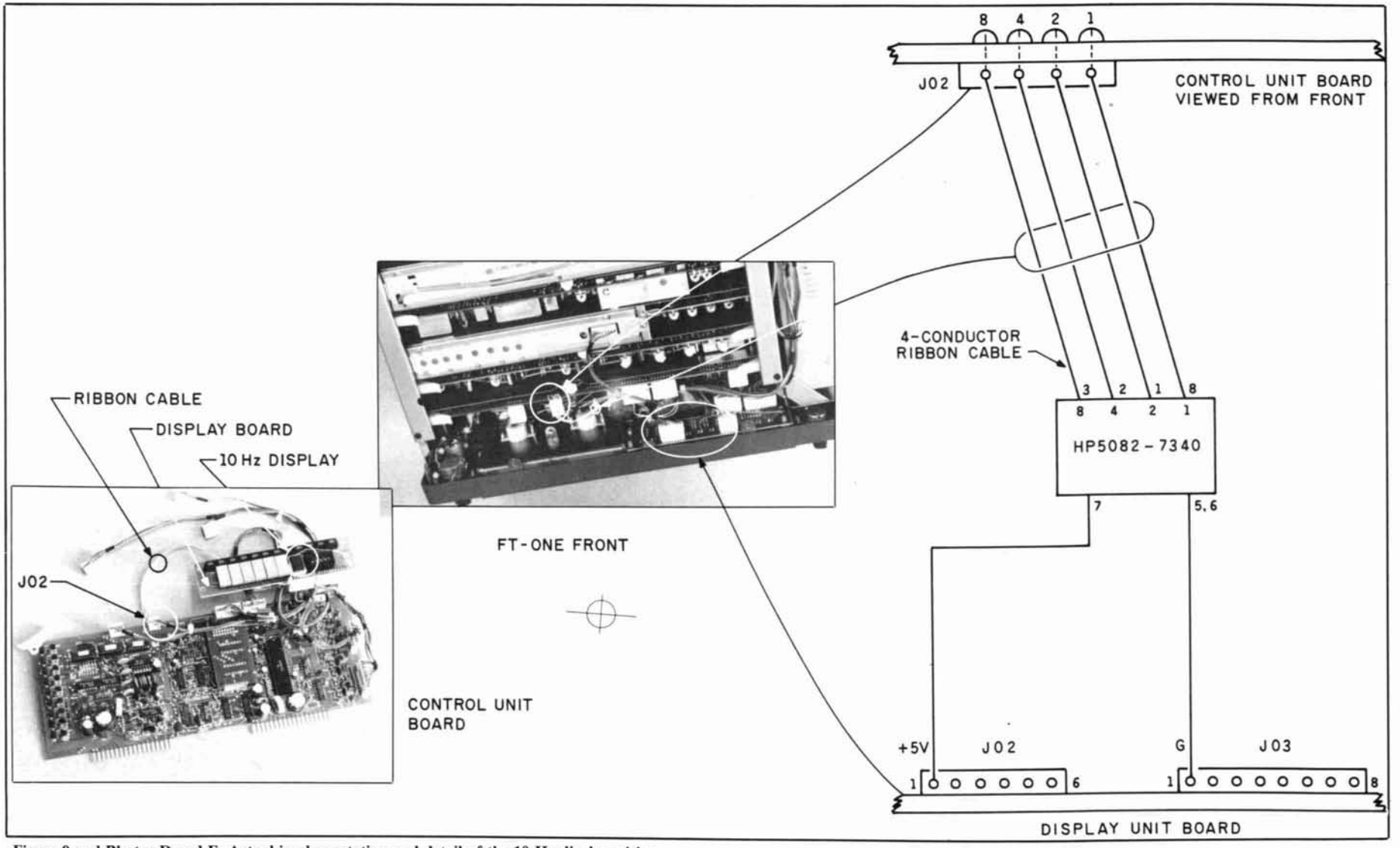

Figure 9 and Photos D and E. Actual implementation and detail of the 10-Hz display wiring.

rest of the layout, and spray paint the back of the entire window with flat black to create a good square cutout which looks like it belongs in the layout. Again, you need to be skillful and precise about this part of the modification. (If you damage your window, there's still hope. Yaesu will sell you a new one for a nominal fee. Order smoke filter part no. R7072790A.) Once you've passed this point, the rest of the project is very easy. Tape a piece of transparent red plastic over the window from the back. This will keep the display hidden, but will pass the light from it. Simply reinsert the entire plastic assembly back into the transceiver and tighten all screws. Put meter assembly in its place and reinstall meter switch from the front panel.

Obtain a small pegboard with holes centered on 0.100 inch. Cut it into a square that slightly exceeds the size of your digital display. Insert and bend the pins of the digital display through the holes. Wire the display with a 10-inch long, four-conductor flexible ribbon cable. Solder the +5 volt DC and ground connections as shown in **Figure 9** (which includes **Photos D** and **E**). To do so, you'll have to route two wires (you can use wire-wrap type wire) through one of the holes in the board to the other side for soldering. Then, solder the other end of the ribbon cable into the back of connector JO2 located on the control unit board as shown. Don't forget to ground yourself before touching the sensitive circuits in the FT-ONE.

When connecting the ribbon cable, make sure that the right BCD numbers of the display (1,2,4,8, for example) go to their corresponding number in the connector. This is also shown in **Photo C**. Now you're ready to complete the job. Purchase a couple of pads of double sticky tape (about 1/8 inch thick) and cut them to the little display's board size. Make a sandwich out of the two pads (1/4-inch thick), and apply it to the back of the board. Apply the entire assembly to the FT-ONE's display board at the exact spot between the main display and the clarifier display (**Photo C**). The 10-Hz display should now lineup with the rest of the displays on the board. You may have to readjust the position of the 10-Hz display a few times before tightening the screws. Simply reinsert the control-unit board and reinstall the display board in its place. Watch the position of the 10-Hz digit through the front panel window and readjust if necessary. Finally, tighten all screws. The 10-Hz display should now lineup and be vertically oriented, showing in the center of your new window. The pressure of the double sticky tape will keep the display pressed firmly against the front-panel window from the inside. You are now ready for the smoke test. If everything was wired correctly, your 10-Hz display should light up and read zero when you turn the power on. The display will always reset to zero on power up. Depressing the "FINE" button will also reset the 10-Hz display to zero. With the "FINE" button pushed in, tune across the band. The display should show the correct 10 Hz your radio is tuned to at any given time. If the rig is warmed up and calibrated properly, "what you will see" should be exactly "what you should get" at any frequency. The display will reset and stay on zero when tuning in 100-Hz steps. There will be no need for the mechanical dial which approximates the 10-Hz resolution. And now, for the final touch. With the display installed and working, you'll need to go back to the 54.28-MHz reference trimmer, and recalibrate it slightly after warm up. This is necessary because the BCD lines which activate the D/A converter in the oscillator will now have an extra digital load (the display's inputs) which will change the resulting voltage (and, consequently, the frequency of the oscillator) slightly. This completes the FT-ONE modifications.

Conclusions

This article was intended to show how to upgrade the Yaesu FT-ONE transceiver for improved stability, and take advantage of that stability by displaying it to the last 10 Hz. In doing so, the FT-ONE can be considered an upgraded radio which need not take second place to any piece of modern equipment. I hope you'll take full advantage of these simple and effective modifications, which will bring your FT-ONE transceiver up to today's standards. I'd like to thank Chip Margelli, K7JA, of Yaesu USA for pro viding useful information during the process of redesigning my FT-ONE transceiver. ■

REFERENCES

1. Cornell Drentea, *Radio Communications Receivers*, TAB, 1982.
2. Cornell Drentea, Lee R. Watkins, "Automatically Switched Half-octave Filters," *Ham Radio*, March 1988.
3. Cornell Drentea, "Designing Frequency Synthesizers," RF Expo-1988, Anaheim, California.

Marv Gonsior, *W6FR*
418 El Adobe Place
Fullerton, California 92635

TX IMD PERFORMANCE AND MEASUREMENT TECHNIQUES

Measure your transmitter's linearity performance without a spectrum analyzer.

Here are two techniques for measuring transmitter linearity performance which are applicable to all types of single sideband equipment. The first, and conventional measurement procedure, dictates the use of well-calibrated laboratory-grade test equipment—basically, a spectrum analyzer. However, a much less conventional, alternative method is available which provides essentially the same data and doesn't require costly equipment.

Background

In an earlier article, I discussed the intermodulation distortion (IMD) characteristics of the Kenwood TS-930S.[1] IMD is defined as the "measured distortion of a linear amplifier as expressed in power in decibels below the amplifier's peak power, as generally specified for Amateur equipment, or below that of one of two [equal] tones employed to produce the complex test signal."[2] Those test data revealed that the laws of physics still hold true today. Generally, you reduce the output to a minimum required; employ the minimum VSWR between the exciter and its load, with the use of a tuner, if necessary, to preclude the shutdown mode which generates distortion; operate as close to Class A as the situation permits; and use proper loading and minimal or no speech processing. If you adhere to all of these principles, you may expect to obtain the highest quality signal possible—provided that any further amplification is *fully* capable of linearly reproducing the input signal. This means that a following amplifier must be at least −6 dB more linear than the exciter when the distortion voltages could add in phase, or −10 dB better to minimize, if not eliminate, any degradation of the exciter. I believe that too few amplifiers will stand this test.

An alternative IMD measurement technique

Recently, I tried a significantly different and simplified IMD measurement technique, suggested by Dan Hearn, N5AR, with exceptionally good success. Amateurs who have some basic equipment can obtain some reasonably good TX IMD measurements, because many modern radios have narrow-band filters (not mandatory, but very desirable), as well as a good dynamic range of at least 90 dB.

In addition to a good receiver, you'll need a shielded dummy load, a two-tone generator, and a step attenuator. The step attenuator is necessary because some S meters may not be linear, nor sufficiently accurate. You could dispense with the step attenuator and rely on the S meter **for relative readings only** unless it is exceptionally well calibrated. Refer to **Figure 1** for the block diagram of the test setup.

Using a TS-950SD as my test transmitter and a TS-930S as my measuring instrument

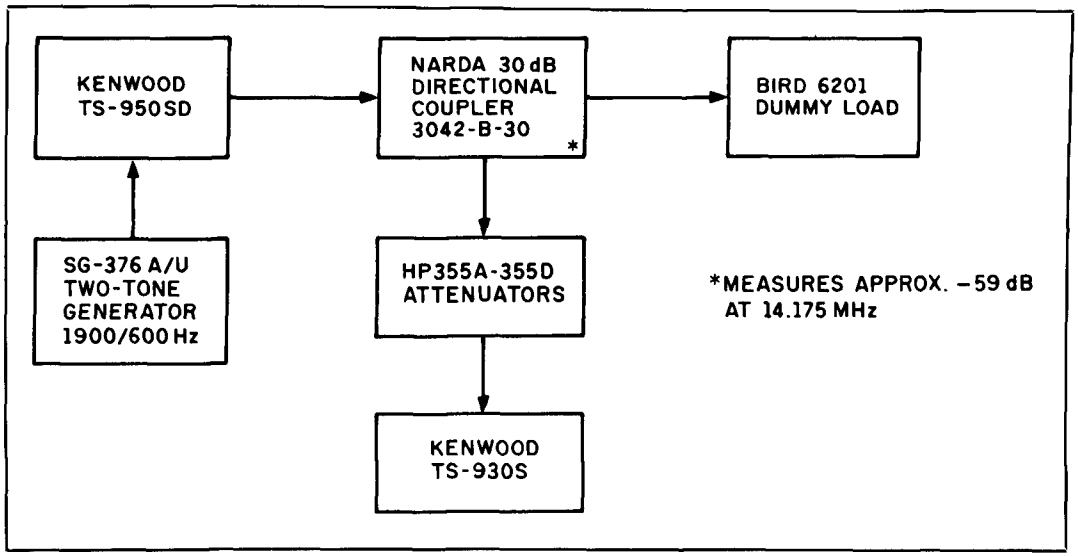

Figure 1. Block diagram of the alternative IMD test setup.

with cascaded 500-Hz filters, I obtained some rewarding results which essentially verified those of my spectrum analyzer. This isn't really surprising because the analyzer is basically nothing more than a sophisticated combination of a swept receiver, with very high selectivity, and a display. Consequently, it became apparent to me that odd-order distortion products could be observed and measured on a good *well shielded*, or isolated, *reasonably selective* receiver. In other words, the receiver becomes a selective RF voltmeter with greater dynamic range and less noise than many very high-quality spectrum analyzers.

The methodology

Here's how to proceed. Place a well-shielded and grounded dummy load on the transmitter under test. Lightly couple the "receiver/analyzer" to the dummy load. Place the step attenuator between the coupler and the receiver so the incoming signal can be attenuated by at least 65 dB. Verification of this number can be done by first

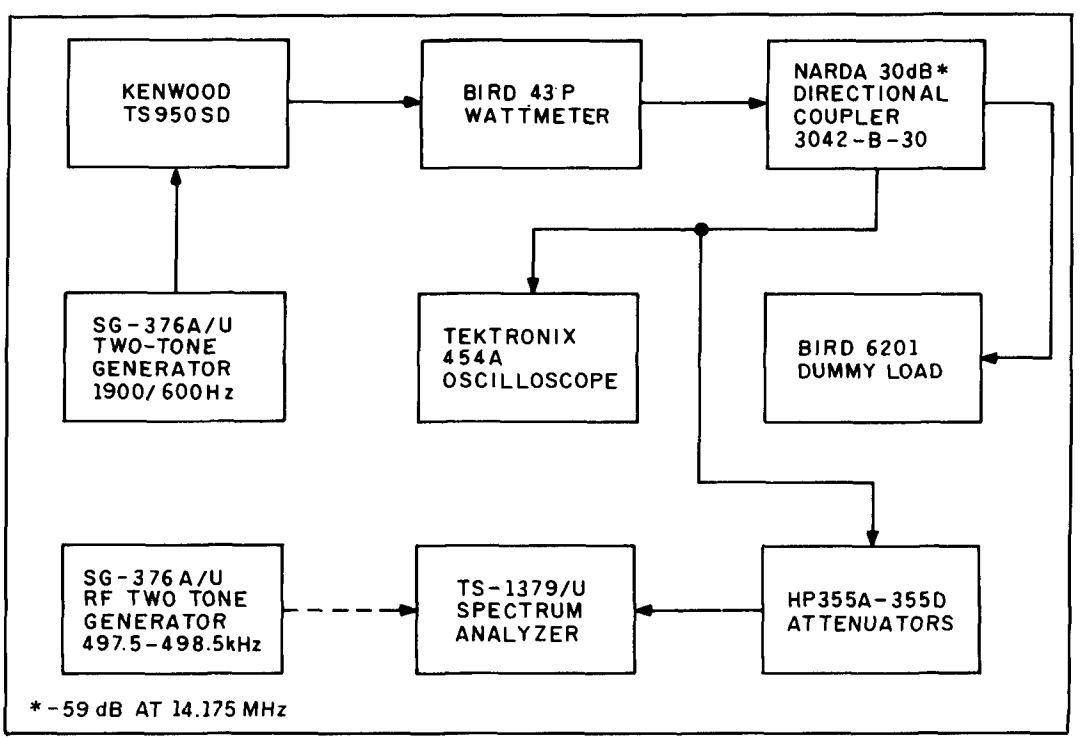

Figure 2. 50-ohm test setup.

calibrating the receiver's S meter and then using it to verify the 65 dB of attenuation. If you are unable to do so, this is an indication that some signal is bypassing the attenuator, and further isolation is needed to ensure maximum accuracy. At this point, you'll want to make one of the two reference carrier signals something along the lines of S9 plus 40 dB from the two-tone generation, and carefully tune higher in frequency (if the transmitter is in the USB mode). Note the odd-order signals and their respective amplitudes. In SSB, these appear at an appropriate difference between the two-tone spacing from the signal frequency, and their levels should be checked against the step attenuator. A side benefit is that you will be checking the linearity and accuracy of your receiver's S meter! Now, by varying your power, loading, VSWR, Icq, etc., you'll obtain basic data regarding your exciter's or system's linearity performance. While doing so, you'll also be able to null the balanced modulator while listening to it in the receiver/analyzer. This is an added benefit because this modulator is often overlooked for extended periods, and may have drifted out of balance.

As a practical example, take a frequency of 14,175 kHz and use two tones (600 and 1900 Hz) within the transmitter's passband. Make sure the tones are not harmonically related and that the transmitter is operating in USB. Call them f1 and f2. When tuning above the suppressed carrier frequency, you'll hear the two-tone test signals at 14,175.6 and 14,176.9 kHz, and each 1300 Hz (the difference between the tones) thereafter, depending on the accuracy of the receiver and the two test-tone frequencies. The IMD products may be any combination of $n \times f_1$, $m \times f_2$, where n and m are any positive or negative integers. Two excellent sources of the analysis of these products are found in Eimac's Application Bulletin number 12, and the classic text book on SSB by Pappenfus, Bruene, and Schoenike[3] At this point, you need only use the step attenuator to read off the relative amplitudes of the respective odd-order distortion products from one of the primary tones – recognizing that the results are being referenced to one tone as described earlier. Because of this, you must remember to *add* –6 dB to each measurement in order to reference the PEP for general comparative purposes. I have always felt that, while the two-tone test is the universally recognized standard, it would have been considerably more informative if it were based upon additional numbers of tones – more closely simulating the complex waveform and resulting impedance of the human voice. To that end, white noise modulation is perhaps the ultimate means of determining the distortion characteristics of a linear system.

Conventional IMD measurement

The conventional measurement test setup was used as shown in **Figure 2**. Those data gave me reasonable confidence that the alternative measurement technique was a valuable tool within reach of most Amateurs. I verified the calibration of the TS-1379A/U spectrum analyzer's log attenuation scale by using two Narda coaxial 20-dB fixed attenuators, type 757 C, which have a specified accuracy of plus or minus 0.2 dB. I used these in conjunction with calibration-certified Hewlett Packard-type 355A and 355D attenuators in series. The two-tone audio generator, the SG-376A/U, has a specified IMD level of –66 dB, as referenced to the PEP, which precludes any portion of its distortion products appearing in the IMD measurements.

The results

My spectrum analyzer results of measured power versus IMD performance of the TS-950SD are tabulated in **Table 1**. Note that all of my measurements were made with the reference to the PEP in order to preclude any differing interpretations of the data because Amateur equipment is universally specified in this manner. However, most commercial equipment and component IMD data are specified with respect to *one* tone of an equal pair of tones, yielding a –6 dB lesser number. **Figure 3** is an interesting TX audio frequency response versus Po comparison that attests to the superior performance digital signal processing (DSP) as compared with a filter-type SSB generation. My measurements were taken on a sample of one. However, judging by those data, it appears that, allowing for production variations and operational parameters, similar results should be attainable. As further evidence to this, my IMD test measurements correlate very closely with those of DL1BU[4] We both noted that varying the ALC from minimum to normal is desirable and beyond that will only result in distortion products being affected adversely. Zero ALC, from normal, represented a 3 dB improvement in the third-order product, while over 12 dB of ALC yielded a 3 dB degradation. The "all knobs to the right" type of operation will only diminish your signal quality and inter-

PEP watts*	Odd order products, −dB**					
	3	5	7	9	11	13
50	39	45	50	54	59	61
75	40	44	49	53	58	60
100	41	46	52	56	60	62
125	40	47	51	55	59	62
150	38	46	50	54	58	60

*14,175 kHz, USB, 6 dB ALC, no RF processing, 1900 and 600 Hz tones.
**Referenced to the PEP.

Table 1. TS-950SD TX spectrum analyzer IMD measurements s/n 10400098*

fere with adjacent frequencies, providing no resulting increase in readability.

Table 2 shows the test data obtained with the alternative receiver/analyzer measurement technique. You can compare it with the spectrum analyzer data in **Table 1**. As shown, it does provide basic information which is reasonably accurate, but you must remember that on-the-air IMD quality is the result of the *system* performance; that is, the sum of *all* distortion products such as those which may be contributed by the final amplifier itself.

SSB design considerations

Hopefully, there will be a trend to include higher voltage transistors, digital signal processing techniques, reduced receiver phase noise, and reduced transmitted noise in more SSB equipment in the near future. For example, higher voltage transistors result in greater efficiency from higher Q and will generate less noise. Of course, the IMD specifications should improve with time through the use of better devices. Some factory-published specifications of contemporary equipment, which are referenced to the PEP, are shown in **Table 3**. These represent a notable improvement over earlier equipment, especially in the area of the lower order products.

Finally, you can expect relatively close performance to that which tubes have provided in the past—with one exception. Tubes, by their design, generally generate

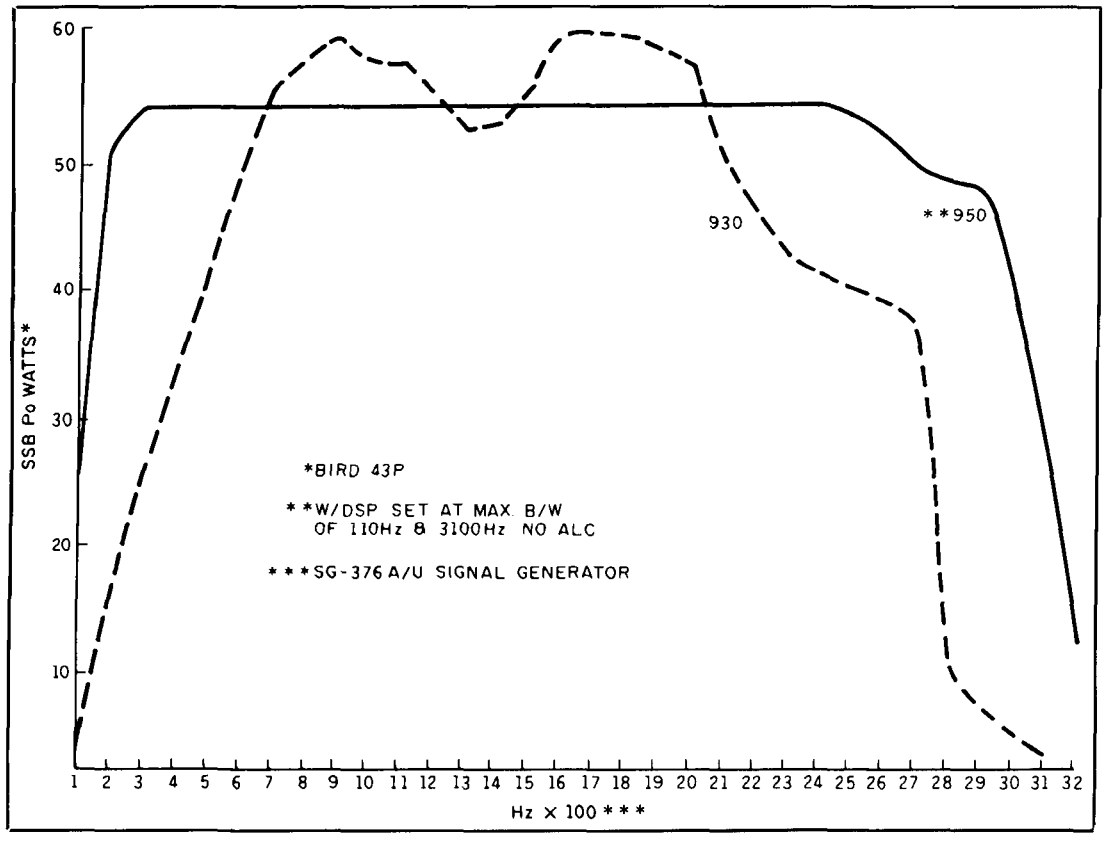

Figure 3. TX audio frequency response versus Po comparison.

PEP watts*	Odd order products, −dB**					
	3	5	7	9	11	13
50	37	40	53	58	60	61
75	40	43	46	50	58	62
100	39	44	51	55	60	61
125	40	45	52	56	61	62
150	38	44	53	55	60	61

*14,175 kHz, USB, 6 dB ALC, no processing, 1900 and 600 Hz tones.
**Referenced to the PEP.

Table 2. TS-950-SD receiver/analyzer IMD measurements s/n 10400098*

Manufacturer	Model	Third order IMD/−dB	PEP out
Kenwood	TS-940S	37	100
Kenwood	TS-950SD	37	150
Yaesu	FT-1000	36	150*
Yaesu	FT-767GXII	35	100
Ten-Tec	Paragon	30	100
Ten-Tec	Omni V	30	100
ICOM	IC-765/781	**	—

*Specified level with 200-watt capability.
**Not specified by manufacturer.

Table 3. Manufacturers' published TX IMD specifications referenced to the PEP.

fewer higher odd-order distortion products than solid-state devices and tend to create less overall distortion. This should result in a more pleasing, higher-quality signal. However, as Helge Granberg, K7ES, points out, "high-order distortion causes disturbances to adjacent communication channels, whereas low-order distortion only relates to the quality of the modulation."[5] In view of this, it's significant to consider *all* distortion products in weighing the merits of the quality of a SSB transmitter.

In my earlier work with the TS-930S, I obtained substantial IMD reduction by operating the 28-volt MRF-422 output transistors nearer to Class A—especially in the area of the higher order products, and at lower power levels. I didn't perform the bias modification to raise the p.a. quiescent collector current (Icq) for these tests because the basic characteristics of the MRF-429s used in the TS-950SD tend to preclude this. Also, Motorola has indicated that, with their MRF-429 devices, little would be gained with high Icq unless you were to operate them at Class A. However, under that condition, the efficiency would obviously suffer. Unfortunately, as in that case, reciprocity is always lurking. Ultimately, I believe the use of power FETs will probably provide a superior solution to the existing general use of bipolar transistors. In the interim, 50-volt bipolar devices are a very positive step in the right direction.

Conclusions

The IMD test results from a spectrum analyzer are significant to Amateurs concerned with their intrinsic transmitted signal quality.

For TX IMD measurement, without the use of the conventional spectrum analyzer, it may be demonstrated that you may gain valuable knowledge of SSB TX IMD performance using relatively basic equipment and a good-quality, selective receiver.

Operators who take pride in their transmitted signal quality and exercise all the established caveats outlined here, will be assured of a very clean signal. If all signals on the already crowded bands were capable of that level of performance, it would make operating a greater pleasure for everyone.

Acknowledgement

My sincere thanks to Dan Hearn, N5AR, for his basic receiver/analyzer concept and thought-provoking suggestions regarding the alternative technique for IMD measurement.

REFERENCES

1. Marv Gonsior, W6FR, "More Operational Notes on the TS-930S," *Ham Radio*, April 1988, page 23.
2. Helge Granberg, K7ES, "Measuring the Intermodulation Distortion of Linear Amplifiers," *Motorola RF Data Manual*, Second Edition, 1981, pages 3-42/44.
3. E.W. Pappenfus, Warren B. Bruene, and E.O. Schoenike, *Single Sideband Principles and Circuits* McGraw Hill, New York, 1964.
4. Guenter Schwartzbeck, DL1BU, *cqDL*, December 1989, page 750.
5. Helge Granberg, K7ES, AR165S, *Motorola RF Device Manual*, Vol. II, Rev. 3, page 7-313.

David M. Barton, *AF6S*
14842 Nelson Way
San Jose, California 95124

THE WONDERFUL TRANSFORMER POWER SPLITTER

This versatile device has many uses in the Amateur station

Power splitters have many uses including parallel operation of multiple RF amplifiers, driving multiple-antenna arrays, and operating more than one receiver from a single antenna without interaction. These devices are also called power dividers and combiners. Splitters can divide power two or more ways and provide various phase relationships between outputs. Some types of splitters are intended for rather narrow purposes and won't be discussed here. But all splitters provide isolation between outputs, so power reflected from one output port doesn't end up in the other. Among other advantages, this isolation minimizes the effects of load mismatches. Because splitters are passive, power can flow through their ports equally well in either direction, which is why the same devices are sometimes called combiners.

Amateurs are probably most familiar with the Wilkinson power divider. It's simple and rugged, and is made from two quarter-wave transmission-line sections and one resistor. This device is a good choice for single-band antenna arrays, especially in the VHF/UHF range, where the line sections are physically short. Microwave designers use strip-line techniques to make tiny Wilkinson dividers on ceramic (or other) substrates. They have at their disposal a number of interesting transmission-line based splitters. At even higher frequencies, waveguide structures perform the same roles. In the HF range, transmission-line splitters become large, but lumped inductors and capacitors can be substituted. However, unlike the transformer splitters described here, all splitters based on transmission lines or lumped reactances are inherently narrow-band devices. None would cover even two Amateur bands, much less the entire HF range.

How the transformer splitter works

Operating on the same principle as the hybrid transformer invented in the early days of telephony, the transformer splitter exploits advances in ferrite technology to extend operating frequency range into VHF and beyond.

Figure 1 shows a basic two-port transformer splitter. It has a total of four "ports." Resistors R1, R2, R3, and R4 are connected to these ports. For initial clarity, I'll make the three windings (n1, n2, and n3) identical. To accommodate identical windings, R2 and R3 must be twice the value of R1, while R4 must be the same as R1.

You can substitute an AC signal generator for any of the resistors, provided the generator output impedance equals the value of the resistor it replaces. **Figure 2** shows a generator in place of R1, and the relationship among the load values. In an ideal transformer, the volts-per-turn in every

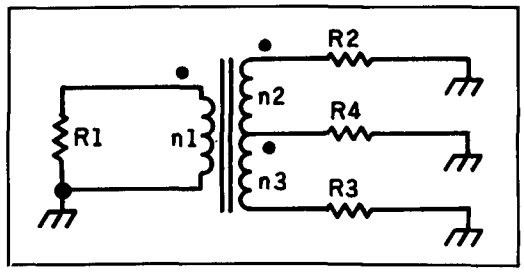

Figure 1. Basic circuit.

winding is the same. With identical windings, the voltages across each are identical. Then V1 = V2 – V4 = V4 – V3 (the dots on the schematic indicate winding phasing).

Looking at the circuit, it becomes clear that if R2 = R3, then V4 must be zero. This is because the voltages on n2 and n3 are equal and connected in series-aiding. With equal loads on the two output ports, all the current which flows in port 3 must also flow in port 2. This leaves no current for port 4. Also, since the only secondary current flows around the outer loop via n2, R2, R3, and n3, the voltage at port 3 must be 180 degrees out of phase with that on port 2. This hookup creates a 180-degree splitter. Furthermore, at port 1, R2 and R4 appear to be in parallel—a perfect match for the generator's output impedance. The generator delivers all its available power to these two loads; exactly half to goes each, which is 3 dB less than the generator's output.

What about imperfect loads? You can investigate this possibility by moving the generator to one of the output ports. Look at **Figure 3** and you'll see a generator driving port 2 and a resistor (R1) on port 1, because you are now interested only in tracking reflected power entering port 2.

Applying Kirchoff's first law

The sum of the products of each winding's current and turns (keeping winding senses the same) must be zero like the sum of currents entering a point, or Kirchoff's first law. Mathematically, this is I1*n1 + I2*n2 + I3*n3 = 0 (each current's number refers to both its winding and its port). All windings are identical in this example, so I1 + I2 + I3 = 0. Kirchoff's first law imposes I4 = I2-I3. The result, with the turns ratios and resistive values chosen, is I1 = I4 = I2 and I3 = 0. For a better understanding of this situation, visualize R1 as being across winding n2. This is equivalent to the actual circuit, because the turns ratio n1:n2 is 1:1. Now R1 and R4 are simply in series (excitation current in our ideal transformer can be ignored). Current entering port 2 flows via R1 to exit at port 4. Because resistors R1 and R4 are equal, V4 = V2/2, and the voltage across n2 is also V2/2, Since voltage across n3 must also be V2/2, voltage at port 3 (V3) is zero, confirming that no current can flow via port 3.

R1 and R4 are presented to the generator at port 2 in series, and the value of each is half this generator's impedance, so the match is perfect. Also, power divides equally between a pair of ports, leaving no power for

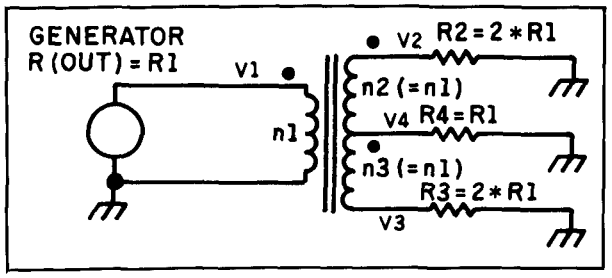

Figure 2. Generator driving port 1.

an additional port. The circuit's symmetry makes it obvious that power entering port 3 would also go only to ports 1 and 4. A general pattern emerges: Power entering any port exits two others, but not a third. This is true if the source and dummy impedances are matched, whether or not the two load impedances are matched. Notice that in **Figure 3**, the voltages on ports 1 and 4 are in phase. If you consider port 2 the input, ports 1 and 4 the outputs, and port 3 the dummy, you have a zero-degree splitter! The difference in principle between a zero and 180-degree splitter relates only to which port is which.

As only half the reflected power from an output port is routed back to the generator, the VSWR at the input port is always less than the VSWR at the output ports. Also, power division between output ports tends to be maintained despite load differences, because reflected power from one port doesn't go to the other, as it would if loads were simply connected in parallel or series. In practice, a real transformer and dummy load will introduce some imbalance, but operation is basically as described.

Impedance considerations

Practical splitters must generally match the same impedance on all ports. Turns ratios n1:n2 and n1:n3 of the square root of 2 (1.414) can accomplish this on ports 1, 2, and 3, and the easily-made ratios 7:5 and 10:7 are both close enough. Port 4, the dummy port in a 180-degree splitter, need *not* have the same impedance as the other ports,

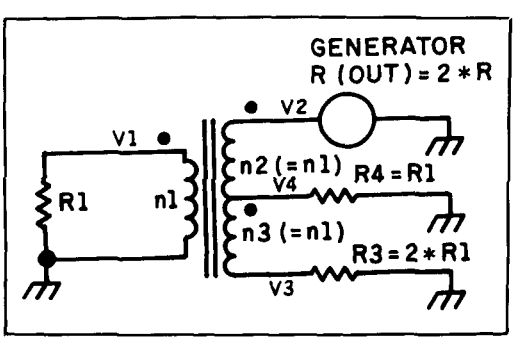

Figure 3. Generator driving port 2.

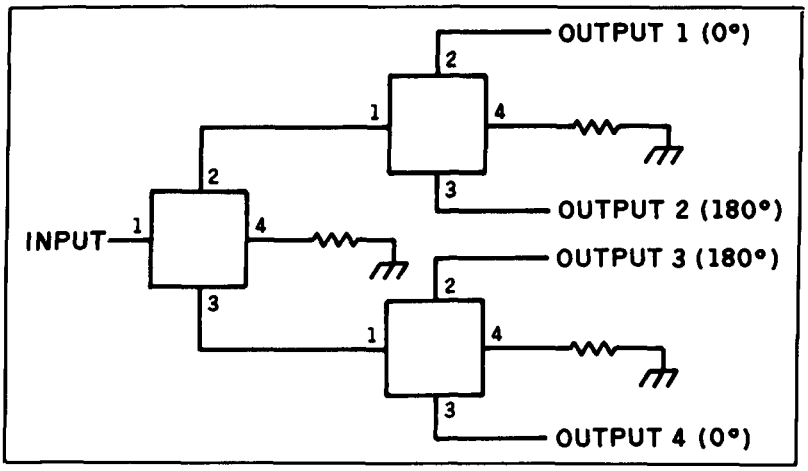

Figure 4. Four-output splitter made from two 2-output splitters (phases shown assume all splitters are 180-degree type).

because its dummy-load resistor can be whatever value is needed (25 ohms in a 50-ohm splitter). To allow for worst- case (open or short-circuit) loads, this resistor should be rated for half the maximum generator power. In high-power applications, you might wish to use a standard 50-ohm dummy load, using a second transformer to transform port 4 impedance to 50 ohms. By adding this second transformer, you can obtain a general-purpose, four-port splitter, usable as either a zero or 180-degree splitter, with an external resistor on whichever port needs the dummy. Generally, the best-balanced zero-degree splitter uses port 4 as the input and port 1 as the dummy. In this case, winding 1 can have the same turns as n2 with a 25-ohm dummy used, but you'll still need the extra port-4 matching transformer.

Four-way splitter

Figure 4 shows how three two-way splitters can be combined to form a four-way splitter. Such a "binary tree" system can be expanded to provide any 2-to-the-n number of outputs. In all cases, input power divides equally among all outputs, and the phase of each output depends on the splitter configuration used. Interestingly enough, the larger the tree, the greater the fraction of reflected power terminated in dummy loads (and the lower the input VSWR).

Each splitter sends half the reflected power it receives to its dummy and half to its input port. Each previous-level splitter sends half of *that* power back toward the generator, and so on. Consequently, you can allow for any possible *antenna* failure by rating each dummy load at the maximum power normally delivered to any *one* output port. Also, a backward tree of splitters can be used to combine all the reflected power, delivering it to a single dummy load (on the ground, if that's more convenient).

Splitter applications

In a large broadside array, you can use a mix of zero and 180-degree splitters to minimize the length of interconnecting feedline. You may do so by using the shortest integral number of electrical half wavelengths which will reach each driven element from its splitter. Splitters can also provide unequal power distribution among loads. It's well known that equally spaced arrays have best side-lobe suppression when feed currents are distributed as in Pascal's triangle.[1] For a three-element linear array, the ratio is 1:2:1—a 1:4:1 power ratio. However, maximum gain occurs when currents are equal. A 1:2:1 power ratio, easily accomplished using splitters, might be a good compromise. **Figure 5** shows how you can recombine two outputs of a four-way splitter tree to provide twice as much power to output 2 as to outputs 1 and 3.

Output phases are arbitrary; however, the signals driving the splitter connected to output 2 must have that splitter's phasing. Of course mutual coupling between elements may affect antenna currents, but the splitters do guarantee both the driving impedance and available power to each element. This is an important advantage in array design and modeling. By preventing power reflected by one element from reaching another, the system avoids array-phasing errors as well as power imbalance.

Figure 6 shows a simple two-receiver coupler. The receiver antenna signal and receiver RF input, available at the back of most transceivers, are intercepted (disconnected from each other) and routed via the

splitter, which sends half the received antenna power to a second receiver. The compelling reason to use a splitter, rather than simply connecting the receivers in parallel, is that the input filter of one receiver tuned to another band could easily present a near short circuit to the input of the other receiver. A splitter's inter-port isolation eliminates the problem. Of course, two receivers using the same antenna each get only half the signal power, or 3 dB less than when not sharing the antenna. But given the sensitivity of modern receivers, you probably won't notice this half S-unit loss.

Commercial splitters

A low-power splitter can be surprisingly small. Commercial units available from Mini-Circuits* range from metal boxes with connectors to tiny surface-mount devices. These units aren't very expensive and their level of performance is amazing. For example, Mini-Circuit model PSC-2-1 ($10) is a 50-ohm, two-way, in-phase unit in a hermetically sealed package designed for PC mounting. It covers 0.1 to 400 MHz, with isolation better than 20 dB from 1 to 400 MHz. These low-cost commercial splitters are designed for low-power applications limited to a few watts.

Low-power homebrew splitter

If you have the materials, a low-power splitter that performs well from 1.8 to 50 MHz is actually very easy to build. Two cores are required for a universal splitter, or for a zero-degree splitter, but a 180-degree splitter can be built on a single core. For many applications, including the operation of two receivers from one antenna, phase relationships don't matter, so the simpler splitter is the best choice.

Ferrite core material is the best choice for broadband uses because its permeability is much higher than powdered iron and requires fewer turns. This is important not only to make construction easier, but to make coupling tighter and minimize bandwidth-limiting stray inductance and capacitance. High Q and DC current-handling capability, features of powdered-iron cores, aren't needed. I chose a 0.375-inch diameter core over a smaller one to make it easier to build. Fair-Rite material no. 43 is a good choice for small splitters in the HF range.

By making a few measurements on a test winding of 5 turns on a Fair-Rite core no. 2643002401, I determined that 10 turns would be sufficient for nl at the lowest frequency. This made each half of the tapped winding 7 turns. Using no. 29 AWG solder-strippable magnet wire in a semi-trifilar winding, I began by first folding about 2 feet of the wire back on itself twice, making three parallel strands. I left one end about 2 inches longer than the loop at the same end. Cinching all three wires from the other end in the chuck of a small variable-speed drill (a hand-powered "egg beater" drill would be easier to control), I pinched the opposite end in my hand while running the drill slowly until

*Mini-Circuits (catalog), Box 350166, Brooklyn, New York 11235-003, 718/934-4500.

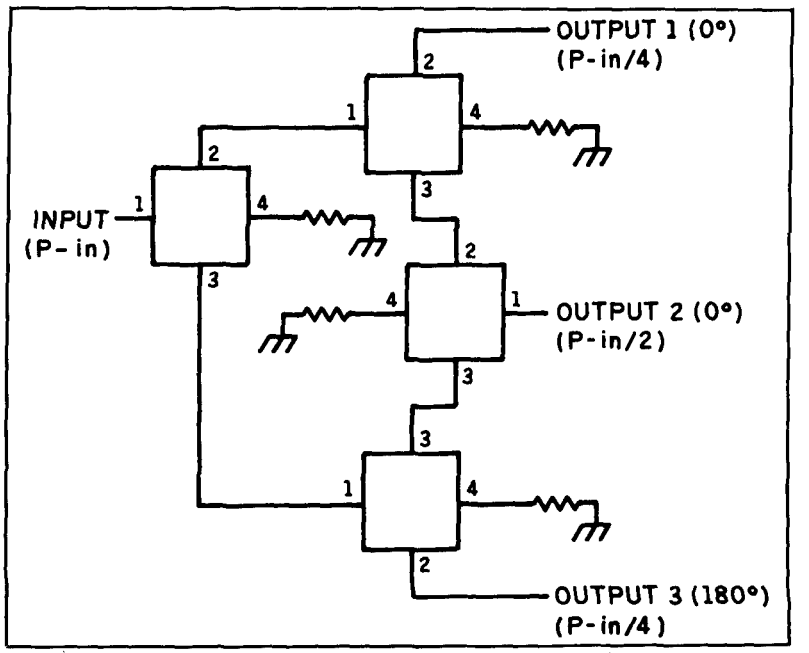

Figure 5. Linear-array drive scheme using four splitters (phases shown assume 180-degree splitters at all locations).

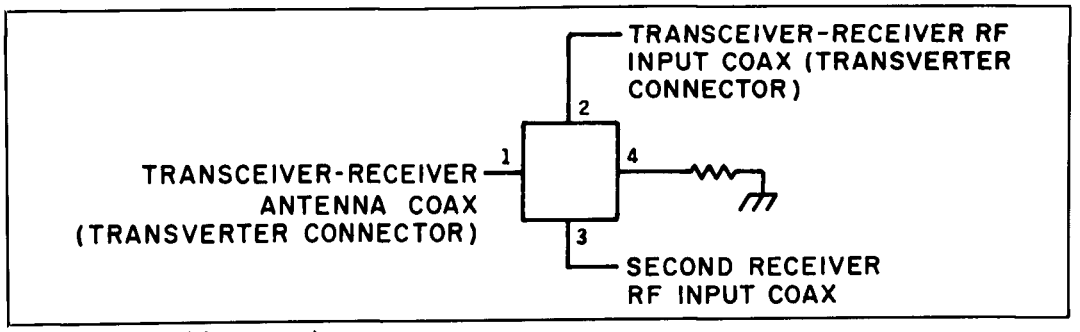

Figure 6. Splitter driving two receivers.

there were from 5 to 10 turns per inch. Next, I put the end with the overhanging strand through the core, leaving enough of the loop extended to strip and solder. Holding this end, I wound the other end until it passed through the hole seven times. Then, I untwisted the single wire on the first end so it could be wound separately and added three more turns of just this one wire, placing its turns between those of the trifilar winding.

Now all I had to do was strip all the wires and sort them out. First, I found the other end of the long wire using an ohm meter and twisted that pair together, so I wouldn't lose track of them. They form n1. Next, I clipped one meter lead to one of the remaining wires and, looking at the wires exiting the coil, found the one to which it was *not* connected. I twisted and soldered that wire to the wire attached to the meter lead. This junction is the center tap of the n2-n3 winding (port 4 in **Figure 2**). The other two remaining ends are ports 2 and 3. It really makes no difference which is which, unless you need to establish the phase relationship between port 1 and ports 2 and 3.

Testing

It's a good idea to test your splitter, just to make sure everything is right. You'll need a signal generator whose output impedance is 50 ohms. Your station's receiver can be the RF detector. Solder coax connectors or short lengths of small 50-ohm coax, each with a connector at the other end, to the splitter ports and solder all the grounds or outer conductors together at the splitter. Also solder a 24-ohm 1/4-watt resistor from the winding center tap to the coax ground. The 50-ohm termination needed for the test can be a 51-ohm 1/4-watt resistor soldered inside a coax connector, or you can use a 50-ohm dummy load on any length of 50-ohm coax.

To test for forward-power transmission, connect the generator directly to the receiver to calibrate its output level, with your receiver's built-in attenuator switched in or set to at least 20 dB, for a reading between S9 and 20 dB over S9. Next, insert the splitter, connecting the generator to port 1, the receiver to port 2, and the termination to port 3. The S meter should read about 3 dB lower (half an S unit). Try this on the highest and lowest bands of interest, making sure to recalibrate at each new frequency. You'll also want to terminate port 2 and connect the receiver to port 3. The results should be identical.

Test for isolation just as the theory describes it. Connect the generator to port 2, the termination to port 1, and the receiver to port 3. The S meter should read at least 20 dB lower (3 to 4 S units), but try switching out attenuation to restore the original reading. Generally, a receiver's attenuator is much more accurate than its S meter, so you can make a much more accurate measurement by reducing attenuation until the reading is nearest that with the splitter out and then using the meter only for interpolation.

I tested a sample splitter, built as described, from 1.8 to 50 MHz using accurate lab equipment. My results indicated isolation better than 20 dB and forward loss less than 0.5 dB, over the entire range.

High-power splitters

You could build a splitter which can safely handle 2 kW. You'd need a ferrite toroidal core with a permeability greater than 100 and a bulk resistivity of 100 megohm-centimeters, or more. Core size should be similar to that of a balun or transmission-line transformer for the same frequency range.

As the size of a transformer increases to accommodate higher power, it becomes difficult to obtain tight coupling between windings. Increased winding length is part of the problem, as is the use of thick wire insulation. Construction techniques similar to some of those in W2FMI's book *Transmission Line Transformers*[2] are almost certainly the answer. ■

REFERENCES

1. John D. Kraus, *Antennas (2nd edition)*, McGraw-Hill, 1988.
2. Jerry Sevick, W2FMI, *Transmission Line Transformers, Amateur Radio Relay League*, Newington, Connecticut, 1987.

Norm Foot, *WA9HUV*
293 East Madison Avenue
Elmhurst, Illinois 60126

A HIGH-LEVEL SSB MODULATOR FOR S BAND

Obtain 5 watts PEP output on the 3456-MHz Amateur band

I wondered if I was up to the challenge of operation on the 3456-MHz band. I wanted sideband modulation and a minimum of 5 watts PEP from the transmitter. This is usually accomplished using a low-level mixer driven by a 144-MHz SSB source and a 3312-MHz local oscillator (LO). The mixer would then be followed by as many S-band amplifier stages as necessary (perhaps three or four) to achieve the 5-watt level at 3456 MHz.

A review of the literature indicated that generating a few milliwatts of RF power at 3456 MHz ought to be easy, but that obtaining adequate S-band SSB power (even 100 mW) would be another matter entirely.

Early attempts

Other experimenters have tried various techniques. One uses a double-balanced mixer (DBM) followed by a 3-stage MMIC amplifier employing devices like the Avantek MSA0885 or Mini-Circuits MAR-8A. (The MMICs are surface mounted on a special Teflon® pc board.) I built one of these MMIC amplifiers, but wasn't fully satisfied with the results. Besides requiring an isolator to make the amplifier stable, another, very expensive, power transistor stage was necessary to generate a full 100-mW output at 3456 MHz. Perhaps I'm too conservative, but I like to have a little extra drive so it won't be necessary to operate everything at full throttle. I needed to find another way to achieve this intermediate power level.

While contemplating this problem, I identified at least three power-amplifier options which could boost the 100-mW level to 5 watts: a surplus high-power traveling-wave tube amplifier (TWTA), a high-power S-band transistor amplifier, or a surplus tube amplifier. Unfortunately, the TWTAs and transistor amplifiers were quite expensive (several hundred dollars each), and my budget restrictions necessitated the use of the surplus tube amplifier.

A very informative article written by Keith R. Ericson, KØKE, called "Another 3456 Transverter,"[1] describes the use of surplus AT&T cavity amplifiers with GE 416B ceramic tubes. These units have been available from Fair Radio* for some time. They can supply 5 watts of RF output at 3456 MHz. Ericson's article describes simple modifications he made to put them on the air.

The power gain of the surplus GE 416B cavity amplifiers is 10 dB when driven with a low-level signal, and slightly less with drive levels in the range of 0.25 to 0.5 watt. These tubes require 300 to 450 volts DC on the plates, and 6.3 volts AC on the filaments. When a pair is connected in cascade, 100 mW (20 dBm) drive will reliably provide 5 watts output.

Using the GE 416B cavity amplifier

Surprisingly, the solution to the intermediate (100 mW) power problem in-

*Fair Radio Sales Company, P.O. Box 1105, 1016 E. Eureka Street, Lima, Ohio 45802.

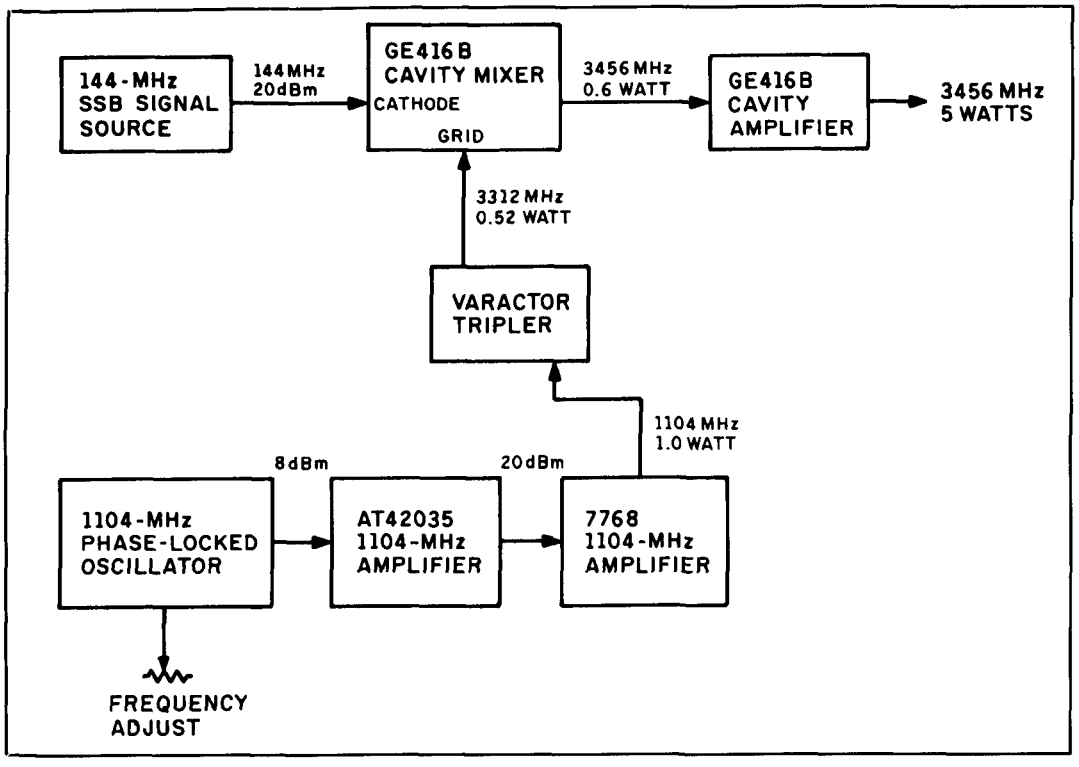

Figure 1. Block diagram of transmitter.

volved using one of the low-cost surplus GE 416B cavity amplifiers. Instead of developing a low-level SSB signal at 3456 MHz and amplifying it with a chain of three or four S-band amplifiers, as other experimenters have done,[2,3] I made some simple modifications which let me use one of the cavity amplifiers as an up-converter. With 144 MHz SSB on the cathode and 3312 MHz at the input, I obtained over 1/2 watt PEP power output at 3456 MHz! **Figure 1** shows how. Only about 100 mW of 144-MHz SSB signal is needed, while approximately 0.5 watt of 3312-MHz local-oscillator power is required.

There are a number of significant advantages to this approach. One is that the up-converting cavity stage also serves as a narrow-band RF filter. When followed by another cavity (amplifier) stage, the 3456-MHz power output is over 5 watts, while the 3312-MHz LO signal is down over 40 dB at the output due to the frequency selectivity of the cascaded cavities.

Local oscillator power for the high-level up-converter is generated by a homebrewed passive tripler which uses an SRD. It's similar to the ones we used a few decades ago to get on 1296 MHz by tripling our 432-MHz signal. This S-band tripler is driven by about 1 watt of 1104-MHz power, providing a 1/2-watt output. It's considerably easier to generate power at 1104 MHz than at 3456 MHz, so tripling is accomplished at high level. As a signal source, I used a phase-locked oscillator (PLO) similar to the one described in the winter edition of *Communications Quarterly*,[4] but changed the crystal frequency to 1.078125 MHz. The PLO drives an Avantek AT42035 medium-power transistor, which in turn drives a 7768 tube amplifier. I used the 7768 amplifier because I happened to have it on hand, but there are other tubes and transistors that will do as well at 1104 MHz.

Now that I've identified the technique used for generating high-level S-band SSB power, I'll describe the modifications you must make to change the GE 416B amplifier to a converter. First, however, I'll discuss the 3456-MHz system that I use, to give you an overview of the whole transverter system.

The transverter

I was able to simplify the transverter system considerably by using two transmission lines on the tower instead of one. This is illustrated in the block diagram of **Figure 2**. A 50-foot length of 1/2-inch Heliax feeds 3456-MHz power to a Transco T/R switch at the top of the tower. In the receive mode, 50 feet of 9913 coax cable brings the output of the low-noise amplifier (LNA) down to the station. The Transco is the only RF relay used in the system. Note that 10 dBm of LO power for the receiver is fed by a directional coupler and an attenuator to the down-converter from the tripler output. The PLO

runs continuously, contributing to the stability of the system. To tune the transverter, I added a voltage variable capacitor (varicap) across the PLO crystal and varied the capacitance with a potentiometer on the front panel. This let me vary the 3456-MHz frequency by ±50 kHz.

I used a modest 21-inch diameter spun-aluminum dish antenna and a "coffee-can" type feedhorn, like those I originally described in the May 1976 issue of *Ham Radio*.[5] I reduced the diameter from that of the original 1-pound coffee can to the 2-1/2 inch diameter of a soup can. I positioned an SMA coaxial fitting with a 0.085-inch long probe 1.42 inches from the back wall. Dish gain is 20.5 dB. I hope to substitute a 3 or 4-foot dish for the 21-inch unit to obtain more gain. I don't recommend the use of a snow sled; most don't focus well and, therefore, have high losses.

Converting the GE 416B amplifier

Converting one of the surplus GE 416B cavity amplifiers to an up-converter is relatively easy. Unscrew the brass cylinder at the rear and slide it away from the tube socket. Then pull the tube socket off the GE

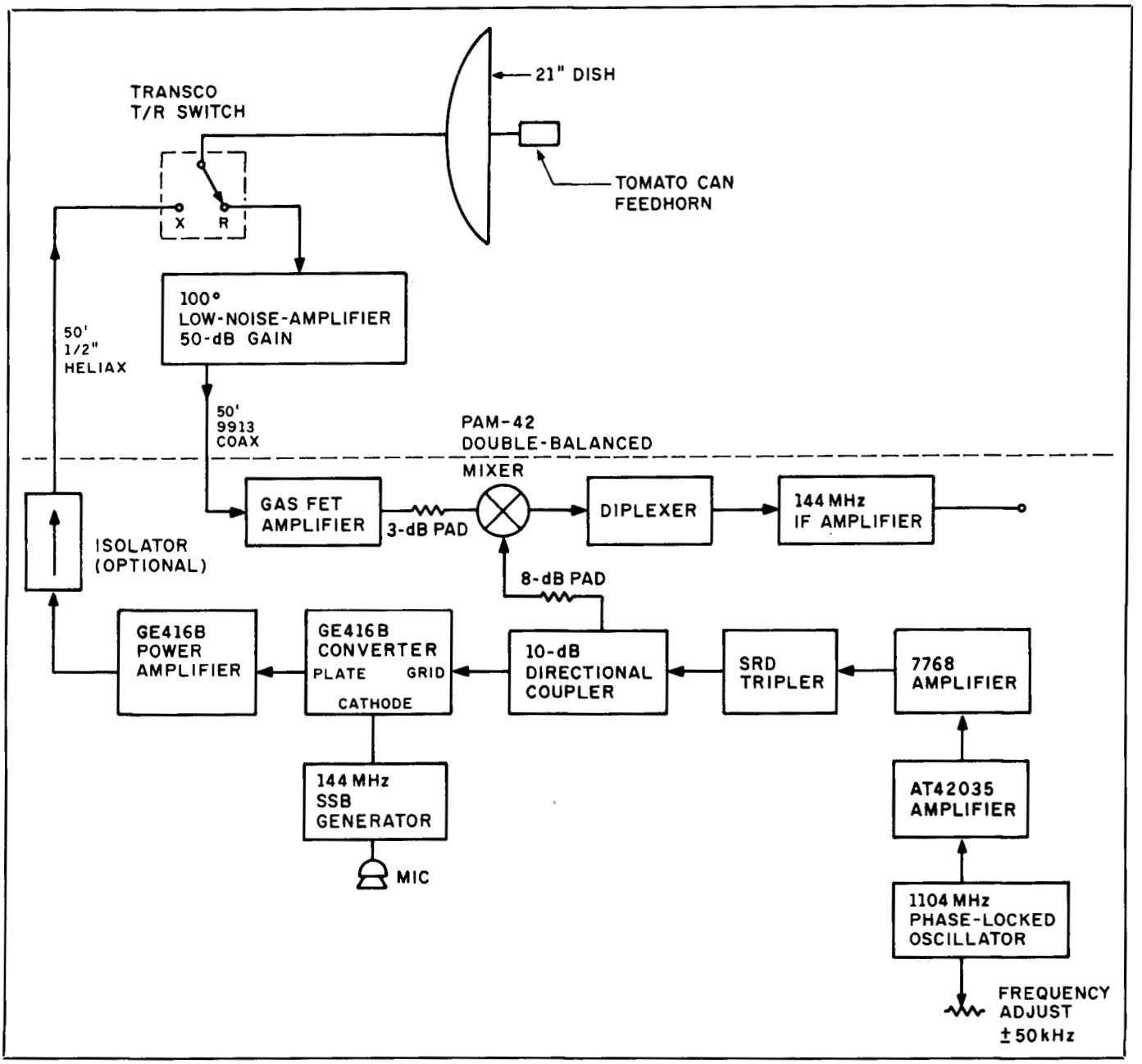

Figure 2. WA9HUV 3456-MHz transverter overall block diagram.

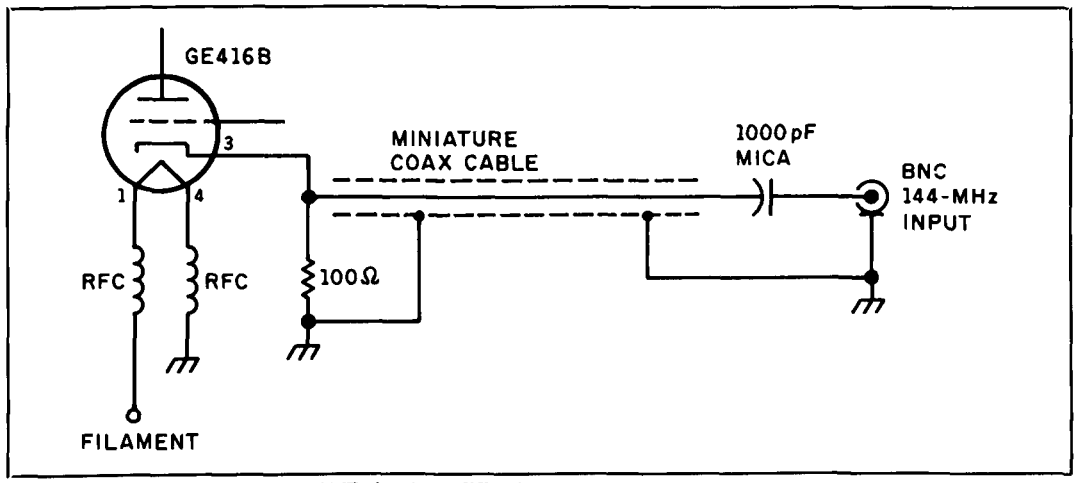

Figure 3. Schematic diagram, GE 416B circuit modification.

416B. The socket includes identifying pin numbers as follows:

1. Filament (high side).
2. NC.
3. Cathode (with 100-ohm resistor to ground).
4. Grounded filament.

Disconnect the high-side filament wire from the socket. Insert a 0.05-μH RF choke between the wire and pin 1. Remove the ground connection between pin 4 and ground and insert a 0.05-μH RF choke from pin 4 to ground. Using a suitable length of miniature coaxial cable, solder the center conductor to socket pin 3 and connect the braid to ground. Feed the coaxial cable through the hole in the brass cylinder. Plug the socket back onto the tube and screw the cylinder back in place.

The far end of the miniature cable is connected through a 1000-pF mica blocking capacitor to the center pin of a BNC fitting, with braid on ground. The location of the blocking capacitor and BNC connector isn't critical, nor is the length of the interconnecting coaxial cable. About 100 mW of 144-MHz SSB signal is fed to the BNC connector to modulate the up-converter. **Figure 3** shows the schematic of the modification.

Feed a 1/2 watt of 3312-MHz LO power to the modified GE 416B converter input. Tune the input cavity to 3312 MHz, and adjust the output cavity to 3456 MHz. Power output should be about 1/2 watt, ample to drive the power amplifier to a full 5-watts output.

Final comments

Construction of Amateur equipment for operation at S-band poses many interesting challenges. If you have access to a high-powered TWTA with high gain (20 to 40 dB for example), then an exciter with a few milliwatts output can provide 10 to 50 watts or more of TWTA output, depending on the type of TWTA. One drawback is that the TWTA requires a fairly complicated power supply, with relatively high voltages of both polarities, plus good regulation. And, like any other type of tube device, linearity is realized only up to the point of saturation. The purchase of a TWTA is probably not for the budget-minded; but if you have one, I recommend that you use it.

On the other hand, the modified surplus GE 416B cavity amplifier, configured as an up-converter, will provide at least 1/2 watt output directly at 3456 MHz. When driving a GE 416B power amplifier, final output should be more than 5 watts. These readily available devices are my choice for operation on the 3.3 to 3.5 GHz Amateur band.

In **Figure 2**, I show an overall station configuration that allows transverter operation with a minimum of special microwave parts. The LNA includes a built-in isolator to prevent oscillation when in transmit mode. I bought an Avantek unit for $5 at a hamfest and modified it. I removed the probe in the coax-to-waveguide input transition, and mounted an input SMA fitting on the side of the unit. Without this fitting, you'd need another waveguide-to-coaxial transition to get back to coax.

You may elect not to use the isolator at the power amplifier output. While the one I used has almost 1.0-dB loss, it probably reduces VSWR loss on the transmission line, which may or may not make up for the isolator loss.

Finally, in the receiver section, I used a Mini-Circuits PAM-42 DBM, integrated on the converter pc board, as the receiver's down-converter. I used pads on the DBM inputs and a diplexer on the output. Except for

the type of DBM, the circuit is identical to the one I used in my 1296-MHz converter.[6]

At 3456 MHz the loss on the 9913 section of cable is relatively high at S band, but this is of little consequence in view of the high gain of the LNA. In recent tests, S-9 signals were heard at a round-trip distance of 100 miles from a 10-watt 3456-MHz signal bounced off a tall building. While activity at 3456-MHz isn't overwhelming in the Chicago area, at least five stations are on the air—including myself and a 3456-MHz beacon that operates 24 hours a day. A beacon like this can be an indispensable tool when taking your first steps on 3456 MHz! My hat is off to Garry, K3SIW/9, for this accomplishment, and to Ron, W9ZIH, for his patience in running 3456-MHz tests. See you on 3456!

NOTE: To obtain a surplus GE 416B cavity amplifier from Fair Radio Sales Company, ask for the following items:

1 - ED63919-31 Amplifier
2 - ED51566-30 Tuner/Transducer
1 - Mating 6-prong Jones connector

The tuner/transducers are waveguide transitions for connecting the RF in and out of the amplifier. You'll add coax fittings on the waveguide transitions. ■

REFERENCES

1. Keith R. Ericson, KØKE, "Another 3456-MHz Transverter," *Central States VHF Proceedings*.
2. Dave Mascaro, WA3JUF, "A 3456-Linear Transverter," *Ham Radio*, January 1989, page 68.
3. Jim Davey, WA8NLC, "A No-Tune Transverter for 3456 MHz, *QST*, June 1989, page 20.
4. Norm Foot, WA9HUV, "Upgrade Your 1296-MHz Converter With This PLO," *Communications Quarterly*, Winter 1991, page 93.
5. Norm Foot, WA9HUV, Cylindrical Feedhorns for Parabolic Reflectors," *Ham Radio*, May 1976, page 16.
6. Norm Foot, WA9HUV, "A High-Performance 1296-MHz Converter," *Communications Quarterly*, Spring 1991, page 101.

PRODUCT INFORMATION

Miniature Soldering Iron

M.M. Newman Corporation offers an industrial-grade soldering iron that features a positively grounded tip for prototype and repair work on loaded pc boards.

The Antex Model G/3U minature soldering iron provides power comparable to a conventional 30-watt iron and accepts over 40 types of slide-on tips. For more information, contact M.M. Newman Corporation, 24 Tioga Way/P.O. Box 615, Marblehead, Massachusetts 01945.

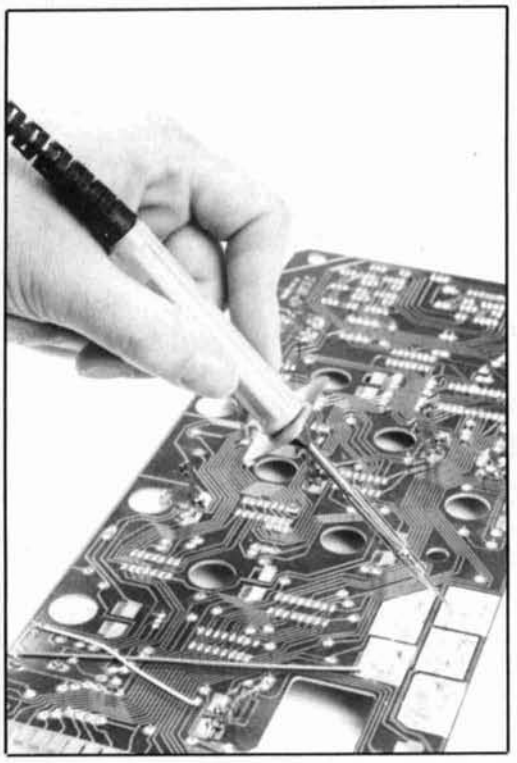

Universal Voltage Monitor ICs Available

The MC34161/MC33161 series of universal voltage monitor ICs is now available from Motorola Inc. These devices can be used in a variety of voltage sensing applications and for implementing over, under, and window detection of positive and/or negative voltages.

The circuit consists of two comparator channels, each with hysterisis, a pinned-out 2.54 volt reference, two open collector outputs capable of sinking in excess of 10 mA, and a "mode select" input for programming the functions of the two comparator channels. The devices are fully functional from 2.0 to 40 volts for positive voltage sensing and from 4.0 to 40 volts for negative voltage sensing.

These ICs are available in 8-pin dual-in-line (P suffix) and surface mount (D suffix) plastic packages for operation over two temperature ranges: 0 °C to −70 °C, and −40 °C to +85 °C.

Samples are available. Contact Motorola Inc.—Media Relations P.O. Box 52073, Mail Drop 56-102, Phoenix, Arizona 85072 for details. To obtain technical data on the universal voltage monitor IC contact: Motorola Literature Distribution, P.O. Box 20912, Phoenix, Arizona 85036. Ask for data sheet MC34161/D.

Bryan Bergeron, *NU1N*
30 Gardner Road, Apt. 1G
Brookline, Massachusetts 02146

AN AUDIO IMAGING SYSTEM FOR ENHANCED CW RECEPTION

An introduction to auditory system concepts, plus a practical application

As anyone experienced in security systems will tell you, the most sensitive alarm system available, even in this era of high-technology electronic instrumentation, is a guard dog's ears. Similarly, the most effective audio filter available for CW work, despite the years devoted to the development of sophisticated active and passive electronic devices, is the human auditory system. As long as the audio signals are presented to the ear in an appropriate format, there's simply no electronic apparatus that can even begin to approach the brain's signal processing abilities. This article describes a filter system, designed to enhance the reception of continuous tone signals in a noisy environment (that is, CW signals with moderate to heavy QRN and QRM), which makes optimum use of the inherent filtering capabilities of the human auditory system.

Introduction

Audio frequency vibrations in the air are a relatively simple physical phenomenon, easily modeled with elementary mathematics. However, the interpretation of these vibrations (sound) by the human auditory system is a complex and not yet completely understood process that has a basis in mathematics, neurology, anatomy, and human perception. As such, the idea that a given audio signal is more easily resolved from other signals and noise when presented in a stereophonic fashion (see **Figure 1**) rather than in a monophonic one (see **Figure 2**), requires some understanding of each of these areas. What follows is a brief introduction to some of the more basic concepts of the auditory system (sound localization, audio imaging, and psychoacoustics). I'll also discuss some practical applications of these concepts, including a CW imaging system.

Sound localization

Sound localization is the ability of the auditory system to determine the physical location of a sound source by auditory cues. To gain an intuitive understanding of sound localization, imagine the following scenario: You're standing in an open field, and, off in the distance and to your right, lightning strikes a tree, creating tremendous vibrations in the air which you interpret as a cracking noise. Even if your eyes were closed during the strike, the audio cues available would allow you to identify its direction with reasonable accuracy (maximum auditory acuity is about one degree of arc[1]). Not only would the audio vibrations reach your right ear first, but the amplitude of the vibrations

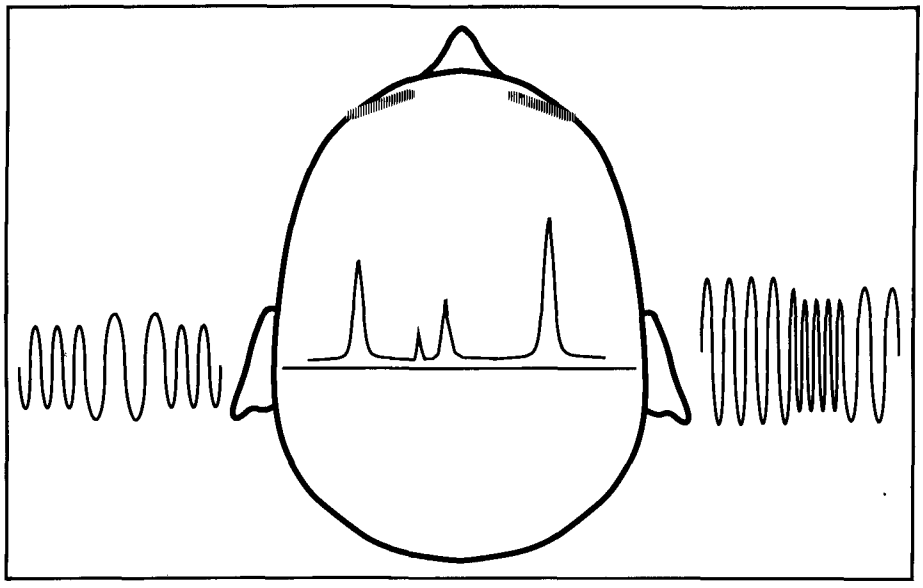

Figure 1. When audio signals of slightly different phase and amplitude are applied to each ear, the human auditory system creates an audio image of the source, localized along an imaginary line drawn between both ears. This effect, which is commonly experienced when one listens to stereophonic music, can be used to discriminate between multiple CW signals and noise. By spatially separating the audio images of each signal and noise source, you can more easily identify and accurately monitor a particular signal. For clarity, the audio signals in this and in *Figure 2* are shown as arriving external to the outer ears. In reality, the signals presented to the ears directly by stereo headphones.

reaching the right ear would be greater than those reaching the left. This, in part, is due to the shadowing effect of your head. The bulk of your head would be between the audio source and your left ear, while your right ear would be in direct line with the source. Sound localization then, is at least partially a function of both relative time delay (phase) and relative audio signal amplitude.[2,3]

The original duplex theory of localization, advanced near the turn of the century, states that relative differences in amplitude are responsible for localization of high-frequency signals, while relative time or phase differences are responsible for localization of low-frequency signals[4]. However, modern studies have revealed a time difference component in high-frequency localization.[5,6,7,8] It's likely that the auditory system's sensitivity to relative amplitude differences may be mediated by different mechanisms at low and high frequencies.[9,10]

Contemporary models of sound localization, while recognizing the significant contributions of relative intensity and phase, also take into account a number of other factors, including:

- The directional characteristics of the pinnae (external ears), which modify the intensity spectrum reaching each ear.[11] Although we would probably all agree that, on an intuitive basis, the external ears are directly involved in sound localization, it is not obvious that the external ears are predominantly useful for localizing frequencies greater than about 6 kHz.[12]
- The characteristics of the audio frequency vibrations.[13] For accurate localization, even at 6 kHz and above, audio signals must have a bandwidth of at least 1 kHz; pure tones are not localized accurately at frequencies below 6 kHz.[14] This is due in part to the auditory system's insensitivity to relative differences of time or phase for pure tones at high frequencies.[15] If you've worked around switching power supplies, high voltage TV power supplies, or piezoelectric tone transducers, you've probably experienced the difficulty of locating the source of a relatively pure tone first hand. For everyday wideband sounds, directional hearing is most accurate in the low-frequency range.[16]
- Information from other sense organs.[17] The correlation between the auditory cues and information from the vestibular (position and movement sense organ in the ears), visual (eyes), and kinesthetic (motion and position sense organs in the muscles, tendons, and joints) systems is used in sound localization. For example, rotating the head from side to side varies the relative amplitude and phase relationships of signals reaching the ears dynamically, providing the auditory system with additional data points

which can be used to more accurately localize the signal source.

Audio imaging

Audio imaging is a complex phenomenon that builds upon the concepts discussed in the section on sound localization. However, where the term sound localization is commonly used to describe the perceived position of an audio source in a flat or two-dimensional sense, audio imaging refers to the more complex, three-dimensional perception of a sound source. Audio imaging involves more than a simple notion of audio source direction and distance. The sensation you experience when listening to a good stereophonic recording through a well-designed stereophonic sound system is an example of audio imaging. In a good recording, you can imagine or deduce the relative positions of each instrument and the vocalist. The auditory system produces an *audio image* of the sound source, in a manner akin to the way our binocular visual system processes visual signals to create 3-D visual images.

Intra-aural versus free-space sources

When discussing audio imaging, it is necessary to determine whether the audio source is *intra-aural* (provided by headphones) or *free space* (provided by loudspeakers). Free-space systems are different from intra-aural systems because the wavefront interactions that occur in free space are not found in intra-aural systems. Also, the shadowing effect of the head, as well as the directional characteristics of the external ears, aren't relevant to intra-aural systems. The predominant *perceptual* difference between intra-aural and free-space systems occurs where the audio image is formed.

Listen to your favorite stereophonic tape or record, first through stereo headphones, and then through a stereo speaker system. Do you notice the difference in the location of the audio image? If you listened to a properly engineered stereophonic recording through loudspeakers, you should have heard the audio image extracranially; that is, outside of your head. However, if you listened to the same piece of music through headphones, the sounds should have seemed to come from within your head, localized on an imaginary line drawn between both ears. Audiologists commonly evaluate a person's ability to perceive this lateralization of sound within the head. The lateralization test, also referred to as phase audiometry, is commonly used to evaluate the audio image location as a function of relative interaural phase differences.[18]

Although difficult, it is possible to present audio signals through stereo earphones which give the perception that the source is external—as though the audio signals are

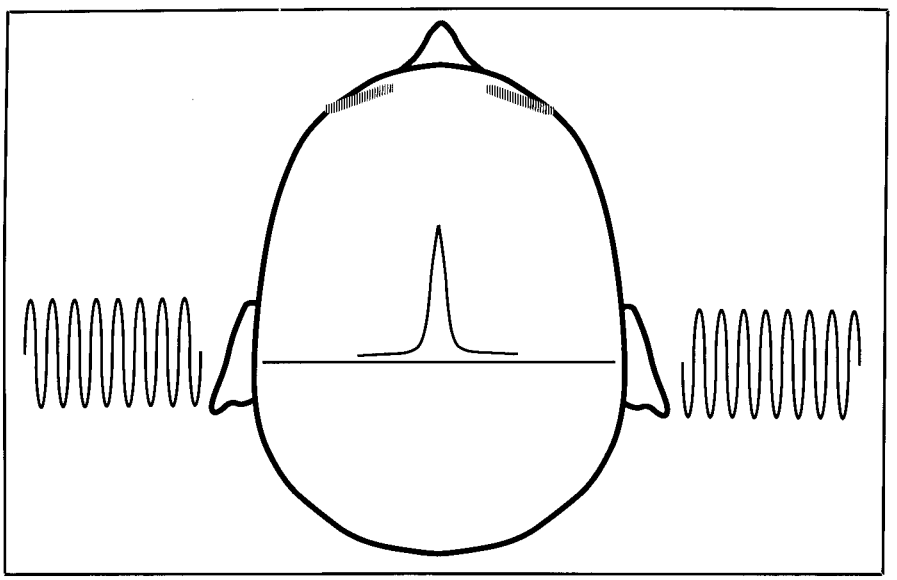

Figure 2. Monitoring a monophonic audio signal, i.e., presenting both ears with a signal of the same spectral content, creates the perception of a single, clumped image of multiple signals and noise, localized near the center of the head. Although this is the traditional means of monitoring CW signals, this approach defeats many of the innate filtering capabilities the auditory system, and requires the operator to rely strictly on the tonal qualities of each signal for discrimination.

produced by a loudspeaker system.[19,20,21] The military is currently funding experiments aimed at improving pilot performance by providing audio images of information which supplies data about events occurring at different spatial locations relative to the aircraft via the pilot's headset.[22]

Due to the complexity of adequately modeling free-space audio imaging, and the popularity of headphones among CW operators, the remainder of this article assumes that you have an intra-aural signal source.

Image resolution

The auditory system's sensitivity to interaural differences (resolution) diminishes when the audio images are located away from midline (the middle of the imaginary line drawn between both ears) because of relative interaural differences of signal phase or intensity.[15,23] This effect suggests that the audio image of desired signals should be positioned, via modification of interaural phase or amplitude relationships, near the midline. Conversely, the audio images of unwanted signals and noise should be positioned as far from midline as possible.

The use of signal phase shifting or delay as the *sole* means of introducing spatial separation in an audio image isn't widespread because the resulting image isn't as well defined and is more difficult to localize then it is when intensity differences are also used,[2] especially at low frequencies.[24] When phase shifting is used to produce a well-defined image, it should not exceed 90 degrees and should be limited to low-frequency signals. Phase shifts greater than 90 degrees produce a broad image of each component within a signal.[24] This means the individual components within the audio image extend from one ear to the other, and the perceived spatial separation between the individual components is greatly reduced. It's interesting to note that the auditory system's sensitivity to interaural level differences is relatively constant across a wide range of frequencies,[9] except for a region near 1 kHz where it is slightly elevated.[15]

Psychoacoustics

Several properties of the human auditory system defy explanation on a strictly mathematical or anatomical basis and are best understood in terms of human perception; that is, psychoacoustics. The psychoacoustic properties most applicable to CW communications are the precedence effect, binarual fusion, and perceived intensity.

When two signals are presented intra-aurally, and within 40 ms of each other, they are perceived as one signal coming from the direction of the first signal.[25] This phenomenon is known as the *precedence effect*.

For instance, if a 1-kHz tone of 20-ms duration is applied to the left ear and an identical signal is applied to the right ear 20 ms later, the auditory system will perceive this as a single 1-kHz tone of 40-ms duration, applied to the left ear. Audio signals separated by 50 ms or more are perceived as having a distinct echo.

Binaural fusion, sometimes referred to as the stereophonic effect, is the perception of a single auditory image when earphones present signals with different relative phase and intensity to each ear.[26] As I mentioned earlier, the resulting image is heard within the head, located along a plane between the ears.

The *perceived intensity* of a sound is a function of the audio signal's duration. Audio signals longer than about 250 ms require the same intensity to be heard, while shorter durations require an increase in signal level to appear at the same level. A decade duration change (from 500 to 50 ms, for example) is equivalent to a 10-dB intensity adjustment.[27] For example, two 1-kHz signals of the same amplitude, one 500 ms in duration and one 2 seconds long, would be perceived as having the same intensity. In order for a 1-kHz signal of 50-ms duration to be perceived as having the same intensity as the 500-ms signal, its actual amplitude must be 10 db greater than that of the 500-ms signal.

Practical applications

What are the practical applications of these findings? Well, virtually all consumer audio electronics make use of some form of audio imaging, sound localization, or psychoacoustics. For example, stereo width expanders have been used for years to widen stereo images from small portable radios. This expansion involves adding phase shifted right-channel signal to the left channel, and phase shifted left-channel signal to the right channel. By increasing the amount of out-of-phase signal, the audio image appears to be much wider than the actual spacing between speakers.

Stereo synthesizers are popular for converting monophonic signals into simulated stereo signals by keeping one signal intact and phase shifting the other.[28] Phase shifting

was once popular (as in the Sansui Matrix System) for encoding and decoding four-channel or "quad" music. The result was a sense of concert hall ambience of complex indirect sounds heard in a large enclosure.[3] Modern surround-sound decoders provide similar results through phase shifting, albeit with a slightly different encoding/decoding scheme.

Perhaps the most obvious application of audio imaging is found in the music industry. Sophisticated audio processing schemes—commonly implemented digitally—have been applied to recordings, instruments, microphones, etc., in an effort to present a particular audio image. I've put together a system which uses this same technology to significantly enhance one's ability to clearly recognize a particular CW signal in the presence of other signals and noise.

A CW imaging system

Although a wide assortment of digital multi-effects processors for home recordings are available, complete with programmable and factory-supplied filters, memory, etc., you can assemble a CW imaging system for a very modest investment in equipment. The simplest approach is to use a commercial sound decoder sold for home stereo systems. I have used two such systems—the M-360 Sound Effects Decoder (Surround Sound, Inc., Santa Monica, California) and the Heathkit AD-2550 Surround Sound Decoder (Heath Company, Benton Harbor, Michigan)—with good results. Both of these decoders use filter and delay circuits, together with on-board stereo audio amplifiers, to reconstruct encoded audio signals from many of the more popular movies available on video tape.

In normal operation, these decoders add a selectable delay between channels, both to make the listening room seem larger, and to eliminate sibilance distortion (the "tearing" sound on the letter S). The signal delay, upon which both of these effects are based, is commonly made possible by a bucket brigade device or BBD. Although BBDs are generally analog input and output devices, they can perhaps be best understood by likening them to a common digital shift register. In its simplest incarnation, a shift register is a series of flip-flops connected so each flip-flop assumes the state of the preceding flip-flop with each clock cycle.[29,30] Although shift registers are most commonly used to implement shift operations in computer CPUs and for converting between serial and parallel data, they can also be used as digital delay devices which provide delays an integer number of clock cycles in length.[31,32]

In a similar fashion, a BBD, which may contain several thousand stages, can be used to add incremental delays to an audio signal path. For example, the Heathkit Surround Sound Decoder uses an MN3008 BBD, a 2048 stage unit, to provide a delay of between 15 and 30 ms in the signal. However, instead of relying on a series of digital flip-flop elements, BBDs consist of an array of capacitors and clocked switches.[33] After an input signal has been sampled, it is propagated from one capacitor to the next at a rate defined by the system clock. The voltage at the end of the capacitor series drives a differential amplifier, producing the output signal. Like all forms of analog-to-digital converters, the frequency response of a BBD is limited by the sampling frequency.[34]

In addition to their normal decode functions, sound decoders commonly provide a standard *mono enhance* feature that adds synthesized stereo to front channels, derived center-to-center channels, bass to the subwoofer channel, and synthesized surround-sound effects to the rear channels. For the purposes of intra-aural or headphone-based CW imaging, only the synthesized stereo available from the front channels is used.

Because they are essentially closed-architecture devices, operation of commercial decoder systems is straightforward. Simply apply the monophonic audio signal to the input ports, set the mode to mono enhance, and connect a set of stereo headphones to the front channel output ports. The audio delay can then be adjusted until the optimal signal image is perceived.

Unless you also plan to use the decoder with your home stereo system, the commercial decoder approach is somewhat expensive (about $200 plus for a unit). A less costly approach, which not only provides a system with more flexibility than the commercial "black box" systems, but also lets you experiment with audio phase and amplitude relationships at a lower level, is to use discrete filter, delay, and amplifier components. Although most Amateurs active in CW already have access to a suitable low-pass audio filter, circuit descriptions for simple low-pass audio filters are given in most of the Amateur reference texts. You can also fabricate a simple delay circuit for just a few dollars in parts. A BBD chip, like the MN3008, and a compatible clock source, like the MN3101, along with a handful of bypass and coupling capacitors, are all that

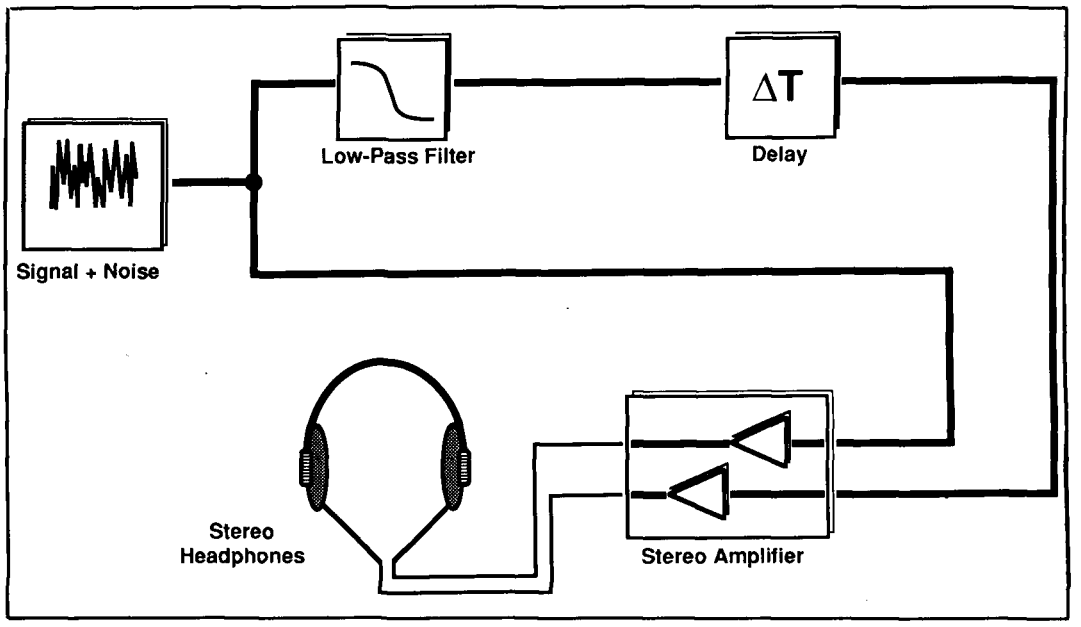

Figure 3. The basic configuration of a CW imaging system. The signal source, which contains multiple CW signals as well as noise, is split into two paths. Signals in the first path are applied directly to the input of a stereo amplifier. Signals in the second path undergo both low-pass filtering and phase shifting or delay before being directed to the second channel of the stereo amplifier. The processed signal is then made available to the operator through a set of stereo headphones.

you need to build a simple and effective delay circuit.

Inexpensive preassembled delay units, sold as Electronic Reverb devices, are also available. The Realistic Electronic Reverb (RS No. 32-1110A) can be purchased for about $14 on sale, and the RadioKit Springline Mono Reverb Unit (RadioKit No. 41-01602) sells for under $40. The stereo audio amplifier for this system can be your home stereo, or a simple two-chip device based on the LM386 audio amplifier IC. The only other piece of equipment you'll need is a pair of stereo headphones. Although virtually any stereo headphones capable of adequately reproducing communications frequencies (300 to 3000 Hz) will do, a pair with circumaural design will produce the best imaging effect. Circumaural headphones, unlike those of supra-aural or open-air design, form a tight-fitting oval around the ear to block out extraneous sounds.

Figure 3 illustrates the basic configuration of a discrete component CW imaging system. As you can see from the figure, the complex signal to be processed is first split into two paths. One is sent directly to one channel of a stereo amplifier, while the other is subjected to low-pass filtering and delay. As a result of this processing, signals with different spectra reach each ear, creating the imaging effect illustrated in **Figure 1**.

Figure 4 shows how easily a practical CW imaging system can be integrated into the framework of your existing station. The monophonic CW signal source, supplied by the phones jack of your HF transceiver, is processed by a low-pass filter, a delay device, and a stereo amplifier. In this system, I use a Realistic 5-Band Mono Frequency Equalizer (RD No. 32-1115) for low-pass filtering, and the Realistic Electronic Reverb unit for the delay. Low-pass filtering is provided by the graphic equalizer, set for 12 dB gain at 60 Hz, 0 dB at 240 Hz, and −12 dB at 1, 3.5, and 10 kHz. After low-pass filtering, the signal is then delayed by the reverb unit which is set to provide approximately 80 ms of delay.

In addition to variable delay, the reverb unit has a number of settings, which are, for the most part, unused in this application. For example, the microphone gain control is set to 0, since, as is the case of the graphic equalizer, the low-impedance line input and output connectors are used instead of the high-impedance microphone I/O ports. The reverb's repeat control, which defines the number of echoes in the signal, is also set to 0. The depth control, which varies the strength of the delayed sound in relation to the original signal, is set to near maximum (8, on a scale of 0 to 10). Although the exact control values for these parameters will vary from one reverb unit to the next, these parameters should be specifiable, even on the simplest unit. After inserting the delay in the signal path, the processed signal, like the

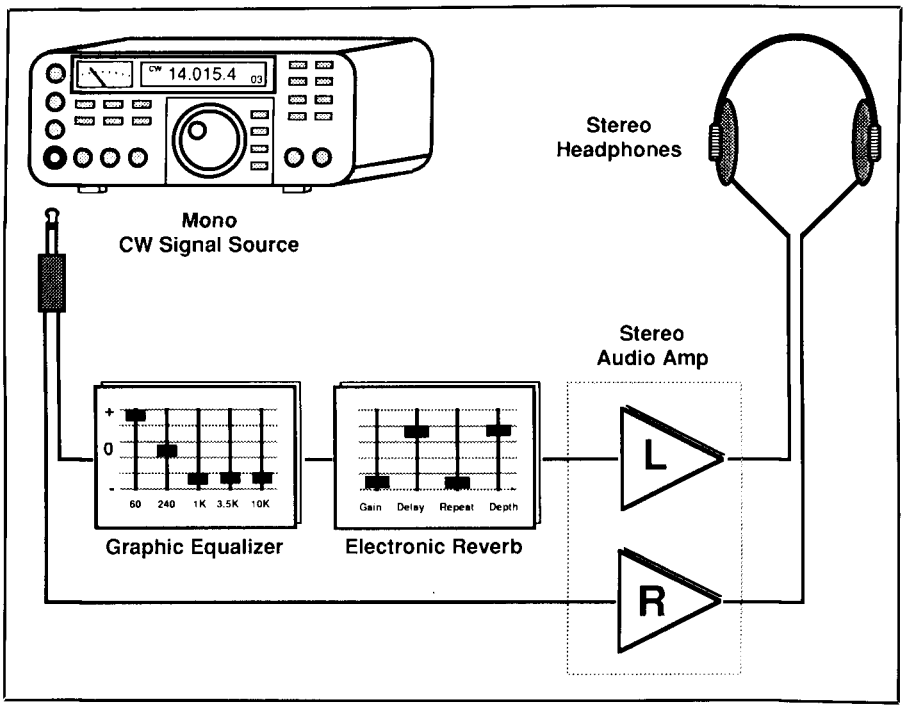

Figure 4. A practical configuration for an actual CW imaging system. The audio output from the headphone jack of an HF transceiver is split into two paths, as illustrated in *Figure 3*. Low-pass filtering is provided by a graphic equalizer, and the delay is introduced by an electronic reverb unit. The original and processed signals are then sent to a stereo amplifier, consisting of two LM386 ICs, and then to a pair of stereo headphones.

unprocessed signal, is amplified separately by a stereo amplifier constructed of a pair of inexpensive LM386 ICs, before being passed on to a pair of stereo headphones.

Operation

In normal operation, the suggested values for filtering, depth of reverb, etc., should be varied to suit the nature of the signal source and your personal preferences. Based on the experimental findings I've described here, you should strive to move the desired signal image as close to midline as possible.

For example, assume that there are four signals very near each other in frequency, say at 500, 700, 900, and 1000 Hz, and that the desired signal is at 900 Hz. For optimum spectral discrimination, you should manipulate the low-pass filtering and delay so the 900-Hz signal falls on or near the midline. This corresponds to the condition illustrated in **Figure 1**, assuming that the spectral maxima represent, from left to right, the 500, 700, 900, and 1000-Hz signals.

Summary

I've described an inexpensive and effective audio filtering system for CW which relies on the inherent capabilities of the human auditory system to synthesize an internalized audio image, based on relative differences in signal phase and amplitude. The system should be especially useful during high density traffic conditions like those experienced when contesting. ■

REFERENCES

1. I.P. Howard and W.B. Templeton, *Human Spatial Orientation*, London, 1966.
2. J. Blauert, *Spatial Hearing*, MIT Press, Cambridge, 1983.
3. L. Feldman, *Four-Channel Sound*, Howard W. Sams & Company, Inc., Indianapolis, Indiana 1973.
4. L. Raleigh, "On Our Perception of Sound Direction," *Philos Magazine*, 13: 1907, pages 214-232.
5. L.R. Bernstein and C. Trahiotis, "Lateralization of Sinusoidally Amplitude-modulated Tones: Effects of Spectral Locus and Temporal Variation," *Journal of the Acoustic Society of America*, 78: 1985, pages 514-523.
6. G.B. Henning, "Some Observations on the Lateralization of Complex Waveforms," *Journal of the Acoustic Society of America*, 68: 1980, pages 446-454.
7. J.M. Nuetzel and E.R. Hafter, "Lateralization of Complex Waveforms: Spectral Effects," *Journal of the Acoustic Society of America*, 69: 1981, pages 1112-1118.
8. W.A. Yost, "Lateral Position of Sinusoids Presented with Interaural Intensive and Temporal Differences," *Journal of the Acoustic Society of America*, 70: 1981, pages 397-409.
9. D.W. Grantham, "Interaural Intensity Discrimination: Insensitivity at 1000 Hz," *Journal of the Acoustic Society of America*, 75: 1984, pages 1191-1194.
10. E.R. Hafter, "Spatial Hearing and the Duplex Theory: How Viable is the Model?" *Dynamic Aspects of Neocortical Function*, Neurosciences Research Foundation, Rochester, 1984, Edelman, Gall, and Cowan, editors.
11. M.B. Gardner and R.S. Gardner, "Problems of Localization in the Median Plane: Effect of Pinnae Cavity Occlusion," *Journal of the Acoustic Society of America* 53: 1973, pages 400-408.
12. S.K. Roffler, and R.A. Butler, "Localization of Tonal Stimuli in the Vertical Plane," *Journal of the Acoustic Society of America*, 43: 1968, pages 1260-1266.
13. R.A. Butler, and N. Planert, "The Influence of Stimulus Bandwidth on Localization of Sound in Space," *Perception and Psychophysics*, 19: 1976, pages 103-108.
14. R.A. Butler and C.C. Helwig, "The Spatial Attributes of Stimulus Fre-

quency in the Median Sagittal Plane and Their Role in Sound Localization," *American Journal of Otolaryngology*, 4: 1983, pages 165-173.
15. W.A. Yost, and R.H. Dye, "Discrimination of Interaural Differences of Level as a Function of Frequency," *Journal Acoustic Society America*, 83(5): 1988, page 1846-1851.
16. G. Liden and M. Korsan-Bengtsen, "Audiometric Manifestations of Retrocochlear Deafness," *Adv. Oto-Rhino-Laryngol*, 20: 1973, page 271.
17. D.R. Perrott, Ambarsoon, and J. Tucker, "Changes in Head Position as a Measure of Auditory Localization Performance: Auditory Psychomotor Coordination Under Monaural and Binaural Listening Conditions," *Journal of the Acoustic Society of America* 82(5): 1987, pages 1637-1645.
18. R. Nilsson and G. Liden, "Sound Localization with Phase Audiometry", *Acta Otolaryngol*, 81: 1976, page 291.
19. G.L. Calhoun, G. Valencia, and T.A. Furness, "Three-dimensional Auditory Cue Simulation for Crew Station Design/Evaluation," *Human Factors Society 31st Annual Meeting*, 1987, pages 1398-1402.
20. T.J. Doll, "Synthesis of Auditory Localization Cues for Cockpit Applications," *Human Factors Society 30th Annual Meeting*, 1986, pages 1172-1176.
21. F.L. Wightman, D.J. Kistler, and M. Perkins, "A New Approach to the Study of Human Sound Localization," *Directional Hearing*, Yost and Gourevitch, editors, Springer-Verlag, New York, 1987.
22. R.D. Sorkin, F.L. Wightman, D.S. Kistler, and G.C. Elvers, "An Exploratory Study of the Use of Movement-correlated Cues in an Auditory Head-up Display," *Human Factors*, 31(2): 1989, pages 161-166.
23. E.R. Hafter, R.H. Dye, N.M. Neutzel, and H. Aronow, "Difference Thresholds for Interaural Intensity," *Journal of the Acoustic Society of America*, 61: 1977, pages 829-833.
24. F.O. Edeko, "Image Localization and Interchannel Phase Difference: Using the Wavefront Reconstruction Approach to Predict Image Position in Stereophonic Systems," *Electronics and Wireless World* 93(1618): 1987, pages 799-802.
25. H. Wallach, E.B. Newman, and M.R. Rosenweig, "The Precedence Effect in Sound Localization," *American Journal of Psychiatry* 62: 1949, pages 315-336.
26. R.B. Newman, S.A. Gelfand, "Characteristics of Sound," *Handbook of Modern Electronics and Electrical Engineering*, Belove, Hopkins, Nelson, Rosenstein, and Shinners, editors, John Wiley & Sons, New York, 1986.
27. J. Zwislocki, "Theory of Auditory Summation," *Journal Acoustic Society America*, 32: 1960, page 1046-1060.
28. P. White, "On the Button" *Home & Studio Recording*, 2(10): 1989, pages 58-59.
29. P. Horowitz and W. Hill, "Digital Electronics," *The Art of Electronics*, Cambridge University Press, Cambridge, 1980.
30. M.J. Wilson, "Digital Basics," *ARRL Handbook for the Radio Amateur*, Wilson, editor, American Radio Relay League, Newington, Connecticut, 1987.
31. F.J. Hill and G.R. Peterson, *Introduction to Switching Theory and Logical Design*, Wiley, New York, 1981.
32. T.W. Parsons, "Flip-Flops and Registers," *Handbook of Modern Electronics and Electrical Engineering*, Belove, editor, John Wiley & Sons, New York, 1986.
33. A.B. Grebene, H.H. Stellrecht, W.F. Davis, C.S. Meyer, R.C. Huntington, and D. Cave, "Integrated Circuits and Microprocessors," *Electronic Engineer's Handbook*, McGraw Hill, New York, 1982, Fink and Christiansen, editors.
34. L.C. Ludeman, *Fundamentals of Digital Signal Processing*, Harper & Row Publishers, New York, 1986.

PRODUCT INFORMATION

Sixteenth Edition of *The ARRL Antenna Book* Released

The ARRL has just released the 16th edition of *The ARRL Antenna Book*. This antenna builder's classic has been extensively revised and updated to reflect the latest antenna designs and technology. There are extensive sections on computer modeling and design optimization, with explanations for both the beginner and more experienced amateur. The book includes an expanded chapter on antenna and transmission-line measurements, along with chapters on safety, fundamentals, loops, limited space designs, multi-element antennas, log periodic, Yagis, and quads. Information on VHF/UHF antennas for home and mobile use is also included. *The ARRL Antenna Book* is over 736 pages long and contains over 900 charts and figures. To order a copy, contact the CQ Bookstore at (800)457-7373.

New Power Switching Regulator Available

A new monolithic power switching regulator IC with an on-chip output switch capable of controlling currents in excess of 5.0 amps is available from Motorola. The MC34167 switching regulator is available in a 5-pin TO-220 type plastic power package in both commercial and industrial temperature range versions. The device contains the primary functions required in step-down and voltage-inverting configurations with a minimum of external components.

The MC34167 has an internal temperature-compensated reference, a fixed frequency oscillator with on-chip timing, a latching pulse width modulator for single pulse metering, a high gain error amplifier, and a high current output switch transistor. Protective features include cycle-by-cycle current limiting, undervoltage lockout, and thermal shutdown. There's also a low power standby mode that reduces power supply current to 36 μA.

Samples are available. Contact Motorola Inc.—Media Relations, P.O. Box 52073, Mail Drop 56-102, Phoenix, Arizona 85072. To obtain technical data on the power switching regulator write to the Motorola Literature Distribution Center, P.O. Box 20912, Phoenix, Arizona 85036. Ask for data sheet MC34167/D

Correction

Incorrect Equation

The legend in **Figure 1** of "The Quad Antenna: Rectangular and Square Loops," by R.P. Haviland, W4MB, from the Spring 1991 issue contains an incorrect equation. Somewhere in the drafting process, a factor of 2 was lost in the expression for omega. It should read $\Omega = 2\ln(2\pi b/a)$. **Ed.**

John Tyskiewicz, *W1HXU*
77 W. Euclid Street
Hartford, Connecticut 06112

SUPER YAGI BEAM

All the best features of the Yagi and the loop are combined into one antenna.

The optimum and most cost-effective Yagi-type beam, has four elements mounted on a long boom. The full-wave element in a quad or a loop-type antenna, has a 2-dB gain advantage over the half-wave Yagi element. Many feel that a three-element loop is equal to a four-element Yagi on a longer boom![1,2] Some also contend that the loop is better when antenna height is at a modest elevation. However, the relative simplicity and strength of the Yagi has predominance over power gain for many experimenters. My "Super Yagi" combines some of the desirable features of the Yagi and the loop.

At a glance, the antenna in **Photo A** appears to be a normal three-element Yagi. Closer inspection reveals three additional wire sections. A commercial or ham version of the Yagi can be easily converted into a

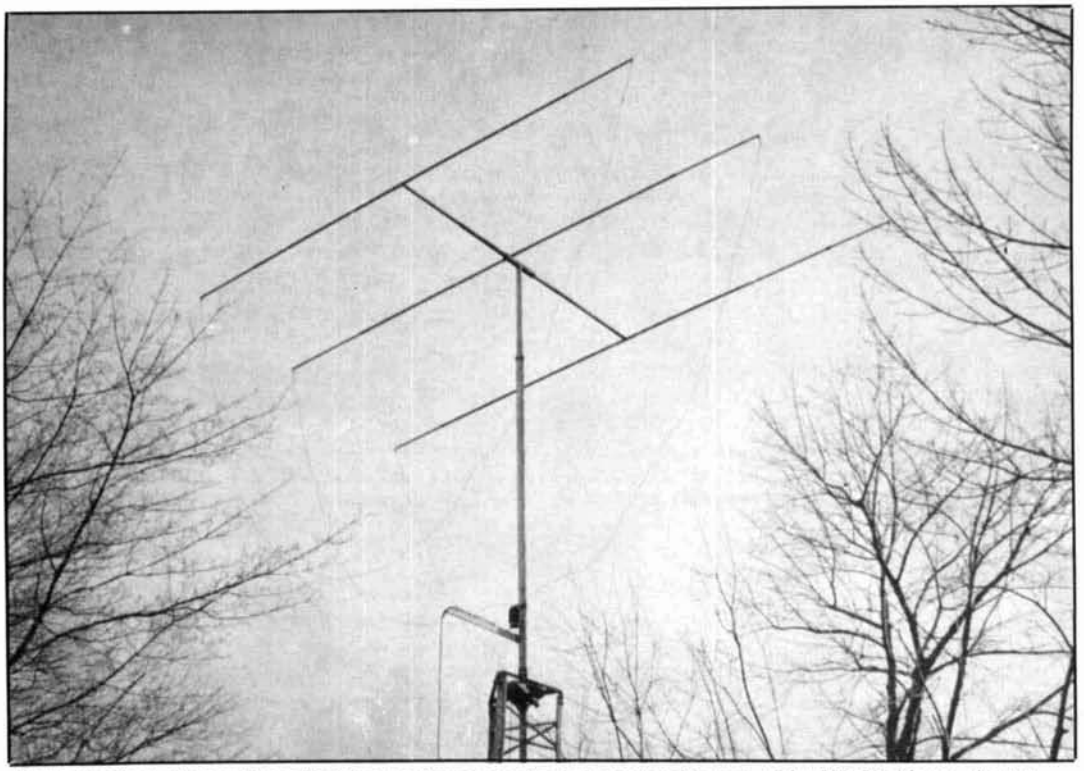

Photo A. The 3-element Super Yagi has the firepower of a 4-element and longer, wider Uda-Yagi beam. A mast yardarm fixture below the choke balun guides the RG-59 feedline around the tower.

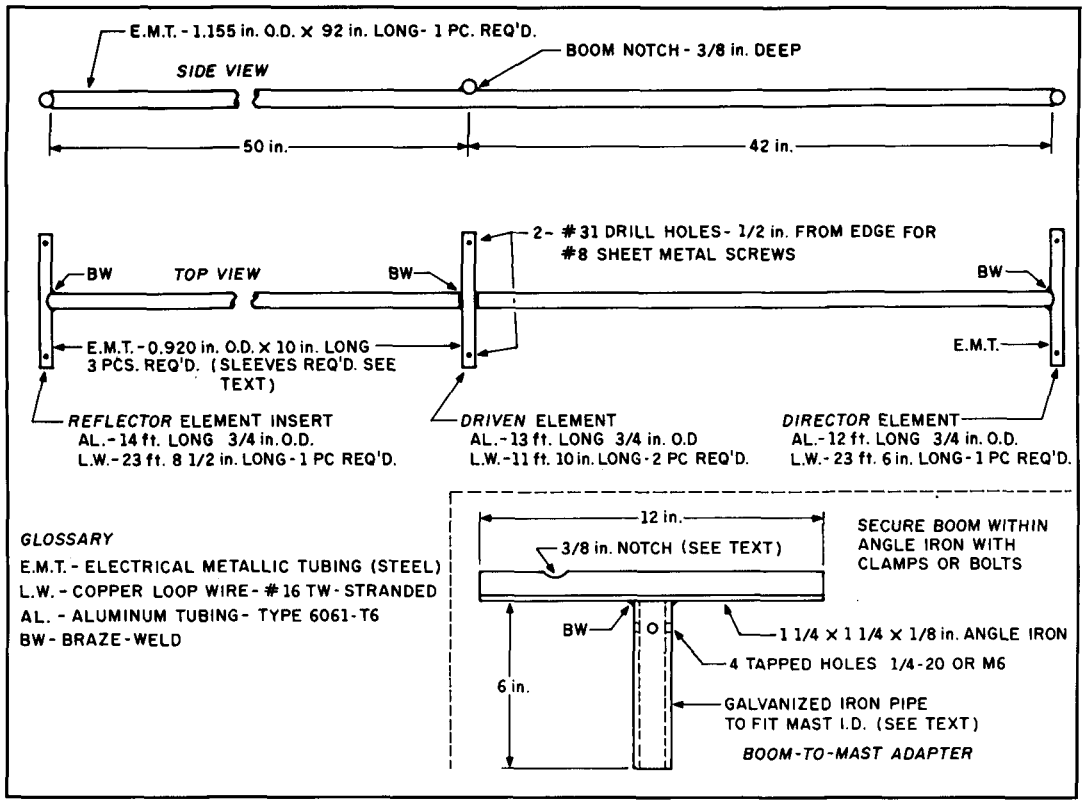

Figure 1. Element-to-boom unit and mast adapter.

Delta Loop by shortening the elements to 1/3 wavelength and adding a 2/3-wavelength long wire suspended from the ends. By virtue of its general appearance and 99 percent Yagi construction, the antenna is a Super Yagi.

The Super Yagi is different from the Delta Loop beam described by K8ANV[3] His triangular elements are perched at their apex and extend above the boom. This creates a mechanical engineering problem with the larger beams, necessitating extraordinary element-to-boom and mast hardware to keep it from toppling[4]

Materials and construction

I used steel EMT (electrical metallic tubing), pipe, angle iron, wire, and sheet metal from a scrap-metal yard. New EMT and thermoplastic-covered wire are available from electrical supply shops. These shops also carry anti-corrosion grease.

All the pertinent construction data for a 10-meter three-element Super Yagi array is shown in **Figures 1** and **2**. To start, shape the boom ends using a hacksaw, grinder, or file until they match the smaller 10-inch long EMT parts, then make the boom notch. The fit need not be precise; the molten bronze used in the brazing process will fill any gaps. Braze the boom to the zinc-coated EMT. This will generate considerable smoke and is better done outdoors. If you do your brazing in a basement workshop, shut off any smoke and fire detectors, and make sure you have adequate ventilation.

The tricky part of this operation is to create a permanently aligned, monolithic structure. First tack-weld or braze the 10-inch EMT piece to the boom notch at one spot. If necessary, straighten the tubing to obtain a 90-degree fit perpendicular to the boom. Apply another tack opposite the first, before starting the finish weld at a new spot. Tack the 10-inch reflector portion into place and insert the reflector element, or it's central portion (also the driven element), into position. Step back and sight down the boom for the parallel elements. Repeat this operation for the director assembly. Chip off and joint-wire brush the glassy weld flux before painting the boom. If you don't, the flashed-on zinc coating will corrode.

Boom to mast adapter

If you make a unit similar to the one shown in **Figure 1**, you'll find that the O.D. pipe size is generally incompatible with the I.D. mast size, and will require shims or sleeves. The clearance notch in the angle iron is needed to prevent interference with the driven element. The location of this

notch is determined by the center of gravity point of the assembled beam. The loop wires can be coiled and fastened to the boom, and the assembly balanced on a sawhorse.

Elements

My elements came from an old 6-meter beam. I extended the 3/4-inch O.D. tubing to the specified 12, 13, and 14-foot dimensions with 5/8-inch O.D. tubing. When joining aluminum sections to each other, or to other metal parts, always coat them with anti-corrosion conductive paste or grease.

Make six 1-inch long, 3/4-inch diameter I.D. sleeves from aluminum or galvanized-metal sheeting, leaving a wide clearance gap for the no. 8 sheet-metal screws. Bevel the I.D. ends of the 10-inch EMT element holders with a tapered reamer or file to ease sleeve insertion. The hole size in the EMT is the thread-root diameter for a better grounded element.

Loop wire

I attached the no. 16 plastic-covered TW stranded wire to a tubular element as shown in **Figure 2.** This technique prevents wire from flexing and eventually breaking at the soldered joint. If you use plastic tape for the outer wrapper, bind it with wire at the last turn to keep the tape from unraveling.

Feed system

You may retain the type of matching system already in use. The relative input impedance for a loop-type beam is quite good with a direct 73-ohm coax feed. If you're a purist, you'll want to insert the 73-ohm matching section between the loop and a 52-ohm feed line.

My RG-59 cable was extra long, so I used the uncut portion for a choke balun. Add one, if your installation is wired for 52-ohm cable.

Choke balun

Make elongated holes for the coax in the PVC or ABS pipe-stock coil form (see **Figure 2**) to avert displacement of the central wire conductor by cold-flow migration in the polyethelene core. Don't kink the coax.

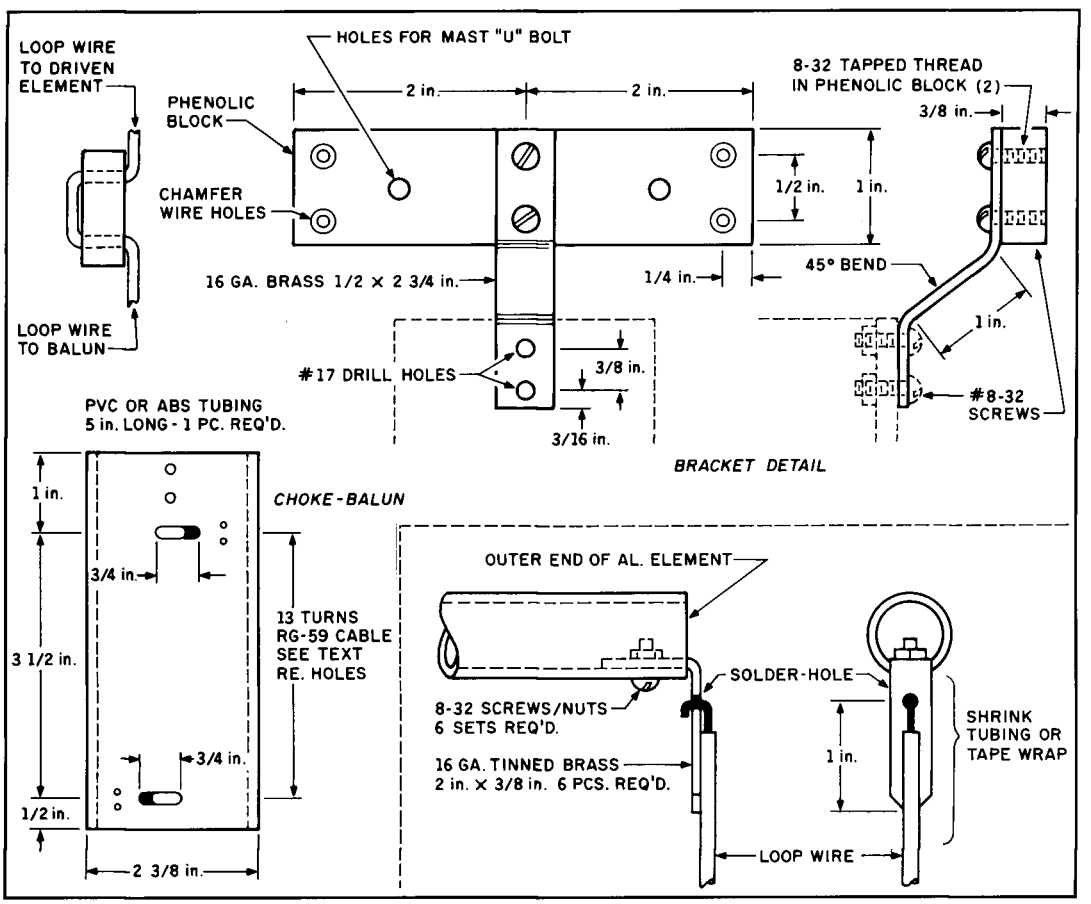

Figure 2. Driven-element connector block, choke-balun, bracket, and loop-wire attachment.

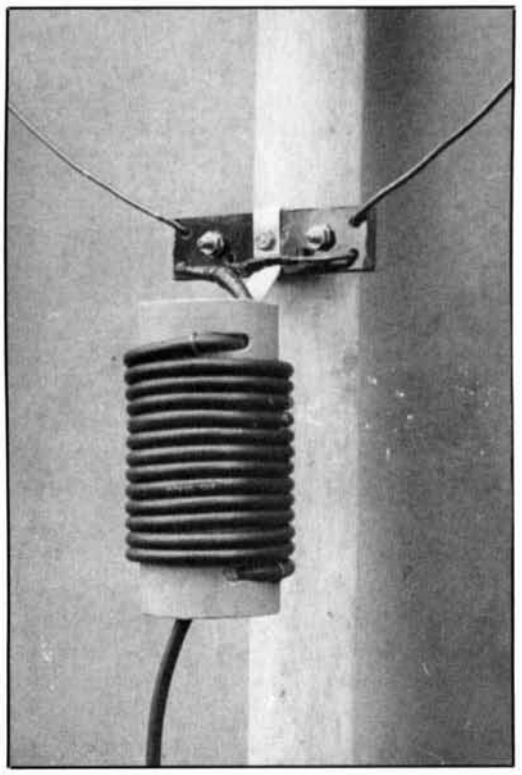

Photo B. Closeup of connector block, choke balun and Delta-Loop wire extensions. Secure bracket with two fasteners as shown in bracket detail drawing.

Start with a pilot hole and follow with a 1/4-inch drill. Maneuver the electric hand drill to a relatively tangential position and cut with the lands or side. Do the final trimming with a knife. Fasten the cable to the coil form with a U-shaped length of no. 16 copper wire pushed through the small diameter holes astride the cable and twist-locked inside the coil form.

Connector block

The connector block, also shown in **Figure 2**, is held in place by the mast U bolt. I made one from 3/16-inch diameter brazing rod with threaded ends. I insulated it from the aluminum mast with plastic tape wrapping to prevent acid rain electrolysis. The coil support bracket has a 45-degree bend for greater separation between the metal mast and choke coil.

Attach the assembled unit (**Photo B**) to the mast, 9 feet below the antenna boom. Lace the loop wire through the chamfered holes and solder it to the RG-59. Make sure the joints are sealed over. The suspended and **slack** loop wire will assume a hyperbolic outline.

Basic design

I used *The ARRL Antenna Handbook* equation for the prototype. Initial tests revealed that the resonant frequency and low SWR was considerably higher than desired. I extended the loop wires and obtained the following:

$$Lft = \frac{1042}{MHz}$$

The reflector is 2 to 3 percent longer and the director is 2 to 3 percent shorter.

This over-simplified equation, doesn't allow for different tube-to-wire ratio, shape factor, element spacing, height above ground, or nearby wires. Element spacing is a major factor. Changing the director spacing from 0.1 to 0.2 wavelength, lowered the magic number in the equation to 1022.

SWR notes

Figure 3 is a smooth SWR plot based on nine spot readings. The meter was inserted in the feed line at the transmatch or tuner. With the meter between the transmitter and tuner, you can obtain a SWR of 1:1 across the entire band.

Although it would appear desirable to maintain a constant bottom-end separation, practical experience has shown that variations due to normal wind exposure produce an insignificant effect—especially with wide element spacing. My present 15-meter prototype beam has no. 18 gauge stranded wire with Teflon™ insulation for its drop wires and works great "as is" during blustery New England weather. In a severe environment, you can stablize the loop's bottom loop wire with a boom-length stick connected to the wires and mast. ■

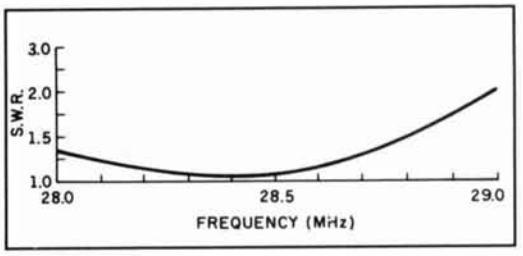

Figure 3. SWR of Super Yagi with 0.12-wavelength reflector and 0.1-wavelength director spacing.

REFERENCES

1. J.E. Lindsay, Jr., W0HTH, "Quads & Yagis," *QST*, May 1968, pages 11-19.
2. R.P. Haviland, W4MB, "The Quad Antenna," *Ham Radio*, August 1988, pages 34-47.
3. H.R. Habig, K8ANV, "Delta Loop Beam," *QST*, January 1969, pages 26-29.
4. L. McCoy, W1ICP, "Big Horn Delta Beams," *CQ*, June 1988, pages 28-31.

Yardley Beers, *WØJF*
740 Willowbrook Road
Boulder, Colorado 80302

MAKING HIGH-Q AIR-CORE COILS

The "basket-weave" coil revisited.

Through perhaps the mid-1950s, any good electronics lab had a corner devoted to coils. Usually, you'd find a coil-winding machine with a rack of gears and a Boonton Q meter. Above this, there'd be a shelf of coil forms and a collection of powered iron cores and slugs. But the young designer could fumble for days trying to wind a coil, because there were no user's manuals. Often an old-timer would take pity, and show him how. The following article, by Yardley Beers, W0JF, follows in that tradition. While many modern circuits can do without a seriously designed coil or transformer, high-power and antenna-matching circuits need the real thing. We hope you'll find this article helpful should you ever need such a coil.

Hunter Harris, W1SI,
COMMUNICATIONS QUARTERLY
Editorial Review Board

Do you need a high-Q coil for an antenna coupler you're building, or as a loading coil for an antenna? Do you want to avoid the cost and inconvenience of obtaining commercial stock? You can make a coil easily with common materials by following the directions given here. The design is an old one, known as the "basket weave." It was popular in the late 1920s, but is now largely forgotten.

Some examples

Photo A shows two samples of coils I've made. The one on the left has an inductance of 20 μH and a measured Q of 350 at 3.8 MHz and 270 at 1.8 MHz. It has 15-1/2 turns of no. 12 plastic-coated wire with a diameter of 3-1/8 inches.

The one on the right has an inductance of 70 μH and a Q of 155 at 3.8 MHz and 200

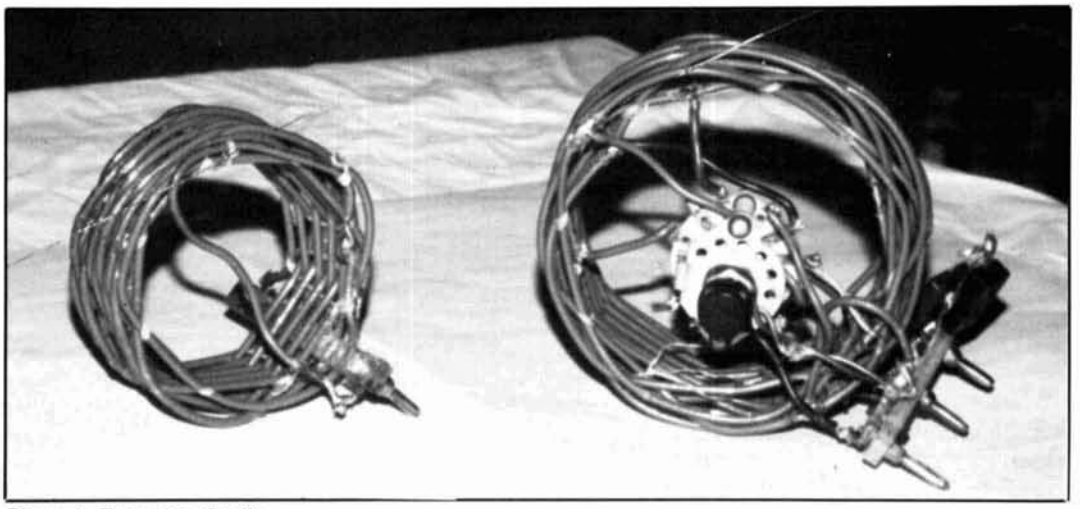

Photo A. Examples of coils.

at 1.8 MHz. It has 21 turns of no. 12 plastic-coated wire and a diameter of 4-1/4 inches. The coil is an auto transformer for matching the impedance of 50-ohm coax to a 38-foot base-loaded vertical antenna at 1.8 MHz. It has taps for shifting the resonance within the band. The tap for the ground is 2 turns from the end connected to the coax. A coil of nearly the same inductance and diameter, using no. 14 wire and no taps, has a Q of 300 at 1.8 MHz.

Choosing the radius and the number of turns

To select the radius, you must first decide what inductance you want the coil to have and the type of wire you need. If you're going to use high power, consult wire tables to find the minimum required diameter.

The wire size and type of insulation determine the number of turns per inch K. But, remember that only two-thirds of the turns lie on the surface of a nail. If you take the number of turns per inch from a wire table, make sure to multiply this number by 3/2.

If the desired inductance in microhenries is L, the radius of the coil in inches is given by

$$R = \sqrt[3]{\frac{200\,L}{9\,K^2}}, \qquad (1)$$

and the number of turns is given by

$$N = \sqrt{\frac{18\,L}{R}}, \qquad (2)$$

The length of wire required is

$$X = 2\pi\,NR \qquad (3)$$

If you build the coil according to these formulas, you should find that, approximately,

$$B = 0.9\,R \qquad (4)$$

Therefore, the length of the coil is within ten percent of the radius.

Derivation of formulas

I'll sketch the main ideas used in the derivations without giving all of the steps. You can find the following formula, known as the Wheeler formula, in many handbooks and textbooks. It gives a good approximation of the inductance of a solenoid.

$$L = \frac{N^2R^2}{9\,R + 10\,B} \qquad (5)$$

or, expressing B in terms of K and N,

$$L = \frac{N^2R^2}{9\,R + 10\,KN} \qquad (6)$$

As it stands, this formula is useful mainly in calculating the inductance (L) of an existing coil. In the situation assumed here, you know L and K and want to find N and R. If you were to solve **Equation 6** for N, you would need to know R, as well as L and K. If you were to wind a coil on a piece of tubing, you'd use the radius of the tubing for R. Here, where there's a free choice of radius, I've imposed the condition that, for a given L and K, the length of wire X is a minimum. I used calculus and algebra to obtain **Equations 1, 2,** and **4.**

At low frequencies, the resistance of a wire is independent of the shape in which it is bent. Therefore, the resistance of the coil is a minimum and its Q a maximum for a given L and K. Because the magnetic field of the coil causes a redistribution of the current in the wire at high frequencies, the resistance depends upon the shape in a complicated way. While it's probably not true that the Q is exactly the maximum possible, it is logical to suppose it's near to the maximum. At any rate, the condition that the wire length be a minimum results in a reduction in the amount of the wire used and in the weight of the coil.

Mechanical construction

Begin by determining the radius of your coil and the number of turns it will need. Next, wind the coil on a group of nails driven into a board at equal distances around a circle. The winding scheme I use is shown in **Figure 1.** The wire goes on the

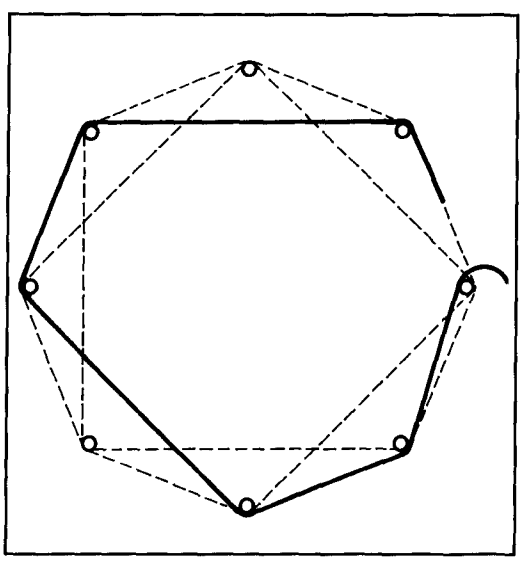

Figure 1. Construction method for basket weave coils.

outside of two adjacent nails, on the inside of the next nail, back on the outside of the next two, and so on, until the winding is complete. If the number of nails isn't an integral multiple of 3, no two adjacent turns will lie completely on top of one another, and each turn will be separated over most of its length from the adjacent turns. I use either 8 or 16 nails. The positions for 8 can be laid out easily using a 45°-45°-90° triangle. If you use 16, you can locate the additional nails by eye.

When you've finished the winding, apply household cement and tie the coil together as a rigid structure. Do this by forcing the winding up from the board slightly, so you can slip pieces of string under the coil. Wrap string around the turns in two or three places between nails, partly on the outside and partly on the inside of the coil, in such a way as to squeeze the turns together. Tie the strings. (These strings are temporary.) Apply household cement to the coil in a few places, but avoid cementing the coil to the nails or the string.

When the cement has hardened, carefully extract an adjacent pair of nails. Using a small wire as a needle, and with the help of tweezers or a pair of needle-nosed pliers, wrap a couple of turns of string around the wires at their crossing point in the space between where the extracted nails were located. Pull the ends of the string tight and tie them. Repeat the procedure with another pair of nails on the opposite side of the circle. Continue removing nail pairs until all of the nails have been extracted and the coil is completely free. Remove the temporary bindings and cement the coil thoroughly.

I find waxed lacing cord is best kind of string to use. This is now hard to find, but waxed dental floss is a good substitute.

The coil on the left in **Photo A** has had a strip of plastic with smoothed corners forced through the space where a nail was located. The strip contains two banana plugs. This strip contributes to the rigidity of the coil. The coil on the right is supported by its leads from a strip containing banana plugs. With other coils, I've used two strips bolted together with spacers—one is forced through the winding and the other holds banana plugs.

Adjusting the inductance

Because of inevitable small errors, the coil probably won't have exactly the inductance you expect. Since it's more convenient to have too many turns than too few, I generally wind one more turn than the number I've calculated, and expect to adjust the inductance downward. In a few cases, I've gone through the tedious process of actually removing turns and replacing the strings as I proceed. It's easier to leave a free end and make the connection with a tap. To provide rigidity, I've made the plastic strips extra long so I can use a machine screw to tie down the free end.

In cases where I've had to add a turn or two, I've spliced a piece of wire onto one of the leads of the coil, shaped it by hand to conform with the shape of the coil, and tied it down.

I leave one or both leads free of the string structure, so I can make fine adjustments to the inductance. By bending these leads, I can vary the inductance continuously by an amount equivalent to one turn. In **Photo A** the lead that goes diametrically across the coil on the left is used for this purpose.

I hope you'll try this old standby the next time you need a high-Q air-core coil. It's easy to make and inexpensive, too! ■

PRODUCT INFORMATION

Application Note Available on HP Impedance-matching Design Tool

A new Hewlett Packard application note, "Designing Impedance-matching Networks with the HP 8751A," describes how design engineers can use the conjugate-matching function of the HP 8751A network analyzer to design impedance-matching networks. This eight-page note, AN 1202-1 (Lit. 5091-1506E), explains the conjugate-matching function and how it works using a design example.

For those individuals not fortunate enough to have access to an HP 8751A, the note includes a review of impedance-matching theory, the use of a Smith chart, and an excellent list of references.

The note is available free of charge from: Hewlett Packard, 3000 Hanover Street, Palo Alto, California 94304.

George W. Carson, *K4GDG*
Route 4, Box 632
Crossville, Tennessee 38555

MODIFYING THE HEATH SB220 LINEAR AMPLIFIER

Better performance from a veteran workhorse

Corrections to this article can be found on page A1 of this issue.

Although I was disappointed with my Heath SB220's performance, I knew the basic design was capable of much more and decided to make some improvements.* Most of the changes I added are shown in the schematic in **Figure 1**. The following steps detail my modifications. Remember that *lethal* voltages are present in this amplifier. Before attempting any work, remove all sources of power and discharge the HV and bias supplies!

Parasitic suppressors and plate connectors

To reduce parasitic oscillation, use the plate parasitic suppressors shown in **Figure 2** of **Reference 1**.

I elected to replace the 3-500Z plate connectors (shown on page 3 of **Reference 2**) with homemade ones (see **Figure 3**). The modified 3 1/8-inch connectors are shorter, resulting in a greater separation from the top shield, increased heat dissipation, and less stray capacitance. I cut these to a 3/4-inch length from 1-inch diameter aluminum stock. If 1-inch diameter stock isn't available, a larger size will do. Groove the sides to improve the plate seal cooling. (You can do this easily in a lathe using a hacksaw blade for a tool.) Next, carefully bore 4 3/8-inch holes into each heatsink to provide a snug fit over the 3-500Z anode caps. Drill the top of the heatsink and tap it for a 6-32 1/4-inch brass screw for electrical connections 5/32-inch from the outer edge. Also drill and tap for a 6-32 setscrew into the heatsink side about 3/16 inch down from the top. This is used to clamp the heatsink to the tube anode.

Underneath the amplifier, route the RF drive to the tube filaments through a pair of 10-ohm 2-watt metallized (non-inductive) resistors, each in series with a 0.01-μF disc ceramic capacitor. These work as additional parasitic suppressors (see **Figure 4, Reference 3**).

Shielding

Replace the point-to-point wiring with shielded wiring. The SB220 makes extensive use of common chassis grounding.

ALC changes

To make the ALC level adjustable, install a 100-k pot on the front panel. Cut and reroute the lead from resistor R11 going to the voltage divider formed by resistors R3 and R4 to the center arm of the newly installed 100-k ALC level control. One leg of the ALC pot goes to ground, the other—via a shielded lead—to the hot side of capacitor C4. Replace capacitor C47 (1000 pF) with a 200-pF disc. Remove capacitor C49 and resistor R22.

Antenna relay changes

Replace the lead from the RCA connector on the rear apron (relay control) to the antenna relay RL1 with shielded wire. Place a 1N4002 diode and 200-ohm 1/2-watt resistor in series with the keying line to reduce transients at the transceiver relay contacts[3]. The keying line may be broken by installing it in series with a SPDT miniature switch on the front panel to provide a "standby" condition for the amplifier.

The flexible pigtails on the antenna relay are a little light considering the RF currents involved. Parallel additional pigtails, sal-

*The SB220 amplifier is a proven workhorse, but its ability to achieve maximum ICAS ratings with 3-500Z tubes is limited by its lack of air system sockets and chimneys, a weak HV supply, and tuning capacitor voltages. But it was designed when FCC rules dictated a 1000-watt maximum DC input power, rather than the present 1500-watt maximum output rule. Ed.

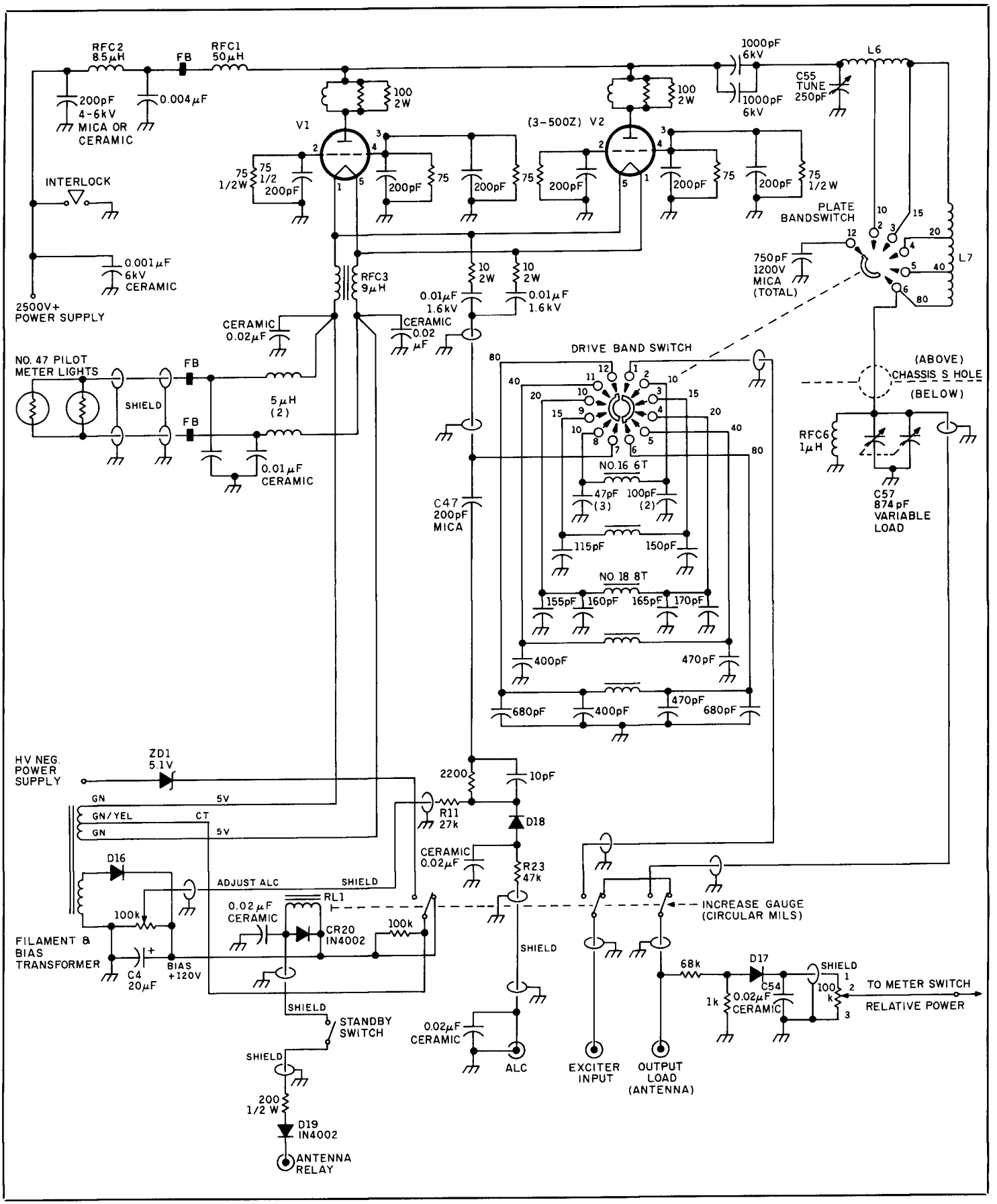

Figure 1. Modified SB220 Amplifier schematic.

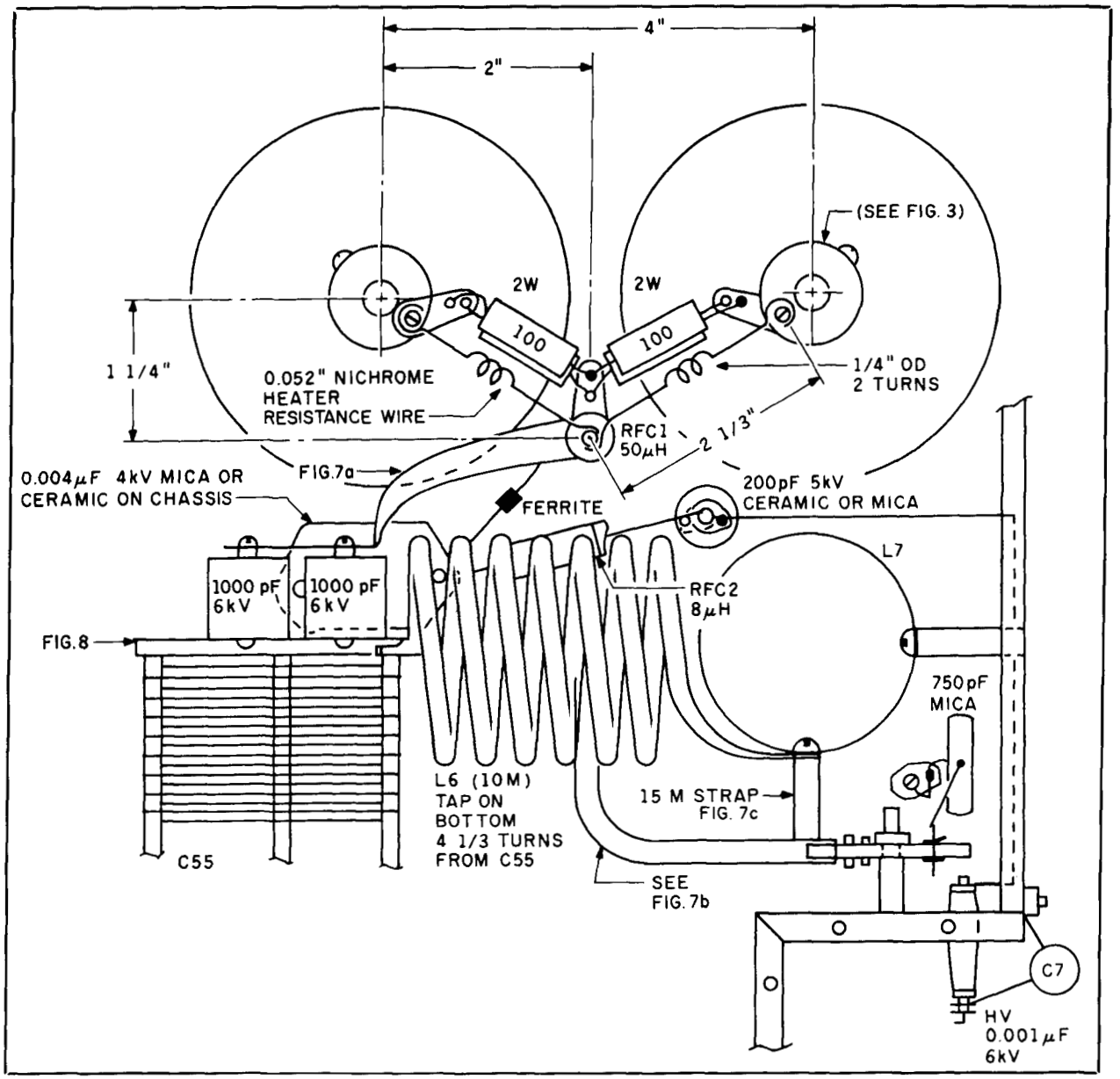

Figure 2. Mechanical detail of modified parasitic suppressors. A heavier conductor was used for the two 1000-pF 6-kV ceramic capacitors. Ten and 15 meter revised taps were used for the bandswitch.

vaged from junk relays, across the existing pigtails. Ideally, 4080 circular mils is needed, equivalent to a no. 14 conductor. The flexible relay arms are about 2437 circular mils. This is a limiting factor, unless you replace RL1 with a heavier duty relay.

Relative power meter bypassing

Replace the wiring associated with R26, the relative power metering control, with shielded wire.

Meter lamp bypassing

To further isolate the meter lamps from RF drive that may be present on the filament winding, you'll need to install further bypassing. A 2 to 5-μH choke is connected in line with each of the leads at the no. 47 meter lamp terminals to the transformer side of the filament choke, RFC3. Run shielded wire to the lamps. Isolate the RF chokes with ferrite beads and 0.01-μF disc capacitors (**Figure 5**).

Improving the efficiency of the input pi-network

The input matching circuits of the SB220 may present a high enough VSWR to be troublesome for modern solid-state exciters. This was most noticeable on the 10 and 20-meter Amateur bands. Modifying the plate and grid circuits netted a better match and increased drive[4,5].

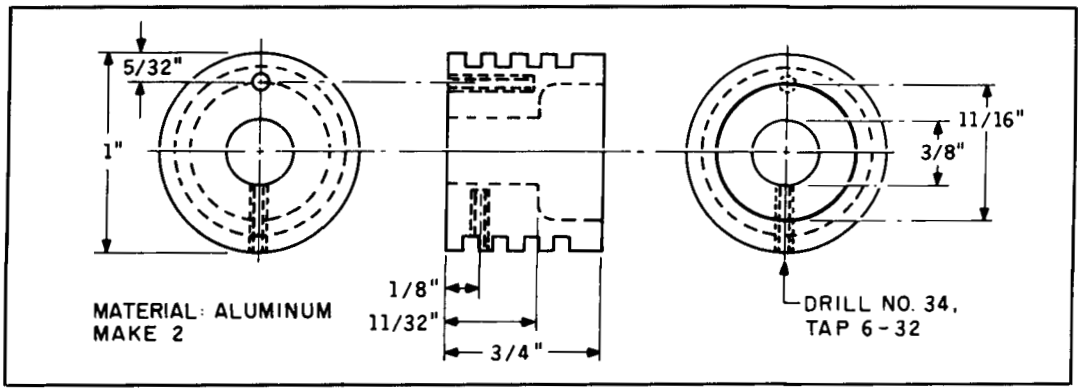

Figure 3. Modified anode connectors.

Ten-meter input network changes

Remove L1, the 10-meter input coil, and rewind the coil with six turns of no. 16 wire spaced evenly over 5/8 inch of the coil form. Solder the coil pigtails to the coil posts leaving about 2-1/2 inch long pigtails to reach the bandswitch terminals. Because it will be necessary to tune the coil later, you may have to loosen a stuck slug with acetone at this point. Discard the no. 22 wires used by Heath between the bandswitch and coil and install the new coil. It's important to trim the pigtails from the coil to the bandswitch terminals as short as possible while providing proper dress and spacing to other input coil wiring (see **Figure 6**).

Discard the original capacitors associated with L1—C33, 34, and 35. Note that C33, C34, and one leg of the coil go to switch terminal 8; C35 and the other coil lead go to switch terminal 2. (Refer to page 14 of **Reference 2.**) They will be replaced by three 47-pF capacitors in parallel for C33 and 34,

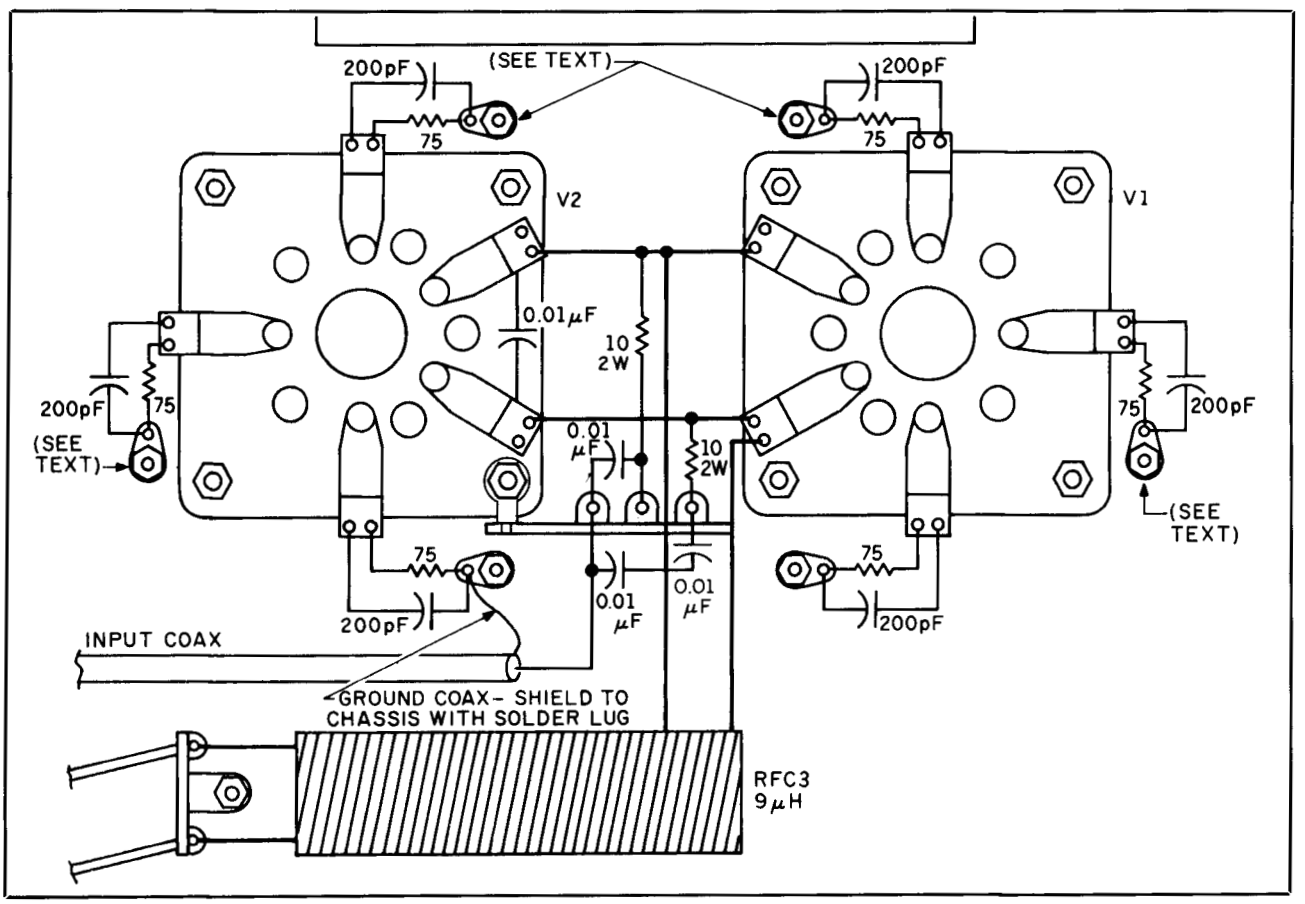

Figure 4. Detail of revised mechanical and electrical connections to grids of V1 and V2. Note grounding of shielded braid of input coaxial line to solder lugs and new mounting locations on chassis.

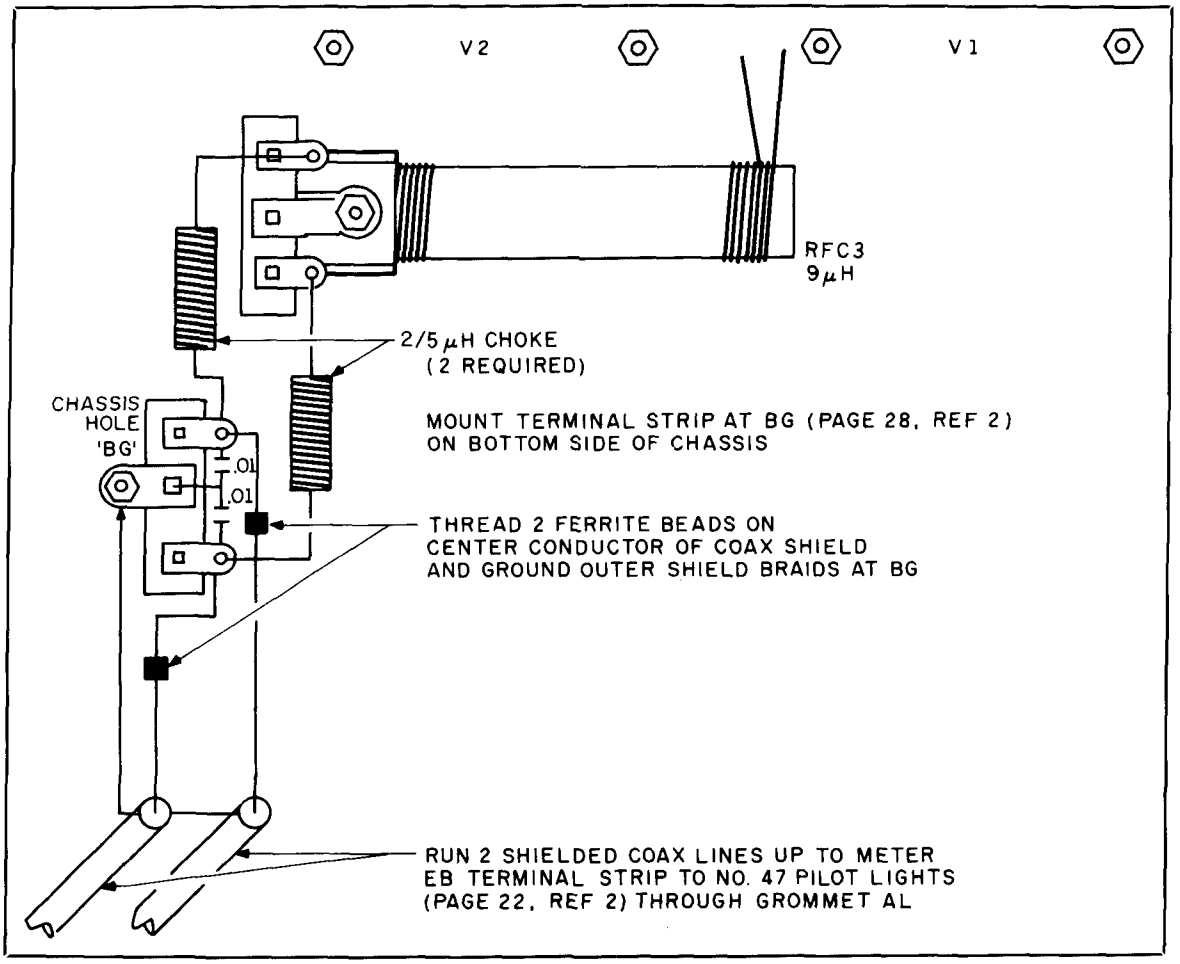

Figure 5. Electrical and mechanical detail of isolation of the filament 5-volt supply to shielded leads for no. 47 meter-pilot lights.

and by two paralleled 100-pF capacitors for C35. Provide a new chassis return for the capacitors by mounting a solder lug on the chassis beneath the bandswitch. I found a clear spot to drill the solder lug mounting hole about 5/8 inch to the right of the switch center line.

Twenty-meter input network modifications

The 20-meter input coil (L3) is modified in a manner similar to the 10-meter coil. Replace the winding with eight turns of no. 18 wire space wound to a 5/8-inch winding length. Don't forget to add a few drops of acetone to the slug so you can adjust it for minimum VSWR to the exciter later. Remove and discard capacitors C38 (100-pF) and C39 (220 pF).

Spot a hole on the chassis below and to the left of the center line of the switch assembly, and mount a solder lug. Install a new 335-pF 1000-volt mica capacitor (C39) from terminal 4 on the bandswitch to the solder lug. For C38, parallel two or three 1000-volt micas for a total of 315 pF, and connect them between the solder lug and terminal 10 on the bandswitch. Reinstall the 20-meter coil, then cut and dress the no. 18 wire leads to terminals 4 and 10 of the bandswitch, and solder the connections (see **Figure 6**)[4,5].

The 15, 40, and 80-meter input circuits give an acceptable match and VSWR, plus adequate drive. However, I suggest replacing the no. 22 coil pigtails with heavier no. 16 or 18 wire while it's convenient to do so.

Grounded-grid parasitic suppression

First, locate and remove the 1-mH chokes (RFC4 and 5) from grid pins 4 of V1 and V2 sockets and ground. Discard these two chokes. Drill a hole in the chassis and mount a solder lug near each of the pins 2,3, and 4 at both of the 3-500Z sockets (see **Figure 4** and page 86 of **Reference 3**). For V1, relocate the ground lead connections for 200-pF capacitors C16, C19, and C26 to the closest solder lug just installed. Do the same for capacitors C27, C28, and C31 at the socket for V2. Parallel a 75-ohm 1 or 2-watt non-inductive metallized resistor with each

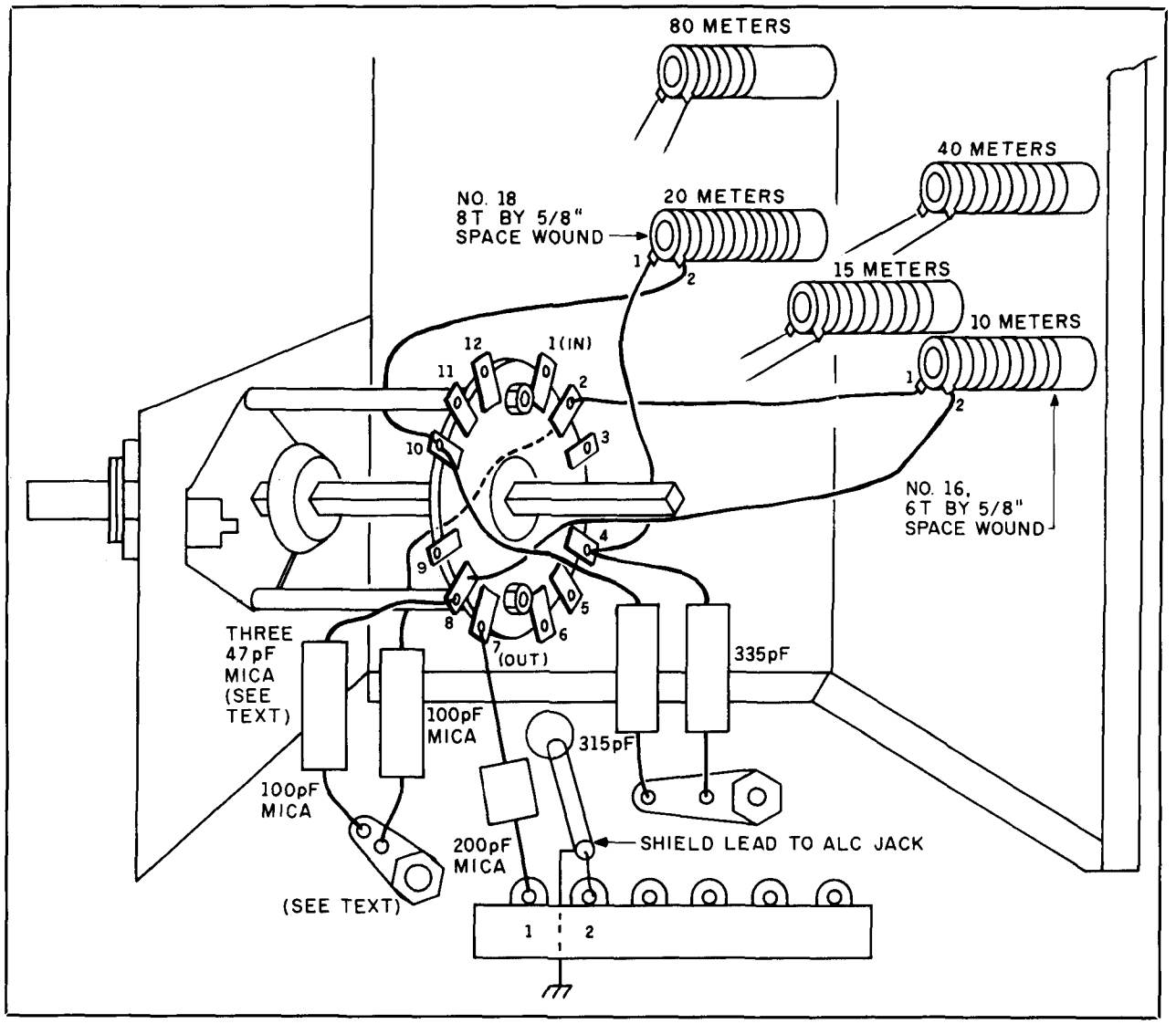

Figure 6. Changes to grid coils and pi network (mica 1000-volt capacitors to increase available grid drive). Coils are wound wire (10 meters) with pigtails extended to band switch. (Twenty meters is wound with no. 18 SEC wire.)

of the the six 200-pF capacitors, from each socket grid-pin solder lug to a ground solder lug.*

Filament voltage drop

The voltage drop across the V1 socket pin connections to the tube filament pins was 0.21 volt. The voltage drop at the V2 socket pin was 0.54 volt! I calculated the resistive loss to be 10.875 watts total, or about 34 BTUs of heat. This additional heat is very detrimental to the tubes' seals. It also shows as low filament voltage and current.

Carefully remove the tubes and clean and burnish all of the tube pins. Using no. 600 emery or crocus cloth rolled on a thin rod, carefully clean the inside of the socket contact fingers.** Remove the spring clips on each socket terminal and carefully increase the tension on each (ten clips total). These clips are highly tempered, so don't over stress them. Age and heat takes a toll on their malleability.

Loading capacitor C37 changes

A seemingly unimportant length of no. 18 wire, about 3/4 inch long, connects the common wipers (terminal 6) of the PA plate bandswitch to the flat strap extension on the stators of loading capacitor C37. Parallel solder a 3/4-inch length of no 12 wire to the existing wire to reduce the I^2R loss inherent in this short connection. The current is more than 4.5 amps at a peak power of only 1 kW when working into a 50-ohm load.

*R.L. Measures' article on grounded amplifier parasitic suppression in the April issue of *Ham Radio* recommends the use of 75-ohm resistors with at least a 1 or 2 watt dissipation rating. Based on personal experience, I concur with his decision to use the higher wattage resistors. Ed.

**See "Cleaning Electronic Hardware," by WA1FB, *Ham Radio*, June 1990, page 57.

Repositioning RFC1 and RFC2

Remove capacitors C6 and C7 (both 0.001-μF doorknobs) and replace them with different value capacitors. One of them will be used again later in the PA modification. Remount RFC1, the PA 50-μH choke, on a standoff insulator (**Figure 2**) allowing a 1/2-inch clearance from the tube envelopes while aligning it with the top of the plate connector caps. On the chassis below and to the left of the plate choke, mount a 4-kV 0.004-μF transmitting-type capacitor. Use a ferrite bead on the jumper wire between the two capacitors. Dress the high-voltage cable from the 200-pF capacitor along the bottom of the chassis and up along the PA compartment to the feedthrough insulator near the electrolytic stack.

Plate circuit changes

Two 0.001-μF capacitors replace the single DC blocking capacitor C29 in the PA tank circuit. The added capacitor is one of the "old" C6 or C7 doorknobs salvaged from earlier changes made on the PA deck.

Replace the 3-inch length of metal braid with a 5-inch long by 7/16-inch wide length of 0.03-inch thick copper strap (twist to fit), as shown on page 56 of **Reference 2** and in **Figure 7A**. Using mounting holes as shown in **Figure 2**, run the strap over to the modified capacitor mounting bracket shown in **Figure 8**. You can use the original bracket or mount the two 0.001-μF doorknobs on a new plate made of 0.06-inch thick copper. This modification shortens the RF path and puts more space between the 10 and 15-meter plate coil sections and the top plate of the cabinet.

Ten-meter tank circuit modifications

Clip and remove the 10-meter tap from

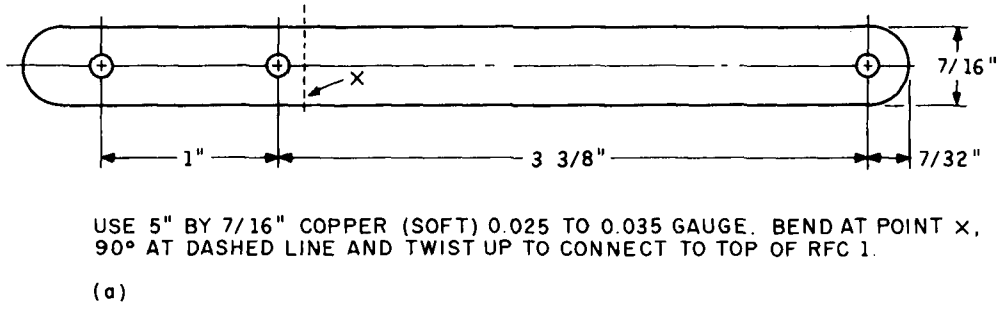

Figure 7A. The 5 by 7/16-inch by 0.03-gauge copper strap from plate parasitic suppressors and plate choke (RFC1) to the two 1000 pF 6 kV capacitors. Note the 90-degree bend and the 90-degree longitudinal twist to connect to top of choke.

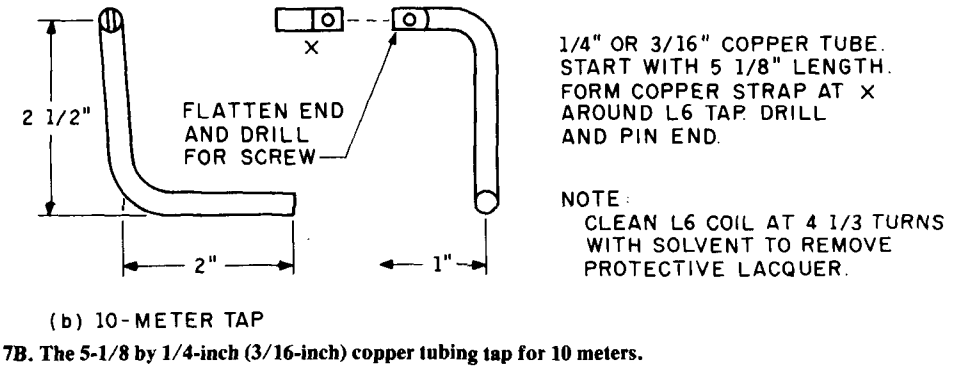

Figure 7B. The 5-1/8 by 1/4-inch (3/16-inch) copper tubing tap for 10 meters.

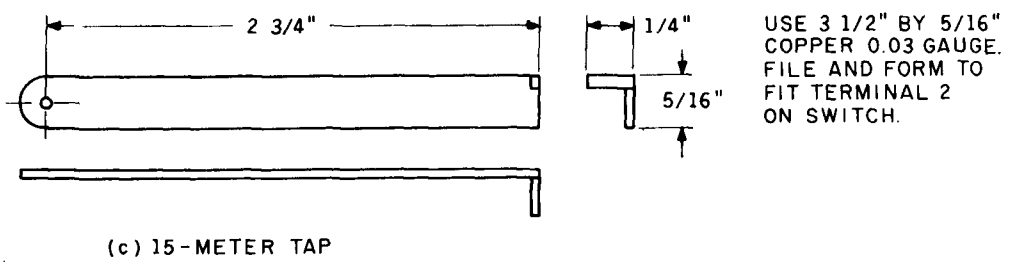

Figure 7C. The 3-1/2 by 5/16-inch by 0.03-gauge soft copper strap for the 15-meter tap.

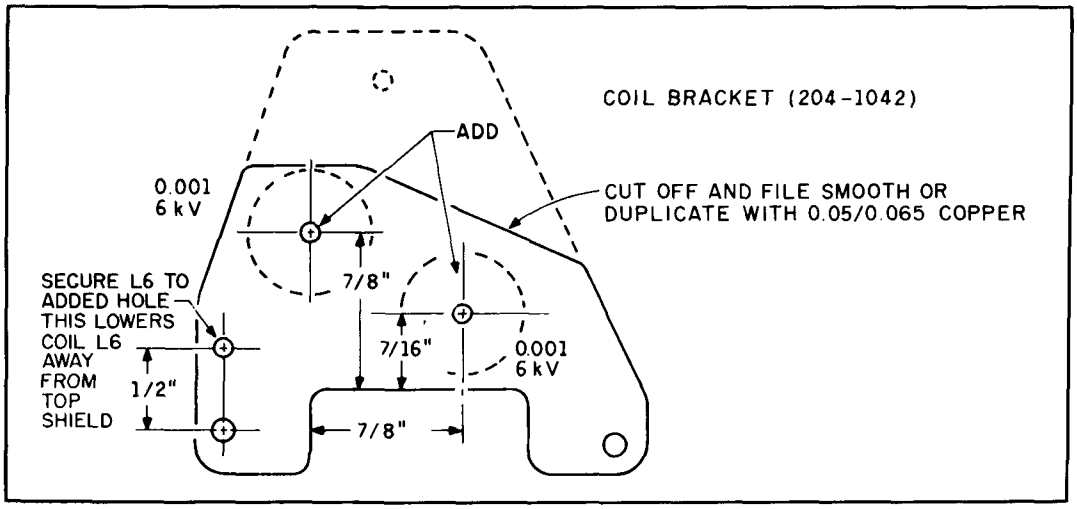

Figure 8. Modified coil bracket (204-1042) for mounting two 1000-pF 6-kV ceramic doorknob capacitor.

coil L6 to the bandswitch. Replace it with a 3/16-inch or 1/4-inch diameter length of soft copper tubing 5-1/8 inches long (see **Figure 7B**). Tap L6 at 4-1/8 turns from tuning capacitor C55. The tubing takes a 1-inch vertical upward bend to the tap on L6. A small copper strap wrapped around coil L6 at the tap point aids in connecting the coil to the tubing. Bend the tubing 90 degrees so the end of the tubing is aligned with the two wafer solder terminals at position 2 of the PA bandswitch. It will dress parallel to the bottom of the chassis. Solder the tubing to the wafer contacts (see **Figure 2**).

Fifteen-meter PA tank circuit changes

Replace the no. 14 wire tap connected from the junction of L6 and L7 (15-meter coil) to the bandswitch with 0.03-inch thick, 3 3/4-inch long by 5/16-inch wide copper strap. Drill a no. 29 hole in one end of the strap and connect it at the junction of coils L6 and L7. Taper cut the other end of the strap, making a 90-degree bend so it will fit into and line up with the solder holes of the wafer contacts at terminal 3 of the PA bandswitch. Before soldering, carefully position the strap so it has at least a 1/4-inch clearance to other nearby coil tap wires (see **Figure 7C** and **Figure 2**).

Eighty-meter loading improvements

Eighty-meter PA tuning can be enhanced by increasing the load padding capacitor C56 from its present 500-pF value to about 750 pF. Either replace the capacitor, or add a parallel 250-pF mica (1200-volts minimum) to the existing 500-pF capacitor.

Odds and ends

As a final touch, add extra self-tapping sheet metal screws to the flange mounts on the left side and top of the PA chassis enclosure. Add enough screws so there isn't more than 2 or 3 inches between them. This will minimize variable cavity currents in the chassis assembly.

Conclusion

I find these modifications provide increased stability during tuning and operation. Erratic plate meter jitters, or jumps in power output, while tuning were eliminated. And when carefully loaded and tuned, there were no more arcs in the PA plate tuning capacitor. This capacitor has only 0.07-inch spacing, which is adequate for only 3 kV.

The measured power output was increased by more than 250 watts on 10 meters, 200 watts on 15 meters, 100 watts on 20 meters, and by 100 watts on the 40-meter band.

REFERENCES

1. R.L. Measures, AG6K, "Improved Anode-Parasitic Suppression for Modern Amplifier Tubes," *QST*, October 1988, page 36.
2. *Heathkit Assembly Manual SSB220* (595-1122-04).
3. R.L. Measures, AG6K, "Hints and Kinks: Improving SB220," *QST*, February 1989, page 42.
4. *The ARRL Handbook*, The Amateur Radio Relay League, Newington, Connecticut.
5. William Orr, W6SAI, *The Radio Handbook*.

BIBLIOGRAPHY

1. R.L. Measures, AG6K, "G.G. Amplifier Parasitics," *Ham Radio*, April 1986, page 31.
2. William Orr, W6SAI, "Grounded Grid Amplifiers," *Ham Radio*, September 1986, page 42.
3. R.L. Measures, AG6K, "Calculating Power Dissipation in Parasitic-Suppressor Resistors," *QST*, March 1989, page 25.
4. William Orr, W6SAI, "Grounded Grid Amplifier II," *Ham Radio*, October 1986, page 38.
5. Ed Mariner, W6XM, "Matching Linear Amplifiers to Transceivers," *Ham Radio*, October 1986, page 73.
6. Joe Reisert, W1JR, "High-Power Amplifiers II," *Ham Radio*, February 1985, page 38.

Corrections to this article can be found on page A1 of this issue.

ELNEC
Advanced Antenna Analysis Program

Fast to learn and easy to use, ELNEC lets you analyze nearly any type of antenna in its actual operating environment. Describe your antenna with ELNEC's unique menu structure and spreadsheet-like entry system and watch it generate azimuth and elevation plots, report beamwidth, front/back ratio, takeoff angle, gain, and more. Save and recall antenna files. Print plots on your dot-matrix or laser printer.

ELNEC uses the full power, versatility, and accuracy of MININEC computing code while making antenna description, analysis, and changes worlds easier. With ELNEC there's no messing with "pulses" - just tell it where on a wire you want a source or load to go, and ELNEC puts it there. And keeps it there, even if you change the antenna. Interested in phased arrays? ELNEC has true current sources for accurate analysis.

ELNEC runs on any PC-compatible computer with at least 360k RAM, CGA/EGA/VGA/Hercules, and 8/9 or 24 pin Epson-compatible or HP LaserJet/DeskJet printer. Two versions are available, optimized for use with and without a coprocessor.

There's no copy-protection hassle with ELNEC -- it's not copy protected. And of course there's extensive documentation.

ELNEC is a terrific value for only $49.00 postpaid. (Please add $3.00 for airmail outside N. America.) VISA and MasterCard orders are accepted -- please include card number and expiration date. Specify coprocessor or noncoprocessor version. Order or write for more information from:

Roy Lewallen, W7EL
P.O. Box 6658
Beaverton, OR 97007

SIGNAL-TO-NOISE
Voting Comparator

Improve coverage by adding receivers

- Expandable to 32 Channels
- Continuous Voting
- 19″ Rack Mountable
- Select/Disable Switches for Manual Override
- Can be used with RF Links or Dedicated Lines
- LED Indicators
- Hundreds in Service
- More

—Competitively Priced—
For more information call or write:

Doug Hall Electronics
815 E. Hudson St.
Columbus, Ohio 43211 • (614) 261-8871
FAX 614-261-8805

Iron Powder and Ferrite Products

Fast, Reliable Service Since 1963
Millions of Parts in Stock for Immediate Delivery.
Low Cost Experimental Kits.

Small Orders Welcome
Ask For Our FREE 78 Pages Handbook/Catalog

Toroidal Cores,
Shielding Beads,
Shielded Coil Forms,
Ferrite Rods,
Pot Cores, Baluns, Etc.

AMIDON. Associates

VISA MasterCard 2216 East Gladwick Street, Dominguez Hills, California 90220

Telephone: (213) 763-5770 FAX: (213) 763-2250

JOIN AMSAT
Support the Amateur Space Program

AMSAT Has Established Amateur Radio As a Permanent Resident in Space!

From operating any of 12 Amateur satellites circling the globe today to participating in Amateur Radio activities from the Space Shuttle, the benefits of space based Amateur Radio are available to you by becoming an *AMSAT* member. Our volunteers design, build and launch state-of-the-art satelites for use by Radio Amateurs the world over. We provide educational programs that teach our young people about space and Amateur Radio. Most of all, we provide our members with an impressive array of member benefits including:

- Operating aides such as discounted tracking software and land line BBS.
- An extensive network of volunteers to provide you local technical assistance.
- The AMSAT Journal, your bi-monthly periodical devoted to the Amateur Space program.

It's Fun! It's Easy! It's Exciting!

JOIN TODAY. For more information, call or write for your free information packet. Or send your dues now, check or charge: $30 U.S., $36 Canada/Mexico, $45 all else. ($15 towards the AMSAT journal.)

AMSAT, P. O. Box 27, Washington, D.C. 20044
(301) 589-6062; Fax: (301) 608-3410

CQ SUMMER SIZZLERS

Call Toll Free: 800-457-7373

8 AM - 5 PM ET

ANTENNA BOOK BUYERS GUIDE

ARRL ANTENNA BOOK NEW!
by Jerry Hall, K1TD,
The 16th edition of this antenna classic represents over two years of hard work by editor K1TD. 700 figures and charts cover just about every subject imaginable. Some of the highlights are: Chapters on Loop antennas, multi-band antennas, low frequency antennas, portable antennas, VHF and UHF systems, coupling the antenna to the transmitter and the antenna, plus p-l-e-n-t-y more. 700+ pages. ©1991.
❑ AR-AM **Softbound $19.95**

BEVERAGE ANTENNA HANDBOOK by Victor Misek, W1WCR
Misek delves deep into the secrets of the single wire Beverage and SWA (Steerable Wave Antenna) with helpful hints and tips on how to maximize performance based upon wire size, height above ground, overall length and impedance matching. Transformer design information for both termination and freeline matching is completely revised. ©1987. 80 pages, 2nd Edition.
❑ VM-BAH **Softbound $14.95**

YAGI ANTENNA DESIGN by Dr. James Lawson, W2PV
W2PV was known world-wide as one of the most knowledgeable experts on antenna design and optimization, Loop antennas, the effects of ground, Stacking, Practical design and Practical Amateur Yagi antennas. Every Ham should get a copy for their bookshelf. ©1986. 1st Edition.
❑ AR-YD **Hardbound $14.95**

THE AMATEUR RADIO VERTICAL HANDBOOK by Captain Paul H. Lee, USN (ret.), N6PL
Based upon the author's years of work with a number of different vertical antenna designs, you'll get plenty of theory and design information along with a number of practical construction ideas. Included are designs for simple 1/4 and 5/8-wave antennas, as well as broadband and multi-element directional antennas. ©1984, 2nd edition.
❑ CQ-VAH **Softbound $9.95**

W1FB's ANTENNA NOTEBOOK by Doug DeMaw, W1FB
Antennas have been one of DeMaw's passions in Amateur Radio. He has worked with countless designs of all shapes and configurations. This fully illustrated book gives you how-to instructions on a number of different wire and vertical antennas. Also includes information on radial systems, tuners, balun and impedance transformers. ©1987, 120 pages.
❑ AR-AN **Softbound $7.95**

LOW BAND DX'ING by John Devoldere ON4UN, 2nd Edition
Based upon years of practical on-the-air experience, learn the secrets of how ON4UN has been so successful on the low bands. Extensive coverage is given to transmit and receive antennas. Dipoles, inverted V's, slopers, phased arrays and Beverages. Also covered: propagation, transmitters, receivers, operating, software and an extensive Low Band bibliography.
❑ AR-UN **Softbound $9.95**

EASY-UP ANTENNAS for Radio Listeners and Hams by Ed Noll W3FQJ
This book covers basic do-it-yourself antennas for SWL's, AM and FM BCB'ers, present and prospective Ham and scanner listeners. Includes dipoles, verticals, beams, long wires, and several special types and configurations. Also has time saving look-up dimension tables, constants and other helpful hints for antenna design. 1st edition, 164 pages, ©1988.
❑ 22495 **Softbound $16.95**

NOVICE ANTENNA NOTEBOOK by Doug DeMaw, W1FB
Novices have long wondered what is the best all around antenna for them to install. Up until now, this was a difficult question to answer. Aimed at the newly licensed Ham, DeMaw writes for the non-engineer in clear, concise language with emphasis on easy-to-build antennas. Readers will learn how antennas operate and what governs performance. Also great reading for all levels of Amateur interest. 1st Edition, ©1988.
❑ AR-NAN **Softbound $7.95**

ANTENNAS by John Kraus, W8JK
Kraus' classic antenna book has been extensively revised and up-dated to reflect the latest state-of-the-art in antenna design and theory. Includes over 1,000 illustrations and nearly 600 worked examples and problem solutions. Chapters cover basic concepts, print sources and point source arrays, dipoles, helixes, broadband and frequency independent antennas, special applications and tons more of information. 2nd edition. 917 pages ©1988.
❑ MH-35422 **Hardbound $59.95**

REFLECTIONS- Transmission Lines and Antennas by Walt Maxwell, W2DU
Over the years, many myths and half truths have become "fact." Noted antenna expert Maxwell debunks them with clear, concise and accurate explanations. The first seven chapters are taken from his QST column "Another Look At Reflections." Seventeen additional chapters contain new and unpublished material covering matching networks, antennas and how to use Smith charts. Also available is a MS-DOS disk with programs taken from the book. © 1990 1st Edition 384 pages
❑ AR-RTLA **Hardbound $19.95**
❑ FAR-RTLADOS **(MS-DOS Disk) $9.95**
❑ AR-RTDOS **Program and disk $2 off $27.90**

ANTENNA IMPEDANCE MATCHING by ARRL
One of the most comprehensive books ever written on the use of Smith charts in solving impedance matching problems. 224 pages full of helpful information and solutions to tricky matching problems. ©1989.
❑ AR-IMP **Hardbound $14.95**

ARRL ANTENNA COMPENDIUM, Vol. 1 by ARRL Staff
QST gets far more antenna articles than it can publish. This collection is taken from the best submissions and represents a wide range of subjects — from quads and loops to general information — this book has it! ©1985. 1st Edition.
❑ AR-AC1 **Softbound $9.95**

ANTENNA COMPENDIUM Vol 2 - Includes MS-DOS program listings
Antennas are the #1 topic of interest among amateurs. ARRL annually receives far more articles than it can use in QST. So, they decided to publish them in THE ANTENNA COMPENDIUM. These never been published articles run the range from simple, easy-to-construct antennas to sophisticated designs. Six program listings are included. You can also get the programs on a MS-DOS disk for an additional charge. ©1989, 1st edition 208 pages.
❑ AR-AC2 **Softbound Book Only $11.95**
❑ FAR-AC2 (MS-DOS) **Disk Only $9.95**
❑ AR-FAC2 BUY 'EM BOTH SPECIAL *SAVE $3.95* **Book & Disk $17.95**

TRANSMISSION LINE TRANSFORMERS by Jerry Sevick, W2FMI
Contains complete explanation and discussion of transmission line transformers and ow to use them. Written by one of the experts in the field - this book is full of helpful information. 1990. 2nd Edition. 272 pages.
❑ AR-TLX **Hardbound $19.95**

By Bill Orr W6SAI & Stu Cowan W2LX

❑ RP-WA	**WIRE ANTENNA HANDBOOK** - Wire antennas for all installations	$11.95
❑ RP-CQ	**ALL ABOUT CUBICAL QUAD ANTENNAS** - The "quad book"	$ 9.95
❑ RP-VA	**ALL ABOUT VERTICAL ANTENNAS** - Everything you want to know	$10.95
❑ RP-AH	**THE RADIO AMATEUR ANTENNA HANDBOOK** - Complete guide to antennas	$11.95
❑ RP-BA	**BEAM ANTENNA BOOK** - All kinds of beams	$11.95

CQ BOOKS

KEYS, KEYS, KEYS, by Dave Ingram, K4TWJ
Sending Morse code by hand has become a lost art in this day of keyers and computerized code machines. Dave Ingram's new book on keys, however, is a triubte to how it used to be done in "the old days." Loaded with pictures, this new book shows just about every key that was ever used in both Amateur and professional telegraph circuits – from simple "cootie keys" and miniature spy keys to gold plated presentation models – they're all in this book. Also gives you insights on how to collect, restore and use your classic keys. Great for the collector, old timer or newcomer. ©1991.
❑ CQ-KEY **Softbound $9.95**

PROPAGATION HANDBOOK - Principles, Theory, Prediction by Ted Cohen, N4XX & George Jacobs, W3ASK
If you are confused by the science of propagation, this book is for you. The authors are noted experts and write in such a way that experts and beginners alike will find this book to be most helpful. Includes a complete explanation of lonospheric propagation principles; what are the D, E and all those F layers and what do they mean, as well as two sections on the Sun and how it effects radio wave propagation. There's a primer on how to predict propagation plus much more. Great book to have on hand. 2nd Edition. 150 pages. ©1991.
❑ CQ-PH **Softbound $9.95**

PACKET USER'S NOTEBOOK
by Buck Rogers, K4ABT
This new book has been put together by CQ's Packet editor and packet pioneer, Buck Rogers, K4ABT. Written with the beginner in mind, the Packet Notebook is full of handy tips, hints and suggestions on how to get the most out of your packet system. Includes a brief history, a how to get started section, standards, flow control and information on radio to TNC to computer interconnections for just about every radio. Good book to have on every packeteer's desk. ©1989. 1st edition. 132 pages.
❑ CQ-PKT **Softbound $9.95**

THE AMATEUR RADIO VERTICAL HANDBOOK
by Cpt. Paul H. Lee, USN (Ret.), N6PL
Based upon the author's years of work with a number of different vertical antenna designs, you'll get plenty of theory and design information along with a number of practical construction ideas. Included are designs for simple 1/4 and 5/8 wave antennas, as well as broadband and multi-element directional antennas. ©1984, 2nd edition.
❑ CQ-VAH **Softbound $9.95**

CQ COUNTIES AWARD BOOK
The only way to keep track of your counties worked is to have a copy of this book in your shack. All counties are listed by state and band for easy record keeping. This is one of amateur radio's most challenging awards. Make sure you have "the offiicial" record book available.
❑ CQ-RB **Softbound $1.25**

1992 EQUIPMENT BUYER'S GUIDE NEW!
Fully up-to-date. Complete listing of equipment available from the various equipment and accessory manufacturers. Includes radios and accessories plus helpful hints and tips and a complete listing of addresses and telephone numbers. ©1991
❑ CQ-EQP92 **Softbound $4.95**

1991 ANTENNA BUYER'S GUIDE
Looking for the latest in antennas? It's all here in the CQ Antenna Buyer's Guide. Crammed full of articles, product information and a who's who section listing all of the manufacturers and importers. Get your's now and start planning for antenna projects. ©1991
❑ CQ-ANT91 **Softbound $4.95**

ORDER INFORMATION

Call (800) 457-7373

AMERICAN EXPRESS VISA MasterCard

8AM-5PM ET
ORDERS ONLY

For More Information about an order call (603) 878-1441
24 Hour Fax Line (603) 878-1951
Shipping and handling: $4.00 to US and Canadian address via US mail. Shipping via UPS Brown $5.00 to US address only. COD orders add an additional $5.00. UPS Red or Blue cost plus $4.00 handling. Foreign orders shipped via US mail F.O.B. Greenville, NH, plus a $4.00 handling charge. Prices subject to change without notice.

CQ's BOOKSTORE

GREENVILLE, NH 03048
Div. of CQ Communications Inc.

SURPLUS SALES OF NEBRASKA

AEA's AT-300 ANTENNA TUNER
Close-Out Special
$139.00
Please add $6.50 per Tuner for UPS (U.S. only). $6.50 credit towards shipping on any DX order.

RG-8 style COAX
Times "IP-8"
The last coax you'll ever need! Imperveon cable by Times has self-healing Xelon® jacket, is moisture, sunlight, and corrosion resistant and is not affected by cold, heat, condensation or TIME. With IP-8, you have protection from all of nature's elements leading to eventual failure of other RG coax. Electrical specs and dimensions are comparable to other RG-8 cable, with less loss. It's flexible too!
35¢ per foot (plus shipping)

CATALOG 6
Available Now! In the USA, send $3 for your copy via First Class Mail. DX please send $5 for Airmail. Payment is refundable with your first $25 catalog purchase. Offer expires 3/92.

TEN-TEC • AEA • B&W • SGC • SPIDER • COLLINS PARTS • TEN-TEC ENCLOSURES • DIODES • PACKET RADIO SYSTEMS • FINGER STOCK • MICROWAVE COMPONENTS • TOROIDS • RF • RF • RF • CONNECTORS, ANY KIND, LITERALLY • MECHANICAL FILTERS • RELAYS • INDUCTORS • SEMICONDUCTORS • TEST EQUIPMENT • TWT • OSCILLATORS • RESISTORS • TRANSFORMERS • SWITCHES • POTENTIOMETERS • METERS • VACUUM RELAYS • VACUUM CAPACITORS • TRANSMITTING COMPONENTS • POWER SUPPLY PARTS • CABLE • WIRE: ANTENNA, MAGNET, HIGH VOLTAGE, HOOK-UP • TUBES • FEED-THRUS • COMPUTER PARTS • TRIMMER CAPS • ANTENNAS • EMI FILTERS • CORDS

SURPLUS SALES OF NEBRASKA
1315 Jones St. • Omaha, NE 68102
402-346-4750 • fax: 402-346-2939

Measure Up With Coaxial Dynamics Model
83000A RF Peak Reading Wattmeter

Take a PEAK with Coaxial Dynamics "NEW" Model 83000A, designed to measure both FWD/RFL power in CW and FM systems simply and quickly. Then with a "FLIP" of a switch, measure "PEAK POWER" in most AM, SSB or pulse systems. Our Model 83000A features a complete selection of plug-in-elements plus a 2 year warranty. This makes the Model 83000A an investment worth looking at. So go ahead, take a "PEAK", you'll like "WATT" you see!

Contact us for your nearest authorized Coaxial Dynamics representative or distributor in our world-wide sales network.

COAXIAL DYNAMICS, INC.
15210 Industrial Parkway
Cleveland, Ohio 44135
216-267-2233
1-800-COAXIAL
Telex 98-0630

Service and Dependability... a Part of Every Product

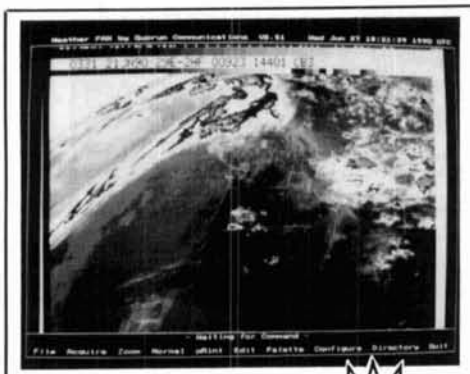

Quorum introduces the first totally integrated system for the reception of weather satellite images directly on your personal computer. Selection of HF NAFAX, GOES WEFAX, GOESTAP, METEOSAT, NOAA and METEOR APT (including satellite downlink frequency selection) are made under complete program control from your PC keyboard.

The easy to learn and use Menu driven program allows you to capture, store, retrieve, view and print images with a few simple keystrokes. Images can be colorized from a palette of up to 262,000 colors when using a VGA display.

System configurations capable of NAFAX reception start at $399.00 while fully capable systems can be configured for $1500 to $2000.00, providing professional quality at low prices.

For complete information and a Demo Disk, call or write:

Quorum Communications, Inc., 1020 S. Main St. Suite A, Grapevine, TX 76051 (817) 488-4861. Or, download a demo from our Bulletin Board by calling (817) 421-0228 using 2400 baud, 8 data bits and No parity.

NOW! SUPER SVGA SUPPORT

Receive Weather Satellite Images and Charts on your PC with Quorum's Totally Integrated and Affordable Weather Facsimile System

QUORUM COMMUNICATIONS

PCBoards

P-C-B ARTWORK MADE EASY !
Create and Revise PCB's In a Flash

* HERC, CGA, EGA, VGA, SUPER-VGA
* HELP SCREENS
* EXTREMELY USER FRIENDLY
* AUTO GROUND PLANES
* DOT- MATRIX, LASER and PLOTTER ART
* GERBER and EXCELLON OUTPUT
* CREATE YOUR OWN FILMS with 1X ART
* LIBRARIES
* DOWNLOAD DEMOS from 24 hr. BBS!

REQUIREMENTS: IBM PC or Compatible, 384 K RAM DOS 3.0 or later. IBM compatible printers, HP Laser

PCBoards - layout program 99.00
(PCBoards HP or HI PEN PLOTTER DRIVER 49.00)
PCRoute - auto-router 99.00
SuperCAD - schematic pgm. 99.00
Demo Pkg. - (includes all 3 programs) 10.00

Call or write for more information
PCBoards
2110 14th Ave. South, Birmingham, AL 35205
1-800-473-PCBS / (205)933-1122
BBS / FAX (205)933-2954

DOWN EAST MICROWAVE

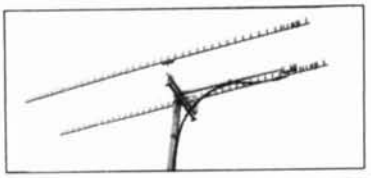

MICROWAVE ANTENNAS AND EQUIPMENT

- Loop Yagis • Power Dividers • Dish Feeds
- Complete Antenna Arrays • Linear Amps
- Microwave Transverters & Kits • GaAs FET Preamps and Kits • Microwave Components
- Tropo • EME • Weak Signal • OSCAR • FM
- Packet • ATV
- 902 • 1269 • 1296 • 1691 • 2304 • 2400 • 3456 • 5760
- 10,386 MHz

ANTENNAS

2345 LYK	45 el	Loop Yagi Kit	1296 MHz	$95
1345 LYK	45 el	Loop Yagi Kit	2304 MHz	$79
3333 LYK	33 el	Loop Yagi Kit	902 MHz	$95
1844 LY	44 el	Loop Yagi Assembled	1691 MHz	$105
3B Feed	Tri Band Dish Feed 2.3, 3.4, 5.7 GHz			$15

Many others and assembled versions available. Shipping extra.

LINEAR AMPS AND PREAMPS

2303 PA	1.2 to 1.3 GHz	3w out	13.8 VDC	$130
2318 PAM	1.24 to 1.3 GHz	20w out	13.8 VDC	$205
2335 PA	1.24 to 1.3 GHz	35w out	13.8 VDC	$325
2340 PA	1.24 to 1.3 GHz	higain 35w out	13.8 VDC	$355
2370 PA	1.24 to 1.3 GHz	70w out	13.8 VDC	$695
1302 PA	2.2 to 2.5 GHz	3w out	13.8 VDC	$430
13 LNA	2.3 to 2.4 GHz	preamp	.6 dB NF	$140
23 LNA	1.2 to 1.3 GHz	preamp	.6 dB NF	$95
33 LNA	900 to 930 MHz	preamp	.6 dB NF	$95
1691 LNA WP	1691 MHz	mast mounted preamp	.8 dB NF	$140

Kits, Weatherproof Versions and other Frequencies Available

NO-TUNE TRANSVERTERS AND TRANSVERTER KITS

900, 1269, 1296, 2304, 2400, 3456, 5760 MHz

SHF 902K	902 MHz Transverter	40mW, 2m IF	Kit $139
SHF 1296K	1296 MHz Transverter	10mW, 2m IF	Kit $149
SHF 2304K	2304 MHz Transverter	10mW, 2m IF	Kit $205
SHF 3456K	3456 MHz Transverter	10mW, 2m IF	Kit $205

OSCAR and other frequencies available, also Amps and package versions wired and tested.

Write for more information. Free catalog available.

DOWN EAST MICROWAVE
Bill Olson, W3HQT
RR1 Box 2310, Troy, ME 04987
(207) 948-3741 Fax: 207-948-5157

ATV CONVERTERS • HF LINEAR AMPLIFIERS

AMATEUR TELEVISION CONVERTERS

ATV2 420–450	$ 44.95 Kit
ATV3 420–450 (GaAS–FET)	$ 49.95 Kit
ATV4 902–928 (GaAS–FET)	$ 59.95 Kit

AUDIO SQUELCH CONTROL for ATV
SIL ..... $ 39.95 Kit

2 METER VHF AMPLIFIERS

35 Watt Model 535A	$ 79.95 Kit
75 Watt Model 875A	$119.95 Kit

Available in kit or wired/tested

HF AMPLIFIERS per MOTOROLA BULLETINS

Complete Parts List for HF Amplifiers Described in the MOTOROLA Bulletins.

AN758 300W $160.70	EB63 140W $ 88.65
AN762 140W $ 93.25	EB27A 300W $139.20
AN779L 20W $ 83.79	EB104: 600W $351.65
AN779H 20W $ 93.10	AR305 300W $383.52
AR313 300W $403.00	

NEW!! 1K WATT 2–50 MHz Amplifier

POWER SPLITTERS and COMBINERS
2–30MHz

600 Watt PEP 2–Port	$ 69.95
1000 Watt PEP 2–Port	$ 79.95
1200 Watt PEP 4–Port	$ 89.95

100 WATT 420–450 MHz PUSH–PULL LINEAR AMPLIFIER – SSB–FM–ATV

KEB67–PK (Kit)	$159.95
KEB67–PCB (PC Board)	$ 18.00
KEB67–I (Manual)	$ 5.00

For detailed information and prices, call or write for our free catalog.

UNIVERSAL DIGITAL FREQUENCY READOUT
TK–1 (Wired/tested) $149.95

HEAT SINK MATERIAL

Model 99 Heat Sink (8.5 × 12 × 1.6)	$24.00
CHS-8 Copper Spreader (8 × 8 × ¾)	$22.00

We also stock Hard–to–Find parts

CHIP CAPS–Kemet/ATC
METALCLAD MICA CAPS–Unelco/Semco
RF POWER TRANSISTORS
MINI–CIRCUIT MIXERS

SBL–1 (1–500Mz)	$ 6.50
SBL–1X (10–1000Mz)	$ 7.95

ARCO TRIMMER CAPACITORS

VK200–20/4B RF Choke	$ 1.20
56–590–65–3B Ferrite Bead	$ .20

Broadband HF Transformers

Add $ 3.50 for shipping and handling.

VISA

CCI Communication Concepts Inc.
508 Millstone Drive • Xenia, Ohio 45385 • (513) 426-8600
FAX (513) 429-3811

MasterCharge

K2AW'S FAMOUS HI-VOLTAGE MODULES

20,000 IN USE IN OVER 50 COUNTRIES.

SAME DAY SHIPPING MADE IN U.S.A.

HV14-1	**14KV-1A**	**250A. SURGE**	**$15.00**
HV10-1	**10KV-1A**	**250A. SURGE**	**12.00**
HV 8-1	**8KV-1A**	**250A. SURGE**	**10.00**
HV 6-1	**6KV-1A**	**150A. SURGE**	**5.00**

Plus $2.00 Shipping—NY Residents Add 8% Tax

K2AW's "SILICON ALLEY"
175 FRIENDS LANE WESTBURY, NY 11590 516-334-7024

HIGH-ACCURACY ANTENNA SOFTWARE

MN 4.0 is the fastest, most powerful, and most accurate MININEC antenna-analysis program available. MN corrects fundamental problems in the MININEC algorithm for improved accuracy. MN features 3-D views of antenna geometry and wire currents, presentation-quality polar and rectangular plots, automatic wire segmentation, automatic frequency sweep, symbolic dimensions, skin-effect modeling, near-field calculation for TVI and RF-hazard analysis, up to 254 pulses for complex models, simple definition of sources and loads, and pop-up menus. MN 4.0, $85. MNC 4.0 (1.6-2.4 times faster, coprocessor required), $110. MNH 4.0 (huge-model option), $25.

YO 4.0 automatically optimizes Yagi antennas for maximum forward gain, best pattern, and minimum SWR. YO handles designs from HF to microwave. YO models stacked Yagis, Yagis over ground, skin-effect, dual driven-elements, element tapering, mounting plates, and matching networks. YO runs hundreds of times faster than MININEC. YO is calibrated to NEC for high accuracy and has been extensively validated against real antennas. YO is intuitive, highly graphical, and fun to use. YO 4.0, $100. YOC 4.0 (1.7-2.7 times faster, coprocessor required), $130.

NEC For Yagis 1.0 provides highest-accuracy analysis of Yagi designs with the professional-standard Numerical Electromagnetics Code. NEC For Yagis 1.0, $50. Coprocessor, hard disk, and 640K memory required.

MN and YO come with comprehensive antenna-design libraries and include both coprocessor and extra-fast no-coprocessor versions. All programs include extensive documentation and an easy-to-use, full-screen text editor. Add 6% CA, $5 overseas. VISA, MasterCard, U.S. check, cash, or money order. For IBM PC, 3.5" or 5.25" disk.

Brian Beezley, K6STI, 507-1/2 Taylor, Vista, CA 92084
(619) 945-9824, 0700-1800 Pacific Time

AMATEUR TELEVISION

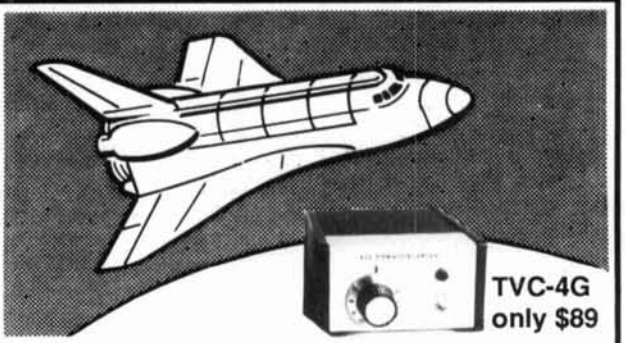

TVC-4G only $89

SEE THE SPACE SHUTTLE VIDEO

Many ATV repeaters and individuals are retransmitting Space Shuttle Video & Audio from their TVRO's tuned to Satcom F2-R transponder 13. If it is being done in your area on 70 CM, all you need is one of our TVC-4G ATV 420-450 MHz downconverters, add any TV set to ch 3 and 70 CM antenna. Others may be retransmitting weather radar during significant storms. Once you get bitten by the ATV bug - and you will after seeing your first picture - show your shack with the TX70-1A companion ATV transmitter for only $279. It enables you to send back video from your camcorder, VCR or TV camera. ATV repeaters are springing up all over - check page 411 in the 90-91 ARRL Repeater Directory. Call for a copy of our complete 70, 33 & 23 CM ATV catalog.

(818) 447-4565 m-f 8am-5:30pm pst. **Visa, MC, COD**
P.C. ELECTRONICS **Tom (W6ORG) Maryann (WB6YSS)**
2522 S. Paxson Ln Arcadia CA 91007

TOROID CORES

- **Iron Powder**
- **Ferrite**
- **Shielding Beads**
- **Ferrite Rods**
- **Split Beads**

Small orders welcome. All items in stock for immediate delivery. Low cost experimenter's kits: **Iron Powder, Ferrite.** The dependable source for toroidal cores for 25 years.

Call or write for free catalog and tech data sheet.

PALOMAR ENGINEERS
Box 455, Escondido, CA 92033, USA
Tel. (619) 747-3343

ADVERTISER'S INDEX

AMSAT 99
Alinco Electronics 7
Amidon Associates 99,103
Astron Corporation 104
Beezley, Brian, K6STI 102
Coaxial Dynamics 101
Communications Concepts, Inc. 102
CQ Bookshop 100
Down East Microwave 102
HAL Communications 9
Hall Electronics 99
ICOM America, Inc. COV.II,1
K2AW's Silicon Alley 102
Kantronics 5
Kenwood USA COV.IV,2
L.L. Grace Communications Products 10
Lewallen, Roy, W7EL 99
OPTOelectronics 8
PC Boards 101
PC Electronics 102
Palomar Engineers 103
Quorum Communications 101
Spectrum International, Inc. 103
Surplus Sales of Nebraska 101
Yaesu ..... COV.III

We'd like to see your company listed here too. Contact Arnie Sposato, N2IQO, at (516) 681-2922 or FAX at (516) 681-2926 to work out an advertising program to suit your needs.

HIGHLY EFFICIENT AND BROADBAND BALUNS AND UNUNS

Available as do-it-yourself kits and packaged and tested units

- Baluns and ununs matching 50 ohms to impedances as low as 3.125 ohms and as high as 800 ohms
- Specified efficiencies: **95% to 99%** (depending upon impedance-levels)
- Designs optimized for bandwidth, efficiency, impedance-level and safety margins
- Power categories (conservative ratings)
  Low-power: 150 watts continuous
  High-power: 1 KW to 5 KW continuous
- 48 design kits available from our 58 page handbook
- New designs upon request (assuming feasibility)
- Each DO-IT-YOURSELF KIT includes data sheet, construction techniques, circuit diagrams, photographs and all components
- PACKAGED and TESTED units come with unconditional money back guarantee for 1 year

W2FMI

These baluns and ununs (unbalanced-to-unbalanced transformers), exclusively designed by **Dr. Jerry Sevick, W2FMI**, are improved versions of those described in his book Transmission Line Transformers, 2nd ed. (Newington: ARRL, 1990). Therefore, many new and useful transformers are readily made available. Some examples are baluns and ununs with transformation ratios of 1:5:1, 2:1, 6:1 and 12:1. Many multimatch ununs are also included.

For a free catalog and a list of 48 designs contact:

AMIDON ASSOCIATES INC.
VISA TEL: 213-763-5770 MasterCard
FAX: 213-763-2250
P.O. Box 956, Torrance, CA 90508

CALL TODAY FOR A LIMITED INTRODUCTORY OFFER

Best Sellers
(800) 457-7373

REFLECTIONS- Transmission Lines and Antennas
by Walt Maxwell, W2DU

Over the years, many myths and half truths have become "fact." Noted antenna expert Maxwell debunks them with clear, concise and accurate explanations. The first seven chapters are taken from his QST column "Another Look At Reflections." Seventeen additional chapters contain new and unpublished material covering matching networks, antennas and how to use Smith charts. Also available is a MS-DOS disk with programs taken from the book. © 1990 1st Edition 384 pages

❑ AR-RTLA	Hardbound		$19.95
❑ FAR-RTLADOS	(MS-DOS Disk)		$9.95
❑ AR-RTDOS	(Program and Book)	Save $2.00	$27.90

Please add $3.75 for shipping and handling

CQ Bookstore
Greenville, NH 03048

K.V.G. CRYSTAL PRODUCTS

9 MHz CRYSTAL FILTERS

MODEL	Application	Bandwidth	Poles	Price
XF-9A	SSB	2.4 kHz	5	$ 75.00
XF-9B	SSB	2.4 kHz	8	105.00
XF-9B-01	LSB	2.4 kHz	8	145.00
XF-9B-02	USB	2.4 kHz	8	145.00
XF-9B-10	SSB	2.4 kHz	10	185.00
XF-9C	AM	3.75 kHz	8	110.00
XF-9D	AM	5.0 kHz	8	110.00
XF-9E	FM	12.0 kHz	8	120.00
XF-9M	CW	500 Hz	4	80.00
XF-9NB	CW	500 Hz	8	165.00
XF-9P	CW	250 Hz	8	199.00
XF-910	IF noise	15 kHz	2	20.00

10.7 MHz CRYSTAL FILTERS

XF-107A	12 kHz	$105.00
XF-107B	15 kHz	105.00
XF-107C	30 kHz	105.00
XF-107D	36 kHz	120.00
XF-107E	40 kHz	125.00
XF-107S139	100 kHz	175.00

41 MHz CRYSTAL FILTER

XF-410S02	$199.00

Write for full details of crystals and filters.
Shipping: $6.00 Shipping: FOB Concord, MA
Prices subject to change without notice.

VISA MasterCard

Spectrum International, Inc.
P.O. Box 1084 Dept. Q
Concord, MA 01742 U.S.A.
Phone: 508-263-2145
FAX: 508-263-7008

ASTRON CORPORATION
9 Autry
Irvine, CA 92718
(714) 458-7277

ASTRON POWER SUPPLIES

• HEAVY DUTY • HIGH QUALITY • RUGGED • RELIABLE •

MODEL VS-50M

SPECIAL FEATURES

- SOLID STATE ELECTRONICALLY REGULATED
- FOLD-BACK CURRENT LIMITING Protects Power Supply from excessive current & continuous shorted output
- CROWBAR OVER VOLTAGE PROTECTION on all Models except RS-3A, RS-4A, RS-5A, RS-4L, RS-5L
- MAINTAIN REGULATION & LOW RIPPLE at low line input Voltage
- HEAVY DUTY HEAT SINK • CHASSIS MOUNT FUSE
- THREE CONDUCTOR POWER CORD except for RS-3A
- ONE YEAR WARRANTY • MADE IN U.S.A.

PERFORMANCE SPECIFICATIONS

- INPUT VOLTAGE: 105-125 VAC
- OUTPUT VOLTAGE: 13.8 VDC ± 0.05 volts (Internally Adjustable: 11-15 VDC)
- RIPPLE Less than 5mv peak to peak (full load & low line)
- All units available in 220 VAC input voltage (except for SL-11A)

SL SERIES

MODEL	Colors Gray	Colors Black	Continuous Duty (Amps)	ICS* (Amps)	Size (IN) H × W × D	Shipping Wt. (lbs.)
• LOW PROFILE POWER SUPPLY						
SL-11A	•	•	7	11	2¾ x 7⅞ x 9¾	11

RS-L SERIES

MODEL	Continuous Duty (Amps)	ICS* (Amps)	Size (IN) H × W × D	Shipping Wt. (lbs.)
• POWER SUPPLIES WITH BUILT IN CIGARETTE LIGHTER RECEPTACLE				
RS-4L	3	4	3½ x 6⅛ x 7¼	6
RS-5L	4	5	3½ x 6⅛ x 7¼	7

RM SERIES

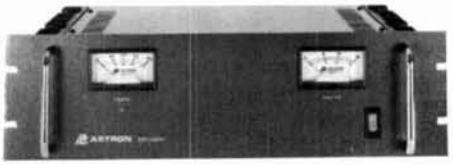

MODEL RM-35M

• 19" RACK MOUNT POWER SUPPLIES MODEL	Continuous Duty (Amps)	ICS* (Amps)	Size (IN) H × W × D	Shipping Wt. (lbs.)
RM-12A	9	12	5¼ × 19 × 8¼	16
RM-35A	25	35	5¼ × 19 × 12½	38
RM-50A	37	50	5¼ × 19 × 12½	50
RM-60A	50	55	7 × 19 × 12½	60
• Separate Volt and Amp Meters				
RM-12M	9	12	5¼ × 19 × 8¼	16
RM-35M	25	35	5¼ × 19 × 12½	38
RM-50M	37	50	5¼ × 19 × 12½	50
RM-60M	50	55	7 × 19 × 12½	60

RS-A SERIES

MODEL RS-7A

MODEL	Colors Gray	Colors Black	Continuous Duty (Amps)	ICS* (Amps)	Size (IN) H × W × D	Shipping Wt. (lbs.)
RS-3A		•	2.5	3	3 × 4¾ × 5¾	4
RS-4A	•	•	3	4	3¾ × 6½ × 9	5
RS-5A		•	4	5	3½ × 6⅛ × 7¼	7
RS-7A	•	•	5	7	3¾ × 6½ × 9	9
RS-7B	•	•	5	7	4 × 7½ × 10¾	10
RS-10A	•	•	7.5	10	4 × 7½ × 10¾	11
RS-12A	•	•	9	12	4½ × 8 × 9	13
RS-12B		•	9	12	4 × 7½ × 10¾	13
RS-20A	•	•	16	20	5 × 9 × 10½	18
RS-35A	•	•	25	35	5 × 11 × 11	27
RS-50A	•		37	50	6 × 13¾ × 11	46

RS-M SERIES

MODEL RS-35M

MODEL	Continuous Duty (Amps)	ICS* (Amps)	Size (IN) H × W × D	Shipping Wt. (lbs.)
• Switchable volt and Amp meter				
RS-12M	9	12	4½ × 8 × 9	13
• Separate volt and Amp meters				
RS-20M	16	20	5 × 9 × 10½	18
RS-35M	25	35	5 × 11 × 11	27
RS-50M	37	50	6 × 13¾ × 11	46

VS-M AND VRM-M SERIES

MODEL VS-35M

• Separate Volt and Amp Meters • Output Voltage adjustable from 2-15 volts • Current limit adjustable from 1.5 amps to Full Load

MODEL	Continuous Duty (Amps) @13.8VDC	@10VDC	@5VDC	ICS* (Amps) @13.8V	Size (IN) H × W × D	Shipping Wt. (lbs.)
VS-12M	9	5	2	12	4½ × 8 × 9	13
VS-20M	16	9	4	20	5 × 9 × 10½	20
VS-35M	25	15	7	35	5 × 11 × 11	29
VS-50M	37	22	10	50	6 × 13¾ × 11	46
• Variable rack mount power supplies						
VRM-35M	25	15	7	35	5¼ × 19 × 12½	38
VRM-50M	37	22	10	50	5¼ × 19 × 12½	50

RS-S SERIES

MODEL RS-12S

• Built in speaker

MODEL	Colors Gray	Colors Black	Continuous Duty (Amps)	ICS* Amps	Size (IN) H × W × D	Shipping Wt. (lbs.)
RS-7S	•	•	5	7	4 × 7½ × 10¾	10
RS-10S	•	•	7.5	10	4 × 7½ × 10¾	12
RS-12S	•	•	9	12	4½ × 8 × 9	13
RS-20S	•	•	16	20	5 × 9 × 10½	18

*ICS—Intermittent Communication Service (50% Duty Cycle 5min. on 5 min. off)

FT-1000

A Few Expert Opinions...

"...The most important performance aspects of any transceiver are ease of use and basic receiver performance. The FT-1000 excels at both...The FT-1000...has a very strong receiver; it has the best overall performance and the highest third order input intercept of any commercial radio ever tested in the ARRL lab...The FT-1000 needs little for me to consider it the ultimate contesting and DXing machine available today..."
— QST Magazine

"The FT-1000 is an excellent top flight transceiver in all respects. It has all the features one would expect in a radio of this class...Of all the top of the range models..., the FT-1000 is the friendliest to use. The ergonomics has been well thought out with simple and obvious control of all functions..." — Radio Communications (U.K.)

"The FT-1000 is indeed a fascinating new generation of HF transceiver...The receiver side is very impressive. The sensitivity, dynamic range, and selectivity figures are more than adequate for today's needs..." — CQ Magazine

"Until now a RF output power of 100 watts applied as the norm for semiconductor component shortwave transceivers; some newer high class units offered 150 watts. The FT-1000 is set for a maximum RF output of 200 watts. During normal SSB and CW use the power transformer remains hand warm — an improvement over the past when a transformer would occasionally 'burn up'..." — cq DL (Germany)

"The biggest attraction of the FT-1000 is the very quiet receiver. In a side-by-side comparison between the FT-1000, the ICOM IC-781, the ICOM IC-765, and the Kenwood TS-950, the FT-1000 came out the winner by a long shot... when comparing its receiver to those found in current equipment of the like monetary value from other manufacturers, the FT-1000 beats all."
— 73 Magazine

YAESU

*Performance without compromise.*SM

One-Year Limited Warranty on all Amateur Radio Products
Specifications subject to change without notice.

©1991 Yaesu USA, 17210 Edwards Road Cerritos, CA 90701 (213) 404-2700

KENWOOD

The only transceiver that could replace our best seller

The TS-450S.

Kenwood's goal is to always offer our customers the most sophisticated achievements in technology. So, when it came time to enhance our best selling TS-440S transceiver, we didn't hesitate.

The resulting TS-450S and TS-690S transceivers offer a combination of versatility, flexibility, sensitivity, and selectivity unparalleled in their price range.

The TS-450S offers competition class reception and 100 W transmission capabilities on all nine Amateur bands in SSB, CW, FM, and FSK modes, with 40 W on AM. The TS-690S also offers 50 W on six meters.

For amazingly clear reception, Advanced Intercept Point (AIP), greatly improves the receiver's dynamic range to an incredible 108 dB. An optional Digital Signal Processor, DSP-100, offers even further sound clarity by tailoring the incoming and outgoing audio passband signals.

You'll find the TS-450S and TS-690S provide truly outstanding sensitivity over the entire band. Innovative "triple conversion" also assures superior stability and accuracy, particularly above 24.5 MHz, for improved DXing.

Other refinements include: convenient split frequency operation, advanced filter functions, optional automatic antenna tuner, and 100 memory channels with flexible scanning selections.

Accessories include: **PS-33** 20.5A power supply, **PS-53** 22.5A heavy duty power supply, **SP-23** external speaker, **AT-450** internal automatic antenna tuner, **AT-300** external automatic antenna tuner, **DSP-100** digital signal processor unit, **VS-2** voice synthesizer, **SO-2** TXCO, **MB-430** mobile mount, **PG-2X** DC cable, **TU-8** CTCSS encoder, **YG-455C-1** 500Hz CW filter for 455kHz IF, **YG-455CN-1** 250Hz CW narrow filter for 455kHz IF, **YK-88S-1** 2.4kHz SSB filter for 8.83MHz IF, **YK-88SN-1** 1.8kHz SSB filter for 8.83MHz IF, **YK-88C-1** 500Hz CW filter for 8.83MHz IF, **YK-88CN-1** 270Hz CW filter for 8.83MHz IF, **YK-455C-1**, 500Hz CW filter for 455kHz IF

KENWOOD U.S.A. CORPORATION
COMMUNICATIONS & TEST EQUIPMENT GROUP
P.O. BOX 22745, 2201 E. Dominguez Street
Long Beach, CA 90801-5745
KENWOOD ELECTRONICS CANADA INC.
P.O. BOX 1075, 959 Gana Court
Mississauga, Ontario, Canada L4T 4C2

KENWOOD

. . . pacesetter in Amateur Radio

Kenwood meets or exceeds all specifications. Contact your dealer for a complete listing of specifications and accessories. Specifications are subject to change without notice. Complete service manuals are available for all Kenwood transceivers and most accessories. One year warranty in the U.S.A. only.

Mr & Mrs George W Carson
1100 Randolph Rd
Crossville, TN 38571-7296

February 29, 1992
George W. Carson, K4GDG
~~Route 4,~~ Box ~~632~~ 1100 RANDOLPH Rd
Crossville, TN 38~~55~~ 38571
(~~615~~) 277-3221
931

RE: ERROR CORRECTIONS
ARTICLE, PAGE 91, COMMUNICATIONS QUARTERLY, SUMMER 1991

Page 91, 1st Column, 3 3/4" up from bottom of page 91: "Modified 3 1/8 connectors" correct to 1" diameter connector.

Page 91, 1st Column, 2 3/8" up from bottom of page: "carefully bore 4 3/8 holes" correct to 11/16" diameter hole to depth of 13/32". NOTE: Figure 3 drawing is correct and you can use 1 1/4" or 1 1/2" diameter aluminum stock if available!

Figure 2, Page 93: 10 Meters tap on L-6 at 4-1/3 turns drawing is in error. (Page 98, 6 5/8" up from bottom first column states correct modification at 4 1/8 turns from tuning capacitor C55). NOTE: If you use different tuning capacitor (C-55) substituting 10/300 vacuum variable, be aware that you do not increase stray capacity of the L C circuit C-55 and L-6 or it will lower ceiling of top tune capabilities at 29,700 KHz. If you can lower stray capacity more you can tap farther out and increase inductance tap of L-6 for 10 Meters which will increase Q and output too. I limited modifications to the basic design merely to improve output and stability which was very bad, meters jumped and variable tune capacitor arced over prior to modifications and power was down.

Additional Reference, Suggested Reading: Page 34, R. L. Measures, AG6K, "Parasitics Revisited II", QST, October 1990.

I put two new tubes 3-500Z Eimac in and revised the parasitic suppressor configuration to:

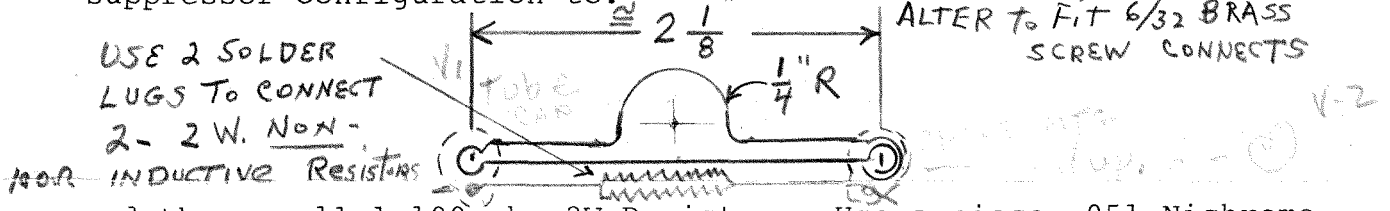

and the parallel 100 ohm 2W Resistors, Use a piece .051 Nichrome furnace heater resistor wire (#16) and fold back. I uncoiled two pieces from a 4500W 240V element!

Additional References:

Page 43, R. L. Measures, "Parasitics II", QST, December 1990 (input net).

Page 25, R. L. Measures, "Circuit Improve SB 220", QST, November 1990.

Page 80, Bill Orr, W6SAI, "Loose Filament Pins on the 3-500Z", CQ, May 1991.

Page 43 R L Measures Parasitics II QST Dec. 1990
" 25 " CIRCUIT IMPROVE SB220 Nov 1990
" 80 BILL ORR W6SAI CQ MAY 1991 Loose fil. PINS on the 3-500 Z